Microbial Community Study of Brine Evaporation Ponds: Identification and Analysis of the Total Organic Carbon Problem

VRISHTHI RAMBARAN

217080193

A Research Dissertation submitted in fulfilment of the academic requirements for the degree of:

Master of Science in Biological Science

School of Life Sciences

College of Agriculture, Engineering and Science

University of KwaZulu-Natal

Westville

South Africa

December 2020

As the candidate's supervisors, we have approved this thesis for submission.

[redacted]

Signed by Dr. Aluwani Nemukula

(Supervisor)

[redacted]

Signed by Dr. Paul A. Joslin

(Co-supervisor)

[redacted]

Signed by Prof. Y. Naidoo

(Co-supervisor)

PREFACE

The research contained in this dissertation was completed by the candidate while based in the Discipline of Biological Sciences, School of Life Sciences of the College of Agriculture, Engineering and Science, University of KwaZulu-Natal, Westville, South Africa. The research was financially supported by the National Research Foundation.

The contents of this work have not been submitted in any form to another university and, except where the work of others is acknowledged in the text, the results reported are due to investigations by the candidate.

[redacted]

Signed: Dr. A. Nemukula

Supervisor

Date: 29/01/2021

[redacted]

Signed: Dr. P. Joslin

Co-Supervisor

Date: 02/02/2021

[redacted]

Signed: Prof. Y. Naidoo

Co-Supervisor

Date: 29/01/2021

DECLARATION: PLAGIARISM

I, **Vrishthi Rambaran**, declare that:

(i) the research reported in this dissertation, except where otherwise indicated or acknowledged, is my original work;

(ii) this dissertation has not been submitted in full or in part for any degree or examination to any other university;

(iii) this dissertation does not contain other persons' data, pictures, graphs or other information, unless specifically acknowledged as being sourced from other persons;

(iv) this dissertation does not contain another persons' writing, unless specifically acknowledged as being sourced from other researchers. Where other written sources have been quoted, then:

a) their words have been re-written, but the general information attributed to them has been referenced;

b) where their exact words have been used, their writing has been placed inside quotation marks, and referenced;

(v) this dissertation does not contain text, graphics or tables copied and pasted from the Internet, unless specifically acknowledged, and the source being detailed in the dissertation and in the References sections.

Signed: Vrishthi Rambaran

Date: 29/01/2021

ABSTRACT

Salt is an important compound as it is used by humans for everyday life. Salt production can occur from two processes: the use of seawater which is evaporated leaving the salt behind or the use of brine which is obtained from underground sources and undergoes the same process of evaporation as the seawater. The focus for this research will be on the microorganism population in salt produced from underground brine sources such as the source used by Botswana Ash (Pty) Ltd (Botash) which is the salt works that provided the samples for this research paper. The most important microorganism found in salt evaporation ponds is the green algae *Dunaliella salina* (*D. salina*) as discovered by previous studies. The main focus of this study was the identification of the microorganisms that are found within the salt evaporation ponds and the effect that the dominant *D. salina* population will have on the salt production process and also whether the dominant *D. salina* species can be used for production of important by-products to generate another source of income. The population genetics study on the samples from the various evaporation ponds at Botash has revealed the presence of many different microorganisms such as the bacterium Salinabacter, and the green algae *Dunaliella salina* which was revealed to be the dominant species. Other species such as archaea were also discovered within the salt evaporation ponds at Botash. The green algae *D. salina* was focused upon due to its dominance within the higher salinity ponds where it serves as the primary producer. The growth rate of the dominant *D. salina* species was observed in different conditions such as saline concentrations and different nitrogen sources. The results found that *D. salina* grows best at 3M salinity with NO_3 or Urea as the nitrogen source. A study of the growth of *D. salina* when environmental factors were controlled showed that *D. salina* prefers high temperatures and high saline conditions for growth. *D. salina* also produces high value products such as beta carotene and Extra Polysaccharides (EPS). The production of these compounds are linked to the environmental conditions as it was found that beta carotene production is optimized when the cells are placed under stress during nitrogen starvation. EPS production occurs under all environmental conditions. The results from this research paper show that if the microbial community is controlled and optimized useful by-products can be produced, whilst minimal harm is done to the quality of salt produced.

DEDICATION

To my parents Binesh and Jothi, and my sister Sharmishta, thank you for being patient and understanding during the course of my research. This dissertation is dedicated to you.

ACKNOWLEDGEMENTS

First and foremost, I would like to express my gratitude and appreciation to the National Research Foundation for the financial support throughout this dissertation.

To my supervisor, Dr Aluwani Nemukula: thank you for allowing me the opportunity to pursue my further studies in academia. Your open-door policy, unwavering support and indispensable wisdom never went unnoticed. Thank you for always being there to help when it was needed and providing guidance on the way forward when the path was lost and never giving up on me.

To my co-supervisors Dr Paul Joslin and Prof. Yougasphree Naidoo: Thank you for accepting me as your student. Thank you Dr Joslin for always checking up on me and expanding my understanding of microbial communities. Your swift response to all queries big or small never went unnoticed. Thank you very much for everything. Thank You Prof. Yougasphree Naidoo for always being there when I needed advice and correcting all my grammatical errors, your advice and swift response was truly appreciated.

To Balopi at Botash: Thank you for always being ready to provide samples and information regarding the workings at the salt evaporation ponds at Botash. The information provided by you allowed for the completion of this dissertation.

To my labmate Reuben Rampersadh: Thank you for always being ready to assist me whenever I needed assistance and always inspiring me to push forward with my research no matter the situation.

To my best friends in Office 04-013a thank you for always being there when I needed to vent and always helping out when I needed assistance. The inspiration provided by you all has helped me through my research. Thank you for all the amazing times we have had.

Lastly, a heartfelt thank you to my family, friends and most importantly Lord Krishna without whom I would never have reached this stage.

Contents

LIST OF FIGURES

LIST OF TABLES

LIST OF ABBREVIATIONS

D. salina	*Dunaliella salina*
FTIR	Fourier-transform infrared spectroscopy
LC-MS	Liquid chromatography–mass spectrometry
GC-MS	Gas chromatography–mass spectrometry
HPLC	High Performance Liquid Chromatography
TOC	Total Organic Carbon
Botash	Botswana Ash (Pty) Ltd
β-carotene	Beta Carotene
EPS	Extra Polysaccharides
NO3	Nitrate
NH4	Ammonia
NaCl	Sodium Chloride
RSM	Response Surface Methodology

CHAPTER 1: INTRODUCTION

Salt evaporation ponds are one of the many methods used to obtain salt crystals for use in industry (Silva *et al*., 2017). They are formed naturally or are engineered in order to obtain the salts present in brine water arising from various sources such as underground sources and the sea (Athearn *et al*., 2009). Such saltpans allow for the evaporation of the water present, thus leaving the salt crystals behind (Önal, 2015). This process requires time and high levels of sunlight. Thus, salt evaporation ponds are generally found in places that receive high levels of sunlight (Takekawa *et al*., 2015).

As pointed out, salt evaporation ponds rely heavily on evaporation in order to achieve the result of salt crystals (Javor, 2002). Thus, salt evaporation ponds are exposed to the atmosphere and are therefore also exposed to contamination by various microorganisms present therein (Javor, 2002). These microorganisms are useful to the salt production process as they darken the colour of the salt evaporation ponds, thus helping to speed up the absorption of heat and the evaporation process (Javor, 2002). The salt crystals produced in salt evaporation ponds are generally of high purity since the starting material which is sent through the evaporation ponds, i.e. the brine and seawater, contain the desired purity of salt in high concentrations (Ravizky & Nadav, 2007).

The salt evaporation ponds function by channelling the brine and seawater through various ponds of different concentrations (Ahmed *et al*., 2001). Brine is obtained from underground stores whilst seawater is obtained from the ocean (Oren, 2019). Brine usually contains other organic compounds such as sulphur, in considerable concentrations as opposed to seawater which has NaCl present as the main organic compound with other compounds present in smaller quantities (Javor, 2002). The ponds are joined via raceways (channels) that allow the concentrated brine or seawater to move to the next concentrating pond (Heng *et al*., 2019). The final pond is known as the crystallizer pond. This is the pond in which the salt crystals are formed due to increased loss by evaporation of the liquid remaining in the brine and seawater solutions (Javor, 2002).

The microorganisms present in salt evaporation ponds include eukaryotes such as microalgae and prokaryotes like the archaea (Oren, 2019). These organisms have

developed various adaptations to the highly saline environment (Oren, 2019). Communities and ecosystems are formed by the interactions of these microorganisms and their environment (Zarrini *et al*., 2018). These microorganisms, for example, supply food and other resources to one another, thus allowing the survival and growth of the community within the salt evaporation ponds. (Oren, 2019). The presence of these microorganisms assists in the salt production process but can also sully and despoil the final product.

The microbial community of the salt evaporation ponds are highly diversified (Oren, 2019). The main types of microorgamnims generally found in salt evaporation ponds are species such as *Dunaliella*, *Salinobacter* and *Halobacterium* (Kerkar, 2004). These organisms co-exist within the salt evaporation ponds as they all inhabit different ecological niches (Kerkar, 2004). Due to the presence of microorganisms within the salt evaporation ponds, there should be a natural method to control the population of these microorganism (Li *et al*., 2018). The presence of grazers such as Artemia within the salt evaporation is a possible method of controlling the microorganism population (Li *et al*., 2018). Therefore, more information needs to be provided on the presence of Artemia or other potential grazers within the ponds and the effect of these grazers on the microbial population.

Botswana Ash (Pty) Ltd is a company situated in the northern Sua Pan region of Botswana. The company which is commonly referred to as Botash was founded in 1991 (Botswana Ash (Pty) Ltd, 2011). Botash has been one of the leading suppliers of sodium products within the African continent since its inception (Botswana Ash (Pty) Ltd, 2011). Botash has the capacity to produce 300 000 tonnes of Soda Ash and 450 000 tonnes of sodium chloride per annum (Botswana Ash (Pty) Ltd, 2011). Botash has partnered with different research institutions in order to determine the composition and roles of the associated microbial communities on the production process as well as the health of the salt evaporation ponds. Thus, the research reported herein will attempt to better understand the microbial diversity within salt evaporation ponds and their potential effects on production.

The salt evaporation ponds of the company, Botash, in Botswana, produce both salt (sodium chloride) crystals and soda ash. Soda ash, which is commonly known as calcium

carbonate, was initially produced from the ash of plants grown on sodium-rich soils (Eggeman, 2011). Soda ash can also be produced from sodium chloride through the solvay process and this process is used to produce soda ash in high amounts at Botash. The solvay process uses salt brine and limestone to produce sodium carbonate through a chemical reaction. The production of high quality soda ash is of equal importance as high quality salt, as soda ash is in high demand in the industrial industry as it is used to make glass for windows (Eggeman, 2011). Thus, the efficiency of Botash to produce Soda Ash is of high importance due to the economic value of Soda Ash.

The efficiency of Botash in producing both salt and soda ash is affected by the numbers and type of microorganisms present in the salt evaporation ponds (Javor, 2002). The microorganisms within the salt evaporation ponds must be maintained at a certain concentration that allows for the proper production of salt and soda ash (Oren, 2019). The maintenance of the correct level of microorganisms depends on the control of all the factors that affect the growth of the microorganisms such as the presence of nutrients within the salt evaporation ponds (Oren, 2019).

1.1 The rationale of the Study

This project aims to establish the cause of increased amounts of organic matter found in the salt evaporation ponds at the Botash Plant in Botswana. The increased amount of organic matter in the evaporation ponds causes the discoloration of the salt crystals. This, in turn, increases the production time required to manufacture the products made at the Botash Plant (Javor, 2002). The process of salt production requires the presence of microorganisms at low concentrations (Javor, 2002). These microorganisms form a dense benthic carpet on the base of the salt evaporation ponds that prevent leakage of the salt from the evaporation ponds which helps optimise the salt production process (Javor, 2002). The process by which the benthic mats are formed and maintained in the salt evaporation ponds is well researched. However, the presence and effect of motile microorganisms such as the microalga, *Dunaliella salina* in brine evaporation ponds have been known to cause a decrease in the quality of salt produced (Javor, 2002). The reason for the decrease in salt quality could be because the by-products such as beta carotene and EPS produced by *D. salina* coats the salt crystals (Javor, 2002). Therefore, it is imperative

to research the effect of microorganisms such as *Dunaliella* on the products produced within salt evaporation ponds such as sodium chloride and soda ash.

There have been various papers published on the mechanisms of *D. salina* in relation to glycerol production, beta carotene production and optimisation of *D. salina* under various environmental conditions due to the economical benefit attached to the production of the above mentioned products. Beta carotene, in particular, is of importance due to its massive role in the pharmaceutical industry.

There has, however, been very few papers published on the impact of microorganisms such as *D. salina* on the production of salt in brine evaporation ponds (Davis & Giordano, 1995). Research has been mostly dedicated to the production of high-value compounds such as beta carotene which is produced in high concentrations by *D. salina* under various conditions (Shaker, Morowvat, & Ghasemi, 2017).

Research studies had demonstrated effects of *D. salina* on the production and quality of salt produced in brine evaporation ponds. An example is a study that focused on the size and quality of salt crystals produced in the presence of *D. salina* (Giordano, *et al*., 2014). However, knowledge gaps in these areas of research need to be addressed.

The effect of *D. salina* on the products can be managed if the quantity of *D. salina* within the ponds is controlled. Hence, research will need to be done into the control of *D. salina* populations using grazers (Mlingi *et al*., 2019). Grazers can be used to control populations due to the fact that they are organisms that can occur naturally within an environment and, hence, will not have an effect on the balance within the salt evaporation ponds, thus making them the best and safest method of biological control (Li *et al*., 2018). The grazer that has the most potential as a form of biological control is Artemia, due to the fact that they live in saline environments (Mlingi *et al*., 2019). Thus the potential of Artemia as a grazer to control *D. salina* population will be investigated within this paper. Grazers may not occur naturally and will require introduction.

Thus, this study aims to determine the cause of the discoloration of the salt products produced at salt evaporation ponds that contain high levels of biological matter. The study will also aim to establish the reason for the increase in microorganisms within the evaporation ponds and what types of microorganisms are found within the ponds.

1.2 Aims and Objectives of the Study

The current study will aim to generally investigate the cause of the total organic carbon (TOC) increase problem in the Botash Plant evaporation ponds. Is this being caused by *D. salina*? To achieve this, the following objectives were pursued:

1. To analyze the samples obtained from Botash to determine the presence of various microorganisms in the sample
2. To analyze the growth rate of the dominant primary producer *D. salina* in various environmental conditions
3. To analyze the production of pigments and glycerol by *D. salina* in salt evaporation ponds under different conditions
4. To analyze the salt samples obtained from Botash to determine the effect that increased levels of microorganisms such as *D. salina* have on the purity of the salt crystals produced
5. To analyze the relationship between the nutrients present and microbial diversity
6. To analyze the effect of various abiotic factors such as salinity and nutrient availability and temperature on the growth of microorganisms such as *D. salina*
7. To analyze the possibility of optimising the production of useful by-products such as beta carotene from *D. salina* as an alternate source of income for Botash

The present study assumes that the cause of the problem at the Botash salt evaporation ponds is due to the presence of high levels of microorganisms. This study will aim to establish the nature of these communities and their impact on salt and soda ash production at the Botash Plant. The study assumes that the main cause of the problem is the primary producer *Dunaliella salina*. Thus, this study will investigate the reasons for the high presence of *D. salina* in the ponds. The *D. salina* appears to be the source of the organic contamination of the salt produced at the Botash salt evaporation ponds.

1.3 Outline of the Dissertation

This dissertation will be divided into five Chapters as follows:

Chapter 1 (this chapter) presents a the Introduction incorporating the literature review which will cover the background information and general aspects of salt evaporation ponds and how these ponds function in relation to the presence of various microorganisms found within these ponds. This chapter will also focus on the *Dunaliella salina* and the compounds that are found within this microorganism. This chapter will introduce the main theoretical concepts to be used in this study.

Chapter 2 will provide the results pertaining to the analysis carried out regarding the microorganism community within the salt evaporation ponds. The analysis involved the genetic sequencing of all the organisms within the salt evaporation ponds. This sequencing analysis allows for the identification of the organisms within the salt evaporation ponds and how they interact with each other and the environment. The nutrient availability within the ponds will also be analysed as the amount of organisms present within an environment is dependant on nutrient availability.

Chapter 3 will provide the results obtained from the experiments regarding the capability of *D. salina* to inhabit environments with high salinities and different sources of nitrogen. This experiment involved the growing of *D. salina* in different salinities and nitrogen sources. These experiments enabled the better understanding of the growth and survival mechanisms of *D. salina* within the environmental conditions that are found in the salt evaporation ponds. Chapter 3 will also will discuss the Response Surface Methodology experiment that was performed on *D. salina*. Response Surface Methodology refers to a set of experiments following a mathematical equation that allows for the analysis of optimum growth parameters for a particular organism which, in this case, was *D. salina*. The experiments involved the construction of experiments that tested the ability of *D. salina* to survive in different environments. The environmental factors used in this experiment were nutrient source, salinity and temperature. The results from this experiment will lead to a better understanding of the optimum growth conditions for *D. salina*.

Chapter four will encompass the results obtained from the analysis of the salt crystals from Botash and will compare these results to the Extra Polysaccharides that are excreted by *D. salina*. This chapter will aim to identify the purity of the salt crystals and whether the decrease in purity of the salt crystals is as a result of the presence of *D. salina* within the ponds.

Chapter five will focus on the conclusions and rcommendations for further research that can be drawn from this thesis. The possibility of biological control will also be discussed in this chapter.

1.4 Literature Review

1.4.1 Salt and Soda Ash Production

Salt (NaCl) is an ionic compound that holds significance to humans due to its many uses. It may be added to food as a condiment, as a preservative, and is used widely by industry. Salt is obtained through the process of evaporation (Tabor, 1981). Seawater and underground brine sources rich in salt are evaporated by the process of passing these salt-rich solutions through various shallow ponds (Mani *et al.*, 2012). The evaporation process allows for the water present in the solution to be evaporated due to exposure to sunlight which concentrates the salt particles present within the solution (Zhao *et al.*, 2018). The shallow ponds increase in salinity as the process of evaporation proceeds (Kaufmann, 1960). The increase in salinity of the consecutive ponds causes changes in the biodiversity that is present in the salt evaporation ponds (Oren, 2012). There is a vast change in the biodiversity of the microbiota present in salt evaporation ponds as the brine becomes concentrated into salt (Javor, 2002).

The production of salt may be facilitated by different methods. The most popular method of salt production is by using seawater as the precursor and allowing the seawater to evaporate until only the salt remains (Muraveva, 2017). The process of using underground brine sources as the starting resource for salt production is also popular. Botswana Ash (Botash) Company uses an underground brine source as the precursor for both salt and soda ash production. The series of ponds and salt evaporation process is shown in Figure 2.1. Salt is mined and processed as a by-product of economic importance, while soda ash is used in the glass manufacturing industry. The production of high-quality salt and soda ash needs to be ensured for the products to meet industry standards. This relies heavily on the balance of microorganisms within the evaporation ponds. If the balance is not maintained at threshold levels the quality of the products is compromised. Thus, the control of the microorganisms within the evaporation ponds is very important as it affects the quality of the products.

Another product that is of great economical importance and is also produced from salt evaporation ponds is soda ash or sodium carbonate (Kwan, 2017). Soda ash is of

particular importance to Botash as it is in high demand due to the fact that it is used in the making of glass window panes (Eggeman, 2011). Thus, the production of soda ash from salt evaporation ponds is also a main focus of companies such as Botash due to its economical value.

1.4.2 The microbiota present in salt evaporation ponds

The microbiota present in salt evaporation ponds can be divided into the following subsections:

1.4.2.1 *The microbiota found in the microbial mat present at the bottom of the salt evaporation ponds*

A microbial mat is formed by the presence of many different microbial species found at the bottom of salt evaporation ponds with high salinities (Oren, 2010). The microbial mat is formed from layers of different bacterial species which all work together to recyle nutrients to sustain the mat (Biswas & Paul, 2014). The microbial mat is composed of various types of bacteria such as purple sulphur-reducing bacteria (Oren, 2009a). The benthic community found in the salt evaporation ponds are generally found at salt concentrations of 90–240g/L (seawater is typically 35g/L). These communities have different types of microorganisms situated in various regions of this benthic mat in an almost layer-like manner (Airs & Keely, 2003). The upper layer of the microbial benthic mat is generally orange-brown in colour and contains unicellular *Halothece*–type cyanobacteria. Below this layer is a green layer that consists of mainly filamentous cyanobacteria. Underneath the green layer is a purple layer of sulphur bacteria and at the base of this benthic mat community is a black layer of reduced anaerobic sediment and detritus (Oren *et al*., 1995). The benthic mat present on the floor of the evaporation ponds has various ways of producing energy such as sulphur reduction, methane reduction and the use of fatty acids. Thus, this is a mini- ecosystem, that can be used to study the different methods of energy production by different microorganisms under saline

conditions (Oren *et al*., 2009b). The focus of this research is on the planktonic microorganisms found in the brine – specifically, *D. salina*.

1.4.2.2 The microbiota present in the brine solution

The microorganisms suspended in the brine solution are called planktonic microorganisms (Oren, 2012). The planktonic microorganisms that are generally found in the brine solution are organisms such as *D. salina*, different types of archaea (e.g. *Haloquadratum*) and eubacteria such as *Salinobacter*. (Gunde-Cimerman *et al*., 2006). These organisms play special roles in the microbial community and in the process of salt production (Oren, 2009a). These microbes can either facilitate the production of salt by producing an environment favourable to salt production or create an environment detrimental to the production of salt (Davis, 2000). The presence of favourable microbes allows for the increased production of salt, by changing the environment to allow for favourable conditions such as the colouration of the water to allow for quicker evaporation of the water and production of salt (Davis, 2000). The unfavourable plankton microbes within the salt evaporation ponds deplete the amount of sunlight entering the evaporation ponds causing a die out of all the useful benthic microbes present and thus, adding biowaste to the salt produced (Davis, 2000). The dominant species within the plankton environment in both favourable and unfavourable conditions is the green alga *D. salina*.

1.4.3 *The alga, Dunalliela salina*

D. salina belongs to the Phylum Chlorophyta, the Order Volvocales and the Family Polyblepharidaceae (Tafreshi & Shariati, 2009). *D. salina* cells are unicellular, motile as they have flagella which are whip-like structures that allow for movement (Ben-Amotz & Avron, 1987). It lacks a rigid cell wall which makes the species morphologically distinct (Ben-Amotz & Avron, 1987). The cell is instead surrounded by a layer of glycerol (Ben-Amotz & Avron, 1987). *D. salina* is a green alga that generally grows in saline environments (El – Baky *et al*., 2004) and can grow in salinities that range from 9–200g/l

(Lamers *et al*., 2010). *D. salina* cells are generally ovoid in shape but they can be spherical, pyriform, fusiform or ellipsoid, depending on the environment (Polle *et al*., 2008). *D. salina* cells are small, having a width between 3 - 13 µm and a length of 5 – 25 µm (Polle *et al*., 2008).

1.4.3.1 Pigments produced by Dunaliella salina

D. salina produces various pigments in order to enable it to survive and photosynthesize in the harsh environments in which it lives (Xu *et al*., 2018). The green algae, *D. salina* produces pigments such as chlorophylls *a* and *b*, β-carotene and various xanthophylls as well as lutein (Lamers *et al*., 2010), as shown with a carotenoid biosynthetic pathway in Figure 1.1. These pigments enable the *D. salina* cells to survive the harsh environment since they absorb the harsh UV rays produced by the sun and prevent damage to the cells (Bonnefond *et al*., 2017). The highly saline environments in which *D. salina* generally live include salt evaporation ponds which are exposed to high levels of sunlight in order to enable the production of salt crystals by evaporation.

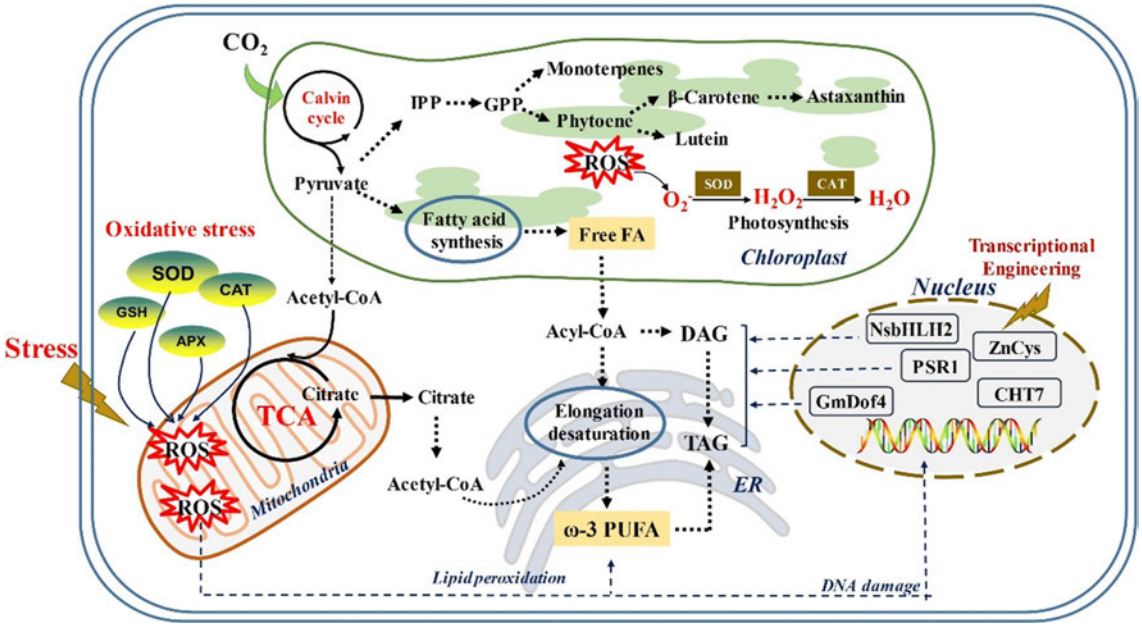

Figure 1.1: Microalgal carotenoid biosynthetic pathway (Sun *et al*., 2018)

The presence of these pigments also, to some extent, helps the process of salt production since these pigments change the colour of the salt evaporation ponds to a pink colour which traps more sunlight, thus speeding up the process of evaporation (Javor, 2002).

These pigments also play an important role in the pharmaceutical industry as beta carotene which is one of the pigments produced by *D. salina* in abundance. They are required by the pharmaceutical industry to produce sun-protective lotions (Zarandi-Miandoab *et al*., 2019). Therefore, much research has been done to understand the mechanisms and conditions that will maximise beta carotene production as this is a difficult pigment to acquire in high concentrations.

1.4.3.2 Dunaliella salina as the primary producer

All organisms in the world require an energy source. The primary producers in most environments are plants and algae that photosynthise (Buchanan *et al*., 2015). The primary food source in saline environments is the microalgae, *D. salina* (Javor, 2002). The cells are not ingested directly but produce glycerol which acts as a primary food source on which all the other microorganisms survive (Ben-Amotz, 2019). The main mechanism for the survival of *D. salina* in saline environments is the presence of glycerol within the cells (Ben-Amotz, 2019). Glycerol is produced by the *D. salina* cells as a mechanism to survive in saline environments. The glycerol forms a protective barrier around the cell and prevents osmotic stress (Oren, 2017). The production of glycerol is very important to *D. salina* as the metabolic pathways that initiate the production of glycerol within its cells are linked to receptors that detect an increase in salinity in the surrounding environment (Fang *et al*., 2017). The glycerol produced by *D. salina* is generally stored within the cell to prevent osmosis. However, some leakage of glycerol into the surrounding environment does occur under certain conditions (Oren, 2017). The glycerol leaked into the surrounding environment acts as a food source for the other microorganisms present within the salt evaporation ponds (Oren, 2017). Thus, the entire ecosystem within the saline environment is dependant upon the production of glycerol by *D. salina*. Although glycerol is produced to help survival, it is also secreted into the environment by the cells which allows for the survival of the ecosystem (Oren, 2017). The reasons for the secretion of glycerol into the environment are various such as leaky cell walls or the excess production of glycerol by the cell (Fang *et al*., 2017).

1.4.3.3 Manipulation of Dunaliella salina to produce by-products of importance

As mentioned above**,** *D. salina* stores and produces various products of economic value (Hans *et al*., 2019). *D. salina* can be induced to produce high-value compounds such as beta carotene, glycerol and fatty acids when grown in conditions favourable to its growth (Ben-Amotz, 2019). The normal concentrations of compounds are not enough to meet the demands of the various sectors that require these compounds. Therefore, growth conditions are manipulated in order to obtain high-value compounds in higher concentrations (Montazeri-Najafabady *et al*., 2016). The manipulations of the growth conditions generally involve the starvation of the cells by the exclusion of certain nutrients which are important to the normal growth of the *D. salina* (Montazeri-Najafabady *et al*., 2016). These exclusions create environments in which *D. salina* is forced to activate the various survival mechanisms it has in order to be able to survive. These mechanisms include the increased production of beta carotene and glycerol which allows the cells to cope with the changes in the environment (Ben-Amotz, 2019). An example of beta carotene as a mechanism for survival is when the cells are exposed to high levels of sunlight. They produce beta carotene which protects the cells from the harsh UV rays (Montazeri-Najafabady *et al*., 2016). Glycerol prevents osmosis in highly saline environments, thus protecting the cells from osmotic shock (Fang *et al*., 2017). Research has been done to determine the role that abiotic factors such as light and temperature have on the maximising of production of high-value compounds. Thus, it has been found that high temperatures and ultraviolet light help increase the production of high-value compounds (Han *et al*., 2019). Thus, much research has been done on the manipulation and growth of *D. salina* to acquire compounds such as beta carotene and glycerol. The previous research mentioned above will be used to perform an optimization study as a means to generate income from the *D. salina* cells present within the Botash ponds.

1.4.3.4 Effect of nitrogen on the growth of D. salina

D. salina has adapted to growth in saline environments. However, it still requires certain nutrients in order to thrive (Chen *et al*., 2015). These nutrients are nitrogen, phosphate, and potassium which enable the efficient growth of *D. salina* in the saline environment

(Chen *et al*., 2015). The presence of nitrogen is most important for the growth of *D. salina* as nitrogen enables the proper functioning and growth of cells as, for example, a key component of amino-acids (Bonnefond *et al*., 2017). The form of nitrogen used by *D. salina* affects the growth and reproduction of the *D. salina* cells (Can *et al*., 2016). Nitrogen can be present as nitrate, ammonia and urea which can affect the uptake and usage of the nitrogen (Can *et al*., 2016). *D. salina* cells generally prefer nitrate as the source of nitrogen as they are adapted to using nitrate as the nitrogen source. However, they can use urea and ammonia as nitrogen sources as well (Ben-Amotz, 2019). The source of nitrogen and its availability within salt evaporation ponds has a significant impact on the growth and reproduction of *D. salina* cells within salt evaporation ponds. This impact will be investigated further.

1.4.3.5 Effect of salinity on D. salina growth

The salinity within the salt evaporation ponds influences the growth of *D. salina* since it must adapt to varying salinities within the salt evaporation ponds (Wei *et al*., 2017). This change in salinity within the ponds causes various changes within the cells (Ahmed *et al*., 2017). These changes result in the production of glycerol and beta carotene which act as factors that allow the cells to survive within the high salinities of the salt evaporation ponds, by protecting the cell against high UV exposure and buffering the cell against osmosis (Oren, 2014). The salinity within the salt evaporation ponds causes an increase in the amount of *D. salina* present within the salt evaporation ponds as it grows best in the salt crystallizer ponds (Oren, 2014). These ponds generally have the highest salinities due to the fact that these ponds are the final stage in the salt solidfiication process (Javor, 2002). The presence of *D. salina* within these ponds allows for faster evaporation due to the fact that the *D. salina* present in the crystallizer ponds have high levels of beta carotene present within their cells which causes a reddish colour to appear within the ponds (Oren, 2014). The effect of salinity on the growth of *D. salina* has been researched in terms of manipulation to produce various high-value compounds. However, the general effects of salinity on growth and the optimal salinity for growth has been less researched.

Therefore, this paper will aim to understand the effect of increasing salinities on the growth and accumulation of products by *D. salina* cells.

1.4.4 *The ecosystem formed within salt evaporation ponds*

The presence of the primary producer *D. salina* allows for various other microorganisms to live within the harsh conditions of salt evaporation ponds (Javor, 2002). The eubacteria and archaea that reside within the salt evaporation ponds have developed mechanisms by which they can use the glycerol produced by *D. salina* as a carbon source (Bardavid & Oren, 2008). The archaea present in salt evaporation ponds have developed a mechanism by which they can use glycerol as a growth substrate and grow at higher rates to the extent that, if left without competing organisms, they cause archaea blooms which turn salt ponds a reddish-pink (Falb *et al*., 2008). Archaea use glycerol as a growth substrate due to the presence of various enzymes within their cells that break it down to derive energy. (Falb *et al*., 2008). Eubacteria can also use glycerol as a substrate on which to grow. However, the bacteria do not grow as well as Archaea on glycerol; except for the species *Salinibacter* (Sher *et al*., 2004). Thus, the Archaea and Eubacteria residing within the salt evaporation ponds survive due to the evolution of mechanisms to use glycerol as a growth substrate (Oren, 2017).

1.4.5 *Nutrients required for Growth*

The proliferation of microorganisms in any environment requires nutrients to be present in concentrations that enable growth (Enache *et al*., 2017). The most important nutrients for the growth of organisms are nitrogen, phosphorus, and potassium (Enache *et al*., 2017). These nutrients are naturally found in most environments and can be used by organisms to replicate and survive (Andrei *et al*., 2012). In saline environments, these nutrients are also found in concentrations that allow for the survival of the organisms present within the salt evaporation ponds (Javor, 2002). The nutrients available within salt evaporation ponds are generally acquired from the brine which is pumped into the salt evaporation ponds (Javor, 2002). This brine has various nutrients present due to the

fact that it is from an underground source and most importantly contains the salt crystals that need to be extracted via a series of evaporation ponds that remove the water present in the brine (Javor, 2002). The nutrients present within the brine are of limited quantities. Hence, the number of microorganisms present within the salt evaporation ponds is controlled by nutrient availability (Javor, 2002). The problem arises when there is an addition of extra nutrients to the ponds through human activities and errors made by the people involved in the salt production process (Javor, 2002). These extra nutrients allow for increased growth of the microorganisms present within the salt evaporation ponds which could have a detrimental effect on the salt production process.

1.4.6 *Other abiotoc environmental factors*

The environmental factors present within the area where the salt evaporation ponds are situated also influence the salt production process (Takekawa *et al*., 2015). The temperature, salinity and changes in wind direction and intensity also have an impact on the salt production process (Takekawa *et al*., 2015). These factors add to the increase in nutrients within the ponds as well as to the change in various dynamics within the ponds that result in an increase in the growth of microorganisms (Javor, 2002). The changes in salinity generally occur during the rainy season which dilutes the salt evaporation ponds, causing a general increase in the number of microorganisms found within the ponds (Javor, 2002). The increase or decrease in temperature causes an increase in the number of microorganisms within the pond due to the creation of favourable conditions for growth such as the correct temperature rane for particular species of microorganisms to reproduce within the salt evaporation ponds (Silva *et al*., 2017). The changes in wind intensity allow for nutrients to flow throughout the salt evaporation ponds due to the fact that this allows for the mixing of the waters from the different ponds and also stirs up the nutrients settled at the bottom of the ponds, thus allowing for the microorganisms within the salt evaporation ponds to have sufficient amounts of nutrients available for rapid growth. The increase in wind intensity and direction also changes the salinities within the salt evaporation ponds (Silva *et al*., 2017).

1.4.7 *The effect of microorganisms on the salt production process*

The presence of microorganisms in brine evaporation ponds has both a positive and negative effect on the process of salt production (Javor, 2002). Organisms such as the bacteria that form part of the microbial mat at the bottom of the salt evaporation pond help in the process of salt production by creating a barrier at the bottom of the evaporation pond that prevents the seepage of the salt from the ponds and allows quality salt to be produced. Whilst organisms such as *D. salina* have a negative effect on the salt produced when present in increased numbers (Javor, 2002). The process of salt production requires a balance of the number of microorganisms present in the evaporation pond to allow for the optimum amount of salt to be produced (Oren, 2005). The presence of *D. salina* in the salt evaporation ponds in controlled numbers is beneficial as it allows for rapid evaporation of the water to produce salt at a faster rate (Bardavid *et al*., 2008). This is due to the presence of beta carotene in the cells of *D. salina* which traps light, thus heating the water quicker (Javor, 2002). The presence of *D. salina* in salterns influence the quality of salt crystals produced, *D. salina* affects the amount of water present inside salt crystals, thus causing a change in the morphology of salt crystals (Giordano *et al*., 2014). *D. salina* affects the salt purity by becoming a carbon coating on the salt crystals that decreases the purity of the crystals and also increases the water concentration within the crystals (Giordano *et al*., 2014). Thus, the presence of microorganisms in salterns needs to be controlled.

1.4.8 *Environmental Control*

Another method for the control of the microorganisms within the salt evaporation ponds is through manual techniques (Javor, 2002). These manual techniques include the curbing of human error such as the use of damaged equipment that leaks carbon into the ponds that allows for the increase in certain nutrients within the salt evaporation ponds (Javor, 2002). Machinery that is used in the production of salt should be serviced regularly as the oil that leaks from these machineries provide a source of carbon for the microorganisms living within the salt evaporation ponds. This causes an increase in the number of microorganisms present within the salt evaporation ponds (Javor, 2002). Another

environmental cause of increased total organic carbon that can be controlled is the wind which increases turbidity and mixing of the different salinities, allowing for an increase in microbial growth (Oren, 2012). This can be controlled by placing pikes that control the flow of water, thus preventing mixing in windy weather (Oren, 2012). The manual control of total organic carbon has been well investigated. However, the research conducted will focus on the cause of increased microorganisms and the growth and adaptation of *D. salina* the primary producer in various environments.

CHAPTER 2: ANALYSIS OF BIODIVERSITY AND NUTRIENT AVAILABILITY WITHIN SALT EVAPORATION PONDS

2.1 Abstract

Biodiversity describes the different species that inhabit an environment. These species live as symbionts and contribute to ecosystem functionalities. The biodiversity within saline environments has always been of interest. The reason is that the high salinity requires certain adaptations for survival within this extreme environment. The biodiversity of the salt evaporation ponds at Botash were investigated. This investigation was performed by the sequencing of the DNA found within three ponds at the Botash site. The nutrient levels within these ponds were also investigated. The results found that most organisms found within these ponds belong to the Archaea and Bacteria Domains of life. The Eukaryotes were represented by the green algae *Dunaliella salina* which was also the dominant species found within the salt evaporation ponds. The high levels of microbes was linked to the presence of high levels of nutrients as presented by the nutrient analysis of the Botash ponds. These results prove the fact that there is biodiversity within even the harshest environments on Earth as long as there is a supply of energy and nutrients.

2.2 Introduction

The biodiversity of salt evaporation ponds shows the vast number of microbes that exist in this world. It depicts this through the various microbes from the different domains of life that grow and interact within the ponds as symbionts (de Melo Soares *et al*., 2018). It also indicates the variety of microorganisms that are able to withstand the harsh environments within salt evaporation ponds and the efficiency of salt evaporation ponds as an environment for the growth of organisms (Oren, 2007).

The organisms from all domains of life that are generally found within salt evaporation ponds are adapted to living in highly saline environments. This information is of

importance as it enables a better understanding of the evolutionary links between the different branches of the tree of life. It also provides information about how diverse each branch of the tree of life is (Casamayor *et al*., 2013). The most efficient method of identifying inhabitants within an environment is genetic sequencing (Zhan *et al*., 2014).

Genetic sequencing is a comparative method which determines the range of different species present within an environment by a genetic compositions' analysis of those species (Madeira *et al*., 2019). This process results in the identification of the 'branch of the tree of life' that the organism originates from (Haile *et al*., 2017). In addition, this tool facilitates the proper classification of an organism as it enables the determination of the characteristics of the organism by comparison to organisms from the same species (Waterman, 2018). This enables a better understanding of the capabilities of the organism to survive in harsh environments such as highly saline ones (Díaz-Cárdenas *et al*., 2017). Genome sequencing also enables us to determine the genes that are used for protein coding and what proteins are produced from these genes (Jeddi *et al*., 2018). This is of importance as the proteins produced by certain organisms are of importance to humans since these proteins are utilised by industry to produce certain products that are beneficial to human health (Zolfaghar *et al*., 2019). The genome sequencing is a complex process that involves multiple steps such as isolation and extraction of DNA (Yaish *et al*., 2016). Technological advancements have permitted for a sample to be taken directly from the environment and used for genetic sequencing of the organisms found within that environment (Yaish *et al*., 2016). Thus, the sequencing of the organisms found within salt evaporation ponds was made possible because the sample obtained could be directly analysed to determine the organisms present within the sample.

Nutrient availability is one of the many factors that contribute to the biodiversity within a certain environment (Kavvadias *et al*., 2017). The main nutrients**,** i.e. nitrogen, phosphorus and potassium that are required for growth need to be present in high quantities to enable growth of organisms within an environment (de Melo Soares *et al*., 2018). The availability of nutrients within environments depend on environmental factors such as soil, wind, sunlight, water movement, decay of organic matter which allow the addition or removal of nutrients from an environment (Topping *et al*., 2016). Human activity also influences the level of nutrients within an environment, activities such as farming and the use of heavy machinery can affect the nutrient levels within environments

(Topping *et al*., 2016). Farming causes an increase in nutrients within environments such as river systems. This is because of the wash-off of fertilizers which result in an increase in algae and invasive plant growth in river systems due to the presence of high levels of nutrients from the fertilizer wash-off (Wurtsbaugh *et al*., 2019). Heavy machinery causes an increase in nutrient levels, particularly in salt evaporation ponds. This is because a lot of heavy machinery is present at salt evaporation ponds for the harvesting of the products produced (Javor, 2002). Heavy machinery generally require oil to function properly and possible oil leakage into the salt ponds causes an increase in carbon levels. As a result, more organisms were seen to thrive within the ponds (Javor, 2002). Thus, the presence of nutrients is of importance and correlates to the growth and biodiversity of species found within environments.

Therefore, it can be concluded that biodiversity and nutrient availability are both linked because without nutrients an organism cannot live or reproduce in the environment. Hence, the nutrient availability and biodiversity within salt evaporation ponds will be reviewed in this chapter. The relationship between the number of microorganisms present and the nutrients available within an environment is of importance as this relationship determines the health of the environment. The relationship maintained between microorganisms and nutrient availability for salt evaporation ponds will be determined as this will enable the better understanding of the dynamics within the salt evaporation ponds.

2.3 Aims and Objectives

The study aims to identify various organisms that reside within the salt evaporation ponds and the effect that nutrient availability has on these populations as mentioned in objectives 1 and 5 for this research thesis.

Objectives

1. To identify the various species that reside within the salt evaporation ponds
2. To identify the link between nutrient availability and species richness

2.4 Methods and Materials

2.4.1 *Sampling*

Samples were obtained from three ponds in the Botash salt evaporation system from the ponds marked with arrows:

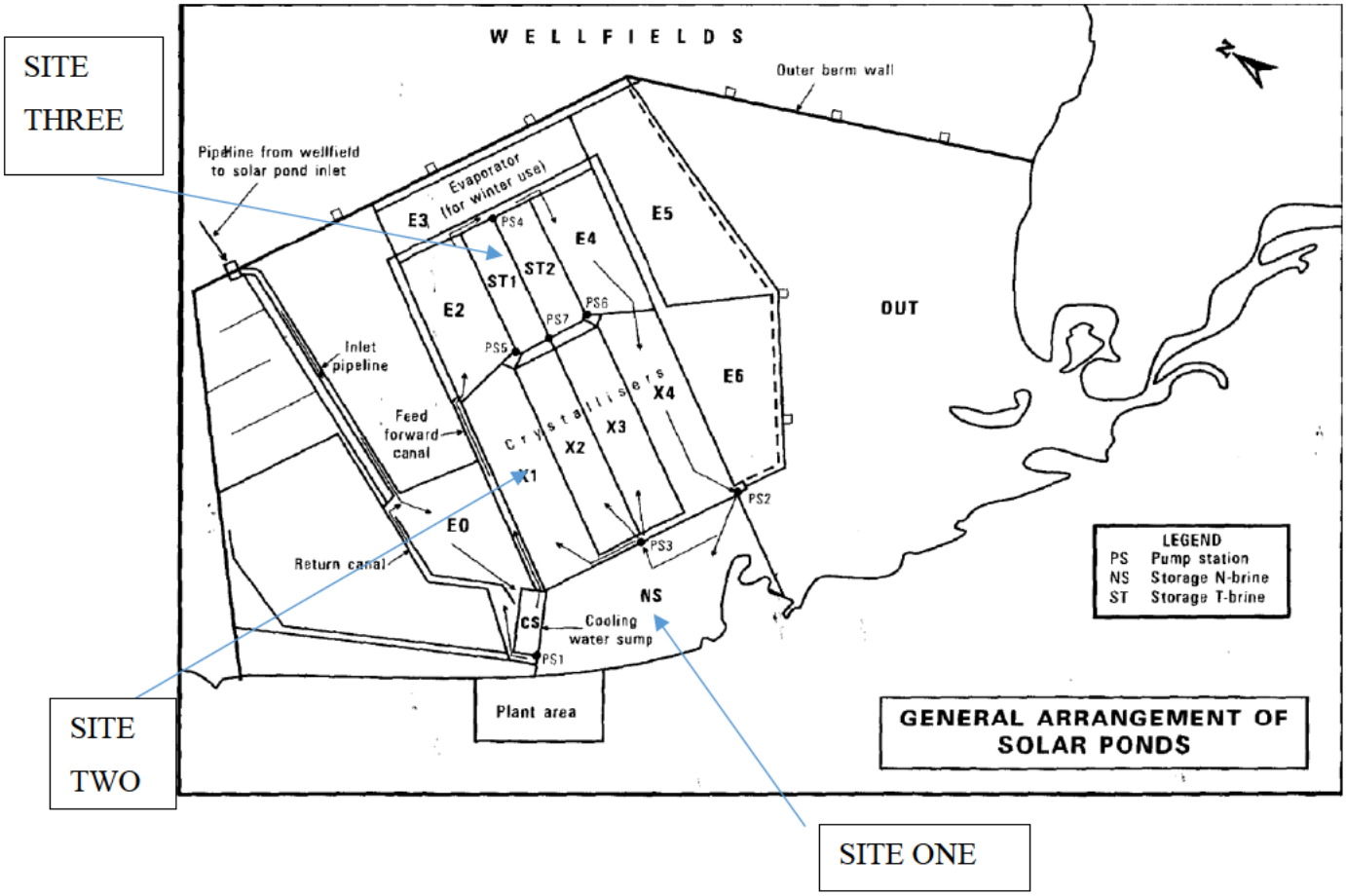

Figure 2.1: Map of Botash Wellfield. Courtesy: Botswana Ash (Pty) Ltd.

These sites where chosen as they represent the areas where brine is stored for long periods of time. The NS Pond is where the natural brine (N-Brine) is stored. The ST Pond is where the transfer brine (T-Brine) is stored and the crystalliser ponds is where the final stage of the salt production process occurs. The samples were obtained from Botash in 500 ml plastic bottles (one bottle per site) as these samples were freighted from Botswana. The samples were then divided into triplicates which were used for the genetic analysis.

2.4.2 *DNA Extraction*

The brine solution triplicate samples from each pond were centrifuged down at 16 000 x g. The phenol-chloroform DNA extraction protocol was used as this protocol is general and will extract DNA from all the microorganisms present. The phenol-chloroform mixture was added to the samples in the V:V ratio. The samples were shaken by hand for twenty seconds. The samples were then centrifuged for five minutes at 16000 x g. The upper aqueous layer was transferred to a fresh tube for ethanol precipitation. Ethanol precipitation was carried out using 1 µl glycogen, 100 ml NH_4OAc and 750 ml 100% ethanol which were added to the samples and kept at -80ºC for one hour. The samples were then centrifuged at -4ºC for 30 minutes at 16000 xg to obtain the DNA pellet. The pellet was then washed three times with 70% ethanol. The pellet was air dryed at room temperature for 5 -10 minutes. The DNA pellet was resuspended in buffer solution and placed on ice.

2.4.3 *PCR Amplification*

The triplicate DNA samples were then amplified using PCR. The samples were amplified by the addition of primers specific to each set of microbes that were possibly present within the samples. These primers hailed from the three domains of life i.e. eukaryotes, bacteria, and archaea.

The following primers were added to the samples for PCR:

Table 2.1: The primers used for analysis of biodiversity.

Primer identification	Target region	Specific Sequence	Reference or source
(FreshH_2O)FWD1	V4 (18S RNA)		41[a,b]
(FreshH_2O)REV1	V4 (18S RNA)	ACTTTCGTTCTTGAT	This study[b]
(Saline)FWD1	V8 (18S RNA)	ATAACAGGTCTGTGATGCCCT	This study[b]
(Saline)REV1	V9 (18S RNA)		23
Bacteria(E786F)	V8	GATTAGATACCCTGGTAG	22
Bacteria (E939R)	V9	CTTGTGCGGGCCCCCGTCAATTC	7[b]
Archaea(Eb787F)		ATTAGATACCCTGGTA	
Archaea(A934R)		GTGCTCCCCCGCCAATTCCT	

The above primers were used to amplify the samples from Botash. Freshwater primers were added as a control to determine the efficiency of the test. The primers added were specific to different groups of organisms and targeted the ribosomal RNA within the microbes as Ribosomal RNA generally displays minimal change between species. Thus,

18S RNA was used as a primer for eukaryotes whilst 16S RNA was used for Archaea and Bacteria.

The PCR reaction for all samples contained 2µl DNA, 12.5µl TopTaq Master mix, 0.5µl of each primer (forward and reverse), 10µl of distilled water, making up a reaction volume of 25µl. The PCR was performed in a thermocycler (BIORAD) under the following conditions for the primers added: 5minutes initial denaturation step at 95°C, followed by 40 cycles of 1 minute denaturation at 95°C, 1 minute annealing at 55°C and 1 minute polymerization at 72°C, and the program ended with a final polymerization step for 7 minutes at 72°C.

2.4.4 *Sequencing*

The samples were then sent to Inqaba Biotech for genetic sequencing. was performed using the Illumina sequencer. The DNA fragments were sequenced in the forward and reverse directions using the primers from the PCR Amplification.

2.4.5 *Data Analysis*

Once the sequences were obtained, the data was trimmed. Sequences of inferior quality were removed from the results obtained through trimming of the sequences. The trimmed results were then blasted against the NCBI database to acquire the species and genus names of evaluated sequences. All sequences were then blasted and the resulting number of organisms per a species was recorded. These results were then run through the MG RAST program to obtain a graphical interpretation of the results. The MG RAST program analysed the results obtained from the NCBI BLAST and sequencing in order to determine the groups of organisms most abundantly found within the salt evaporation ponds.

2.4.6 *Chemical Composition analysis*

The chemical composition of the salt evaporation ponds was analysed in order to determine the amount of different nutrients that are required for the growth of microorganisms' present within the ponds. This analysis was carried out at the laboratory in Botash using various tests that are specific for the analysis of nutrients. The analysis used to determine the various nutrients were nutrient specific i.e. each test was designed to test for a compound within the pond samples. The test for nitrogen was nitrogen specific and would not identify phosphorus, for example.

2.4.7 *Statistical Analysis*

The Pearson Correlation Coefficient test will be used to determine the correlation between the nutrient availability in the form of NO_3 availability and the microbial alpha diversity within the pond. The correlation will be regarded significant at $p<0,05$.

2.5 Results

The following results were obtained from the above analysis performed. The results were obtained in graphical and table forms.

Table 2.2: Chemical Composition of Botash Salt Evaporation Ponds.

Analyte Symbol	Unit Symbol	NS POND		CRYSTALLIZER POND	
		3m depth	18 m depth	6 m depth	20 m depth
pH	pH	10 ± 0,001	8,3 ± 0,001	9,5 ± 0,001	9,8 ± 0,001
Na	mg/L	21100 ± 14869,96	70,7 ± 14869,96	84600 ± 31395,54	40200 ± 31395,54
K	mg/L	1170 ± 821,7712	7,84 ± 821,7712	4290 ± 1704,127	1880 ± 1704,127
Mg	mg/L	0,228 ± 0,574171	1,04 ± 0,574171	0,276 ± 0,09051	0,148 ± 0,09051
Ca	mg/L	***5* ± 2,262742**	8,2 ± 2,262742	***35* ± 10,6066**	***20* ± 10,6066**
F	mg/L	***2* ± 1,403607**	***0,015* ± 1,403607**	***15* ± 8,838835**	***2,5* ± 8,838835**
Cl	mg/L	28200 ± 19864,04	108 ± 19864,04	96400 ± 36274,58	45100 ± 36274,58
NO2 as NO2	mg/L	***6,58* ± 4,617867**	***0,04935* ± 4,617867**	***49,35* ± 29,07977**	***8,225* ± 29,07977**
Br	mg/L	56,9 ± 40,20256	***0,045* ± 40,20256**	***35* ± 34,93107**	84,4 ± 34,93107
NO3 as NO3	mg/L	***8,86* ± 4,917998**	***1,9049* ± 4,917998**	***66,45* ± 39,15604**	***11,075* ± 39,15604**
PO4 as PO4	mg/L	***12,28* ± 8,618147**	***0,0921* ± 8,618147**	***76,75* ± 43,41636**	***15,35* ± 43,41636**
SO4	mg/L	2620 ± 1847,465	7,29 ± 1847,465	8470 ± 3712,311	3220 ± 3712,311
Alk.	mg/L CaCO3	11300 ± 0,001	80 ± 0,001	41300 ± 0,001	16100 ± 0,001
$CO3^{(2-)}$	mg/L CaCO3	5642,236 ± 0,001	1,1992 ± 0,001	20866,08 ± 0,001	7974,68 ± 0,001
$HCO3^{(-)}$	mg/L CaCO3	1072,896 ± 0,001	47,5488 ± 0,001	3639,312 ± 0,001	1572,768 ± 0,001
$OH^{(-)}$	mg/L CaCO3	***0,5* ± 0,001**	***0,5* ± 0,001**	***0,5* ± 0,001**	***0,5* ± 0,001**
I	mg/L	***100* ± 70,00357**	***1* ± 70,00357**	***500* ± 247,4874**	***150* ± 247,4874**
Li	mg/L	***0,01* ± 0,001**	0,003 ± 0,001	***0,05* ± 0,001**	***0,025* ± 0,001**
Be	mg/L	***0,001* ± 0,001**	***0,0001* ± 0,001**	***0,005* ± 0,001**	***0,0025* ± 0,001**

Al	mg/L	0,587 ± 0,001	0,213 ± 0,001	0,923 ± 0,001	0,109 ± 0,001
Si	mg/L	13,2 ± 5,656854	21,2 ± 5,656854	***10* ± 29,34493**	51,5 ± 29,34493
Sc	mg/L	***0,01* ± 0,001**	0,005 ± 0,001	***0,05* ± 0,001**	***0,025* ± 0,001**
Ti	mg/L	0,0078 ± 0,001	0,0122 ± 0,001	0,11 ± 0,001	0,0292 ± 0,001
Mn	mg/L	***0,001* ± 0,001**	0,0078 ± 0,001	***0,005* ± 0,001**	***0,0025* ± 0,001**
Fe	mg/L	***0,1* ± 0,001**	0,24 ± 0,001	***0,5* ± 0,001**	***0,25* ± 0,001**
Co	mg/L	0,0003 ± 0,001	0,000162 ± 0,001	0,0018 ± 0,001	0,00085 ± 0,001
Ni	mg/L	0,0279 ± 0,001	0,0043 ± 0,001	0,229 ± 0,001	0,129 ± 0,001
Cu	mg/L	***0,002* ± 0,001**	0,0012 ± 0,001	***0,01* ± 0,001**	***0,005* ± 0,001**
Zn	mg/L	0,0178 ± 0,001	0,0054 ± 0,001	***0,025* ± 0,001**	***0,015* ± 0,001**
Ga	mg/L	***0,0001* ± 0,001**	0,00008 ± 0,001	***0,0005* ± 0,001**	***0,00025* ± 0,001**
Ge	mg/L	0,0002 ± 0,001	0,00003 ± 0,001	0,0011 ± 0,001	0,0007 ± 0,001
As	mg/L	***0,0003* ± 0,001**	***0,00003* ± 0,001**	***0,0015* ± 0,001**	0,0586 ± 0,001
Se	mg/L	***0,002* ± 0,001**	0,0007 ± 0,001	***0,01* ± 0,001**	0,0155 ± 0,001
Rb	mg/L	0,276 ± 0,001	0,0189 ± 0,001	2,01 ± 0,001	1,11 ± 0,001
Sr	mg/L	0,0766 ± 0,001	0,0943 ± 0,001	0,16 ± 0,001	0,144 ± 0,001
Y	mg/L	0,0181 ± 0,001	0,00022 ± 0,001	0,0125 ± 0,001	0,00125 ± 0,001
Zr	mg/L	0,00232 ± 0,001	0,00006 ± 0,001	***0,0005* ± 0,001**	***0,00025* ± 0,001**
Nb	mg/L	***0,00005*** ± 0,001	0,000016± 0,001	***0,00025*** ± 0,001	***0,00015*** ± 0,001
Mo	mg/L	0,0714 ± 0,001	0,0015± 0,001	0,229± 0,001	0,122± 0,001
Ag	mg/L	***0,002*** ± 0,001	***0,0002*** ± 0,001	0,0258± 0,001	***0,005*** ± 0,001
Cd	mg/L	***0,0001*** ± 0,001	0,00004 ± 0,001	0,00258± 0,001	0,00071± 0,001
In	mg/L	0,00004± 0,001	***0,000001*** ± 0,001	***0,00005*** ± 0,001	***0,000025*** ± 0,001
Sn	mg/L	***0,001*** ± 0,001	***0,0001*** ± 0,001	***0,005*** ± 0,001	***0,0025*** ± 0,001
Sb	mg/L	0,00696± 0,001	0,00018± 0,001	0,0088± 0,001	0,00205± 0,001
Te	mg/L	***0,001*** ± 0,001	***0,0001*** ± 0,001	***0,005*** ± 0,001	***0,0025*** ± 0,001
Cs	mg/L	0,00012± 0,001	0,000034± 0,001	0,0026± 0,001	0,00075± 0,001
Ba	mg/L	0,114± 0,001	0,022± 0,001	0,102± 0,001	0,12± 0,001
La	mg/L	***0,00001*** ± 0,001	0,00015± 0,001	***0,00005*** ± 0,001	***0,000025*** ± 0,001
Ce	mg/L	0,00014± 0,001	0,000306± 0,001	0,0003± 0,001	***0,000025*** ± 0,001
Pr	mg/L	***0,00001*** ± 0,001	0,00005± 0,001	0,0002± 0,001	***0,000025*** ± 0,001

Nd	mg/L	0,00006± 0,001	0,000196± 0,001	0,0013± 0,001	***0,000025***± 0,001
Sm	mg/L	0,00004± 0,001	0,000042± 0,001	0,0005± 0,001	***0,000025***± 0,001
Eu	mg/L	***0,00001***± 0,001	0,00001± 0,001	0,0002± 0,001	***0,000025***± 0,001
Gd	mg/L	0,00006± 0,001	0,000036± 0,001	0,0006± 0,001	***0,000025***± 0,001
Tb	mg/L	***0,00001***± 0,001	0,000006± 0,001	0,0001± 0,001	***0,000025***± 0,001
Dy	mg/L	0,00006± 0,001	0,000036± 0,001	0,0011± 0,001	0,0001± 0,001
Ho	mg/L	***0,00001***± 0,001	0,000008± 0,001	0,0003± 0,001	***0,000025***± 0,001
Er	mg/L	0,00008± 0,001	0,000024± 0,001	0,0014± 0,001	0,0001± 0,001
Tm	mg/L	***0,00001***± 0,001	0,000004± 0,001	0,0002± 0,001	***0,000025***± 0,001
Yb	mg/L	0,00008± 0,001	0,000028± 0,001	0,002± 0,001	0,00015± 0,001
Lu	mg/L	***0,00001***± 0,001	0,000006± 0,001	0,0003± 0,001	***0,000025***± 0,001
Hf	mg/L	0,00006± 0,001	0,000002± 0,001	***0,00005***± 0,001	***0,000025***± 0,001
Hg	mg/L	***0,002***± 0,001	***0,0002***± 0,001	***0,01***± 0,001	***0,005***± 0,001
W	mg/L	0,014± 0,001	0,00068± 0,001	0,099± 0,001	0,0435± 0,001
Tl	mg/L	***0,00001***± 0,001	0,000006± 0,001	***0,00005***± 0,001	***0,000025***± 0,001
Pb	mg/L	0,00068± 0,001	0,00508± 0,001	***0,0005***± 0,001	0,00265± 0,001
Bi	mg/L	***0,003***± 0,001	***0,0003***± 0,001	***0,015***± 0,001	***0,01***± 0,001
Th	mg/L	0,00292± 0,001	0,000074± 0,001	0,0318± 0,001	0,00345± 0,001
U	mg/L	0,121± 0,001	0,003± 0,001	0,428± 0,001	0,544± 0,001

The above table gives the chemical composition of the two ponds that were sampled for the genomic analysis. The table depicts a wide variety of different chemical elements. These compounds are available within the ponds in different concentrations. The most abundant element is Sodium.

The results obtained for the analysis of the sequences are as follows:

Results for the 18S analysis of the NS Pond

Taxonomic Hits Distribution

The charts below represent the distribution of taxa using a contigLCA algorithm finding a single consensus taxonomic entity for all features on each individual sequence.

Genus

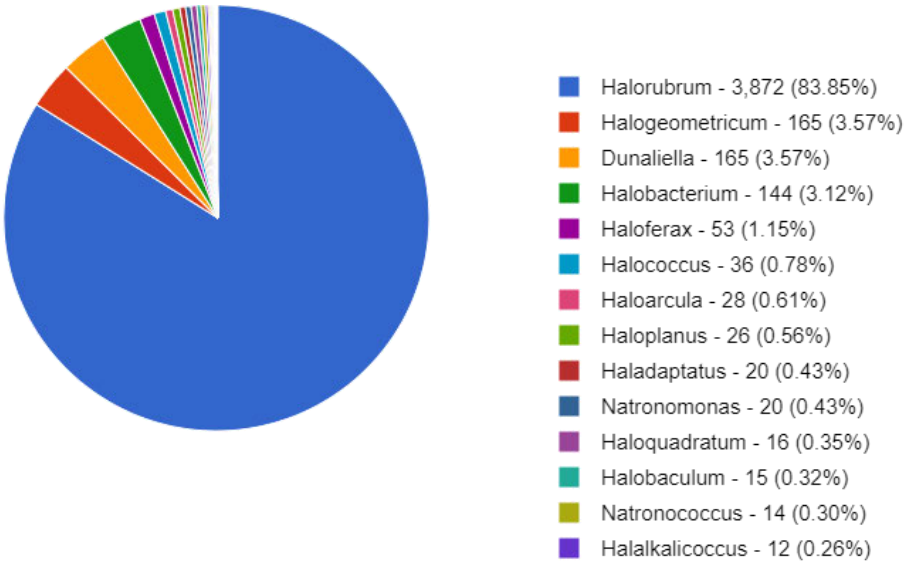

Figure 2.2: The Genus Distribution of the 18S Analysis of the NS Pond.

Alpha Diversity

The α-diversity of this data set is 21 species.

Figure 2.3: The alpha diversity of the 18S Analysis of the NS Pond.

The above image shows the range of α-diversity values in the study 'Botash'. The min, max, and mean values are shown with the standard deviation ranges (σ and 2σ) in different shades. The α-diversity of this metagenome is shown in red.

Alpha diversity summarizes the diversity of organisms in a sample with a single number. The α-diversity of annotated samples can be estimated from the distribution of the species-level annotations.

Annotated species richness is the number of distinct species annotations in the combined MG-RAST data set. Shannon diversity is an abundance-weighted average of the logarithm of the relative abundances of annotated species. The species-level annotations are from all the annotation source databases used by MG-RAST.

Results for the 18S analysis of the WI Pond

Taxonomic Hits Distribution

The charts below represent the distribution of taxa using a contigLCA algorithm finding a single consensus taxonomic entity for all features on each individual sequence.

Genus

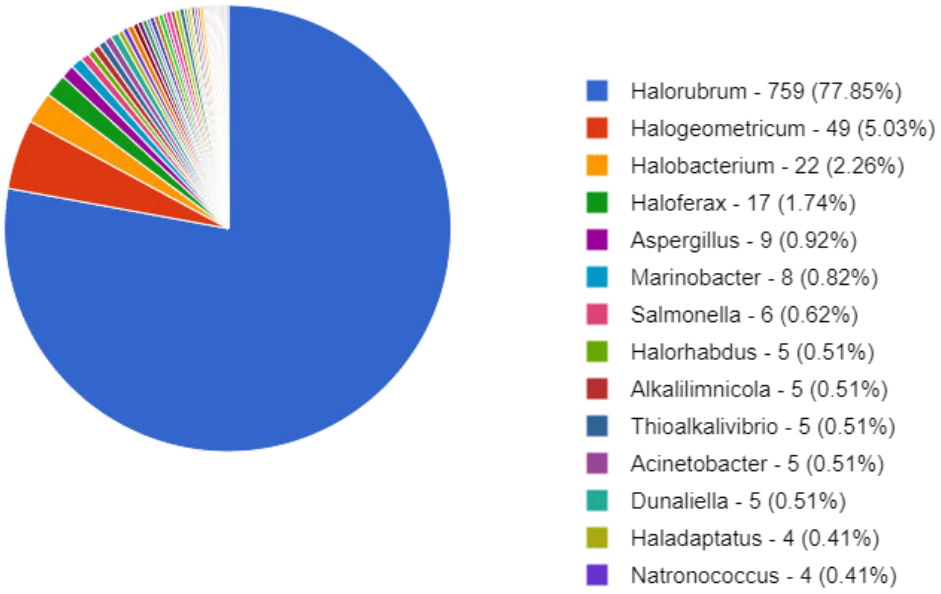

Figure 2.4: The Genus Distribution of the 18S Analysis of the WI Pond.

Alpha Diversity

The α-diversity of this data set is 39 species.

Figure 2.5: The Alpha Diversity for the 18S Analysis of the WI Pond.

The above image shows the range of α-diversity values in the study 'Botash'. The min, max, and mean values are shown with the standard deviation ranges (σ and 2σ) in different shades. The α-diversity of this metagenome is shown in red.

Alpha diversity summarizes the diversity of organisms in a sample with a single number. The α-diversity of annotated samples can be estimated from the distribution of the species-level annotations.

Annotated species richness is the number of distinct species annotations in the combined MG-RAST data set. Shannon diversity is an abundance-weighted average of the logarithm of the relative abundances of annotated species. The species-level annotations are from all the annotation source databases used by MG-RAST.

Results for the 18S Analysis of the ST Pond

Taxonomic Hits Distribution

The charts below represent the distribution of taxa using a contigLCA algorithm finding a single consensus taxonomic entity for all features on each individual sequence.

Genus

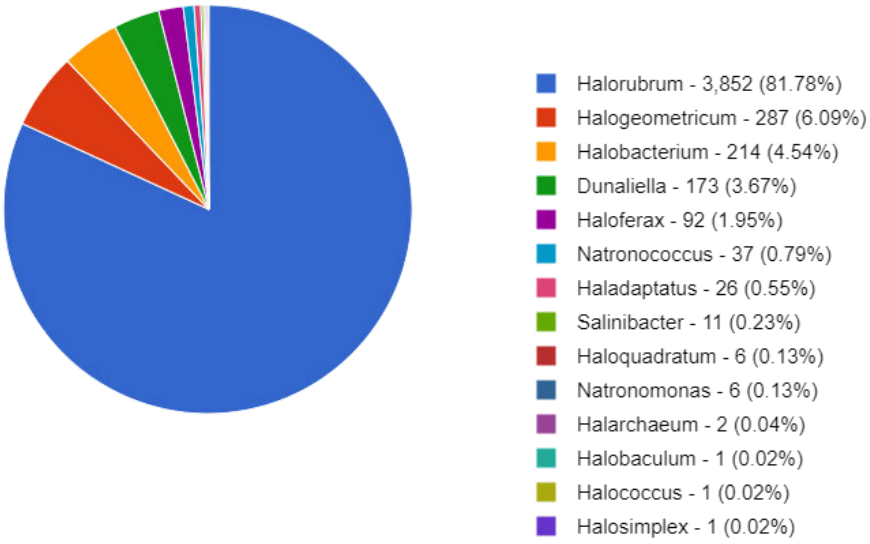

Figure 2.6: The Genus Distribution of the 18S Analysis for the ST Pond.

Alpha Diversity

The α-diversity of this data set is 15 species.

Figure 2.7: The Alpha Diversity of the 18S Analysis for the ST Pond.

The above image shows the range of α-diversity values in the study 'Botash'. The min, max, and mean values are shown with the standard deviation ranges (σ and 2σ) in different shades. The α-diversity of this metagenome is shown in red.

Alpha diversity summarizes the diversity of organisms in a sample with a single number. The α-diversity of annotated samples can be estimated from the distribution of the species-level annotations.

Annotated species richness is the number of distinct species annotations in the combined MG-RAST data set. Shannon diversity is an abundance-weighted average of the logarithm of the relative abundances of annotated species. The species-level annotations are from all the annotation source databases used by MG-RAST.

Results of the 16S Analysis of the NS Pond

Taxonomic Hits Distribution

The charts below represent the distribution of taxa using a contigLCA algorithm finding a single consensus taxonomic entity for all features on each individual sequence.

Genus

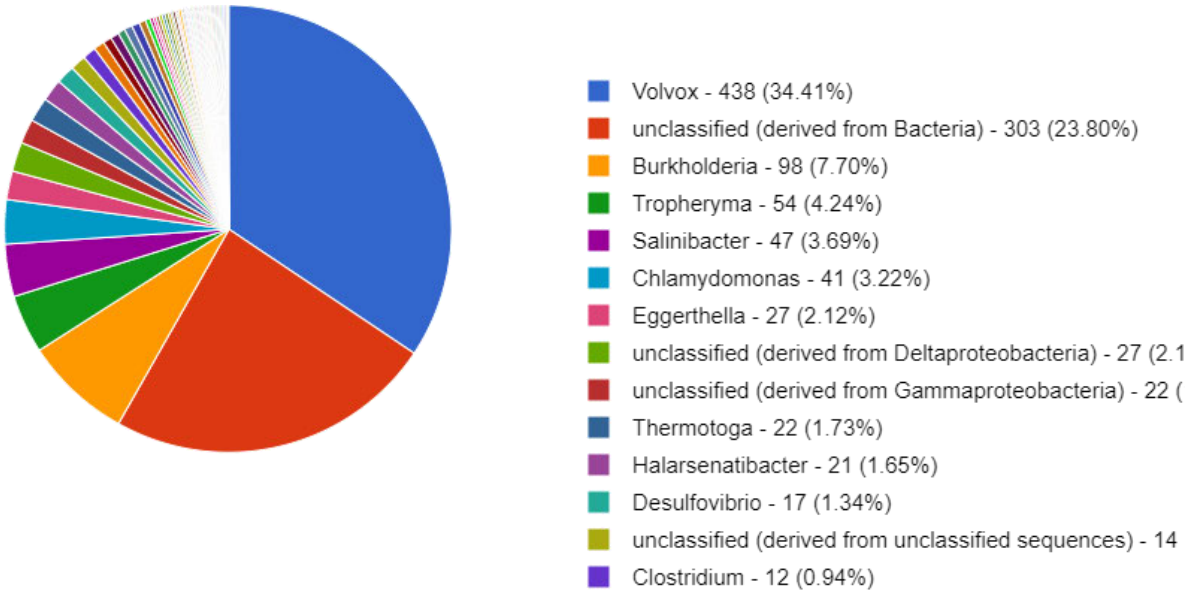

Figure 2.8: The Genus Distribution of the 16S Analysis for the NS Pond.

Alpha Diversity

The α-diversity of this data set is 10 species.

Figure 2.9: The Alpha Diversity of the 16S Analysis for the NS Pond.

The above image shows the range of α-diversity values in the study 'Botash'. The min, max, and mean values are shown with the standard deviation ranges (σ and 2σ) in different shades. The α-diversity of this metagenome is shown in red.

Alpha diversity summarizes the diversity of organisms in a sample with a single number. The α-diversity of annotated samples can be estimated from the distribution of the species-level annotations.

Annotated species richness is the number of distinct species annotations in the combined MG-RAST data set. Shannon diversity is an abundance-weighted average of the

logarithm of the relative abundances of annotated species. The species-level annotations are from all the annotation source databases used by MG-RAST.

Results of the 16S Analysis of the WI Pond.

Taxonomic Hits Distribution

The charts below represent the distribution of taxa using a contigLCA algorithm finding a single consensus taxonomic entity for all features on each individual sequence.

Genus

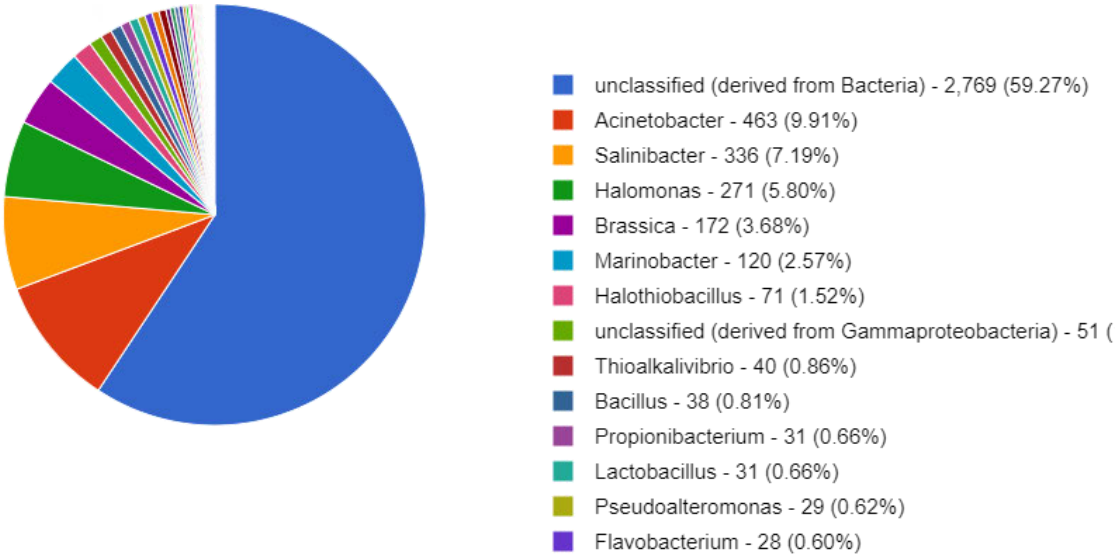

Figure 2.10: The Genus Distribution of the 16S Analysis for the WI Pond.

Alpha Diversity

The α-diversity of this data set is 16 species.

Figure 2.11:The Alpha Diversity of the 16S Analysis for the WI Pond.

The above image shows the range of α-diversity values in the study 'Botash'. The min, max and mean values are shown with the standard deviation ranges (σ and 2σ) in different shades. The α-diversity of this metagenome is shown in red.

Alpha diversity summarizes the diversity of organisms in a sample with a single number. The α-diversity of annotated samples can be estimated from the distribution of the species-level annotations.

Annotated species richness is the number of distinct species annotations in the combined MG-RAST data set. Shannon diversity is an abundance-weighted average of the logarithm of the relative abundances of annotated species. The species-level annotations are from all the annotation source databases used by MG-RAST.

Results of the 16S Analysis of the ST Pond.

Taxonomic Hits Distribution

The charts below represent the distribution of taxa using a contigLCA algorithm finding a single consensus taxonomic entity for all features on each individual sequence.

Genus

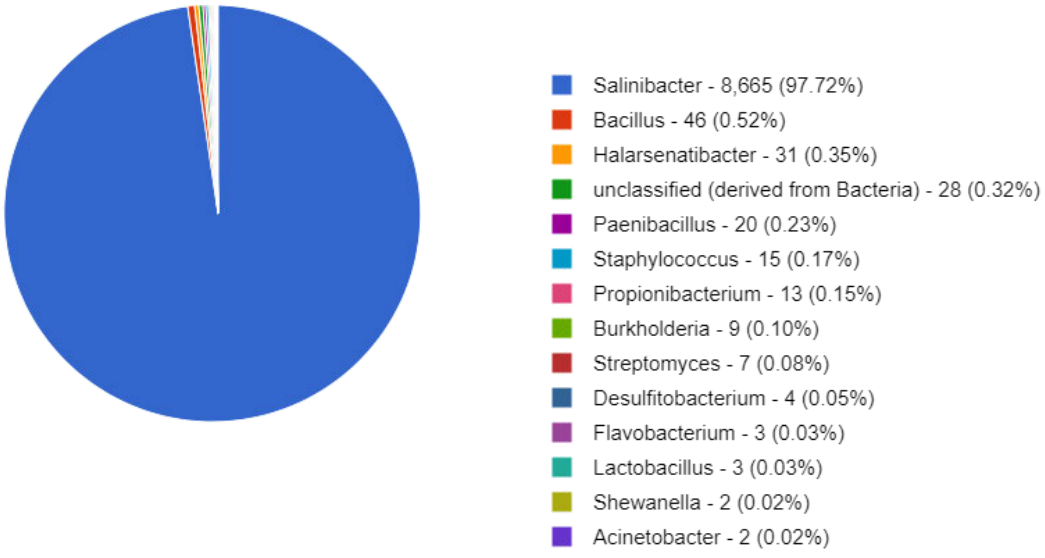

Figure 2.12: The Genus Distribution of the 16S Analysis for the ST Pond.

Alpha Diversity

The α-diversity of this data set is 5 species.

Figure 2.13:The Alpha Diversity of the 16S Analysis for the ST Pond.

The above image shows the range of α-diversity values in the study 'Botash'. The min, max, and mean values are shown with the standard deviation ranges (σ and 2σ) in different shades. The α-diversity of this metagenome is shown in red.

Alpha diversity summarizes the diversity of organisms in a sample with a single number. The α-diversity of annotated samples can be estimated from the distribution of the species-level annotations.

Annotated species richness is the number of distinct species annotations in the combined MG-RAST data set. Shannon diversity is an abundance-weighted average of the logarithm of the relative abundances of annotated species. The species-level annotations are from all the annotation source databases used by MG-RAST.

The pearson correlation coefficient between NO_3 availability and alpha diversity is 0, 8403637 which shows a positive relationship between NO_3 availability and alpha diversity. The p-value for the pearson correlation test is 0, 03619 which is less than $p<0,05$ thus these results are significant.

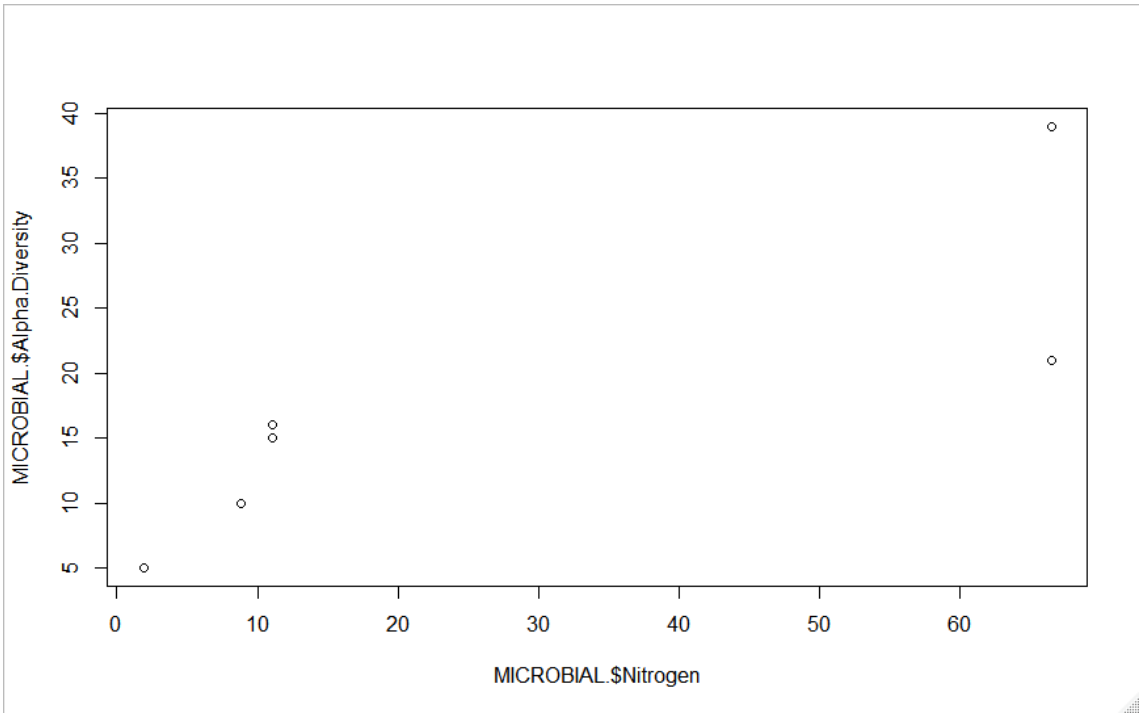

Figure 2.14: The scatter plot depicting the relationship between nitrogen availability and alpha diversity.

Figure 2.14 depicts the relationship between nitrogen availability and alpha diversity of the species found within the salt evaporation ponds. The relationship is clear the higher the nitrogen availability the more diverse the microbial community.

2.6 Discussion

The nutrient levels within the salt evaporation ponds at Botash are generally similar to the nutrient levels within all salt evaporation ponds worldwide (Oren, 2009). The reason for the increase in nutrient levels within the crystallizer ponds afre generally attributed to the evaporation of water that concentrates the nutrients within the ponds (Oren, 2009). This allows for an abundance of different species to be present within the salt evaporation ponds. Nitrogen is present in high levels within salt evaporation ponds. The nitrogen levels are split into nitrite and nitrate and is present in relatively high amounts. The crystallizer pond has 49,35 mg/L of NO_2 and 66,45 mg/L of NO_3, respectively. The presence of nitrogen is fundamental as it a crucial nutrient involved in the growth of organisms such as algae, bacteria, and archaea, hence the notable increase in levels of organisms within the salt evaporation ponds (Griffin *et al*., 2019). The other important

nutrients for the growth of organisms are Potassium and Phosphorus. These elements are also required for the healthy growth and survival of organisms. These elements are also found in high concentrations within the salt evaporation ponds. The concentration of potassium within the crystallizer pond is 4290 mg/L and the concentration of phosphorus within the ST Pond is 76,75 mg/L. These three components are integral to the proper growth of all organisms and the results from the chemical composition of the salt evaporation pond depicts the availability of these components in high levels. Therefore, the diversity and density of the microbial population within the salt evaporation pond is dependent on the fact that there is a good supply of nutrients available for the growth of the microorganisms (Griffin *et al*., 2019). Another important factor to be noted about the chemical composition of the salt evaporation ponds is that there are various other macro and micronutrients present in reasonably high amounts that allow for the abundance of species found within the ponds (Daneshvar *et al*., 2018). The levels of the important macronutrients such as magnesium and calcium are in high enough quantities to allow for the growth of many organisms without competition. The presence of micronutrients such as manganese and iron also allow for the constant growth of the microorganisms as these micronutrients are required for proper growth although in lower concentrations than the macronutrients (Ghafari *et al*., 2018). Thus, the chemical composition of the salt evaporation ponds proves that these ponds indeed have the nutrients available at appropriate levels to allow for and sustain a diversity of different organisms to inhabit the salt evaporation ponds and form a complex ecosystem within these ponds.

The above results depict that there is immense diversity of organisms within the salt evaporation ponds (Fig. 2.2, 2.4, 2.6, 2.8, 2.10,2.12), this diversity can be directly related to nutrient availability within the salt evaporation ponds. The microbial diversity covers all the domains of life. The full breakdown of the diversity can be found in Appendix A.

The Genus distribution is the most important distribution as it describes the organisms within the salt evaporation ponds. The Genus distribution is the most concentrated hierarchy as only organisms that are similar can share the same Genus (Polle *et al*., 2019). The Genus distribution for the 16S analysis of the NS pond shows that the Genus Volvox is most prominent within these ponds. The Genus Salinibacter is also present although it is less prominent than Volvox. The Volvox Genus is a freshwater species of green algae that live in colonies of approximately 50 000 cells (Desnitskiy, 2018). The reason for a

freshwater alga genus such as Volvox being present in salt evaporation ponds could be due to the fact that these algae grow in rain water and the Botash Ponds do experience high rainfall in their rainy seasons, thus allowing for the growth of the green algae (Herron, 2016). The genus Salinibacter which is found in all three ponds in various concentrations is a species of bacteria that is extremely halophilic and originally identified in crystallizer ponds. These bacteria have an orange- red colour due to the novel carotenoid Salinixanthin (Oren, 2013). The WI pond had the majority unclassified bacteria. However, the second most prominent group of Bacteria was the Genus Acinetobacter. This genus is related to several human sicknesses (Zander *et al*., 2016). Thus, the genus results from the 16S analysis reveal that many species of bacteria can be found within saline environments, including disease causing bacteria.

The 18S analysis of the salt evaporation ponds displayed two very prominent Genus's, one Genus for Archaea and one Genus for Eukaryotes. The NS pond had a majority Archaea with the Genus Halorubrum being the most prevalent of the Archaea species. This Genus of Archaea is extremely Halophilic and is generally found in highly saline environments. This genus is generally red pink in colour due to the presence of the pigment bacteriorubin which is a carotenoid produced by this species (Sun *et al*., 2019). The Genus Halorubrum is present in abundance in all three ponds. The genus Dunaliella represents the eukaryotes within all three ponds. This genus is of interest to the pharmaceutical industry as it produces beta carotene which is a red pigment that is used to produce sun protection lotions (Valencia *et al*., 2018). The Dunaliella genus comprises single celled, motile and photosynthetic organisms that are adapted to live in highly saline environments (Polle *et al*., 2019).

The alpha diversity refers to the diversity of species found within an area of the larger ecosystem i.e. the sample. The alpha diversity basically is an indication of the species richness found within a region. The alpha diversity for the different analysis is different, showing that species diversity varies between the prokaryotes and eukaryotes. The alpha diversity is diverse across both the 18S and 16S analysis, showing that different species inhabit both ponds in different concentrations.

The pearson correlation showed that there is a strong relationship between the presence of nutrients and the microbial diversity witnessed within the salt evaporation pond. The

correlation coefficient was 0,8403637 which shows that as the nutrient availability inreases so does the diversity of microbes. The most abundance of microbes can be witnessed within the crystallizer ponds because of the concentration of nutrients within these ponds because of evaporation (Oren, 2009). This result shows that indeed the appropriate supply of nutrients does indeed lead to an increase in microbial diversity. The alpha diversity was the highest in the crystallizer ponds showing the effect that nutrients have on the establishment of microbial communities.

To conclude, the above results prove that the presence of appropriate nutrient levels does indeed affect the level of microbial communities that can inhabit an environment. The presence of nutrients is of vital importance to the sustenance of ecosystems. The nutrients present within the salt evaporation ponds are indeed at required concentrations to allow for the growth and maintenance of microbial communities as can be seen from the microbial diversity. The salt evaporation ponds at Botash play host to a wide array of organisms that hail from all three domains of life. This shows that microorganisms can indeed inhabit even the harshest of environments. The presence of organisms from the Genus *Dunaliella* shows that there is indeed a monetary benefit to having microorganisms present. However, the concentration of microorganisms needs to be lowered in order to maintain a balance between a fully functioning salt production facility and the ecosystems that exist within this facility.

2.7 References

Bacaro, G., Altobelli, A., Cameletti, M., Ciccarelli, D., Martellos, S., Palmer, M.W., Ricotta, C., Rocchini, D., Scheiner, S.M., Tordoni, E. and Chiarucci, A., 2016. Incorporating spatial autocorrelation in rarefaction methods: Implications for ecologists and conservation biologists. *Ecological indicators*, *69*, pp.233-238.

Bachran, M., Kluge, S., Lopez-Fernandez, M., & Cherkouk, A. (2019). Microbial diversity in an arid, naturally saline environment. *Microbial ecology*, *78*(2), 494-505.

Bascompte, J. (2019). Mutualism and biodiversity. *Current Biology*, *29*(11), R467-R470.

Bogaerts, B., Winand, R., Fu, Q., Van Braekel, J., Ceyssens, P. J., Mattheus, W., Bertrand, S.,

Bradley, I. M., Pinto, A. J., & Guest, J. S. (2016). Design and evaluation of Illumina MiSeq-compatible, 18S rRNA gene-specific primers for improved characterization of mixed phototrophic communities. *Appl. Environ. Microbiol.*, *82*(19), 5878-5891.

Casamayor, E. O., Triadó-Margarit, X., & Castañeda, C. (2013). Microbial biodiversity in saline shallow lakes of the Monegros Desert, Spain. *FEMS microbiology ecology*, *85*(3), 503-518.

Cherif, H., Neifar, M., Chouchane, H., Soussi, A., Hamdi, C., Guesmi, A., Fhoula, I., Najjari, A., Ferjani, R., Mahjoubi, M. and El Hidri, D., 2018. Extremophile diversity and biotechnological potential from desert environments and saline systems of southern Tunisia. In *Extremophiles* (pp. 33-64). CRC Press.

Daneshvar, E., Santhosh, C., Antikainen, E., & Bhatnagar, A. (2018). Microalgal growth and nitrate removal efficiency in different cultivation conditions: Effect of macro and micronutrients and salinity. *Journal of Environmental Chemical Engineering*, *6*(2), 1848-1854.

De Keersmaecker, S., Roosens, N., & Vanneste, K. (2019). Validation of a Bioinformatics Workflow for Routine Analysis of Whole-Genome Sequencing Data and Related Challenges for Pathogen Typing in a European National Reference

Center: *Neisseria meningitidis* as a Proof-of-Concept. *Frontiers in microbiology*, *10*, 362.

Desnitskiy, A. G. (2018). Comparative analysis of embryonic inversion in algae of the genus Volvox (Volvocales, Chlorophyta). *Russian Journal of Developmental Biology*, *49*(3), 129-133.

Díaz-Cárdenas, C., Cantillo, A., Rojas, L.Y., Sandoval, T., Fiorentino, S., Robles, J., Ramos, F.A., Zambrano, M.M. and Baena, S., 2017. Microbial diversity of saline environments: searching for cytotoxic activities. *AMB Express*, *7*(1), p.223.

Dubinkina, V. B., Ischenko, D. S., Ulyantsev, V. I., Tyakht, A. V., & Alexeev, D. G. (2016). Assessment of k-mer spectrum applicability for metagenomic dissimilarity analysis. *BMC bioinformatics*, *17*(1), 38.

Ghafari, M., Rashidi, B., & Haznedaroglu, B. Z. (2018). Effects of macro and micronutrients on neutral lipid accumulation in oleaginous microalgae. *Biofuels*, *9*(2), 147-156.

Griffin, J. E., Park, G., & Dam, H. G. (2019). Relative importance of nitrogen sources, algal alarm cues and grazer exposure to toxin production of the marine dinoflagellate Alexandrium catenella. *Harmful algae*, *84*, 181-187.

Haile, S., Pandoh, P., McDonald, H., Corbett, R.D., Tsao, P., Kirk, H., MacLeod, T., Jones, M., Bilobram, S., Brooks, D. and Smailus, D., 2017. Automated high throughput nucleic acid purification from formalin-fixed paraffin-embedded tissue samples for next-generation sequence analysis. *PloS one*, *12*(6), p.e0178706.

Herron, M. D. (2016). Origins of multicellular complexity: Volvox and the volvocine algae. *Molecular ecology*, *25*(6), 1213-1223.

Hugerth, L. W., & Andersson, A. F. (2017). Analysing microbial community composition through amplicon sequencing: from sampling to hypothesis testing. *Frontiers in Microbiology*, *8*, 1561.

Jeddi, M., Karray, F., Loukil, S., Mhiri, N., Abdallah, M. B., & Sayadi, S. (2018). Anaerobic biological treatment of industrial saline wastewater: Fixed bed Reactor

performance and analysis of the microbial community structure and abundance. *Environmental technology*, (just-accepted), 1-29.

Kavvadias, V., Elaiopoulos, K., Theocharopoulos, S., & Soupios, P. (2017). Fate of Potential Contaminants Due to Disposal of Olive Mill Wastewaters in Unprotected Evaporation Ponds. *Bulletin of environmental contamination and toxicology*, *98*(3), 323-330.

Limayem, A., Micciche, A., Nayak, B., & Mohapatra, S. (2018). Prokaryotic community profiling of local algae wastewaters using advanced 16S rRNA gene sequencing. *Environmental Science and Pollution Research*, *25*(1), 704-711.

Ma, Y., Galinski, E. A., Grant, W. D., Oren, A., & Ventosa, A. (2010). Halophiles 2010: life in saline environments.

MacGowan, S. A., Madeira, F., Britto-Borges, T., Warowny, M., Drozdetskiy, A., Procter, J. B., & Barton, G. J. (2020). The Dundee Resource for Sequence Analysis and Structure Prediction. *Protein Science*, *29*(1), 277-297.

Madeira, F., Lee, J., Buso, N., Gur, T., Madhusoodanan, N., Basutkar, P., Tivey, A., Potter, S.C., Finn, R.D. and Lopez, R. (2019). The EMBL-EBI search and sequence analysis tools APIs in 2019. *Nucleic acids research*.

McNeil, L.K., Reich, C., Aziz, R.K., Bartels, D., Cohoon, M., Disz, T., Edwards, R.A., Gerdes, S., Hwang, K., Kubal, M. and Margaryan, G.R., 2007. The National Microbial Pathogen Database Resource (NMPDR): a genomics platform based on subsystem annotation. *Nucleic acids research*, *35*(suppl_1), pp.D347-D353.

de Melo Soares, R. H. R., de Assunção, C. A., de Oliveira Fernandes, F., & Marinho-Soriano, E. (2018). Identification and analysis of ecosystem services associated with biodiversity of saltworks. *Ocean & coastal management*, *163*, 278-284.

Muller, J., Szklarczyk, D., Julien, P., Letunic, I., Roth, A., Kuhn, M., Powell, S., von Mering, C., Doerks, T., Jensen, L.J. and Bork, P., 2010. eggNOG v2. 0: extending the evolutionary genealogy of genes with enhanced non-supervised orthologous groups, species and functional annotations. *Nucleic acids research*, *38*(suppl_1), pp.D190-D195.

Oren, A. a (2013). Salinibacter: an extremely halophilic bacterium with archaeal properties. *FEMS microbiology letters*, *342*(1), 1-9.

Oren, A. b (2009). Saltern evaporation ponds as model systems for the study of primary production processes under hypersaline conditions. *Aquatic Microbial Ecology*, *56*(2-3), 193-204.

Paver, S. F., Muratore, D., Newton, R. J., & Coleman, M. L. (2018). Reevaluating the salty divide: phylogenetic specificity of transitions between marine and freshwater systems. *MSystems*, *3*(6), e00232-18.

Polle, J. E., Tran, D., & Ben-Amotz, A. (2019). History, distribution, and habitats of algae of the genus Dunaliella Teodoresco (Chlorophyceae). *The Alga Dunaliella*, 1-14.

Sun, S., Chen, F., Xu, Y., Liu, J., & Chen, S. (2019). Halorubrum amylolyticum sp. nov., a novel halophilic archaeon isolated from a salt mine. *Antonie van Leeuwenhoek*, *112*(12), 1849-1861.

Tatusov, R. L., Galperin, M. Y., Natale, D. A., & Koonin, E. V. (2000). The COG database: a tool for genome-scale analysis of protein functions and evolution. *Nucleic acids research*, *28*(1), 33–36. https://doi.org/10.1093/nar/28.1.33

Topping, B. R., Kuwabara, J. S., Carter, J. L., Garrett, K. K., Mruz, E., Piotter, S., & Takekawa, J. Y. (2016). Effects of salt pond restoration on benthic flux: sediment as a source of nutrients to the water column. *Journal of Environmental Protection*, *7*(07), 1064.

Valencia, R., Giffard-Mena, I., Cruz-López, R., García-Mendoza, E., & Stephano-Hornedo, J. L. (2018). Growth Profiles, Nutrient composition and Pigments Analysis of Dunaliella salina strain San Quintin. *CICIMAR Oceánides*, *33*(2), 1-11.

Waterman, M. S. (2018). *Introduction to computational biology: maps, sequences and genomes*. Chapman and Hall/CRC.

Wurtsbaugh, W. A., Paerl, H. W., & Dodds, W. K. (2019). Nutrients, eutrophication and harmful algal blooms along the freshwater to marine continuum. *Wiley Interdisciplinary Reviews: Water*, *6*(5), e1373.

Wu, H., & Moore, E. (2010). Association analysis of the general environmental conditions and prokaryotes' gene distributions in various functional groups. *Genomics*, *96*(1), 27-38.

Yadav, A. N., & Saxena, A. K. (2018). Biodiversity and biotechnological applications of halophilic microbes for sustainable agriculture. *Journal of Applied Biology & Biotechnology Vol*, *6*(1), 48-55.

Yaish, M. W., Al-Harrasi, I., Alansari, A. S., Al-Yahyai, R., & Glick, B. R. (2016). The use of high throughput DNA sequence analysis to assess the endophytic microbiome of date palm roots grown under different levels of salt stress. *Int. Microbiol*, *19*, 143-155.

Zander, E., Seifert, H., & Higgins, P. G. (2016). Effects of saline, an ambient acidic environment, and sodium salicylate on OXA-mediated carbapenem resistance in Acinetobacter baumannii. *Antimicrobial agents and chemotherapy*, *60*(6), 3415-3418.

Zhan, A., Bailey, S. A., Heath, D. D., & Macisaac, H. J. (2014). Performance comparison of genetic markers for high-throughput sequencing-based biodiversity assessment in complex communities. *Molecular Ecology Resources*, *14*(5), 1049-1059.

Zolfaghar, M., Amoozegar, M. A., Khajeh, K., Babavalian, H., & Tebyanian, H. (2019). Isolation and screening of extracellular anticancer enzymes from halophilic and halotolerant bacteria from different saline environments in Iran. *Molecular biology reports*, *46*(3), 3275-3286.

CHAPTER THREE: THE EFFECT OF SALINITY AND NITROGEN SOURCES ON THE GROWTH OF *DUNALIELLA SALINA* AND BIOPROSPECTING USING THE RSM METHOD

3.1 Abstract

Macro nutrients such as potassium, nitrogen and phosphorus are essential to cellular viability and are found in varying concentrations within environments. Specifically, the presence of nitrogen within an environment allows for the rapid growth of organisms. Saline environments are generally found throughout the world. Many organisms can grow and thrive within these environments. *Dunaliella salina* is one such organism. To adapt to these saline environments, the cells produce certain compounds such as β-carotene. Beta carotene is an orange compound that is extremely useful to humans as it is a precursor for Vitamin A which is a particularly important nutrient for humans. The aim of this study was to use the adapted Response Surface Methodology Box Behnken to optimize the production of beta carotene and determine the highest bio-productivity for *D. salina*. The experiment was set up according to the Box Behnken Design and was run for 25 days. The results indicated that *D. salina* can grow within the different treatments. The results also showed that 3M NaCl salinity, nitrate as the nitrogen source and 30℃ were the best conditions for *D. salina* growth. The study also established the inverse relationship between bio-productivity and β-carotene production as an increase in bio-productivity decreased β-carotene production.It is clear from these results that *D. salina* responds differently to different conditions, thus allowing for the manipulation of conditions in order to produce certain by-products such as β-carotene. It is concluded that salinity (3M NaCl) and 549µM NO_3 is crucial for optimal *D. salina* growth.

3.2 Introduction

All organisms require nutrients to grow and reproduce. These nutrients are generally found within the environment in different forms and quantities. From the various nutrients required by organisms, Potassium, Nitrogen and Phosphorus are the most essential macronutrients for growth and survival (Shurtz *et al.*, 2017). These nutrients are generally

found in different forms within the environment. However, the most important nutrient for proper growth and functioning of organisms is nitrogen (Gao *et al*., 2018).

Nitrogen is generally found within the environment as nitrate, nitrite or urea. These diverse forms of nitrogen require different pathways for digestion and assimilation (Ross *et al*., 2018). The ability of organisms to absorb nitrogen in its different forms is of utmost importance as it allows organisms to inhabit a wide range of environments (Fan *et al*., 2018).

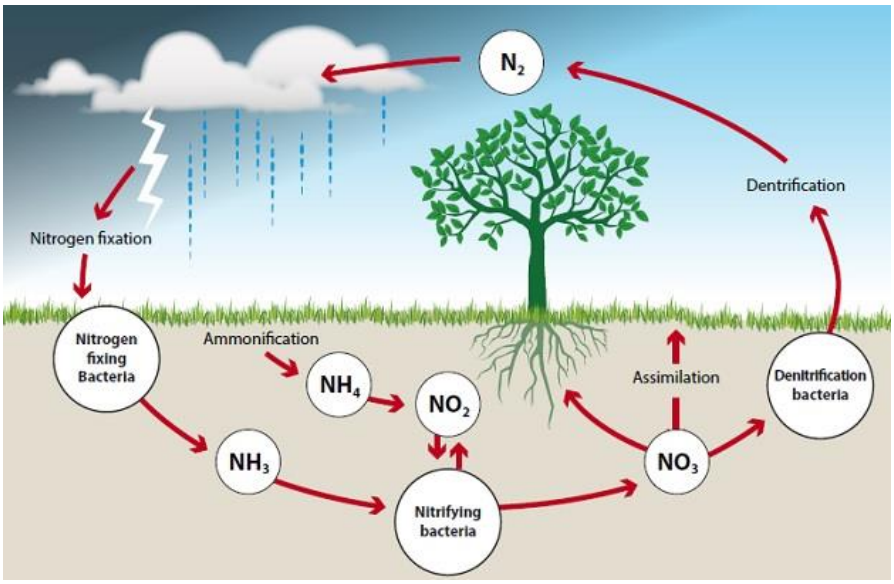

Figure 3.1: The Nitrogen Cycle (Reference: Nitrogen Cycle Picture: Land Management Online Course.).

The nitrogen cycle which is one of the most important cycles, allows for nitrogen fixation and assimilation to the organisms that require the nitrogen the most (Figure 3.1). This cycle is performed in every environment of the world in some form or the other. One such environment is highly saline environments.

Saline environments have higher than normal levels of sodium chloride. These higher sodium chloride levels are measured as salinity (usually in ppt or molar concentration), found in extreme environments ranging from lakes to oceans. Some saline environments such as salt evaporation ponds are man-made. Salt evaporation ponds are used to produce salt and soda ash (Zhao & Filker, 2018). The production of these salts requires the ponds to have increasing levels of salinity as the water known as brine (due to the high levels of salt present) evaporates and the salt begins to concentrate (Abdulsalam *et al*., 2017). The

salt evaporation ponds, therefore, have an increasing salinity gradient, thus allowing for different organisms to inhabit each pond (Takekawa *et al*., 2006). Salt evaporation ponds allow for the establishment of various ecosystems within the different salinities found in the ponds (Javor, 2002). These ecosystems depend on one group of organisms (algae) to act as a primary producer to produce enough food for the rest of the ecosystem (Wu *et al*., 2016). In addition, the primary producer has to effectively survive the saline environment by obtaining nourishment from the nitrogen present within the ponds (Wu *et al*., 2016). Typically, the primary producer within salt evaporation ponds is the green microalga *Dunaliella salina* (*D. salina*).

Bio productivity refers to the rate of increase of the biomass of organisms within an environment (Vaidya & Naik, 2018). The rate of increase is of importance as it allows for a better understanding of the organisms' reactions to changes in the environment. The bio productivity of *D. salina* is of importance as it allows for a better understanding of how the cells function under different conditions. This information can be used to increase the biomass of *D. salina*. The increase in the biomass of *D. salina* allows for an increase in the production of beta carotene as the increased biomass allows for the increased production of beta carotene (Lou *et al*., 2020). Beta carotene production can also be increased within the *D. salina* cells by changing the environmental conditions within which the cells are grown (Lou *et al*., 2020). Environmental conditions such as increased salinity and nitrogen starvation lead to an increase in the production of beta carotene by *D. salina* cells. These conditions do not increase the bio productivity rate but increase the rate at which the biomass present produces the required compounds such as beta carotene (Bonneford *et al*., 2017). Thus, the manipulation of the environment in which the *D. salina* cells are grown allows for the better production of compounds such as beta carotene.

The *D. salina* algae is best known for its ability to produce high levels of β-carotene. Beta carotene is an important compound that is found in vegetables such as carrots. This compound is a member of the carotenes and has a strong orange-red colour. The production of beta carotene is of importance as it acts as a precursor of Vitamin A (Sommer, 2001). Vitamin A is an important vitamin within the body as it helps in normal vision and boosting the immune system (Sommer, 2001). Thus, the intake of beta carotene is necessary as it is used as a precursor for Vitamin A. The average human does not

consume enough beta carotene and, hence, beta carotene supplements are required. A good source of beta carotene is *D. salina* as it produces it in high volumes (Polle *et al*., 2017). The beta carotene produced by *D. salina* is in the correct chemical motif for intake by humans and, thus, it is used as a supplement by humans (Hashemi *et al*., 2020). Specifically, the beta carotene produced by *D. salina* is required by the pharmaceutical industry to produce cosmetics (Bonnefond *et al*., 2017). It is also of importance to the pharmaceutical industry as it is a key ingredient in Sun Protective lotions (Sanchez *et al*., 2016). Thus, the production of beta carotene is of utmost importance.

Along with beta carotene *D. salina* also produces glycerol. The algae generally produce high levels of glycerol to maintain osmolarity in extremely saline environments (He *et al*., 2007). The glycerol produced by the *D. salina* slowly gets excreted into the environment surrounding the cells, allowing for the survival of various other microorganisms within the environment (Monte *et al*., 2020). The growth and proliferation of *D. salina* cells are dependent on the presence of nitrogen within the environment. The production of both beta carotene and glycerol is also dependant on the presence of nitrogen (Bonneford *et al*., 2017, Wu *et al*., 2019). Glycerol production increases as salinity increases. This is due to the osmolarity function of glycerol (Wu *et al*., 2019).

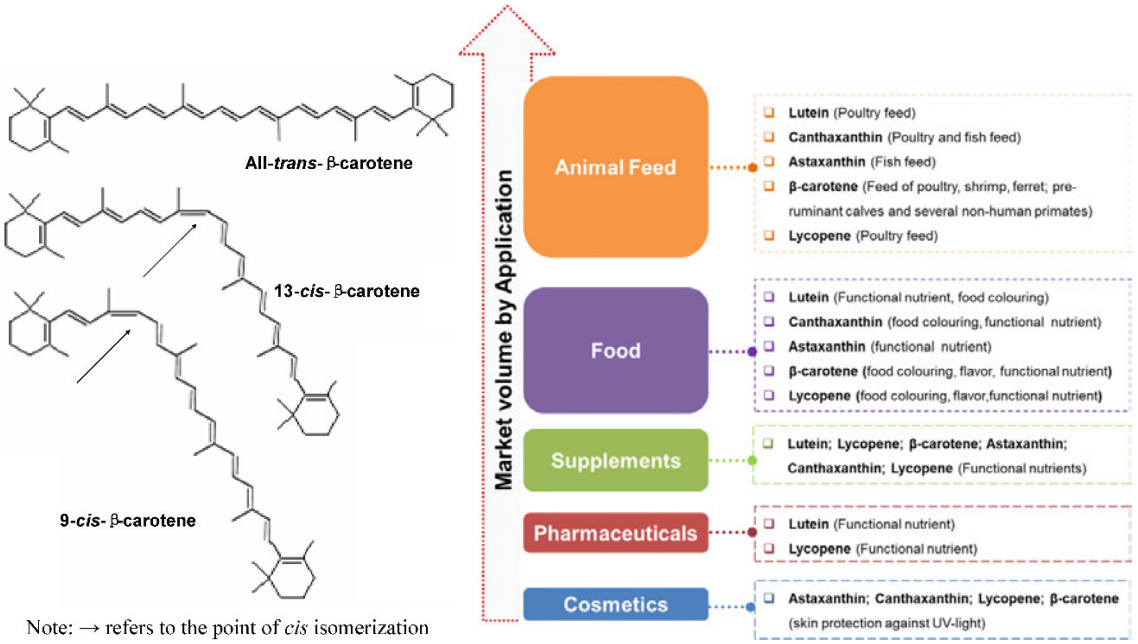

Note: → refers to the point of *cis* isomerization

Figure 3.2: The chemical structure and industrial applications of β-carotene (Reference for pictures: Chemical structure (Khoo *et al*., 2011). Industrial applications (Mussagy *et al*., 2019).

The Response Surface Methodology (RSM) is a mathematical procedure that explores the relationship between various independent variables and their effect on one or more dependant variables (Myers *et al*., 2016). The basic use of RSM is to use a sequence of designed experiments to obtain the optimal response (Myers *et al*., 2016). This procedure allows for the optimization of the independent variables to obtain the optimal response from the dependant variable. RSM can be used to optimize the production of desired compounds from organisms or the growth of the organism. Thus, this procedure can be used to optimize the production of β-carotene from *D. salina* and the RSM will also focus on optimizing the growth of *D. salina* as the only way to reduce an organism is to understand its optimal growth requirements.

3.3 Aims and Objectives

Aims

This chapter aims to fulfil the main objectives 2, 3, 6 and 7 of this research thesis.

Objectives

1. To determine the effect of salinity and nitrogen source on growth rate.
2. To analyse the pigments produced by *D. salina* under different salinities and nitrogen sources and the effect these pigments have on salt production
3. To analyse the glycerol production of *D. salina* under different salinities and nitrogen sources which effects the salt production process.
4. To establish the relationship between environmental factors (NaCl salinity, nitrogen source and temperature) and growth of *D. salina*
5. To determine the effect of environmental factors on β-carotene production

3.4 Materials and Methods

3.4.1 *Algae growth kinetics*

This experiment was conducted in two parts. Part A assessed the effect of varying salinities and different nitrogen sources on the growth and pigment, glycerol production within *D. salina* while part B evaluated the RSM methodology.

The starting culture used for this experiment was obtained from Botash and observed under the microscope to determine the purity of the sample which was then cultivated at 2M NaCl salinity with nitrate (NO_3) in AMCONA media, which is specific for the growth of *D. salina*. The algae culture was grown in 250 ml Erlenmeyer flasks with a seed culture of 30 ml combined with 120 ml of media to give a final volume of 150 ml. The seed culture was inoculated during the exponential phase i.e. the culture was doubling rapidly and the cells within the culture were healthy. The experiment was performed in triplicate. The salinities evaluated during this experiment were 2M NaCl, 2,5M NaCl, 3M NaCl and 3,5M NaCl. The 2M salinity served as the control for this experiment as the *D. salina* cells optimally grow in 2M NaCl salinity. The nutrient experiment was performed using the same starting culture as the salinity experiment. The same volumes were used and the salinity was constant at 2M in the media. However, the nitrogen source was changed. The following nitrogen sources were used: nitrate, ammonia, urea and the control had no nitrogen source. The nitrogen experiment was also performed in triplicate. The flasks for both experiments were stored at ambient temperature (±26°C) in the culture room under constant photon flux density (PFD) of ca. 80 $\mu mol.m^{-2}.s^{-1}$. The light source was Growlux fluorescent tubes (OSRAM, Germany). The flasks were manually shaken in the morning and afternoon to avoid sedimentation of the cells in the media. Optical density (OD_{680nm}) readings were taken using the Shimadzu UV-1280 Spectrophotometer to determine the growth rate of the cultures. The experiment was run for 25 days.

The following conditions were used during this experiment, as determined by the Response Surface Methodology, Box Behnken Design. These conditions were chosen according to the effect these variables have on the growth and beta carotene production of *D. salina*:

Table 3.1: Factors and their significant levels used for this experiment.

FACTOR		-1	0	1
SALINITY (Moles)	X1	2	3	4
TEMPERATURE (℃)	X2	25	28	32
NITROGEN SOURCE	X3	NH_4	NO_3	UREA

Table 3.2: Experimental Design according to the Box Behnken Design Principal.

EXPERIMENT	SALINITY (X1)	TEMPERATURE (X2)	NUTRIENT (X3)
1	4 (1)	28 (0)	UREA (1)
2	4 (1)	32 (1)	NO_3 (0)
3	3 (0)	32 (1)	UREA (1)
4	2 (-1)	25 (-1)	NO_3 (0)
5	3 (0)	25 (-1)	UREA (1)
6	3 (0)	28 (0)	NO_3 (0)
7	3 (0)	28 (0)	NO_3 (0)
8	4 (1)	28 (0)	NH_4 (-1)
9	2 (-1)	28 (0)	NH_4 (-1)
10	3 (0)	32 (1)	NH_4 (-1)
11	3 (0)	28 (0)	NO_3 (0)

12	**2 (-1)**	**28 (0)**	**UREA (1)**
13	**2 (-1)**	**32 (1)**	**NO_3 (0)**
14	**3 (0)**	**25 (-1)**	**NH_4 (-1)**
15	**4 (1)**	**25 (-1)**	**NO_3 (0)**

Each of the above treatments were performed in triplicate. The flasks for the room temperature treatments were stored at ambient temperature (±25°C), the cultures grown at 28ºC and 32ºC were kept in incubators that were constantly maintained at these temperatures in the culture room under constant photon flux density (PFD) of ca. 80 µmol.m^{-2}.s^{-1}. The light source was Growlux fluorescent tubes (OSRAM, Germany). The flasks were manually shaken in the morning and afternoon to avoid sedimentation of the cells in the media. Optical density (OD_{680nm}) readings were taken using the Shimadzu UV-1280 Spectrophotometer to determine the growth rate of the cultures. The experiment was run for 25 days.

During the exponential phase of growth, the bioproductivity and specific growth rate of the cultures were calculated (Eq. 1, 2 and 3). This was done by centrifuging 15ml of each treatment culture and drying the cell mass overnight to get the dry weight of each treatment. The procedure was performed to obtain the initial mass reading and after seven days to obtain the final mass reading. A calculation was performed using both masses to obtain the bioproductivity and specific growth rate of *D. salina* in the different treatments. Dry weight (DW) measurements were also taken at the end of the experiment.

Equation 1: Biomass Productivity

$$\text{BMPr } (mgL^{-1}d^{-1}) = \frac{BM2-BM1}{T2-T1}$$

BM2 – Final Biomass

BM1 – Initial Biomass

T2 – 7th Day

T1 – 1st Day

Equation 2: Specific Growth Rate

$$SGR\ (d^{-1}) = 2{,}303\left(\frac{logN2 - logN1}{T2 - T1}\right)$$

N2 – Final Biomass

N1 – Initial Biomass

T2 – 7th Day

T1 – 1st Day

Equation 3: Dry Weight

$$DW\ (mg/L) = 1000\left(\frac{weight\ of\ fliter + dried\ residue\ (mg) - weight\ of\ filter(mg)}{volume\ used\ (ml)}\right)$$

3.4.2 *Pigment (β-carotene) extraction*

The pigments found within *D. salina* cells were extracted and quantified using rigorous protocols. The extraction protocol used organic solvents such as acetone and petroleum ether. The biomass culture was harvested by centrifuging 50 ml of *D. salina*. The cell pellet was washed by adding distilled water (dH_2O) and re centrifuging to remove impurities. The washing process was repeated 3 times. The washed pellet was left overnight to dry at room temperature. The extraction solvent (acetone) was diluted to a 90% (v/v) concentration and stored in the fridge overnight as the solution needed to be chilled. An ice box was used to chill samples throughout the extraction procedure. The 90% acetone was used to macerate the algae paste to release the pigments from within the cells. The slurry was then mixed with petroleum ether in a 1:1 ratio. Once the petroleum ether was added to the acetone the pigments present within the acetone solution moved into the petroleum layer forming two different layers. The petroleum ether layer was removed with a pipette and placed into coloured tubes to block sunlight as sunlight affects the pigments.

3.4.3 *Pigment (β-carotene) analysis*

The extracted pigments were then analysed by Liquid Chromatography Mass Spectroscopy (LCMS) to determine the presence of different pigments. The Shimadzu LCMS – 9030 was used to perform the analysis, a 40 -100% acetonitrile gradient was used with standard parameters. The samples were also analysed for Optical Density using the Shimadzu UV-1280 Spectrophotometer to determine the abundance of β-carotene using standard equations (Eq. 4 and 5).

Equation 4: Chlorophyll A and B Abundance

$Ca = 11.75 (A662) - 2.350 (A645)$

$Cb = 18.61 (A645) - 3.960 (A662)$

A645 – Absorbance at OD_{645nm}

A662 – Absorbance at OD_{662nm}

Equation 5: Carotenoid Abundance

$Cx+c = 1000 (A470) - 2.270 (Ca) - 81.4 (Cb)/227$

A470 – Absorbance at OD_{470nm}

Ca – Value calculated for Chlorophyll A Abundance

Cb – Value calculated for Chlorophyll B Abundance

3.4.4 *Glycerol extraction*

The glycerol was also extracted from the algae cells amd analysed by Gas Chromatography (GC). Mordhay and Ben-Amotz (1978) proposed extraction protocol for glycerol extraction involved centrifuging 50 ml of the algae culture to produce a pellet. A solvent mixture of ethanol (70%v/v) and chloroform (30%v/v) was added to the cell pellet. The mixture was vortexed for 20 minutes and the samples were recentrifuged leaving the extract layer on top. The samples were then analysed by Gas Chromatography Mass Spectroscopy using the Shimadzu GC-2010 Pro with general spilt parameters at normal concentration to determine the presence of glycerol within the samples.

3.4.5 *Statistical analysis*

The statistical calculations performed for this chapter involved the ANOVA test ran on the different variables that were used in this experiment. The regression coefficient and F-value were also determined from the results obtained. R Studio was used for the ANOVA, regression coefficient and F-value whilst MATHLAB was used for the Response Surface calculations.

3.5 Results

3.5.1 *Part A*

The ANOVA results for the four NaCl salinities had the Sum of Square value of 0.5599 which indicates a large degree of variability within the data set, the F-Value for the NaCl Salinity Experiment is 12,98 which indicates that there is indeed a significant difference between the growth rates for each NaCl salinity treatment. The p-value for this experiment is $2{,}87e^{-07}$ which is less than p<0,005, hence the results are significant. The ANOVA results for the different nitrogen sources experiment had the Sum of Square value of 0.05089 which indicates a very small degree of variability within the data set, the F-Value for the nitrogen source experiment is 7.116 whuch indicates that there is a significant difference between the growth rates for each nitrogen source treatment. The p-value for the nitrogen source experiment is 0.000221 which is less than p<0,005, hence the results are significant.

As shown in Figure 3.3, the growth rate of *D. salina* when exposed to different salinities exhibited a gradual, slow increase, followed by a steady increase and ultimately a plateau phase. This was common for all treatments, except the 3.5M NaCl culture which is strikingly different. After the 25-day period, the 3.5M culture appears to peak rather than follow the norm displayed by the other treatments. The graph shows that the 3M cultures had the highest growth rate and that the 2M culture had the lowest growth rate while the 2.5M and 3,5M cultures appeared to have a similar final rate of growth.

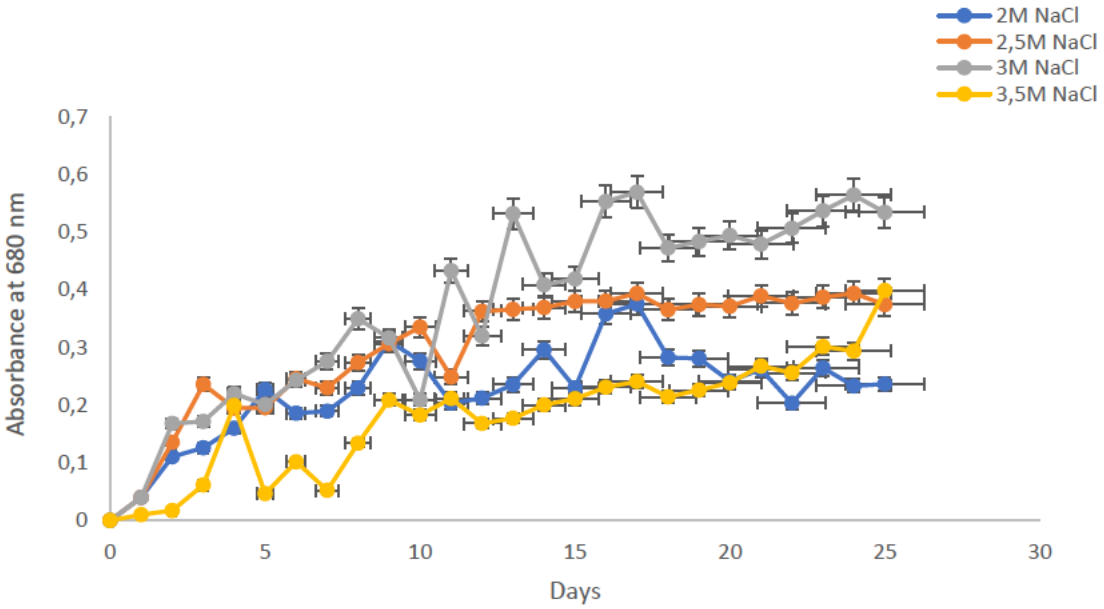

Figure 3.3: The Growth Curves of *D. salina* in different salinities measured using NaCl.

As shown in Figure 3.4, the *D. salina* cells present within each of the above NaCl treatments have reacted differently to the growth media. The cells grown in 2M NaCl treatment (A) have a circular shape and are green in colour showing high levels of pigments. There are very few cells depicted in the 2M NaCl treatment. The cells grown in 2,5M NaCl (B) are more ellipsoid on shape and have a more orange colouring showing the presence of carotenoids. The 2,5M NaCl treatment has the most number of cells present within the image. The cells grown in 3M NaCl (C) have an ellipsoid with high levels of pigments as can be seen by the bright green colour of the cells. The cells grown in 3,5M NaCl (D) have an ellipsoid shape with high amounts of pigments as can be seen by the colour of the cells. The 3M NaCl and 3,5M NaCl have similar number of cells present within the image. The differences in cell numbers within the images could be due to photography errors as all the cells depicted are healthy.

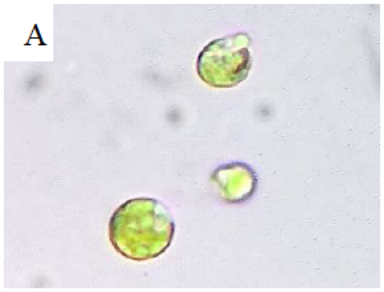

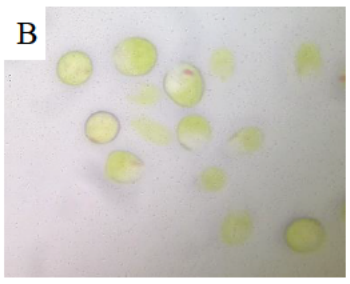

Figure 3.4: Images of *D. salina* cells grown in : A) 2M NaCl Salinity, B) 2,5M NaCl Salinity, C) 3M NaCl Salinity and D) 3,5M NaCl Salinity Treatments.

As shown in Figure 3.5, the growth rate of *D. salina* when exposed to different nitrogen sources. *D. salina* generally exhibits a slow and gradual increase throughout the course of the nitrogen source experiment. The Urea treatment however had a gradual increase followed by an exponential phase which continued till the 25 day mark unlike the other treatments. The graph shows that the highest growth rate was observed for the urea treatment, whilst the control treatment had the lowest growth rate. The sodium nitrate and ammonia treatments had similar growth rates.

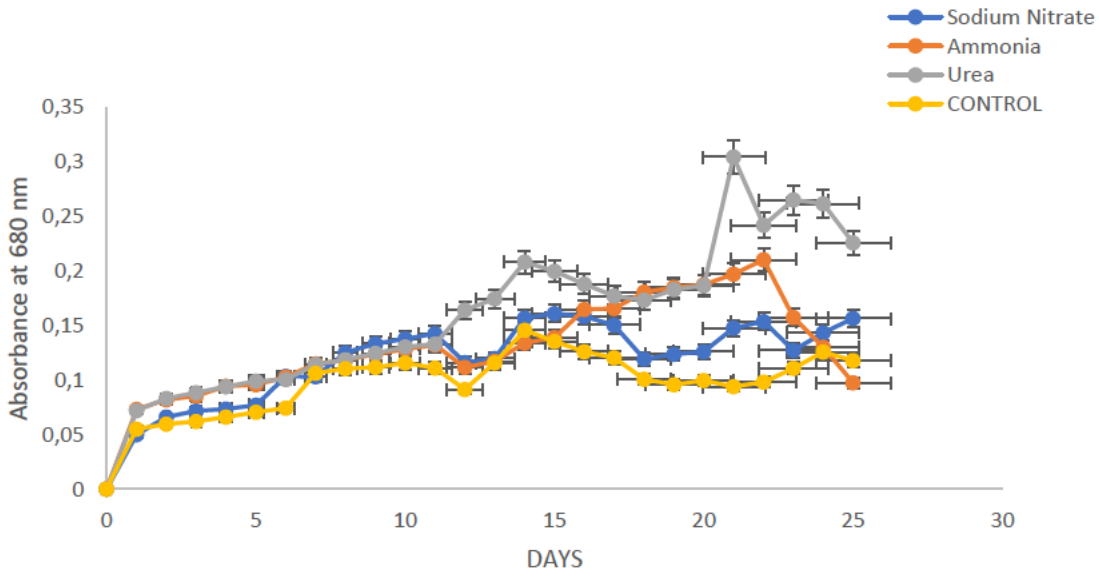

Figure 3.5: The Growth Curves of *D. salina* under different nitrogen source treatments.

As shown in Figure 3.6, the *D. salina* cells reacted differently to the different nitrogen sources. The cells grown in the NO_3 treatment (A) appeared round to ellipsoid in shape and have a strong green colour depicting the prensence of high levels of pigments. The cells grown in the ammonia treatment (B) have a circular to ellipsoid shape and have a lighter colour which depicts the presence of carotenoids within the cells. The cells grown in the urea treatment (C) have a circular shape with a light green colour and orange spots which indicate the presence of carotenoids. The control treatment has circular cells which have a light colour indicating the presence of carotenoids. The number of cells depicted for each treatment are the same except for the control sample which has fewer cells due to the absence of a nitrogen source.

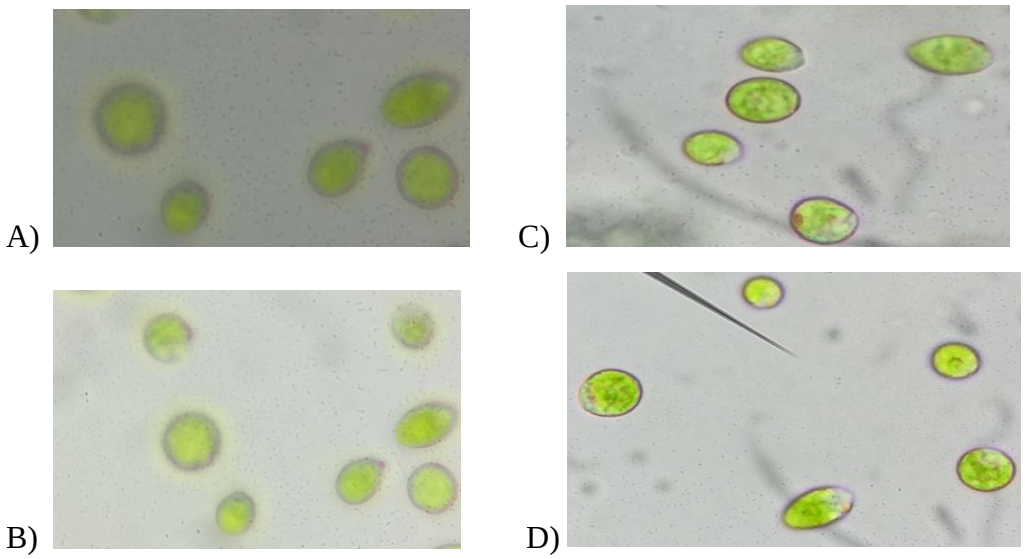

Figure 3.6: Images of *D. salina* cells growin in : A) NO_3, B) Ammonia, C) Urea and D) Control Treatments.

As shown in Figure 3.7 the bioproductivity analysis for the nitrogen source experiment displayed results similar to the growth curves displayed in Figure 3.4. The highest bioproductivity of *D. salina* was displayed in the urea treatment, whilst the lowest bioproductivity was recorded for the control treatment. The ammonia and sodium nitrate treatments had almost the same rate of bioproductivity. The bioproductivity graph gives a better understanding of the growth curves featured in Figure 3.4.

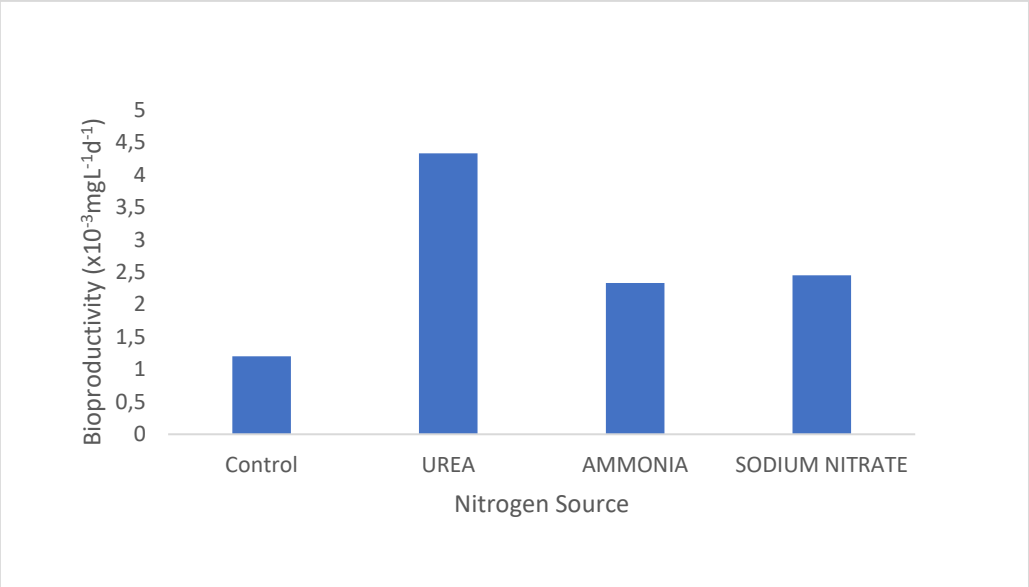

Figure 3.7: The Bioproductivity Rate of *D. salina* under different nitrogen source treatments.

As shown in Figure 3.8, the bioproductivity analysis for the NaCl salinity experiment depict a different picture than the growth curves for the NaCl salinity experiment. The 2M NaCl bioproductivity is the highest due to the fact that the cells were acclimatized to the 2M NaCl and hence did not have to undergo acclimitization. The 3,5 M NaCl had the second highest bioproductivity due to the exponential phase that this treatment underwent at the 20 day time period in Figure 3.3. The 2,5 M NaCl and 3 M NaCl had similar bioproductivity rates.

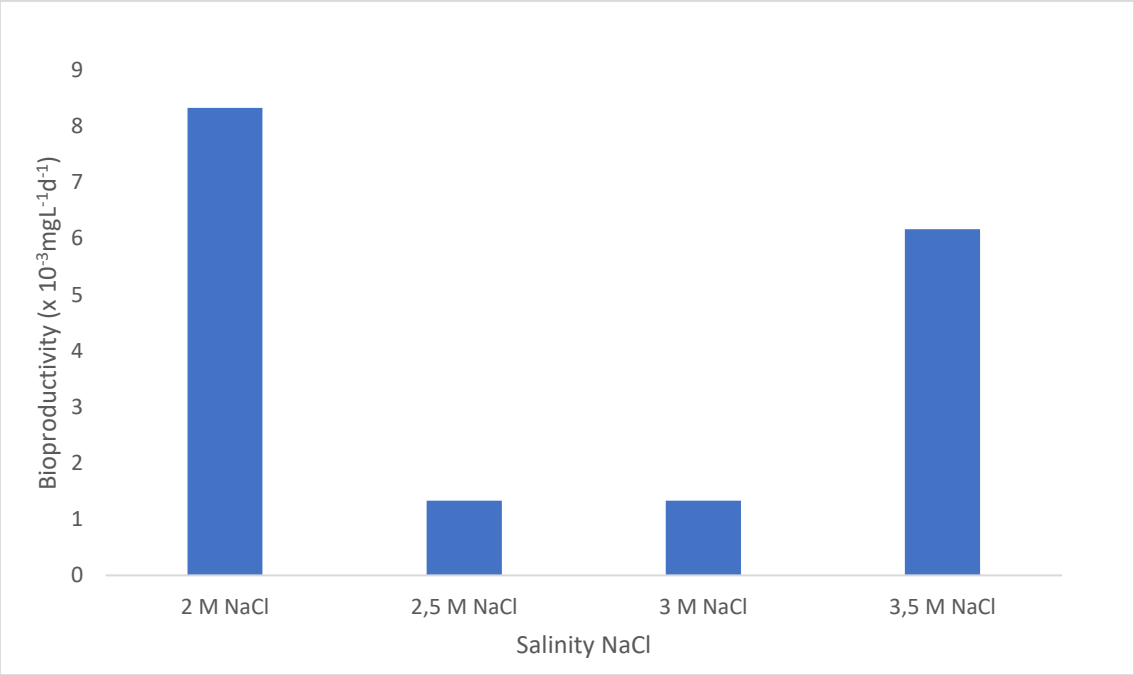

Figure 3.8: The Bioproductivity Rate of *D. salina* under different NaCl salinities.

As shown in Appendix A, the LCMS results for the 2M, 2,5M, 3M and 3,5M NaCl treatments. The results depict the presence of β-carotene which is identified by the peak present at 536 m/z. The LCMS was run to determine all the different carotenoid and pigment molecules present within the *D. salina* extract. The presence of β-carotene in the LCMS proves that *D. salina* indeed produces β-carotene in high concentrations. The LCMS also depicts the presence of chlorophylls A and B, xanthophylls and phycobilins which are all compounds found within the pigment extract of *D. salina*. These results depict the compound richness of the pigments found within the *D. salina* cells. The different NaCl salinities all produced similar LCMS results showing that varying NacCl salinity has a similar reaction on the pigment production of *D. salina*. The LCMS results for the NO_3, ammonia, urea and control treatments were also shown in Appendix A. The results depict the presence of β-carotene which is identified by the peak present at the 536 m/z mark which is the molecular weight for β-carotene. The difference between the results for the NaCl salinity treatments and the nitrogen source treatments is the percentage of the other pigments found within the *D. salina* cells. The percentage of the other pigments found within the *D. salina* cells is greatly reduced in the nitrogen source treatments. This depicts that the difference in nitrogen source has an

impact on the pigments produced by *D. salina*, however the β-carotene produced by the cells remained at the same amount showing that *D. salina* cells have an affinity to producing β-carotene. This is due to the fact that β-carotene is involved in the stress response of *D. salina* cells.

As shown in Appendix A, the GC-MS results for the glycerol production of *D. salina* under the different treatments. The results of the GC-MS show that the only treatments that do not induce glycerol production in the *D. salina* cells are the 2M NaCl treatment and the NO_3 treatment. The other treatments induce glycerol production with the control treatment (Figure 3.24) for the nitrogen source experiment having the highest glycerol peak. The glycerol peaks can be found at the 7 minute retention time for all the treatments that have glycerol present. The reason for the absence of glycerol production for the 2M NaCl treatment and the NO_3 nitrogen source treatment could be due to the adaptability of *D. salina* to these conditions.

3.5.2 *Part B*

The following results were obtained from the RSM Experiment.

Table 3.3: Results of Box Behnken Design RSM for *D. salina*.

Std Order	Run	Salinity	Temperature	Nitrogen	Bioproductivity ($mgL^{-1}d^{-1}$)	β carotene (µg/l)
8	1	4	28	1	0,00133	859,39
7	2	2	28	1	0,00633	941,72
6	3	4	28	-1	0,007	804,21
10	4	3	32	-1	0,00083	1171,69
5	5	2	28	-1	0,003	99,21
13	6	3	28	0	0,00245	598,45
2	7	4	25	0	0,00183	1395,38
14	8	3	28	0	0,00283	612,39
12	9	3	32	1	0,017	505,76
4	10	4	32	0	0,00267	1892,03
3	11	2	32	0	0,033	269,45
15	12	3	28	0	0,00262	624,53

1	13	2	25	0	0,0015	384,74
9	14	3	25	-1	0,00333	490,89
11	15	3	25	1	0,00233	449,6

Table 3.3 represents the results from the optimization experiments in table form. The experiment comprised of 15 runs that were performed over a period of 23 days. The results show that the bio productivity of the treatments is generally within the 0,017 to 0,00083 $mgL^{-1}d^{-1}$ range with the highest bio productivity response occurring for Run 11 which had the *D. salina* grown in 2M of salinity with NO_3 as the nitrogen source and the temperature being 32℃. The beta carotene response for Run 11 was one of the lowest at 269,45 µg. The Run with the highest beta carotene production was Run 10 which had the *D. salina* grown in 4M salinity with NO_3 being the nitrogen source and the temperature being 32℃. The bio productivity for Run 10 was 0,00267 $mgL^{-1}d^{-1}$.

Table 3.4: The ANOVA Results for the bio productivity Response.

Source	Sum of Squares	df	Mean Square	F-value	p-value	
Model	0,0010	12	0,0001	2326,87	0,0004	significant
A-Salinity	5,567E-06	1	5,567E-06	153,64	0,0064	
B-Temperature	0,0000	1	0,0000	1021,91	0,0010	
C-Nitrogen	0,0001	1	0,0001	1587,83	0,0006	
AB	0,0002	1	0,0002	6485,99	0,0002	
AC	0,0000	1	0,0000	558,88	0,0018	
BC	0,0001	1	0,0001	2034,10	0,0005	
A^2	0,0000	1	0,0000	1027,15	0,0010	
B^2	0,0000	1	0,0000	1231,21	0,0008	
C^2	1,730E-06	1	1,730E-06	47,75	0,0203	
A^2B	0,0001	1	0,0001	1403,50	0,0007	
A^2C	0,0000	1	0,0000	774,24	0,0013	
AB^2	0,0001	1	0,0001	2069,99	0,0005	
Pure Error	7,247E-08	2	3,623E-08			
Cor Total	0,0010	14				

Factor coding is **Coded**.

Sum of squares is **Type III - Partial**

The **Model F-value** of 2326,87 implies the model is significant. There is only a 0,04% chance that an F-value this large could occur due to random 'noise'.

P-values less than 0,0500 indicate model terms are significant. In this case A, B, C, AB, AC, BC, A^2, B^2, C^2, A^2B, A^2C, AB^2 are significant model terms. Values greater than 0.1000 indicate the model terms are not significant.

Table 3.5: Best Fit Statistics for the Bio productivity Response.

Std. Dev.	**0,0002**	R^2	**0,9999**
Mean	0,0059	**Adjusted R^2**	0,9995
C.V. %	3,24	**Predicted R^2**	NA(1)
		Adeq Precision	181,5394

Adeq Precision measures the signal to noise ratio. A ratio greater than 4 is desirable. The ratio of 181,539 indicates an adequate signal. This model can be used to navigate the design space.

The equation in terms of coded factors can be used to make predictions about the response for given levels of each factor. By default, the high levels of the factors are coded as +1 and the low levels are coded as -1. The coded equation is useful for identifying the relative impact of the factors by comparing the factor coefficients.

Final Equation for bio productivity Response in Terms of Actual Factors

BioProductivity = 0,940023 - 0,128195Salinity - 0,083891Temperature - 0,058289 Nitrogen + 0,018402Salinity * Temperature + 0,020336 Salinity * Nitrogen + 0,001226 Temperature * Nitrogen - 0,037871 $Salinity^2$ + 0,00183 $Temperature^2$ - 0,000688 $Nitrogen^2$ + 0,001441$Salinity^2$ * Temperature - 0,003764 $Salinity^2$ * Nitrogen-0,000513 Salinity * $Temperature^2$

The equation in terms of actual factors can be used to make predictions about the response for given levels of each factor. Here, the levels should be specified in the original units for each factor.

Table 3.6: ANOVA Results for the Beta Carotene Response.

Source	Sum of Squares	df	Mean Square	F-value	p-value

Model	3,011E+06	12	2,509E+05	1473,25	0,0007	significant
A-Salinity	1,055E+05	1	1,055E+05	619,46	0,0016	
B-Temperature	1,358E+05	1	1,358E+05	797,23	0,0013	
C-Nitrogen	1,250E+05	1	1,250E+05	734,18	0,0014	
AB	93617,64	1	93617,64	549,68	0,0018	
AC	1,550E+05	1	1,550E+05	909,93	0,0011	
BC	97543,78	1	97543,78	572,74	0,0017	
A^2	1,338E+05	1	1,338E+05	785,81	0,0013	
B^2	89030,37	1	89030,37	522,75	0,0019	
C^2	71321,87	1	71321,87	418,77	0,0024	
A^2B	15806,42	1	15806,42	92,81	0,0106	
A^2C	2,843E+05	1	2,843E+05	1669,05	0,0006	
AB^2	4,576E+05	1	4,576E+05	2687,04	0,0004	
Pure Error	340,62	2	170,31			
Cor Total	3,011E+06	14				

Factor coding is **Coded**.
Sum of squares is **Type III - Partial**

The **Model F-value** of 1473,25 implies the model is significant. There is only a 0,07% chance that an F-value this large could occur due to noise.

P-values less than 0,0500 indicate model terms are significant. In this case A, B, C, AB, AC, BC, A^2, B^2, C^2, A^2B, A^2C, AB^2 are significant model terms. Values greater than 0.1000 indicate the model terms are not significant. If there are many insignificant model terms (not counting those required to support hierarchy) model reduction may improve your model.

Table 3.7: Best Fit Statistics for the β-Carotene Response.

Std. Dev.	**13,05**	R^2	**0,9999**
Mean	739,96	**Adjusted R^2**	0,9992
C.V. %	1,76	**Predicted R^2**	NA(1)
		Adeq Precision	147,5668

Adeq Precision measures the signal to noise ratio. A ratio greater than 4 is desirable. The ratio of 147,567 indicates an adequate signal. This model can be used to navigate the design space.

Final Equation for the Beta Carotene Response in Terms of Coded Factors

Beta Carotene = 634,86 + 167,51 A + 184,24 B - 176,81 C + 152,99 AB - 196,83 AC - 156,16 BC + 191,28 A^2+ 159,26 B^2 - 139,64 C^2 - 88,9 A^2B + 378,92 A^2C + 490,8 AB^2

The equation in terms of coded factors can be used to make predictions about the response for given levels of each factor. By default, the high levels of the factors are coded as +1 and the low levels are coded as -1. The coded equation is useful for identifying the relative impact of the factors by comparing the factor coefficients.

The equation in terms of actual factors can be used to make predictions about the response for given levels of each factor. Here, the levels should be specified in the original units for each factor. This equation should not be used to determine the relative impact of each factor because the coefficients are scaled to accommodate the units of each factor and the intercept is not at the centre of the design space.

As shown in Figure 3.25, the graphic presentations show that the interaction between temperature and nitrogen produces the highest bio productivity whilst the interaction between temperature and salinity produces the highest beta carotene production. The reasons for this could be various but it could be possibly due to the fact that high temperatures and high salinities increase the amount of β-carotene produced by *D. salina* cells, whilst the nitrogen source allows for rapid bioproductivity of the *D. salina* cells. The interaction between nitrogen and salinity (E & F) also show high levels of β-carotene production. This result can be linked to the results obtained from the previous chapter regarding the effect of the NaCl salinity and nitrogen source on the β-carotene and bioproductivity of the *D. salina* cells.

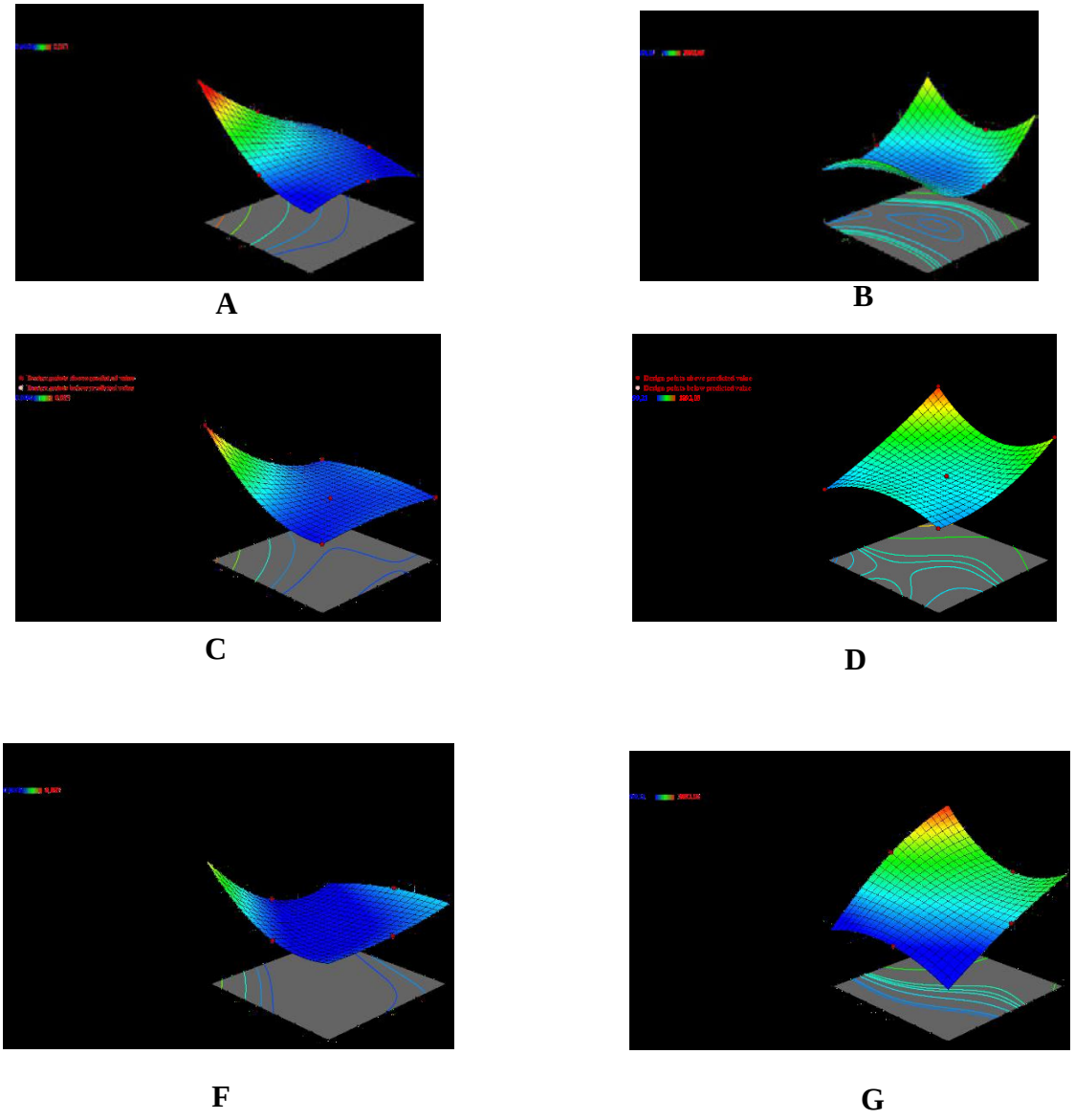

Figure 3.9: The Response Surface Plots (3D) showing the influence of the three variables on the bio productivity (mg/L/d) and the Beta carotene production (µg). This was observed when a pair of parameters were optimized whilst one parameter was kept constant. The interaction between Temperature and Nitrogen source on the bio productivity and beta carotene production is presented in A and B, respectively. The interaction between Salinity and Temperature on the bio productivity and beta carotene production, respectively, is presented in C and D, respectively, whilst the interaction between Salinity and Nitrogen source on the bio productivity and beta carotene production is presented in E and F, respectively.

As shown in Figures 3.10 – 3.12, the growth curves of the various treatments that *D. salina* was exposed to was grouped together according to the temperatures at which the treatments were grown. The reason for this was to allow a clearer picture of the growth rates of the *D. salina* at the different temperature. Figure 3.10 displays the growth rates of the *D. salina* at 25ºC. The highest growth rate occurred for the 3M NaCl and ammonia treatment. The reason for this could be due to the fact that *D. salina* prefers to grow at higher salinities. The 4M NaCl and sodium nitrate treatment also confirms this theory as the 4M NaCl and sodium nitrate treatment also has a relatively high growth rate. The 2M NaCl and sodium nitrate treatment had the most constant growth rate due to previous acclimatization to the conditions.

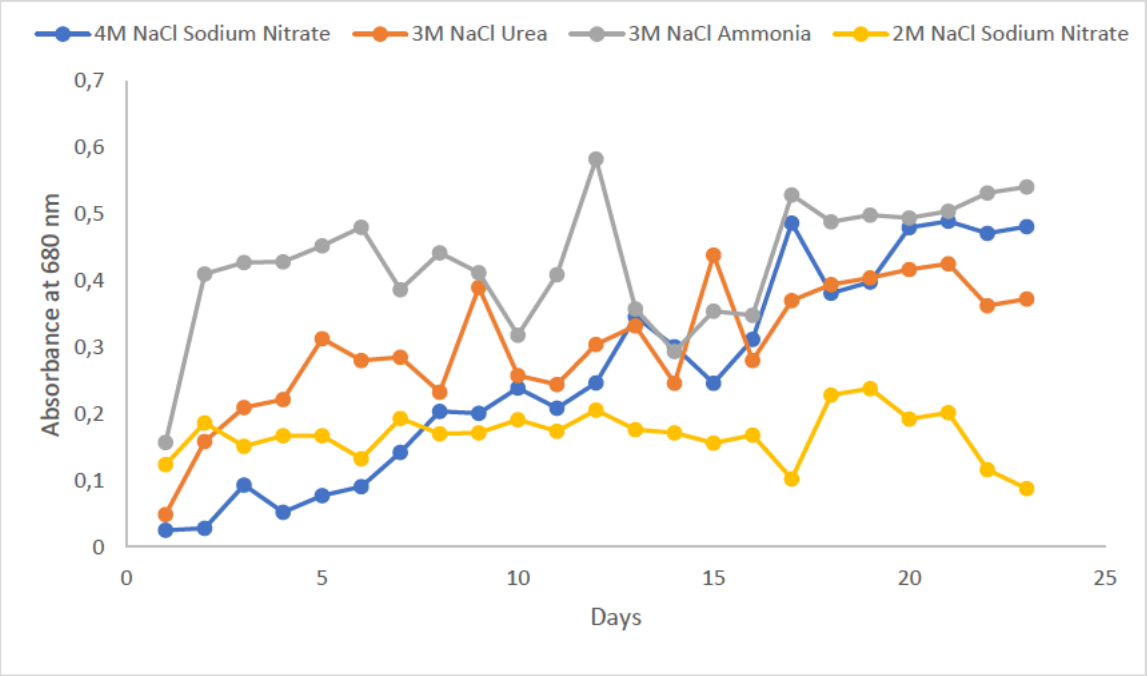

Figure 3.10: The Growth Curves of *D. salina* under different conditions at 25°C.

As shown in Figure 3.11, the growth curves of *D. salina* at 28ºC have constant growth rates. There were five treatments grown at 28°C as this was the middle point for the Response Surface Methodology set up with 4M NaCl and urea having the lowest growth curve. The limiting factor for growth at 4M NaCl is the urea as the treatment with 4M NaCl and ammonia has a higher growth rate. The 3M NaCl and sodium nitrate had the highest growth rate due to the high salinity. The 2M NaCl and urea treatment and the 2M NaCl and ammonia treatment had constant growth rates. The change in growth rate for

certain NaCl and nitrogen source combinations could have been the increased temperature.

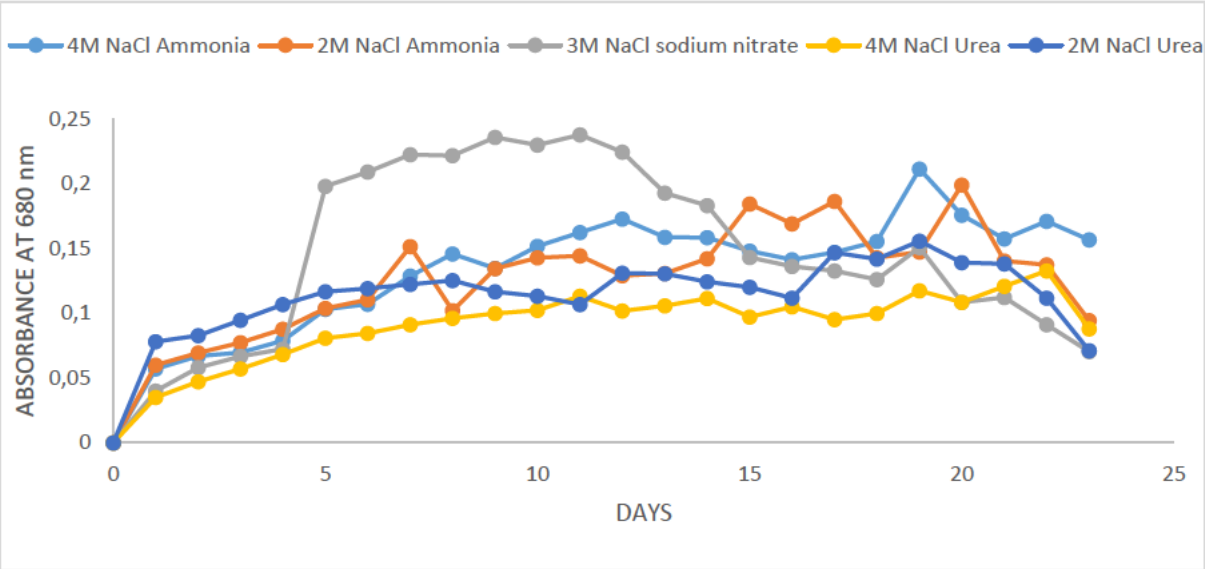

Figure 3.11: The Growth Curves of *D. salina* under different treatments at 28°C.

As shown in Figure 3.12, the growth curves of *D. salina* under different treatments at 32ºC show a constant growth rate. The highest growth rate is observed at 4M NaCl with sodium nitrate. This is due to the fact that *D. salina* prefers high NaCl salinities and sodium nitrate as the nitrogen source. The lowest growth rate was observed for the 2M NaCl with sodium nitrate as the cells were previously acclimatized to these conditions. The 3M NaCl with ammonia and the 3M NaCl with urea had constant growth rate which could have been impacted by the temperature.

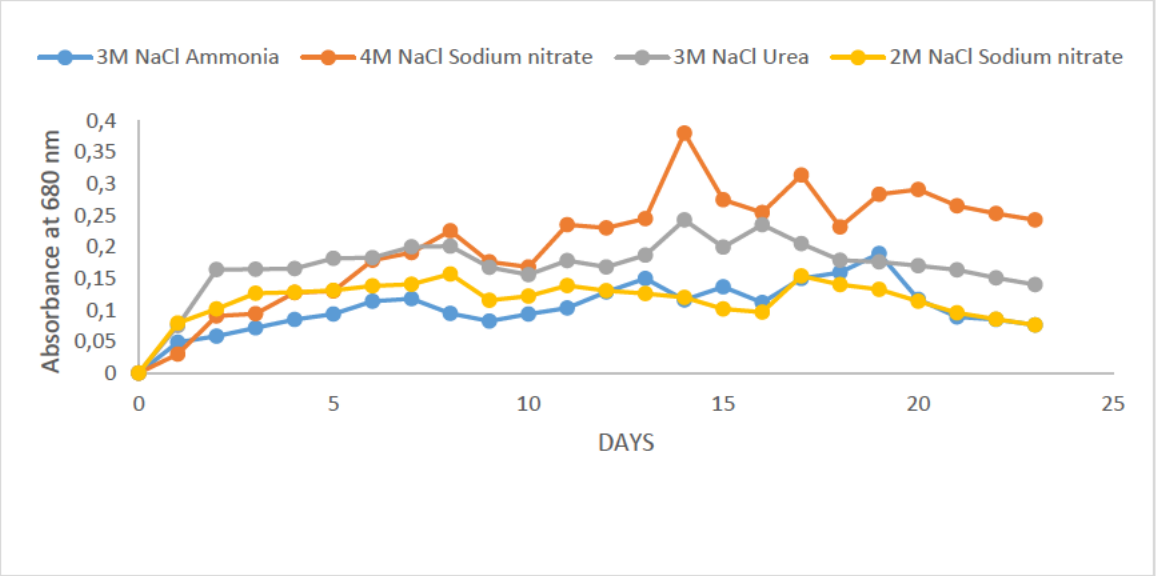

Figure 3.12: The Growth Curves of *D. salina* under different treatments at 32°C.

3.6 Discussion

D. salina has the affinity to grow in various different conditions as determined by the above experiment. The *D. salina* cells were able to grow in various saline concentrations and nitrogen sources. The cells grew best in high NaCl salinities as shown by the 3,5M NaCl treatment (Figure 3.3) and with urea as the nitrogen source as displayed by Figure 3.5. The lowest growth rate for the nitrogen source experiment (Figure 3.5) was observed for the control treatment. The lowest growth rate for the NaCl salinity experiment (Figure 3.3) was observed for the 2,5 M and 2M NaCl treatments. *D. salina* is highly adaptable to various conditions, however the growth rate of *D. salina* within these conditions vary according to the acclimitization of *D. salina*.

The NaCl salinity experiment growth curves in Figure 3.3 depict a picture of the capability of *D. salina* to inhabit the different salinities present within the Botash salt evaporation ponds. The results show that *D. salina* is indeed capable of surviving within high NaCl salinities, however the growth curves for each NaCl treatment showed the rate of acclimitization to each of the NaCl salinities. The fastest acclimitization occurred in the 2M NaCl treatment as shown by the growth curve and the maximum bioproductivity was also found for the 2M NaCl treatment (Figure 3.8). The rate of survival of the *D.*

salina cells within the NaCl treatments were high as can be seen by the bioproductivity of the cells (Figure 3.8). The growth curves for the NaCl salinity experiment showed that the cells are able to grow within the different NaCl salinities, however some growth curves were smoother than others such as the 2,5M NaCl salinity. The 2,5M treatment had a very steady growth curve indicating, that the *D. salina* cells acclimatized efficiently to this salinity. This indicates the cellular metabolism to tolerate this salinity (Gao *et al*., 2019). The rate of cell survival within the 2,5M NaCl treatment was also proved by Figure 3.4 which depicted the highest concentration of cells within the 2,5M NaCl treatment. The cell survival rate at the 3M and 3,5M NaCl treatments were also high even though the growth curves were not steady. The unsteady growth curves were due to the increased salinity which required acclimatization. The cell survival rate in the 3M and 3,5M NaCl was relatively low due to the fact that there were less cells of larger size as seen in Figure 3.4. Thus, the saline concentrations of 3M and 3,5M induced physiological stress as there were less cell counts within these concentrations.

There was however a significant difference between the growth curves of the different NaCl salinity treatments as shown in Figure 3.3. The reason for this difference in the growth curves was the difference in NaCl salinity and the varying responses the *D. salina* cells have to different NaCl salinities. As stated previously *D. salina* is able to inhabit a wide range of salinities, however the cells need time to adapt to these changing environments. This can be seen in the differing growth curves shown in Figure 3.3. The 2M and 2,5M NaCl treatments have the most steady growth curves due to the lower salinities. The 2,5M NaCl growth curve is slightly higher than that of the 2M NaCl treatment, however the bioproductivity of the 2M NaCl treatment is the highest for the salinity experiment. The higher growth curve for the 2,5M NaCl treatment could be due to the presence of more pigments within the cells grown in the 2,5M NaCl treatment as determined by Ahmed *et al*., 2017. The paper by Ahmed *et al*., determined that pigment synthesis increased with increasing salinity, therefore the higher optical densities observed for the higher NaCl treatments as opposed to the 2M NaCl treatment. The 3,5M NaCl had the lowest growth curve that suddenly had an increase in growth rate toward the end of the experiment. Thus, the growth curves of the NaCl treatments varied due to the adaptability of *D. salina* to the different NaCl salinities.

The treatments with the most abundant number of cells was the 2M and 2,5M NaCl treatments, this was due to the fact that the *D. salina* takes less time to acclimitize in lower salinities this was also shown by the paper by García *et al*., 2007. The paper written by García *et al*., 2007 aimed to determine the optimum salinity at which *D. salina* prefers to grow the results showed that the *D. salina* cells acclimitized to lower salinities faster. The results from this paper also showed that the cell size of *D. salina* increased as the salinity increased, thus there are fewer cells at higher salinities, however the cells present at these salinities are larger in size as can be seen in Figure 3.4 (García *et al*., 2007).

As shown in Figure 3.5, the growth curves for the nitrogen treatments follow a more subtle exponential phase. This is because the nitrogen source acts as a food source for the *D. salina* cells which means that nitrogen is consumed at a steady pace to insure normal growth of the cells (Sui *et al*., 2019). The control treatment which contained no nitrogen source reached the plateau the quickest due to the lack of nitrogen which slowed down cell division (Bonneford *et al*., 2017). The treatment that had the highest exponential phase was the Urea treatment, indicating the affinity of *D. salina* to grow and use Urea as the nitrogen source. The reason for *D. salina* being able to use urea as the nitrogen source is due to extracellular secretion that hydrolyse the urea into usable compounds (Sharma *et al*., 2017). This also increased the affinity of *D. salina* to urea as *D. salina* is known to secrete high amounts of EPS (Sharma *et al*., 2017). Figure 3.5 indicates the ability of *D. salina* to use any nitrogen source to grow and multiply and it also indicates that without nitrogen the cells do not multiply very quickly. The use of ammonia as the nitrogen source induced physiological stress within the *D. salina* cells as could be seen by the low growth rate and cell count.

The lowest bio productivity was observed for the control treatment (Figure 3.8). The reason for this is due to the lack of nitrogen which is required by algae cells for growth and reproduction (Espada *et al*., 2020). The highest productivity for all treatments was observed in the 2M treatment. This is due to the cells being in a stable environment and not having to acclimatize to a new environment before exponential growth. The 3,5M treatment had the second highest bio productivity which is an indication of the affinity of *D. salina* cells to grow in salinities as high as 3,5M (Fang *et al*., 2017). The rest of the treatments had average bio productivity, indicating that *D. salina* can indeed survive and grow in these conditions, however not at a fast pace. The highest bio productivity for the

nitrogen source experiment was observed in the Urea treatment. This is because *D. salina* can utilise urea as a nitrogen source efficiently (Lv *et al*., 2016). The nitrate and ammonia treatments had lower bio productivity than the urea treatment. This is because it takes *D. salina* time to acclimatize to changes in the environment. Nitrate is generally the source of nitrogen used whilst making media and, thus, *D. salina* cells are adapted to this nitrogen source and grow at a steady pace. Thus, the bio productivity shown in Figure 3.7 and 3.8 is an indication of the affinity of *D. salina* to grow in various conditions. The cells within all treatments look healthy (Figure 3.6), thus indicating their affinity to grow under different conditions. The number of cells vary within the treatment, indicating differing growth rates. Thus, the pictures of the cells serve as an indication of the viability of the cells within the different nitrogen source treatments.

The reason for the high concentrations of β-carotene as shown in Appendix A is because *D. salina* produces high concentrations of β-carotene under high stress conditions such as a change in nitrogen source or the increase in NaCl salinity (Ahmed *et al*., 2017). The LCMS results also showed the presence of various other pigments related to photosynthesis. The reason for this is due to the fact that the extract given for analysis was a crude extract containing all the pigments present within the *D. salina* cells. The reason for this was to acquire a better understanding of the pigments found within *D. salina* cells. The other peaks observed on the spectrum were obtained from a mixture of different pigments. The peak found at 871 m/z represents the compound Pheophytin A (National Center for Biotechnology Information, 2020). This compound is the primary electron acceptor in photosystem II. It is a chlorophyll molecule that lacks the central Mg^{2+} ion (Klimov, 2003). This molecule is of importance as it is a derivative of chlorophyll. The other molecules such as chlorophyll b and xanthophylls are also identified by peaks within the spectrum. The peak observed at 593 m/z indicates the presence of chlorophyll and its various derivatives as the distance within peaks 593 m/z and 871 m/z indicate the presence of chlorophyll (Milenković *et al.*, 2012). The reason for this is due to the mixing of chlorophyll and its derivatives whilst within the cells the chlorophyll molecule is always changing due to the addition and removal of the Mg^{2+} ion (Milenković *et al*., 2012). The above results for the LCMS indicate that beta carotene is indeed produced in high levels within *D. salina* in all conditions along with all the other pigments required for photosynthesis. The LCMS results therefore provide a very

accurate picture of the pigments required for photosynthesis by the *D. salina* cells. This photosynthesis although beneficial to the *D. salina* cells promotes the increase of microorganisms within the salt evaporation ponds which reduces the quality of salt produced (Javor, 2002).

The presence pigments such as β-carotene is highly beneficial to the salt production process as β-carotene is able to trap high amounts of sunlight (Ahmed *et al*., 2017). The sunlight trapped by β-carotene enables a higher rate of evaporation within the salt evaporation ponds, thus speeding up the salt production process (Javor, 2002). The presence of excessive amounts of β-carotene; however begins to discolor the salt crystals produced at the salt evaporation ponds, thus reducing the quality of salt produced (Javor, 2002).

The GCMS results (Appendix A) obtained for the different treatments indicate that glycerol is indeed produced by the *D. salina* cells. The two treatments that had no glycerol present were the nitrate and 2M treatments. The lack of glycerol could have been because the cells were placed in conditions that are common for the cells as these were the conditions in the stock culture. The retention time of glycerol indicates how long it takes glycerol to pass through the chromatography column (Lv *et al*., 2017). The retention time for glycerol varied among the different treatments. The reason for the variation could be due to the different conditions within the cultures because of the different treatments. The peak areas of the glycerol peaks from the different treatments also varied. This variation is because glycerol is produced in different concentrations in the different treatments. The control treatment for the nitrogen experiment had the highest peak area at 15.84. This result reiterates the fact that the lack of nitrogen does indeed stimulate stress reactions within the *D. salina* cells. Thus, the GC-MS results served as an indication of the effects of each treatment upon the *D. salina* cells. The full breakdown of the compounds within the GC-MS can be found in Appendix A.

The glycerol produced by *D. salina* is useful to the protect the cells from the harsh environment (Lv *et al*., 2017). However, the presence of this glycerol has a negative impact on the salt production process (Javor, 2002). The glycerol produced by *D. salina* is used by the microorganisms residing within the salt evaporation ponds as a food source which allows these organisms to grow within the salt evaporation ponds (Javor, 2002).

The growth of these organisms results in the increased carbon contamination of the salt crystals produced at Botash, reducing the quality of the salt produced and effecting the sale of the salt produced, thus reducing the profit acquired by Botash (Javor, 2002).

The P values for both experiments was below $p<0,005$, thus indicating a significant difference between the different tests and the control. The p-values obtained from the ANOVA tests for the NaCl salinity experiment and the nitrogen source experiment indicate that the change in NaCl salinity has more of an impact on the growth rate than the change in nitrogen source which impacts the amount of pigments and glycerol produced.

The Response Surface Methodology was used to optimize the responses of bio productivity and beta carotene production under the influence of independent variables such as temperature, nitrogen source and salinity. The variables individual and interactive effects upon the bio productivity and beta carotene production were analysed using the Box Behnken Design approach. The reason for analysing the bio productivity and beta carotene responses is that these responses are of importance. The reason for the bio productivity being of importance is that the collaborator in this project Botash has a *D. salina* problem in his crystallizer ponds that he wants investigated. Therefore, a better understanding of the bio productivity of *D. salina* under different conditions will allow for a better approach to the problem. The beta carotene response is important because it could serve as an additional source of income for Botash if the *D. salina* population cannot be controlled.

The results shown in Table 3.3 proves that there is an inverse relationship between the bio productivity response and beta carotene response. The reason for this is that beta carotene is generally produced by *D. salina* cells under stress conditions (Lou *et al*., 2020). Therefore, when the bio productivity is low the beta carotene production is high.

Tables 3.4, 3.5, 3.6, and 3.7 give the results for the ANOVA and Regression statistical analysis of the different variables involved in this experiment. The reason for the ANOVA and Regression values statistical analysis was to determine the statistical significance of the Box Behnken Design used in this experiment. The interaction coefficients of the different variables used in this experiment were all significant because they caused responses from both the bio productivity and beta carotene production. The regression

values indicated that the relationship between the variables and the responses was generally decent. The regression values generally serve as a correlation between the experimental and the predicted values. The higher the Regression values the better the correlation. Thus, it can be concluded that the Box Behnken Design was successful in optimizing the responses from bio productivity and beta carotene production.

The 3-dimensional figures displayed in Figure 3.9 are used to explain the influence that the different variations in the chosen variables have on the responses. They also enable the understanding of the interaction between the variables and the effects these interactions have on the responses (Hosseini *et al.*, 2017). The 3D plots represent the effects of two variables on the response whilst the third variable is kept constant to establish the effect the interaction of the variables has on the responses. Figure 3.9 A and B displayed the effects that the interaction of temperature and nitrogen source have on the responses. The relationship between beta carotene production and bio productivity is inverse. Therefore, an increased bio productivity would have a lower beta carotene production (Morowvat & Ghasemi, 2016). Figure 3.9 C and D show the reason for the inverse relationship between salinity and temperature on bio productivity and beta carotene production is that the higher the salinity the more beta carotene is produced because the cells activate beta carotene as a response to the increased salinity. The increase in temperature causes an increase in bio productivity because *D. salina* generally grows at higher temperatures (Xu & Harvey, 2019).

Figure 3.9 E and F represent the interaction between nitrogen source and salinity. The interaction between salinity and nitrogen has a positive effect on the beta carotene production whilst the bio productivity was the lowest in this interaction, showing that salinity and the nitrogen source used has a negative impact on bio productivity as it causes stress to the *D. salina* cells which allows for the increased beta carotene production (Xu *et al.*, 2018). Thus, the effect of salinity and nitrogen source on the beta carotene production is a positive whilst the bio productivity is drastically reduced in these conditions.

Figure 3.10 depicts the growth curve for the different treatments grown at 25℃. The growth of *D. salina* under these conditions depicts the affinity of *D. salina* to grow at 25℃. The treatment with the highest growth curve was the treatment at 25℃ with 3M

salinity and NH_4 (Ammonia) as the nitrogen source. The reason for the high growth rate of this treatment could be that *D. salina* grows better at higher salinities (Ahmed *et al*., 2017). The nitrogen source of Ammonia does not allow for the rapid growth of *D. salina* because it requires a lot more effort to break down Ammonia into the required nutrients (Dums *et al*., 2018). Therefore, it can be deduced that *D. salina* has an increased affinity to growing in 3M salinity. The lowest growth curve at 25℃ was for the 2M NO_3 treatment. This is because this was the normal conditions under which the *D. salina* was growing. Thus, there was no acclimatization period and the cells continued their constant growth rate. The other three treatments had an acclimatization period in which the growth rate was slow and then steadily began to increase. The normal condition treatment had a constant growth rate throughout (Perez-Boerema *et al*., 2020).

In figure 3.11 the reason for the 3M treatment with nitrate as the nitrogen source allowing for increased bio productivity is that the *D. salina* cells are adapted to being grown in such an environment as 3M is their optimal salinity whilst nitrate is the best source of nitrogen as they are well adapted to using nitrate as the nitrogen source (Ahmed *et al*., 2017). The lowest growth curve was observed for the 4M NaCl and Urea treatment as the salinity was to high and the cells went into physiological stress (Sharma *et al*., 2017).

The highest growth curve (Figure 3.12) for the treatments grown at 32℃ was the treatment using 4M salinity and NO_3 as the nitrogen source. The reason for this is that the increase in temperature affects the cellular mechanisms of *D. salina*, thus allowing them to grow at higher salinities (Wu *et al*., 2016). The lowest growth rate was observed for the 2M NO_3 and 3M NH_4 treatments. This again can be related to the effect that the temperature has on the *D. salina* cells as the physiochemical properties of the cells are changed, thus changing the conditions in which they can live (Wu *et al*., 2016). Thus, it can be concluded that temperature does have an impact on the growth rate of the *D. salina* cells.

In conclusion, the above results serve as an indication that salinity and nitrogen source have a potential impact on the growth rate, pigment and glycerol production of *D. salina* cells. The production of these compounds especially glycerol by the *D. salina* cells has a negative impact on the salt production process at Botash. This negative impact needs to be controlled to allow for better salt production. The beta carotene production of *D. salina*

was also optimized in an attempt to use this by-product as an alternative income source. The results of the RSM showed that there is an inverse relationship between bio productivity and beta carotene production, thus the optimizing of the conditions for beta carotene production within the ponds will naturally reduce the biomass of *D. salina* present. The results show that the optimal temperature for growth of *D. salina* is 30℃ with salinity being 3M and the nitrogen source nitrate as these are the standard conditions within most salt evaporation ponds (Sharma *et al*., 2017). Therefore, these conditions need to be avoided in order to prevent the excessive growth of *D. salina* and the introduction of conditions that allow for optimal beta carotene production must be introduced within the salt evaporation ponds.

3.7 References

Abdulsalam, A., Idris, A., Mohamed, T. A., & Ahsan, A. (2017). An integrated technique using solar and evaporation ponds for effective brine disposal management. *International Journal of Sustainable Energy*, *36*(9), 914-925.

Ahmed, R. A., He, M., Aftab, R. A., Zheng, S., Nagi, M., Bakri, R., & Wang, C. (2017). Bioenergy application of Dunaliella salina SA 134 grown at various salinity levels for lipid production. *Scientific Reports*, *7*(1), 1-10.

Bonnefond, H., Moelants, N., Talec, A., Mayzaud, P., Bernard, O., & Sciandra, A. (2017). Coupling and uncoupling of triglyceride and beta-carotene production by Dunaliella salina under nitrogen limitation and starvation. *Biotechnology for biofuels*, *10*(1), 25.

Dums, J., Murphree, C., Vasani, N., Young, D., & Sederoff, H. (2018). Metabolic and transcriptional profiles of Dunaliella viridis supplemented with ammonium derived from glutamine. *Frontiers in Marine Science*, *5*, 311.

Espada, J. J., Pérez-Antolín, D., Vicente, G., Bautista, L. F., Morales, V., & Rodríguez, R. (2020). Environmental and techno-economic evaluation of β-carotene production from Dunaliella salina. A biorefinery approach. *Biofuels, Bioproducts and Biorefining*, *14*(1), 43-54.

Fang, L., Qi, S., Xu, Z., Wang, W., He, J., Chen, X., & Liu, J. (2017). De novo transcriptomic profiling of Dunaliella salina reveals concordant flows of glycerol metabolic pathways upon reciprocal salinity changes. *Algal research*, *23*, 135-149.

Fan, L., Brett, M. T., Li, B., & Song, M. (2018). The bioavailability of different dissolved organic nitrogen compounds for the freshwater algae Raphidocelis subcapitata. *Science of the Total Environment*, *618*, 479-486.

Gao, X., Cong, Y., Yue, J., Xing, Z., Wang, Y., & Chai, X. (2019). Small RNA, transcriptome, and degradome sequencing to identify salinity stress responsive miRNAs and target genes in Dunaliella salina. *Journal of Applied Phycology*, *31*(2), 1175-1183.

Gao, S., Waller, P., Khawam, G., Attalah, S., Huesemann, M., & Ogden, K. (2018). Incorporation of salinity, nitrogen, and shading stress factors into the Huesemann Algae Biomass Growth model. *Algal research*, *35*, 462-470.

García, F., Freile-Pelegrín, Y., & Robledo, D. (2007). Physiological characterization of Dunaliella sp.(Chlorophyta, Volvocales) from Yucatan, Mexico. *Bioresource technology*, *98*(7), 1359-1365.

Hashemi, A., Moslemi, M., Pajoum Shariati, F., & Delavari Amrei, H. (2020). Beta-carotene production within Dunaliella salina cells under salt stress condition in an indoor hybrid helical-tubular photobioreactor. *The Canadian Journal of Chemical Engineering*, *98*(1), 69-74.

He, Q., Qiao, D., Bai, L., Zhang, Q., Yang, W., Li, Q., & Cao, Y. (2007). Cloning and characterization of a plastidic glycerol 3-phosphate dehydrogenase cDNA from Dunaliella salina. *Journal of plant physiology*, *164*(2), 214-220.

Hosseini, S. R. P., Tavakoli, O., & Sarrafzadeh, M. H. (2017). Experimental optimization of SC-CO2 extraction of carotenoids from Dunaliella salina. *The Journal of Supercritical Fluids*, *121*, 89-95.

Javor, B. J. (2002). Industrial microbiology of solar salt production. *Journal of Industrial Microbiology and Biotechnology*, *28*(1), 42-47.

Khoo, H. E., Prasad, K. N., Kong, K. W., Jiang, Y., & Ismail, A. (2011). Carotenoids and their isomers: color pigments in fruits and vegetables. *Molecules*, *16*(2), 1710-1738.

Klimov, V. V. (2003). Discovery of pheophytin function in the photosynthetic energy conversion as the primary electron acceptor of Photosystem II. *Photosynthesis research*, *76*(1-3), 247-253.

Lou, S., Zhu, X., Zeng, Z., Wang, H., Jia, B., Li, H., & Hu, Z. (2020). Identification of microRNAs response to high light and salinity that involved in beta-carotene accumulation in microalga Dunaliella salina. *Algal Research*, *48*, 101925.

Lv, H., Cui, X., Tan, Z., & Jia, S. (2017). Analysis of metabolic responses of Dunaliella salina to phosphorus deprivation. *Journal of Applied Phycology*, *29*(3), 1251-1260.

Lv, H., Cui, X., Wang, S., & Jia, S. (2016). Metabolic profiling of Dunaliella salina shifting cultivation conditions to nitrogen deprivation. *Metabolomics*, *6*(170), 2153-0769.

Milenković, S. M., Zvezdanović, J. B., Anđelković, T. D., & Marković, D. Z. (2012). The identification of chlorophyll and its derivatives in the pigment mixtures: HPLC-chromatography, visible and mass spectroscopy studies. *Adv Technol*, *1*(1), 16-24.

Monte, J., Ribeiro, C., Parreira, C., Costa, L., Brive, L., Casal, S., Brazinha, C. and Crespo, J.G. (2020). Biorefinery of Dunaliella salina: Sustainable recovery of carotenoids, polar lipids and glycerol. *Bioresource Technology*, *297*, p.122509.

Monte, J., Sá, M., Galinha, C. F., Costa, L., Hoekstra, H., Brazinha, C., & Crespo, J. G. (2018). Harvesting of Dunaliella salina by membrane filtration at pilot scale. *Separation and Purification Technology*, *190*, 252-260.

Mordhay, A. & Ben-Amotz, A. (1978). *Production of glycerol from algae*. US Intellectual Property Office Patent no. US4115949A. Available at: https://patents.google.com/patent/US4115949A/en (Accessed: 20 January 2021).

Morowvat, M. H., & Ghasemi, Y. (2016). Culture medium optimization for enhanced β-carotene and biomass production by Dunaliella salina in mixotrophic culture. *Biocatalysis and agricultural biotechnology*, *7*, 217-223.

Mussagy, C. U., Winterburn, J., Santos-Ebinuma, V. C., & Pereira, J. F. B. (2019). Production and extraction of carotenoids produced by microorganisms. *Applied microbiology and biotechnology*, *103*(3), 1095-1114.

Myers, R. H., Montgomery, D. C., & Anderson-Cook, C. M. (2016). *Response surface methodology: process and product optimization using designed experiments*. John Wiley & Sons.

National Center for Biotechnology Information. PubChem Database. beta-Carotene, CID=5280489, https://pubchem.ncbi.nlm.nih.gov/compound/beta-Carotene (accessed on May 27, 2020)

National Center for Biotechnology Information. PubChem Database. Pheophytin a, CID=135398712, https://pubchem.ncbi.nlm.nih.gov/compound/Pheophytin-a (accessed on May 27, 2020)

Perez-Boerema, A., Klaiman, D., Caspy, I., Netzer-El, S. Y., Amunts, A., & Nelson, N. (2020). Structure of a minimal photosystem I from the green alga Dunaliella salina. *Nature plants*, *6*(3), 321-327.

Polle, J.E., Barry, K., Cushman, J., Schmutz, J., Tran, D., Hathwaik, L.T., Yim, W.C., Jenkins, J., McKie-Krisberg, Z., Prochnik, S. and Lindquist, E. (2017). Draft nuclear genome sequence of the halophilic and beta-carotene-accumulating green alga Dunaliella salina strain CCAP19/18. *Genome Announc.*, *5*(43), pp.e01105-17.

Ross, M. E., Davis, K., McColl, R., Stanley, M. S., Day, J. G., & Semião, A. J. (2018). Nitrogen uptake by the macro-algae Cladophora coelothrix and Cladophora parriaudii: Influence on growth, nitrogen preference and biochemical composition. *Algal research*, *30*, 1-10.

Sanchez, G., Nova, J., Rodriguez-Hernandez, A.E., Medina, R.D., Solorzano-Restrepo, C., Gonzalez, J., Olmos, M., Godfrey, K. and Arevalo-Rodriguez, I. (2016). Sun protection for preventing basal cell and squamous cell skin cancers. *Cochrane Database of Systematic Reviews*, (7).

Sharma, J., Kumar, S., Sharma, P., Gupta, S., Manju, T., Malyan, S., & Bishnoi, N. (2017). Effect of different nitrogen sources on growth of algal consortia. *Annals of Agri-bio Research*, *22*(2), 150-153.

Shurtz, B. K., Wood, B., & Quinn, J. C. (2017). Nutrient resource requirements for large-scale microalgae biofuel production: Multi-pathway evaluation. *Sustainable Energy Technologies and Assessments*, *19*, 51-58.

Sommer, A. (2001). Vitamin A deficiency. *e LS*.

Sui, Y., Muys, M., Van de Waal, D. B., D'Adamo, S., Vermeir, P., Fernandes, T. V., & Vlaeminck, S. E. (2019). Enhancement of co-production of nutritional protein and carotenoids in Dunaliella salina using a two-phase cultivation assisted by nitrogen level and light intensity. *Bioresource technology*, *287*, 121398.

Takekawa, J.Y., Miles, A.K., Schoellhamer, D.H., Athearn, N.D., Saiki, M.K., Duffy, W.D., Kleinschmidt, S., Shellenbarger, G.G. and Jannusch, C.A., 2006. Trophic structure and avian communities across a salinity gradient in evaporation ponds of the San Francisco Bay estuary. *Hydrobiologia*, *567*(1), pp.307-327.

Vaidya, G., & Naik, G. R. (2018). Comparative Evaluation of Bioproductivity Studies of Simarouba, Pongamia and Jatropha for Biodiesel Parameters. *Int J Cur Res Rev*| *Vol*, *10*(5), 46.

Wei, S., Bian, Y., Zhao, Q., Chen, S., Mao, J., Song, C., Cheng, K., Xiao, Z., Zhang, C., Ma, W. and Zou, H., 2017. Salinity-induced palmella formation mechanism in halotolerant algae Dunaliella salina revealed by quantitative proteomics and phosphoproteomics. *Frontiers in plant science*, *8*, p.810.

Wu, Q., Lan, Y., Cao, X., Yao, H., Qiao, D., Xu, H., & Cao, Y. (2019). Characterization and diverse evolution patterns of glycerol-3-phosphate dehydrogenase family genes in Dunaliella salina. *Gene*, *710*, 161-169.

Wu, Z., Duangmanee, P., Zhao, P., Juntawong, N., & Ma, C. (2016). The effects of light, temperature, and nutrition on growth and pigment accumulation of three Dunaliella salina strains isolated from saline soil. *Jundishapur journal of microbiology*, *9*(1).

Xu, Y., & Harvey, P. J. (2019). Carotenoid production by Dunaliella salina under red light. *Antioxidants*, *8*(5), 123.

Xu, Y., Ibrahim, I. M., Wosu, C. I., Ben-Amotz, A., & Harvey, P. J. (2018). Potential of new isolates of Dunaliella salina for natural β-carotene production. *Biology*, *7*(1), 14.

Zhao, F., & Filker, S. (2018). Characterization of protistan plankton diversity in ancient salt evaporation ponds located in a volcanic crater on the island Sal, Cape Verde. *Extremophiles*, *22*(6), 943-954.

CHAPTER FOUR: THE EFFECT OF THE DIFFERENT TREATMENTS ON EXTRAPOLYSACCHARIDES AND THE SALT CRYSTALS

4.1 Abstract

Salt is one of the most important compounds in the world. Salt production can occur in two forms. These are: the process of using seawater as the starting material which is the more popular choice. Underground brine sources are also used as the starting material for salt production. The latter is of interest as salt evaporation ponds contain various forms of microorganisms. The focus has been placed on *D. salina* which is a green microalga that is found in abundance in salt evaporation ponds. These microalgae produce extra polysaccharides that are secreted into the environment. This paper aimed to identify the constituents of the EPS produced by *D. salina* under different conditions and to determine their effect on the salt crystals produced. The EPS was extracted from the media in which the cells were grown during various experiments and sent for HPLC analysis. An FTIR analysis of the salt crystals was also performed. The results depicted the presence of various compounds. The EPS is primarily composed of mono and polysaccharides such as Arabinose which helps with the survival of the cells in saline environments. The other compounds enable communication between the cell and act as a food source for the other microorganisms living within the salt evaporation ponds. The presence of these EPS molecules affects salt purity negatively and thus, more research needs to be done to prevent the contamination of the salt crystals.

4.2 Introduction

Salt is one of the most important compounds in the world. Salt has been used from prehistoric times as a method to flavor and preserve food (Adshead, 2016). Salt is a composition of two chemicals sodium and chloride. These chemicals combine to form a lattice network which gives the salt its crystal appearance (Suhendra, 2016). Salt is

present mostly in the ocean as it is the main mineral constituent of seawater (Cinku & Karabulut, 2020). Thus, the production of salt crystals is of importance as it is the only way to produce salt for human consumption (Suhendra, 2016).

One of the most important microorganisms present within the salt evaporation ponds is the green alga *Dunaliella salina* (*D. salina*). This green alga is generally found within highly saline environments such as salt evaporation ponds. *D. salina* is known for its ability to survive at high salinities (Xu & Harvey, 2019). The *D. salina* cells also produce compounds like beta carotene and extra polysaccharides. *D. salina* produces beta carotene an orange pigment as a technique to protect the cell against the harsh conditions within the salt evaporation ponds such as the high levels of sunlight the cells are exposed to within the salt evaporation ponds (Bonnefond *et al*., 2017). The beta carotene produced by the *D. salina* cells traps the harmful UV rays from sunlight and protects the cell from photodamage (Bonnefond *et al*., 2017). The beta carotene produced is also useful to the pharmaceutical industry as it is used as an ingredient in Sun protective lotions and as a dietary supplement for Vitamin A (Harvey & Ben-Amotz, 2020). The production of extra polysaccharides (EPS) by *D. salina* is of interest as these EPS are excreted by the cells into the environment and affect the quality of the salt produced.

Extra Polysaccharides or EPS are substances that are excreted into the environment by microorganisms (Staudt *et al*., 2004). The EPS excreted by organisms are natural polymers that help the microorganisms adapt to the environment (Staudt *et al*., 2004). *D. salina* also excretes such EPS molecules into the environment (Mishra *et al*., 2011). The EPS molecules produced by *D. salina* enable the cells to survive in the highly saline environment in which they reside. The EPS produced by *D. salina* is of importance to the health industry as the EPS produced by *D. salina* has been shown to affect cancer cell lines (Chawla, 2019). Thus, the production of EPS by *D. salina* is of interest to the health industry. Although the EPS secreted by *D. salina* can be useful to the health industry the secretion of these EPS have a negative impact on the quality of salt produced (Javor, 2002). The EPS produced by *D. salina* coats the salt crystals produced in the salt evaporation ponds thus reducing the quality of salt produced (Javor, 2002). The EPS also reduces the size of the crystals produced and changes the color of the salt crystals (Javor, 2002). There is not much research provided on the possible secretion of EPS by the other

microorganisms within the salt evaporation ponds as these organisms are generally not as dominant as *D. salina* within the salt evaporation ponds.

This chapter will aim to establish the chemical constituents within the EPS produced by *D. salina* cells and determine the presence of these constituents on the FTIR of the salt crystals from Botash. This paper will also determine the effect that the environment has on the amount and constituents of the EPS produced. The *D. salina* EPS analyzed for this chapter was obtained from the various experiments performed in previous chapters such as the RSM study and the saline concentration and nitrogen source study. Thus, this chapter will aim to establish the relationship between the environment, EPS production, and salt quality.

4.3 Aims and Objectives

Aims

This chapter aims to fulfil the main objective 4 of this research thesis.

Objectives

1. To analyze the salt crystals from Botash via FTIR for the presence of impurities.
2. To analyze the EPS produced by *D. salina* under different conditions using HPLC-MS to determine the relationship between the EPS and the impurities on the salt crystals.
3. To determine the effect that the different experimental conditions such as the RSM, salinity and nitrogen experiment have on the EPS produced and the contamination of the salt crystals.

4.4 Methods

The following experimental procedures were performed during this experiment.

4.4.1 *EPS extraction and analysis*

The *D. salina* cells that were exposed to different treatments in the RSM and saline concentration and nitrogen experiments for 25 days. The results of these experiments are detailed in the previous chapters. The reason for using the cells from the above mentioned experiments was because these different experiments highlight a wide range of possible environments in which *D. salina* can grow. Thus, an estimation of the environmental impact on salt purity can be analysed from these results. The following process was performed on the treated *D. salina* cells. The cells suspended in media were obtained and 15 ml of this mixture was centrifuged down. The pellet was used for other extraction protocols whilst the media was used for the extraction of EPS. The EPS was obtained by adding an equal volume of 99% alcohol to the media obtained from the treatments. The mixture was then vortexed for 20 minutes before being put into the -30ºC freezer for four hours. After four hours the EPS had formed a pellet at the bottom of the tube this pellet was washed in 100% alcohol three times to remove impurities. The pellet was then resuspended in distilled water and sent for High-Performance Liquid Chromatography which analyses both the absorbance and mass of the compounds present within the EPS samples.

4.4.2 *Botash salt crystals analysis*

The salt crystals obtained from Botash were analyzed by FTIR as follows: One eighth of the salt crystal sample was mixed with ground potassium bromide crystals. The sample was pressed together with the potassium bromide in a press to obtain a flat nearly clear disc that was placed in the FTIR sample holder. The sample was analyzed in the FTIR apparatus which had been set to scan the sample eight times with a resolution of 2 cm^{-1} and the final format of absorbance for the 400 cm^{-1} to the 4000 cm^{-1} range.

4.4.3 *Analysis of the FTIR Spectra of the Botash Salt Crystals*

The FTIR spectra obtained from the analysis of the salt crystals was analyzed by the input of each of the peaks present on the spectra into a software program, to determine which chemical groups were present in the salt crystals. The software program used in this study was IRPal2.0.

4.5 Results

As shown in Appendix A, the HPLC-MS chromatograms for the various treatments that *D. salina* underwent are depicted. These chromatograms show various peaks at different retention times. The peaks represent various different molecules that are present within the EPS such as polysachharides containing the hydroxyl, carbonyl and alkyl groups as well hexoses and pentoses which are hetero-polysaccharides (Goyal *et al.*, 2019). The most highest concentration was obtained at the 17 minute mark for all treatments. This peak represents the presence of the Arabinose sugar which helps with salt stress (Zhao *et al.*, 2019). The reason for this sugar being present in the EPS is to enable acclimatization to the high salt levels within the Botash salt evaporation ponds. The EPS samples also have various other sugars such as ribose present which help the cell survive within the high salt environments at the Botash ponds. The EPS samples also contain sulphated polysaccharides and aromatic compounds which enable the survival and proliferation of the *D. salina* cells.

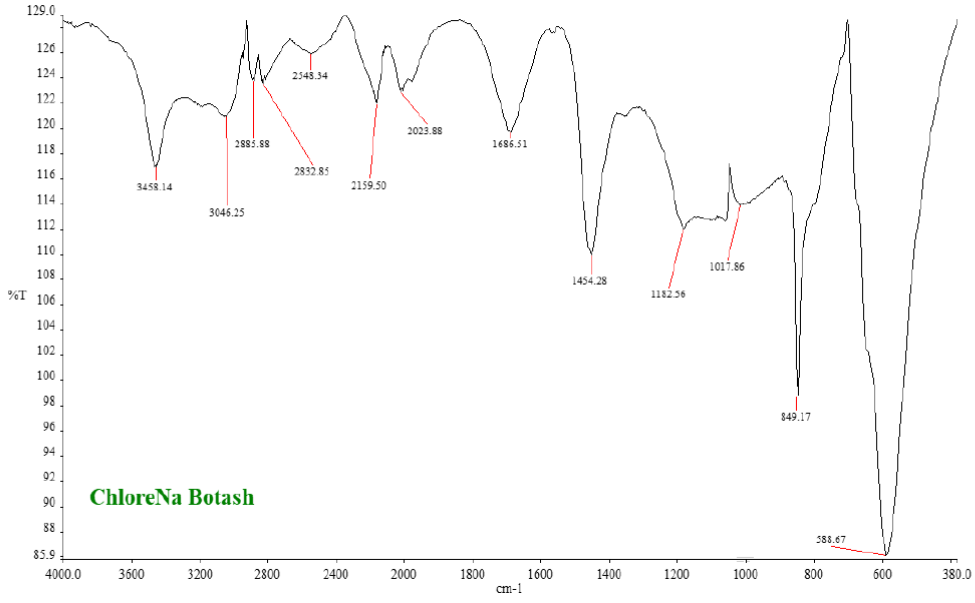

Figure 4.1: FTIR Spectrum of NaCl from Botash.

The results above depict various peaks along the length of the spectrum, these peaks can be found at the following locations 3458 cm^{-1}, 3046 cm^{-1}, 2885 cm^{-1}, 2832 cm^{-1}, 2548 cm^{-}

[1], 2159 cm^{-1}, 2023 cm^{-1}, 1686 cm^{-1}, 1454 cm^{-1}, 1182 cm^{-1}, 1017 cm^{-1}, 849 cm^{-1} and 588 cm^{-1}.

Table 4.1: Chemical Groups present on Salt Crystals.

Peak on FTIR	**Assignment**	**Chemical Groups**
3458 cm^{-1}	NH_2 Stretch	Amine Group
3046 cm^{-1}	NH_4 Group	Ammonia
2885 cm^{-1}	RCH_2CH_3, C-H Stretch	Methyl group
2832 cm^{-1}	R-CHO, C-H Stretch	Aldehyde group
2548 cm^{-1}	RCO-OH Stretch	Carboxyl Group
2159 cm^{-1}	R-N-C Stretch	Carbamide Group
2023 cm^{-1}	R-N=C=S Stretch	Isothiocyanate Group
1686 cm^{-1}	C=N Stretch	Quinones
1454 cm^{-1}	AR C-C Stretch	Nitroso Compound
1182 cm^{-1}	S=O Sulfonyl Chloride	Sulfone Group
1017 cm^{-1}	RCOOR’ C-O Stretch	Esters
849 cm^{-1}	C-H out of plane	Aromatic compounds
558 cm^{-1}	C-Br Stretch	Alkyl Groups

The results obtained from the FTIR analysis can be related to the EPS results due to the presence of similar compounds. There is no statistical test that can be performed due to the lack of quantities in both sets of results, however the different compounds identified in the EPS due to specific retention times are the same compounds that are identified on the FTIR spectra. The presence of hydroxyl, carbonyl and alkyl groups as well hexoses and pentoses which are hetero-polysaccharides are identified in the EPS samples and the FTIR spectra of the salt crystals from Botash. The sugars such as ribose and arabinose are

identified by the presence of alkyl groups on the FTIR spectra of the salgt crystals. Table 4.2 will give the retention times for the various sugars which might be present in the EPS whilst the Table 4.1 shows all the carbon contaminants present on the salt crystals from Botash. The presence of similar compounds in both sets of results prove that the EPS does indeed cause the contamination of the salt crystals.

Table 4.2: The Retention times of Monosaccharides and Polysaccharides Generally found in EPS samples.

COMPOUND	RETENTION TIME
Ribose	12,5 minutes
Xylose	14,6 minutes
Arabinose	17,2 minutes
Fucose	17,4 minutes
Mannose	21,3 minutes
Glucose	22,5 minutes

The table was obtained from the publication of Lopes & Gasper, 2008.

4.6 Discussion

The HPLC results depicted above show the retention times of the various polysaccharide compounds found within the EPS sample obtained from the *D. salina* cells. The retention time of a compound is important as it determines the polarity of a compound. Polarity is the affinity of a compound to water with polar compounds being eluted first from the HPLC column and thus having a low retention time and apolar molecules having higher retention times (Vahteristo *et al*., 1996). The elution of the compounds occurs because of the mobile phase that is passed through the column. The mobile phase is generally water

mixed with acetonitrile in a gradient with the concentration of acetonitrile increasing as the elution process progresses (Vahteristo *et al*., 1996).

The different retention times featured within the chromatograms are proof of the presence of different EPS compunds within the samples obtained from Botash. These EPS are in the form of polysaccharides and monosaccharides (Mishra *et al*., 2011). The monosaccharides are the building blocks for the polysaccharides present within the EPS samples, therefore the monosaccharides are also present within the samples as the polysaccharides are broken down into monosaccharides due to environmental conditions (Elifantz *et al*., 2005). The peak heights at the different retention times display the concentration of the various EPS molecules within each sample.

Table 4.2 displays retention times of the various poly and monosaccharides found within the EPS samples obtained from *D. salina* cells in different journal articles regarding EPS analysis of *D. salina* (Lopes & Gasper, 2008). The above table depicts that there are generally various poly and monosaccharides present within the EPS from *D. salina*. Along with these polysaccharides, there are also sulphated polysaccharides, proteins, and uronic acid along with aromatic compounds present within the EPS (Mishra *et al*., 2011). Thus, the EPS produced by *D. salina* is of importance and use to various sectors as the constituents can be used for various purposes (Natarajan *et al*., 2008).

The sugars mentioned in table 4.2 all have different functions within the EPS. Arabinose sugar which is the most abundant saccharide according to concentration is generally found in nature as a constituent of hemicellulose and pectin (Xu *et al*., 2018). Arabinose is also known to be synthesized by plants like Arabidopsis to enable salt stress tolerance (Zhao *et al*., 2019). The arabinose sugar can also be playing the same role within the EPS as it can also enable the cells to survive in the high salinities which they inhabit. The graphs with the highest concentration of Arabinose with the concentration at 75 mAU were the graphs from the salinity experiment and also the NH_4, and the control treatment from the nutrient experiment. The reason for this could be that the nitrogen source effects the salinity response of the cells thus, triggering more arabinose to be produced (Xiao & Zheng, 2016). The treatments from the RSM also featured arabinose levels of 75 mAU. Figures 10, 11, 15, and 19 all had arabinose levels at 75 mAU. The reason for this is the

presence of NH_4 and high salinities in the treatments that observed the high concentrations of arabinose.

These biological compounds are generally found within the cells or as secretions from microorganisms (Enache *et al*., 2017). The presence of these biological compounds causes a deterioration in the salt produced at Botash, hence the exact nature of these products needs to be known in order to develop a method of removal (Silva-Castro *et al*., 2015). The identification of the biological compounds present on the salt crystals can be completed by matching the pattern of peaks present in the FTIR Spectra from the salt crystals to FTIR spectra obtained from other biological compounds.

The analysis of the FTIR spectra from the salt crystals shows similarities to various biological compounds found in the EPS analysis of *D. salina*. One of the most important biological compounds found on the salt crystals is beta carotene, this can be seen from the spectrum of beta carotene which indicates a peak at around 970 cm^{-1} as shown in Appendix A.

The beta carotene peak in the FTIR Spectra of the salt crystals from Botash can be found at 1017 cm^{-1}, the shift in the spectra of the beta carotene is as a result of the presence of various other biological compounds, which mix together and cause a shift in the spectra of a particular compound (Güven *et al*., 2015).

The presence of arabinose and all the other sugars within the EPS benefits the *D. salina* cells by allowing them to be able to live within the salt evaporation ponds. These sugars are however detrimental to the quality of salt produced as can be seen in the FTIR spectra. The presence of these sugars within the environment leads to the salt crystals produced being coated with a polysaccharide slime (Oren, 2010). The effect of this polysaccharide slime is the increase in carbon and decrease in pure salt produced within the salt evaporation ponds as displayed by the FTIR spectra of the salt crystals. The increase in the EPS coating of the salt crystals decreases the size of the crystals and also increases the water retention of the salt crystals thus, making the salt of inferior quality (Oren, 2010). The carbon contamination of salt is closely monitored and if there is excessive carbon contamination of the salt crystals the salt is not accepted for sale for human consumption (Oren, 2010). The other detrimental aspect of the presence of excessive

carbon contamination is the reduction in the production of soda ash which is more valuable then the salt produced (Oren, 2002).

The different environmental conditions established during the RSM, nitrogen and salinity experiments have an impact on the concentration of EPS compounds produced. All the HPLC-MS results from all these experiments depict that similar EPS compounds are produced under all environmental conditions although in different concentrations and these EPS compounds are the same compounds that are found on the FTIR spectra of the salt crystals. This result proves that no matter the environmental conditions EPS of the same composition is always produced and this EPS results in the decrease in purity of the salt crystals. These results depict that *D. salina* is in fact the cause of the organic contamination of the salt crystals produced at Botash as the EPS compounds produced by *D. salina* in all conditions is the same types of compounds found on the FTIR analysis of the salt crystals from Botash.

The FTIR spectra showed the presence of all the polysaccharides that constitute the EPS of *D. salina*. These compounds pollute the crystallizer ponds and coat the salt crystals which reduces the production of soda ash (Javor, 2002). Soda ash is the main source of income for Botash and any reduction in the production and quality of soda ash is detrimental to Botash. The above results show that EPS is produced in all situations by *D. salina*. This is of concern as these EPS molecules is inhibiting the production of pure quality salt and soda ash. Therefore in order for Botash to become profitable the EPS production of *D. salina* needs to be controlled.

To conclude the presence of EPS is generally useful to the cells and humans if harvested. However, when present in the salt evaporation ponds at the levels shown above it influences the salt crystals produced. The salt crystals produced are of inferior quality and cannot be consumed by humans. The presence of the EPS produced by *D. salina* on the crystals has an impact on the quality of the salt because of the excessive amount of carbon present thus making the salt inconsumable. Therefore, a method to remove the EPS from the ponds before the effect the purity of the salt crystals needs to be investigated.

4.7 References

Adshead, S. A. M. (2016). *Salt and civilization*. Springer.

Bonnefond, H., Moelants, N., Talec, A., Mayzaud, P., Bernard, O., & Sciandra, A. (2017). Coupling and uncoupling of triglyceride and beta-carotene production by Dunaliella salina under nitrogen limitation and starvation. *Biotechnology for Biofuels*, *10*(1), 25.

Chawla, B. (2019). *Effect of Exopolysaccharides Produced under Stress Conditions by Dunaliella Salina on the Growth of Cancer Cell Lines and Peripheral Blood Mononuclear Cells* (Doctoral dissertation).

Çinku, M. C., & Karabulut, S. (2020). *Salt in the Earth*.

Dai, J., Wu, Y., Chen, S. W., Zhu, S., Yin, H. P., Wang, M., & Tang, J. (2010). Sugar compositional determination of polysaccharides from Dunaliella salina by modified RP-HPLC method of pre-column derivatization with 1-phenyl-3-methyl-5-pyrazolone. *Carbohydrate polymers*, *82*(3), 629-635.

Elifantz, H., Malmstrom, R. R., Cottrell, M. T., & Kirchman, D. L. (2005). Assimilation of polysaccharides and glucose by major bacterial groups in the Delaware Estuary. *Applied and environmental microbiology*, *71*(12), 7799–7805. https://doi.org/10.1128/AEM.71.12.7799-7805.2005

Goyal, M., Baranwal, M., Pandey, S. K., & Reddy, M. S. (2019). Hetero-Polysaccharides Secreted from Dunaliella salina Exhibit Immunomodulatory Activity Against Peripheral Blood Mononuclear Cells and RAW 264.7 Macrophages. *Indian journal of microbiology*, *59*(4), 428-435.

Goyal, M., & Baranwal, M. G. (2017). *Characterisation of exopolysaccharides isolated from Dunaliella salina exhibiting immunomodulation in peripheral blood mononuclear cells and RAW 264.7 macrophages* (Doctoral dissertation).

Harvey, P. J., & Ben-Amotz, A. (2020). Towards a sustainable Dunaliella salina microalgal biorefinery for 9-cis β-carotene production. *Algal Research*, *50*, 102002.

Javor, B. J. (2002). Industrial microbiology of solar salt production. *Journal of Industrial Microbiology and Biotechnology*, *28*(1), 42-47.

Liu L, Pohnert G, Wei D. Extracellular Metabolites from Industrial Microalgae and Their Biotechnological Potential. *Mar Drugs*. 2016;14(10):191. Published 2016 Oct 20. doi:10.3390/md14100191

Lopes, J & Gaspar, E. (2008). Simultaneous chromatographic separation of enantiomers, anomers and structural isomers of some biologically relevant monosaccharides. Journal of chromatography. A. 1188. 34-42. 10.1016/j.chroma.2007.12.016.

Mishra, A., Kavita, K., & Jha, B. (2011). Characterization of extracellular polymeric substances produced by micro-algae Dunaliella salina. *Carbohydrate Polymers*, *83*(2), 852-857.

Monte, J., Ribeiro, C., Parreira, C., Costa, L., Brive, L., Casal, S., Brazinha, C. and Crespo, J.G., 2020. Biorefinery of Dunaliella salina: Sustainable recovery of carotenoids, polar lipids and glycerol. *Bioresource Technology*, *297*, p.122509.

Natarajan, S., Lakshmi, D. S., Thiagarajan, V., Mrudula, P., Chandrasekaran, N., & Mukherjee, A. (2018). Antifouling and anti-algal effects of chitosan nanocomposite (TiO2/Ag) and pristine (TiO2 and Ag) films on marine microalgae Dunaliella salina. *Journal of environmental chemical engineering*, *6*(6), 6870-6880.

Oren, A. (2010). Thoughts on the “missing link” between saltworks biology and solar salt quality. *Global NEST J*, *12*(4), 417-425.

Raposo, M. F., de Morais, R. M., & Bernardo de Morais, A. M. (2013). Bioactivity and applications of sulphated polysaccharides from marine microalgae. *Marine drugs*, *11*(1), 233–252.

Seedevi, P., Sudharsan, S., Kumar, S. V., Srinivasan, A., Vairamani, S., & Shanmugan, A. (2013). Isolation and characterization of sulphated polysaccharides from Codium tomentosum (J. Stackhouse, 1797) collected from southeast coast of India. *Adv Appl Sci Res*, *4*(5), 72-77.

Staudt, C., Horn, H., Hempel, D. C., & Neu, T. R. (2004). Volumetric measurements of bacterial cells and extracellular polymeric substance glycoconjugates in biofilms. *Biotechnology and bioengineering*, *88*(5), 585-592.

Suhendra, A. (2016). Increasing The Productivity of Salt Trought HDPE Geomembrane Indonesia Case History in Salt Evaporation Pond. *EJGE*, *11*, 4272-4280.

Vahteristo, L., Finglas, P. M., Witthöft, C., Wigertz, K., Seale, R., & de Froidmont-Görtz, I. (1996). Third EU MAT intercomparison study on food folate analysis using HPLC procedures. *Food chemistry*, *57*(1), 109-111.

Winkelhausen, E., & Kuzmanova, S. (1998). Microbial conversion of D-xylose to xylitol. *Journal of Fermentation and Bioengineering*, *86*(1), 1-14.

Xiao, R., & Zheng, Y. (2016). Overview of microalgal extracellular polymeric substances (EPS) and their applications. *Biotechnology Advances*, *34*(7), 1225-1244.

Xu, Y., & Harvey, P. J. (2019). Carotenoid production by Dunaliella salina under red light. *Antioxidants*, *8*(5), 123.

Xu, X. L., Tong, W. X., Lei, Y. L., & Yao, S. J. (2007). Separation and purification of extracellular polysaccharides from Dunaliella salina. *J Food Sci Biotechnol*, *26*(4), 28-33.

Xu, W., Zhang, W., Zhang, T., Jiang, B., & Mu, W. (2018). L-arabinose isomerases: Characteristics, modification, and application. *Trends in Food Science & Technology*, *78*, 25-33.

Zhang, J., Liu, L., Ren, Y., & Chen, F. (2019). Characterization of exopolysaccharides produced by microalgae with antitumor activity on human colon cancer cells. *International journal of biological macromolecules*, *128*, 761-767.

Zhao, C., Zayed, O., Zeng, F., Liu, C., Zhang, L., Zhu, P., Hsu, C.C., Tuncil, Y.E., Tao, W.A., Carpita, N.C. and Zhu, J.K., 2019. Arabinose biosynthesis is critical for salt stress tolerance in Arabidopsis. *New Phytologist*, *224*(1), pp.274-290.

CHAPTER FIVE: CONCLUSIONS AND RECOMMENDATIONS FOR FURTHER RESEARCH

5.1 Major Findings

Phylogenetic analysis of the species biodiversity within saline environments has been previously investigated, however the focus on salt evaporation ponds has been of less importance. Therefore, **Chapter 2** identified the various species of microorganisms that reside within the salt evaporation ponds at Botash. The microbial diversity established from the analysis of the Botash salt evaporation ponds show that diverse microorganisms all reside within the ponds. The most abundant organisms being the bacterium Salinibacter and the archaea Halorubrum. The eurkaryote green algae *D. salina* was also prominent due to its dominance as the primary producer within the ponds. The results obtained from this chapter could assist with a deeper understanding of microbial community dynamics within salt evaporation ponds.

The effect of nitrogen deprivation and saline concenntrations on the beta carotene production by *D. salina* has been well researched. Therefore, **Chapter 3** identified the effect that saline concentrations and different nitrogen sources had on the bio productivity, beta carotene and glycerol production of *D. salina*. This chapter determined that the bio productivity of *D. salina* is greatest at 2M, 3,5M and when Urea is used as the nitrogen source. The glycerol production by *D. salina* occurred during all treatments except the 2M and NO_3 treatments. The production of beta carotene occurred during all the treatments. These results show that *D. salina* adapts well to different salinities and nitrogen sources and is thus able to survive in harsh environments which could be problematic to Botash.

The understanding of beta carotene production by *D. salina* under varying environmental conditions has been previously researched. Therefore, **Chapter 3** also identified the effect of different environmental factors such as saline concentration, nitrogen source and temperature on the bio productivity and beta carotene production of *D. salina* using the RSM method. The results obtained determined that bio productivity and beta carotene

production are inversely related. The maximum amount of beta carotene was produced when the temperature was 32ºC with 4M salinity and NO_3 as the nitrogen source, whilst the maximum bio productivity was observed at 30℃ with 3M salinity and NO_3 as the nitrogen source. The results obtained depict the fact that beta carotene production does not require high biomass. These results could be used in future research as a method to optimise and upscale for improved production of beta carotene.

The EPS produced by *D. salina* has been researched in relation to different pharmaceutical uses by various other studies. The effect of different environmental conditions on the production of EPS has not been well researched. Therefore, **Chapter 4** identified the effects of different treatments on the production of EPS. The EPS was extracted from the *D. salina* cells that underwent the different treatments mentioned in the previous chapters. The results obtained showed that the EPS produced contains polysaccharides such as Arabinose which enables the cells to inhabit the saline environment.

5.2 Challenges

A major challenge in this study was the optimization of the growth medium in which *D. salina* was grown to allow for optimum growth of batch cultures used for the experimental procedures.

The use of the modified AMCONA medium allowed for fast growth of *D. salina* thus, acting as a solution to this challenge.

5.3 General Discussion

This thesis has shown that there is indeed a vast microbial diversity to be found within salt evaporation ponds. The ponds at Botash play home to various microorganisms from the bacterium Salinibacter and the archaea Halorubrum to the eurkaryotic green alga *D. salina*. These microorganisms form durable ecosystems within the ponds because of the presence of nutrients such as nitrate which allow for growth and survival of the microorganisms. The Botash ponds also have nutrients present in increasing concentrations thus allowing more abundance of microorganisms to grow and survive.

Thus, the nutrients present within the ponds at Botash enable the microbial biodiversity observed within this thesis.

The *D. salina* found within these salt evaporation ponds is an interesting organism as it produces many important compouds such as beta carotene. The production of beta carotene has made this organism well researched in relation to beta carotene production. The organism has not been well researched in relation to growth dynamics and the effect of different environmental factors on the growth of *D. salina*. This thesis has found that *D. salina* grows best at 2M and 3,5M salinity with NO_3 and urea as the nitrogen source. This thesis has also found that *D. salina* is able to produce beta carotene and glycerol under various environmental conditions. This thesis also shows the inverse effect that beta carotene production has on biomass through the RSM experiment. Thus, for optimal beta carotene production biomass must be relatively low.

The EPS extracted from the *D. salina* cells under different treatments shows the effect that various treatments have on the production of EPS. The EPS produced by *D. salina* in turn has a negative impact on the salt problem as it coats the salt and increases the TOC contamination of the salt. This salt is difficult to sell as it is not pure, hence the presence of *D. salina* within salt evaporation ponds can be detrimental to salt production. The EPS produced by *D. salina* has beneficial compounds for pharmaceutical uses, however the presence of these compounds on the salt crystals reduces the purity of the crystals. Thus, the presence of EPS has a negative impact on salt production.

5.4 Future Perspectives

There are various future perspectives that can be drawn from this thesis. The exact relationship between nutrient and microbial diversity can be further researched along with the mechanisms behind the functioninig ecosystem within the salt evaporation ponds. The *D. salina* cells can be further researched as a means to better understand the life processes of these cells in order to control the population and manipulate the cells for high value products. Biological control of the *D. salina* population is of importance as it will allow for the reduction of the TOC on the salt crystals which will increase the purity of the salt. Therefore research into the biological control of *D. salina* must be investigated. The

results obtained from the EPS chapter can be used for future research into optimization of EPS production for particular functions.

5.5 Final Comments and Summary Conclusions

This thesis provided information on various aspects related to the salt evaporation ponds at Botash. The microbial diversity within these ponds was analysed and it was found that there is a vast amount of microbes that live within these ponds. The microbe of interest is *D. salina* which acts as the primary producer within saline environments. *D. salina* is also known for its ability to produce high value products such as beta carotene and glycerol. Therefore this thesis researched the mechanisms behind the production of these compounds. The production of EPS by *D. salina* was also researched in relation to its affect on the quality of salt produced. The results from this thesis show that the presence of microorganisms is both beneficial and harmful to the salt production process and therefore the microbes within salt evaporation ponds need to be controlled.

REFERENCES

Ahmed, M., Arakel, A., Hoey, D., & Coleman, M. (2001). Integrated power, water and salt generation: a discussion paper. *Desalination*, *134*(1-3), 37-45.

Ahmed, R. A., He, M., Aftab, R. A., Zheng, S., Nagi, M., Bakri, R., & Wang, C. (2017). Bioenergy application of Dunaliella salina SA 134 grown at various salinity levels for lipid production. *Scientific reports*, *7*(1), 8118.

Airs, R. L., & Keely, B. J. (2003). A high-resolution study of the chlorophyll and bacteriochlorophyll pigment distributions in a calcite/gypsum microbial mat. *Organic Geochemistry*, **34**(4): 539-551.

Andrei, A. Ş., Banciu, H. L., & Oren, A. (2012). Living with salt: metabolic and phylogenetic diversity of archaea inhabiting saline ecosystems. *FEMS microbiology letters*, *330*(1), 1-9.

Athearn, N. D., Takekawa, J. Y., & Shinn, J. M. (2009). Avian response to early tidal salt marsh restoration at former commercial salt evaporation ponds in San Francisco Bay, California, USA. *Natural Resources and Environmental Issues*, *15*(1), 14.

Bardavid, R. E., & Oren, A. (2008). Dihydroxyacetone metabolism in Salinibacter ruber and in Haloquadratum walsbyi. *Extremophiles*, *12*(1), 125-131.

Bardavid, R. E., Khristo, P., & Oren, A. (2008). Interrelationships between Dunaliella and halophilic prokaryotes in saltern crystallizer ponds. *Extremophiles*, *12*(1), 5-14.

Ben-Amotz, A. (2019). Bioactive compounds: glycerol production, carotenoid production, fatty acids production. *The Alga Dunaliella, Biodiversity, Physiology, Genomics and Biotechnology*, 189-207.

Ben-Amotz, A. and Avron, M. (1987) On the mechanism of osmoregulation in *Dunaliella*. In *Energetic and Structure of Halophilic Microorganism*. ed. Caplan, S.R.and Gizburg, M. pp. 529–541

Bhuvaneshwari, M., Thiagarajan, V., Nemade, P., Chandrasekaran, N., & Mukherjee, A. (2018). Toxicity and trophic transfer of P25 TiO2 NPs from Dunaliella salina to Artemia salina: Effect of dietary and waterborne exposure. *Environmental*

research, *160*, 39-46.

Biswas, J., & Paul, A. K. (2014). Production of extracellular polymeric substances by Halophilic bacteria of solar salterns. *Chinese Journal of Biology*, *2014*.

Bonnefond, H., Moelants, N., Talec, A., Mayzaud, P., Bernard, O., & Sciandra, A. (2017). Coupling and uncoupling of triglyceride and beta-carotene production by Dunaliella salina under nitrogen limitation and starvation. *Biotechnology for biofuels*, *10*(1), 25.

Borowitzka, M.A. and Siva, C.J. (2007) The taxonomy of the genus *Dunaliella*(Chlorophyta, Dunaliellales) with emphasis on the marine and halophilic species. *J Appl Phycol* **19**, 567–590.

Botswana Ash (Pty) Ltd 2011, *Welcome to Botswana Ash*, Botswana Ash (Pty) Ltd, viewed 28 January 2020, <https://botash.bw/>

Buchanan, B. B., Gruissem, W., & Jones, R. L. (Eds.). (2015). *Biochemistry and molecular biology of plants*. John Wiley & Sons.

Can, S. S., Cirik, S., Koru, E., Turan, G., Tekogul, H., & Subakan, T. (2016). Effects of salinity, light and nitrogen concentration on growth and lipid accumulation of the green algae Dunaliella bardawil. *Fresenius Environmental Bulletin*, *25*(5), 1438-1448.

Chen, Y., Tang, X., Kapoore, R. V., Xu, C., & Vaidyanathan, S. (2015). Influence of nutrient status on the accumulation of biomass and lipid in Nannochloropsis salina and Dunaliella salina. *Energy conversion and management*, *106*, 61-72.

Davis, J. S. (2000). Structure, function, and management of the biological system for seasonal solar saltworks. *Global nest journal*, *2*(3), 217-226.

Davis, J. S., & Giordano, M. (1995). Biological and physical events involved in the origin, effects, and control of organic matter in solar saltworks. *International Journal of Salt Lake Research*, *4*(4), 335–347. https://doi.org/10.1007/BF01999117

Daintith, M. (1996). Rotifers and Artemia for marine aquaculture: a training guide.

El-Baky, H. A., El-Baz, F. K., & El-Baroty, G. S. (2004). Production of antioxidant by the

green alga Dunaliella salina. *Int. J. Agric. Biol*, *6*(1), 1560-8530.

Eggeman, T. (2011). Sodium Carbonate. In Kirk-Othmer Encyclopedia of Chemical Technology, (Ed.). doi:10.1002/0471238961.1915040918012108.a01.pub3

Enache, M., Teodosiu, G., Itoh, T., Kamekura, M., & Stan-Lotter, H. (2017). Halophilic microorganisms from man-made and natural hypersaline environments: Physiology, ecology, and biotechnological potential. In *Adaption of Microbial Life to Environmental Extremes* (pp. 201-226). Springer, Cham.

Eryalçın, K. M. (2018). Effects of Different Commercial Feeds and Enrichments on Biochemical Composition and Fatty Acid Profile of Rotifer (Brachionus Plicatilis, Müller 1786) and Artemia Franciscana. *Turkish Journal of Fisheries and Aquatic Sciences*, *18*(1), 81-90.

Falb, M., Müller, K., Königsmaier, L., Oberwinkler, T., Horn, P., von Gronau, S., Gonzalez, O., Pfeiffer, F., Bornberg-Bauer, E. and Oesterhelt, D., 2008. Metabolism of halophilic archaea. *Extremophiles*, *12*(2), pp.177-196.

Fang, L., Qi, S., Xu, Z., Wang, W., He, J., Chen, X., & Liu, J. (2017). De novo transcriptomic profiling of Dunaliella salina reveals concordant flows of glycerol metabolic pathways upon reciprocal salinity changes. *Algal research*, *23*, 135-149.

Giordano, M., Bargnesi, F., Mariani, P., & Cryptogamie, S. (2014). Dunaliella salina (Chlorophyceae) Affects the Quality of NaCl Crystals Dunaliella salina (Chlorophyceae) affects the quality of NaCl crystals, *35*(3), 285–302. https://doi.org/10.7872/crya.v35.iss3.2014.285

Gunde-Cimerman, N., Oren, A., & Plemenitaš, A. (Eds.). (2006). *Adaptation to life at high salt concentrations in Archaea, Bacteria, and Eukarya* (Vol. 9). Springer Science & Business Media.

Han, S. I., Kim, S., Lee, C., & Choi, Y. E. (2019). Blue-Red LED wavelength shifting strategy for enhancing beta-carotene production from halotolerant microalga, Dunaliella salina. *Journal of Microbiology*, *57*(2), 101-106.

Heng, S., Sutheeworapong, S., Prommeenate, P., Cheevadhanarak, S., Kosugi, A., Pason, P., Waeonukul, R., Ratanakhanokchai, K. and Tachaapaikoon, C., 2019. Complete

Genome Sequence of Halocella sp. Strain SP3-1, an Extremely Halophilic, Glycoside Hydrolase-and Bacteriocin-Producing Bacterium Isolated from a Salt Evaporation Pond. *Microbiol Resour Announc*, *8*(7), pp.e01696-18.

Hosseini Tafreshi, A., & Shariati, M. (2009). Dunaliella biotechnology: methods and applications. *Journal of applied microbiology*, *107*(1), 14-35.

Javor, B. (2002). Industrial microbiology of solar salt production. *Journal of Industrial Microbiology and Biotechnology*, *28*(1), 42–47. https://doi.org/10.1038/sj/jim/7000173

Kerkar, S. (2004). Ecology of hypersaline microorganisms.

Komaristaya, V., Bezrodnova, O., & Rudas, A. (2018). A remote sensing approach to assess algal beta-carotene content in solar salt evaporation ponds.

Kwan, M. B. (2017). Appendix VIIIA Yongli (Tanggu) Soda Ash Production, 1946–1953. In *Patriots' Game* (pp. 214-214). Brill.

Lamers, P.P., van de Laak, C.C., Kaasenbrood, P.S., Lorier, J., Janssen, M., De Vos, R.C., Bino, R.J. and Wijffels, R.H. (2010). Carotenoid and fatty acid metabolism in light-stressed Dunaliella salina. *Biotechnology and bioengineering*, *106*(4), 638-648.

Le, T. H., Hoa, N. V., Sorgeloos, P., & Van Stappen, G. (2019). Artemia feeds: a review of brine shrimp production in the Mekong Delta, Vietnam. *Reviews in Aquaculture*, *11*(4), 1169-1175.

Li, R., Cui, X., Zhang, L., Zhang, B., Wang, X., & Sui, L. (2018). Brine characterization and Artemia population dynamics in Bohai Bay solar saltworks, China. *Crustaceana*, *91*(8), 1013-1025.

Ma, Y., Galinski, E. A., Grant, W. D., Oren, A., & Ventosa, A. (2010). Halophiles 2010: life in saline environments.

Mani, K., Salgaonkar, B. B., Das, D., & Bragança, J. M. (2012). Community solar salt production in Goa , India, 1–8.

Mlingi, F. T., Lamtane, H. A., Chenyambuga, S. W., & Lund, I. (2019). First biogeographical survey of Artemia in Tanzania. *Journal of Applied Aquaculture*, 1-13.

Montazeri-Najafabady, N., Negahdaripour, M., Salehi, M. H., Morowvat, M. H., Shaker, S., & Ghasemi, Y. (2016). Effects of osmotic shock on production of β-carotene and glycerol in a naturally isolated strain of Dunaliella salina. *Journal of Applied Pharmaceutical Science Vol*, *8*, 160-163.

Muraveva, E. A. (2017, October). Simulation of salt production process. In *IOP Conference Series: Earth and Environmental Science* (pp. 052018-052018).

Na, J.M., Kang, M.S., Kim, J.H., Jin, Y.X., Je, J.H., Kim, J.B., Cho, Y.S., Kim, J.H. and Kim, S.Y. (2011) Distribution and identification of halophilic bacteria in solar salts produced during entire manufacturing process. *Microbiology and Biotechnology Letters*, *39*(2), pp.133-139.

Önal, O. (2015). Lime stabilization of soils underlying a salt evaporation pond: a laboratory study. *Marine Georesources & Geotechnology*, *33*(5), 391-402.

Oren, A., Kühl, M., & Karsten, U. (1995). An endoevaporitic microbial mat within a gypsum crust: zonation of phototrophs, photopigments, and light penetration. *Marine Ecology Progress Series*, **128**: 151-159.

Oren, A. (2005). Microscopic examination of microbial communities along a salinity gradient in saltern evaporation ponds: a 'halophilic safari'. In *Adaptation to Life at High Salt Concentrations in Archaea, Bacteria, and Eukarya* (pp. 41-57). Springer, Dordrecht.

Oren, A. (2009a). Saltern evaporation ponds as model systems for the study of primary production processes under hypersaline conditions. *Aquatic Microbial Ecology*, *56*(2-3), 193-204.

Oren, A., Sørensen, K. B., Canfield, D. E., Teske, A. P., Ionescu, D., Lipski, A., & Altendorf, K. (2009b). Microbial communities and processes within a hypersaline gypsum crust in a saltern evaporation pond (Eilat, Israel). *Hydrobiologia*, **626**(1): 15-26.

Oren, A. (2010). Industrial and environmental applications of halophilic microorganisms. *Environmental technology*, *31*(8-9), 825-834.

Oren, A. (2012). Salts and brines. In *Ecology of cyanobacteria II* (pp. 401-426). Springer, Dordrecht.

Oren, A. (2014). The ecology of Dunaliella in high-salt environments. *Journal of Biological Research-Thessaloniki*, *21*(1), 23.

Oren, A. (2017). Glycerol metabolism in hypersaline environments. *Environmental microbiology*, *19*(3), 851-863.

Oren, A. (2019). Solar salterns as model systems for the study of halophilic microorganisms in their natural environments. In *Model Ecosystems in Extreme Environments* (pp. 41-56). Academic Press.

Ownagh, E., Agh, N., & Noori, F. (2015). Comparison of the growth, survival and nutritional value of Artemia using various agricultural by-products and unicellular algae Dunaliella salina. *Iranian Journal of Fisheries Sciences*, *14*(2), 358-368.

Polle, J. E., Struwe, L., & Jin, E. (2008). Identification and characterization of a new strain of the unicellular green alga Dunaliella salina (Teod.) from Korea. *J Microbiol Biotechnol*, *18*(5), 821-827.

Ravizky, A., & Nadav, N. (2007). Salt production by the evaporation of SWRO brine in Eilat: a success story. *Desalination*, *205*(1-3), 374-379.

Salari, Z., Kazemi, M. J., & Shirsalimian, M. S. (2019). Isolation and Molecular Identification of Halophilic Microorganisms from Around Saghand Uranium Mine, Saghand Desert, Iran. *Geomicrobiology Journal*, 1-10.

Shaker, S., Morowvat, M. H., & Ghasemi, Y. (2017). Effects of Sulfur, Iron and Manganese Starvation on Growth, β-carotene Production and Lipid Profile of Dunaliella salina. *Journal of Young Pharmacists*. https://doi.org/10.5530/jyp.2017.9.9

Sher, J., Elevi, R., Mana, L., & Oren, A. (2004). Glycerol metabolism in the extremely halophilic bacterium Salinibacter ruber. *FEMS microbiology letters*, *232*(2), 211-215.

Silva, C., González, D., & Suárez, F. (2017). An experimental and numerical study of evaporation reduction in a salt-gradient solar pond using floating discs. *Solar energy*, *142*, 204-214.

Sima, S., Rosenberg, D. E., Wurtsbaugh, W. A., Null, S. E., & Kettenring, K. M. (2020).

Restoring a Saline Lake to a Range of Water Levels with Noisy Data and Diverse Objectives.

Sun, X. M., Ren, L. J., Zhao, Q. Y., Ji, X. J., & Huang, H. (2018). Microalgae for the production of lipid and carotenoids: a review with focus on stress regulation and adaptation. *Biotechnology for biofuels*, *11*(1), 1-16.

Tabor, H. (1981). REVIEW ARTICLE SOLAR PONDSt, (3), 181–194.

Takekawa, J.Y., Ackerman, J.T., Brand, L.A., Graham, T.R., Eagles-Smith, C.A., Herzog, M.P., Topping, B.R., Shellenbarger, G.G., Kuwabara, J.S., Mruz, E. and Piotter, S.L., 2015. Unintended consequences of management actions in salt pond restoration: cascading effects in trophic interactions. *PloS one*, *10*(6), p.e0119345.

Van Stappen, G., Sui, L., Hoa, V.N., Tamtin, M., Nyonje, B., de Medeiros Rocha, R., Sorgeloos, P. and Gajardo, G., 2019. Review on integrated production of the brine shrimp Artemia in solar salt ponds. *Reviews in Aquaculture*.

Veeramani, T., Santhanam, P., Manickam, N., & Rajthilak, C. (2019). Introduction to Artemia Culture. In *Basic and Applied Zooplankton Biology* (pp. 209-224). Springer, Singapore.

Velasco, S. J., Retana, O. D., Castro, M. J., Castro, M. G., & Castro, C. A. E. (2018). Effect of different salinities on the survival and reproductive characteristics of populations of Artemia franciscana Kellogg, 1906 from coastal and inland waters of Mexico. *Journal of Entomology and Zoology Studies*, *6*(2), 1090-1096.

Wei, S., Bian, Y., Zhao, Q., Chen, S., Mao, J., Song, C., ... & Zou, H. (2017). Salinity-induced palmella formation mechanism in halotolerant algae Dunaliella salina revealed by quantitative proteomics and phosphoproteomics. *Frontiers in plant science*, *8*, 810.

Xu, Y., Ibrahim, I., Wosu, C., Ben-Amotz, A., & Harvey, P. (2018). Potential of new isolates of Dunaliella salina for natural β-carotene production. *Biology*, *7*(1), 14.

Yao, Y., Ge, Y., Thomasson, J. A., & Sui, R. (2018). Algae optical density sensor for pond monitoring and production process control. *International Journal of Agricultural & Biological Engineering*, *11*(1).

Zarandi-Miandoab, L., Hejazi, M. A., Bagherieh-Najjar, M. B., & Chaparzadeh, N. (2019). Statistical Optimization of The Four Key Factors on β-Carotene Production by Dunaliella salina Under Laboratory Conditions Using Response Surface Methodology. *Iranian Journal of Pharmaceutical Research*.

Zarrini, G., Rahmani, R., Negahdaripour, M., Mohkam, M., & Ghasemi, Y. (2018). Isolation and identification of culturable aerobic halophilic Archaea associated with salt crystals from Urmia Lake. *Trends in Pharmaceutical Sciences, 4*(2).

APPENDIX A

Chapter 2

Sequence Breakdown

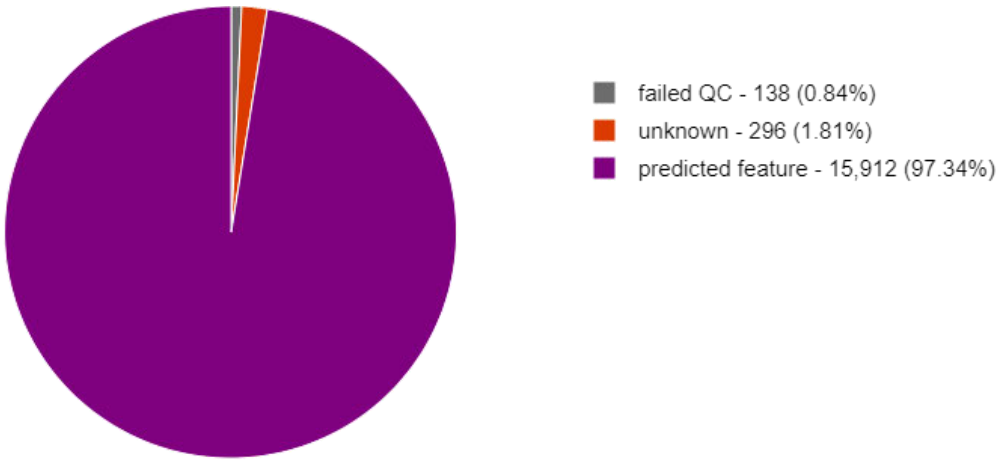

The sequence Breakdown for the 18S analysis of the NS Pond

Of the sequences tested, 138 sequences (0.84%) failed to pass the QC pipeline. Of those, dereplication identified 14,758 sequences as artificial duplicate reads.

Analysis Statistics

Table 7.1: The Analysis Statistics of the 18S Analysis for the NS Pond.

UPLOAD BP COUNT	**4 848 809 bp**
UPLOAD SEQUENCE COUNT	**16 346**
UPLOAD MEAN SEQUENCE LENGTH	**297 ± 27 bp**
UPLOAD MEAN GC PERCENT	**61 ± 4%**
ARTIFICIAL DUPLICATE READS	**14 758**
POST QC bp COUNT	**342 418 bp**
POST QC SEQUENCES COUNT	**1 446**
POST QC MEAN SEQUENCE LENGTH	**237 ± 61 bp**

POST QC MEAN GC PERCENT	**61 ± 6 %**
PROCESSED PREDICTED PROTEIN FEATURES	**6**
PROCESSED PREDICTED rRNA FEATURES	**11 779**
ALIGNMENT IDENTIFIED PROTEIN FEATURES	**3**
ALIGNMENT IDENTIFIED rRNA FEATURES	**11 666**
ANNOTATION IDENTIFIED FUNCTIONAL CHANGES	**UNDEFINED**

Domain

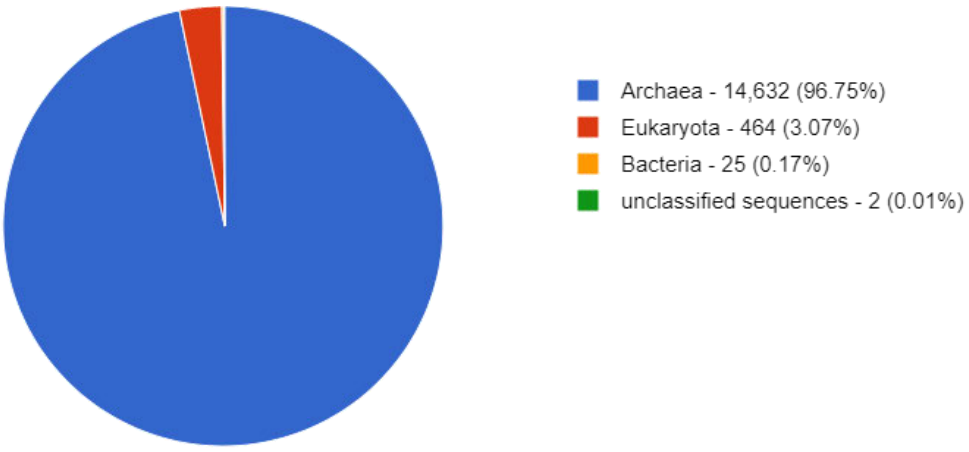

The Domain Distribution of the 18S Analysis of the NS Pond.

Phylum

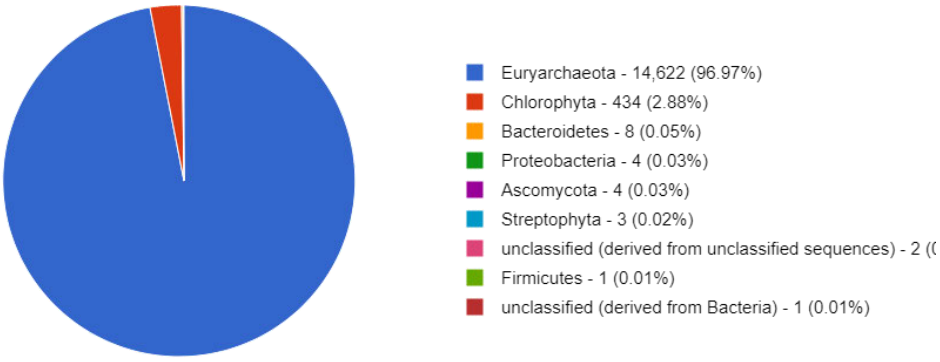

The Phylum Distribution of the 18S Analysis of the NS Pond.

Class

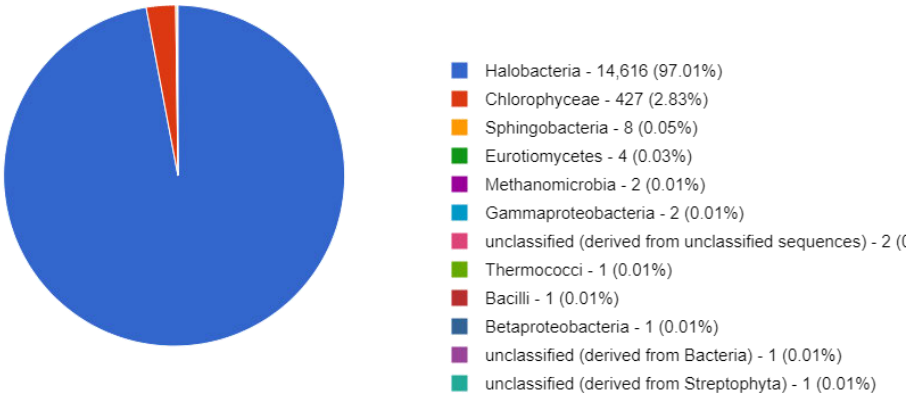

The Class Distribution of the 18S Analysis of the NS Pond.

Order

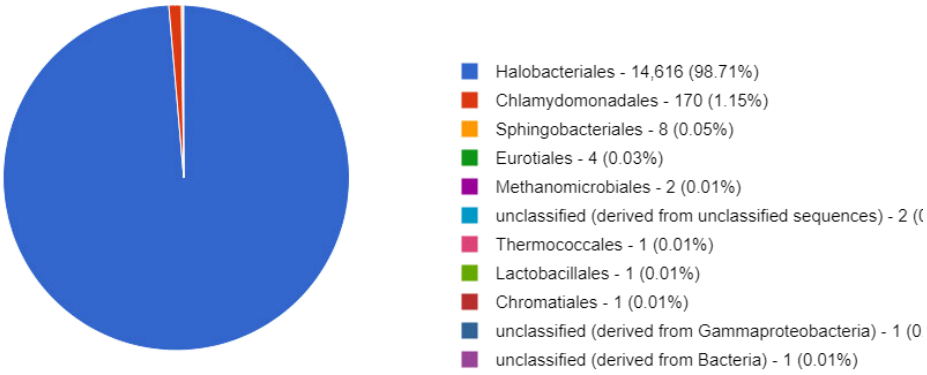

The Order Distribution of the 18S Analysis of the NS Pond.

Family

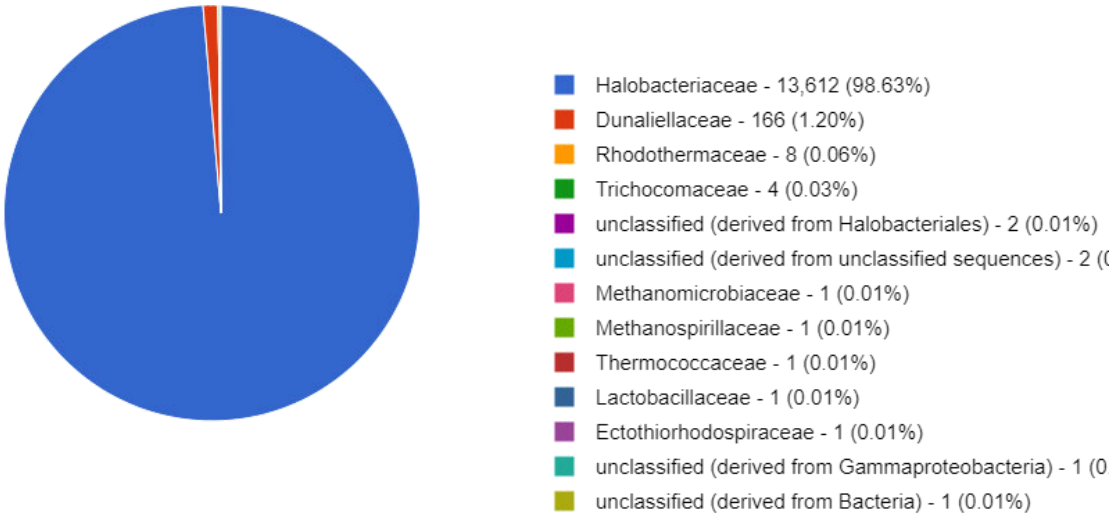

The Family Distribution of the 18S Analysis of the NS Pond.

Rarefaction Curve

The plot below shows the rarefaction curve of annotated species richness. This curve is a plot of the total number of distinct species annotations as a function of the number of sequences sampled. On the left, a steep slope indicates that a large fraction of the species diversity remains to be discovered. If the curve becomes flatter to the right, a reasonable

number of individuals is sampled. More intensive sampling is likely to yield only few additional species.

Sampling curves generally rise very quickly at first and then level off toward an asymptote as fewer new species are found per unit of individuals collected. These rarefaction curves are calculated from the table of species abundance. The curves represent the average number of different species annotations for subsamples of the complete data set.

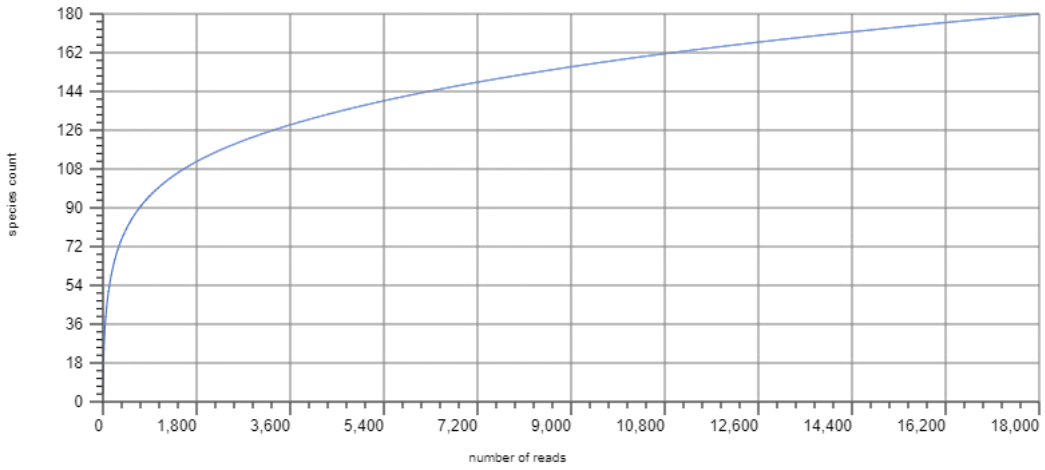

The Rarefaction Curve of the 18S Analysis of the NS Pond.

Sequence Breakdown

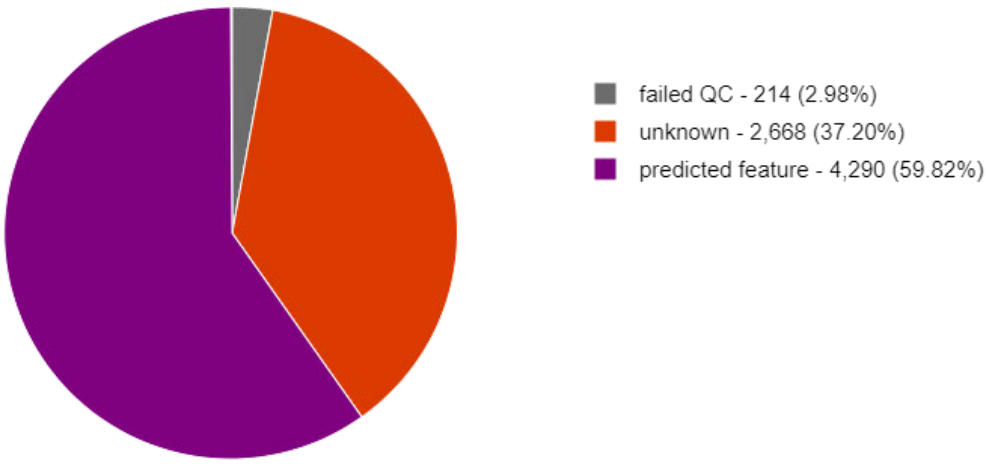

The Sequence Breakdown for the 18S Analysis of the WI Pond.

Of the sequences tested, 214 sequences (2.98%) failed to pass the QC pipeline. Of those, dereplication identified 3,797 sequences as artificial duplicate reads.

Analysis Statistics

Analysis Statistics for the 18S Analysis of the WI Pond.

UPLOAD bp COUNT	**2 158 772 bp**
UPLOAD SEQUENCES COUNT	**7 172**
UPLOAD MEAN SEQUENCE LENGTH	**301 ± 0 bp**
UPLOAD MEAN GC PERCENT	**55 ± 7 %**
ARTIFICIAL DUPLICATE READS: SEQUENCE COUNT	**3 797**
POST QC bp COUNT	**748 251 bp**
POST QC SEQUENCES COUNT	**3 145**
POST QC MEAN SEQUENCE LENGTH	**238 ± 66 bp**
POST QC MEAN GC PERCENT	**58 ± 5 %**
PROCESSED PREDICTED PROTEIN FEATURES	**375**
PROCESSED PREDICTED rRNA FEATURES	**2 614**
ALIGNMENT IDENTIFIED PROTEIN FEATURES	**153**
ALIGNMENT IDENTIFIED rRNA FEATURES	**2 486**
ANNOTATION IDENTIFIED FUNCTIONAL CATEGORIES	**UNDEFINED**

Domain

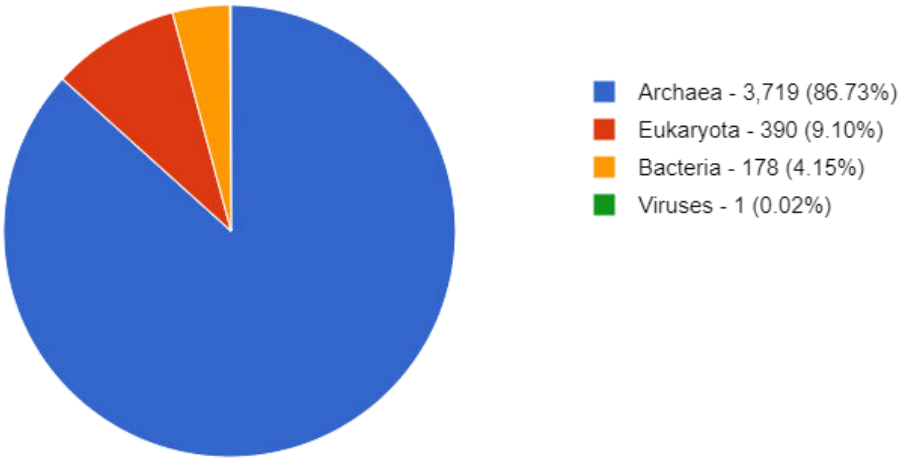

The Domain Distribution of the 18S Analysis of the WI Pond.

Phylum

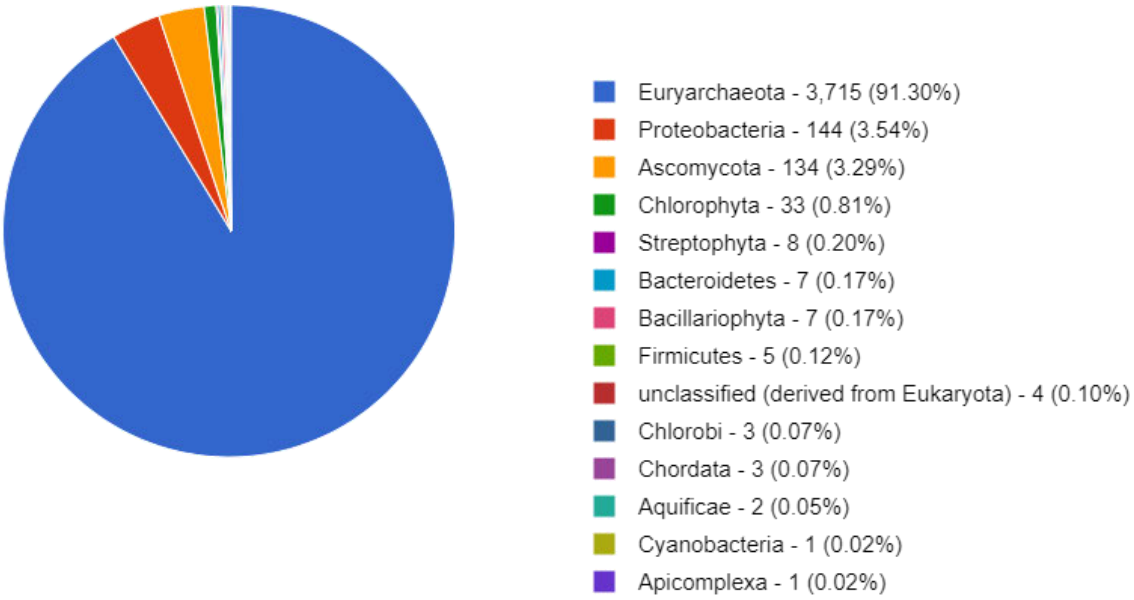

Class

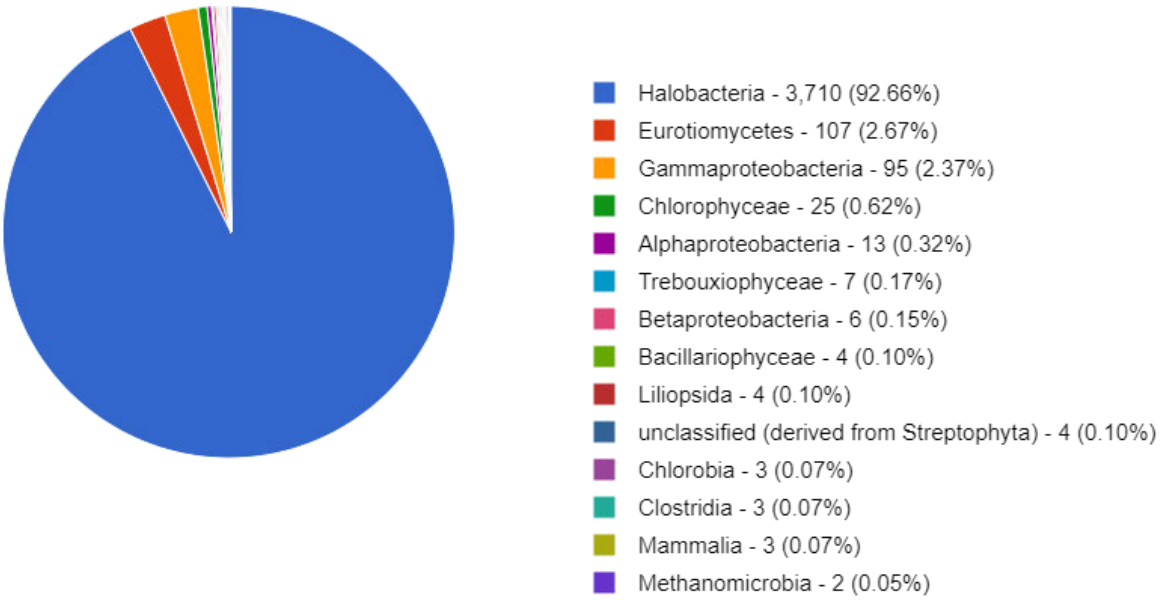
Halobacteria - 3,710 (92.66%)
Eurotiomycetes - 107 (2.67%)
Gammaproteobacteria - 95 (2.37%)
Chlorophyceae - 25 (0.62%)
Alphaproteobacteria - 13 (0.32%)
Trebouxiophyceae - 7 (0.17%)
Betaproteobacteria - 6 (0.15%)
Bacillariophyceae - 4 (0.10%)
Liliopsida - 4 (0.10%)
unclassified (derived from Streptophyta) - 4 (0.10%)
Chlorobia - 3 (0.07%)
Clostridia - 3 (0.07%)
Mammalia - 3 (0.07%)
Methanomicrobia - 2 (0.05%)

Order

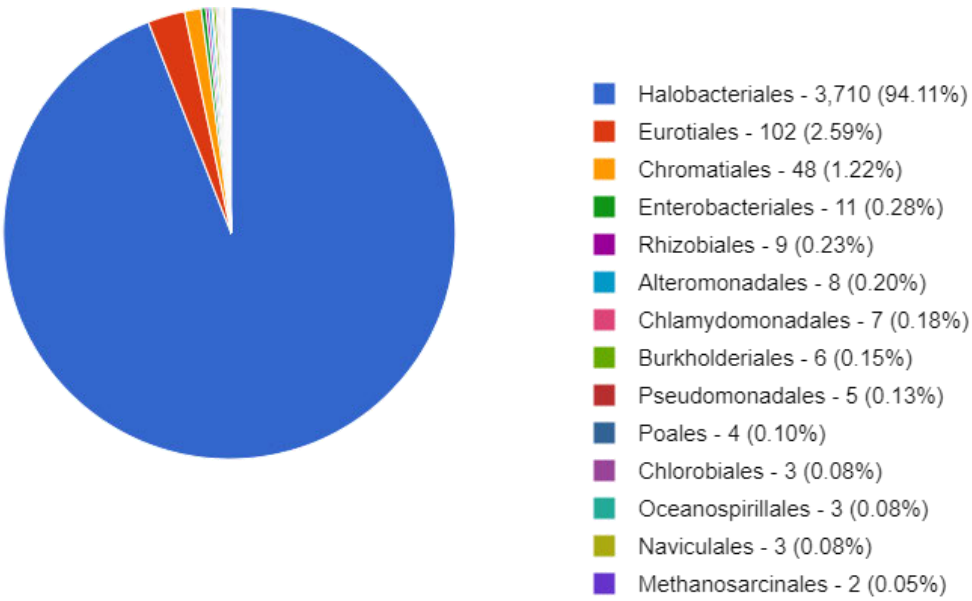
Halobacteriales - 3,710 (94.11%)
Eurotiales - 102 (2.59%)
Chromatiales - 48 (1.22%)
Enterobacteriales - 11 (0.28%)
Rhizobiales - 9 (0.23%)
Alteromonadales - 8 (0.20%)
Chlamydomonadales - 7 (0.18%)
Burkholderiales - 6 (0.15%)
Pseudomonadales - 5 (0.13%)
Poales - 4 (0.10%)
Chlorobiales - 3 (0.08%)
Oceanospirillales - 3 (0.08%)
Naviculales - 3 (0.08%)
Methanosarcinales - 2 (0.05%)

Family

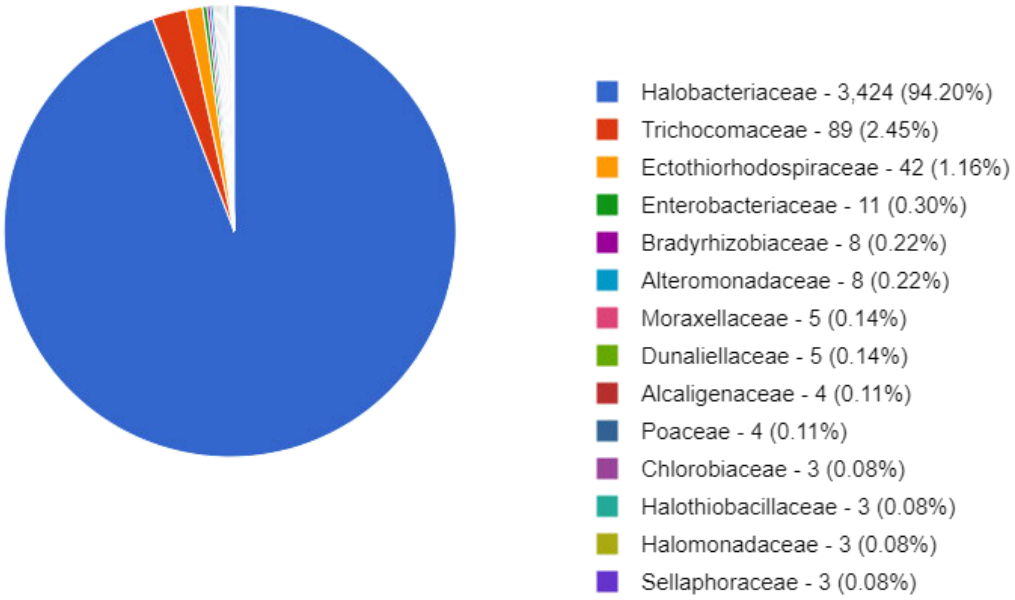

The Family Distribution of the 18S Analysis of the WI Pond.

Rarefaction Curve

The plot below shows the rarefaction curve of annotated species richness. This curve is a plot of the total number of distinct species annotations as a function of the number of sequences sampled. On the left, a steep slope indicates that a large fraction of the species diversity remains to be discovered. If the curve becomes flatter to the right, a reasonable number of individuals is sampled. More intensive sampling is likely to yield only few additional species.

Sampling curves generally rise very quickly at first and then level off toward an asymptote as fewer new species are found per unit of individuals collected. These rarefaction curves are calculated from the table of species abundance. The curves represent the average number of different species annotations for subsamples of the complete data set.

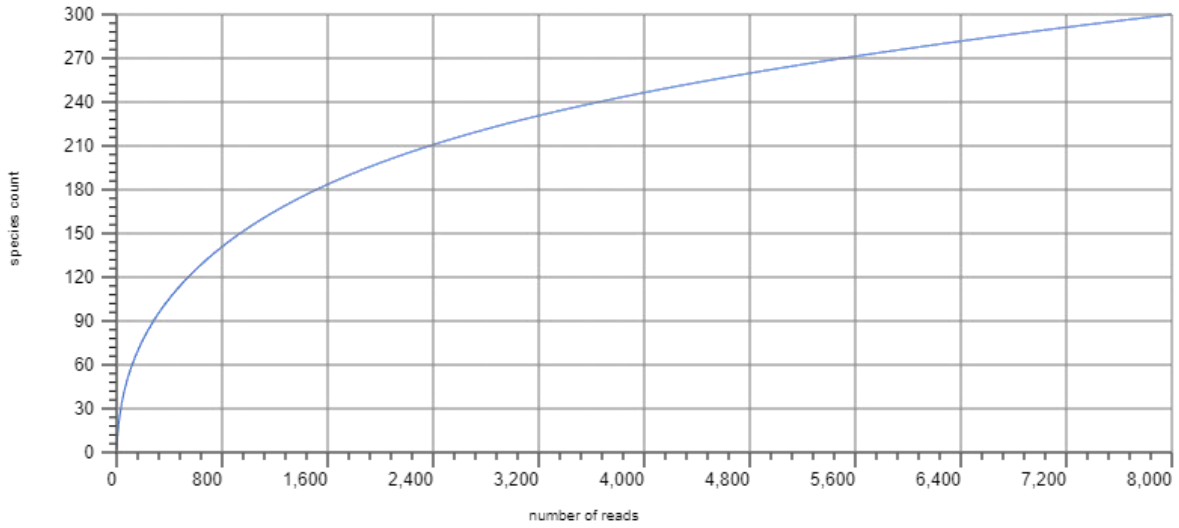

The Rarefaction Curve for the 18S Analysis of the WI Pond. Sequence Breakdown

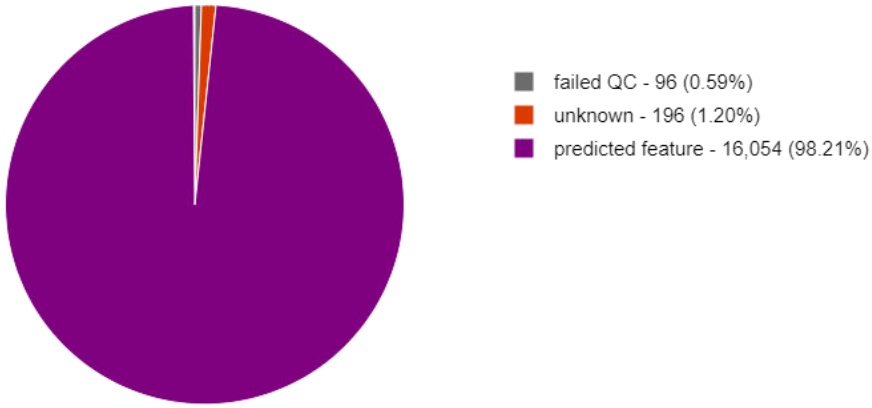

The Sequence Breakdown for the 18S Analysis of the ST Pond.

Of the sequences tested, 96 sequences (0.59%) failed to pass the QC pipeline. Of those, dereplication identified 14,964 sequences as artificial duplicate reads.

Analysis Statistics

The Analysis Statistics of the 18S Analysis for the ST Pond.

UPLOAD bp COUNT	**4 821 563 bp**

UPLOAD SEQUENCES COUNT	**16 346**
UPLOAD MEAN SEQUENCE LENGTH	**295 ± 29 bp**
UPLOAD MEAN GC PERCENT	**59 ± 4 %**
ARTIFICIAL DUPLICATE READS SEQUENCE COUNT	**14 964**
POST QC bp COUNT	**342 163 bp**
POST QC SEQUENCES COUNT	**1 285**
POST QC MEAN SEQUENCE LENGTH	**266 ± 57 bp**
POST QC MEAN GC PERCENT	**58 ± 5 %**
PROCESSED PREDICTED PROTEIN FEATURES	**6**
PROCESSED PREDICTED rRNA FEATURES	**2 647**
ALIGNMENT IDENTIFIED PROTEIN FEATURES	**2**
ALIGNMENT IDENTIFIED rRNA FEATURES	**2 617**
ANNOTATION IDENTIFIED FUNCTIONAL CATEGORIES	**UNDEFINED**

Domain

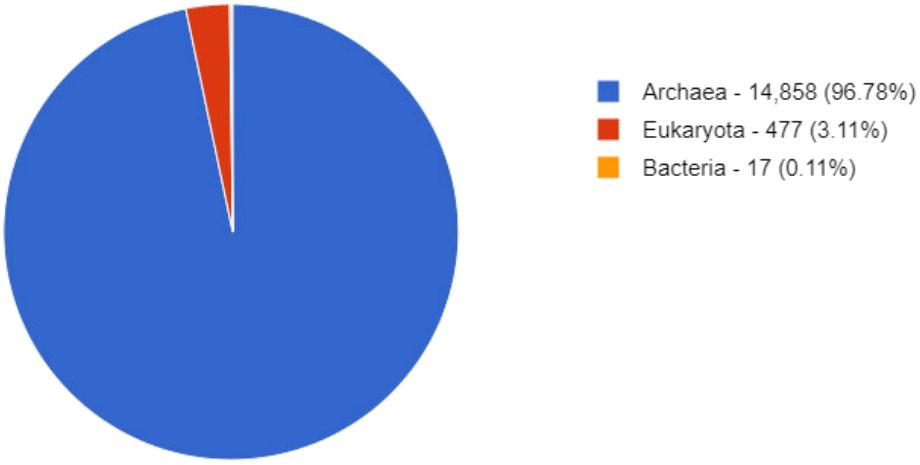

The Domain Distribution of the 18S Analysis for the ST Pond.

Phylum

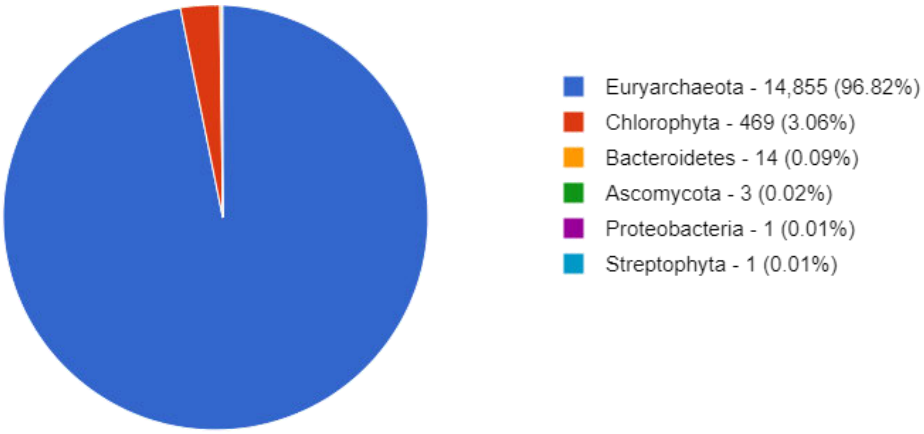

The Phylum Distribution of the 18S Analysis of the ST Pond.

Class

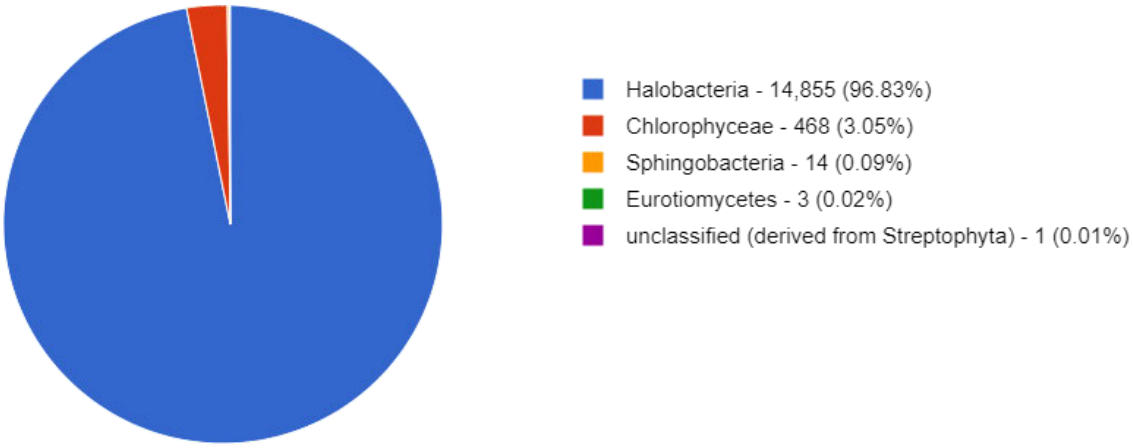

The Class Distribution of the 18S Analysis of the ST Pond.

Order

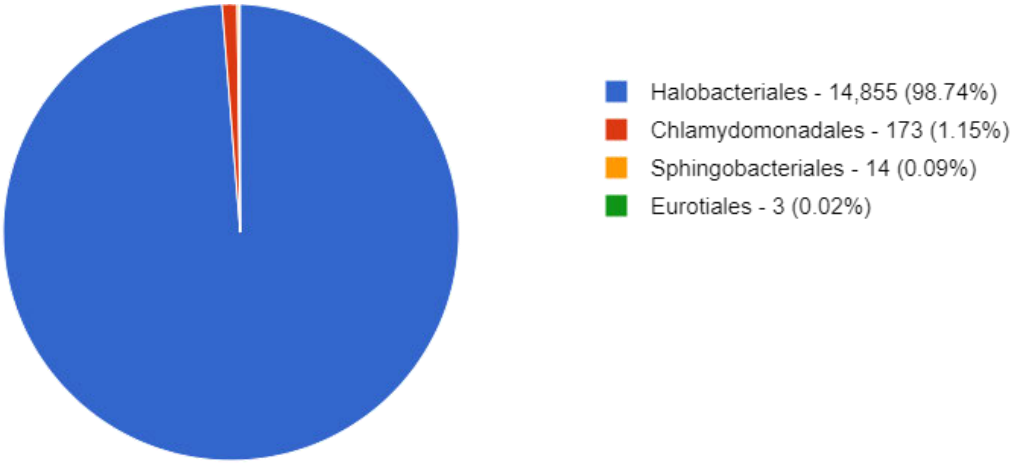

The Order Distribution of the 18S Analysis for the ST Pond.

Family

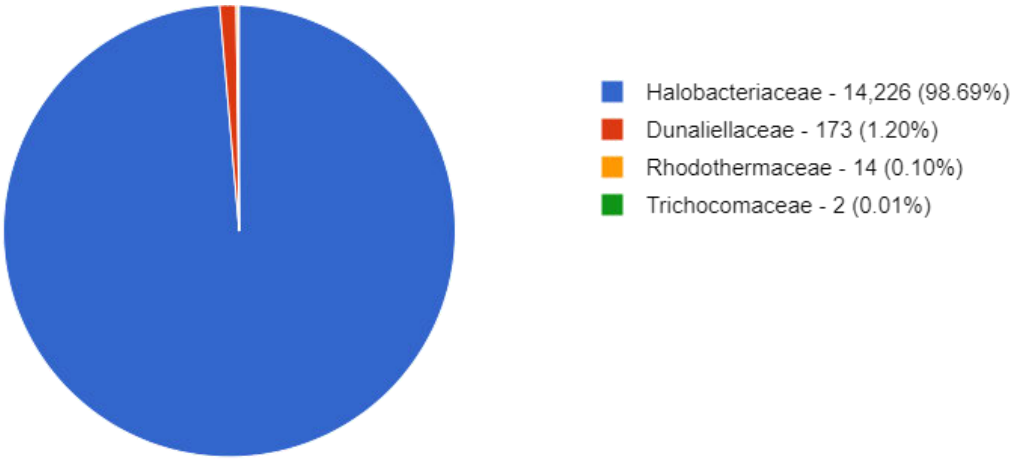

The Family Distribution of the 18S Analysis for the ST Pond.

Rarefaction Curve

The plot below shows the rarefaction curve of annotated species richness. This curve is a plot of the total number of distinct species annotations as a function of the number of sequences sampled. On the left, a steep slope indicates that a large fraction of the species diversity remains to be discovered. If the curve becomes flatter to the right, a reasonable number of individuals is sampled. More intensive sampling is likely to yield only few additional species.

Sampling curves generally rise very quickly at first and then level off toward an asymptote as fewer new species are found per unit of individuals collected. These rarefaction curves are calculated from the table of species abundance. The curves represent the average number of different species annotations for subsamples of the complete data set.

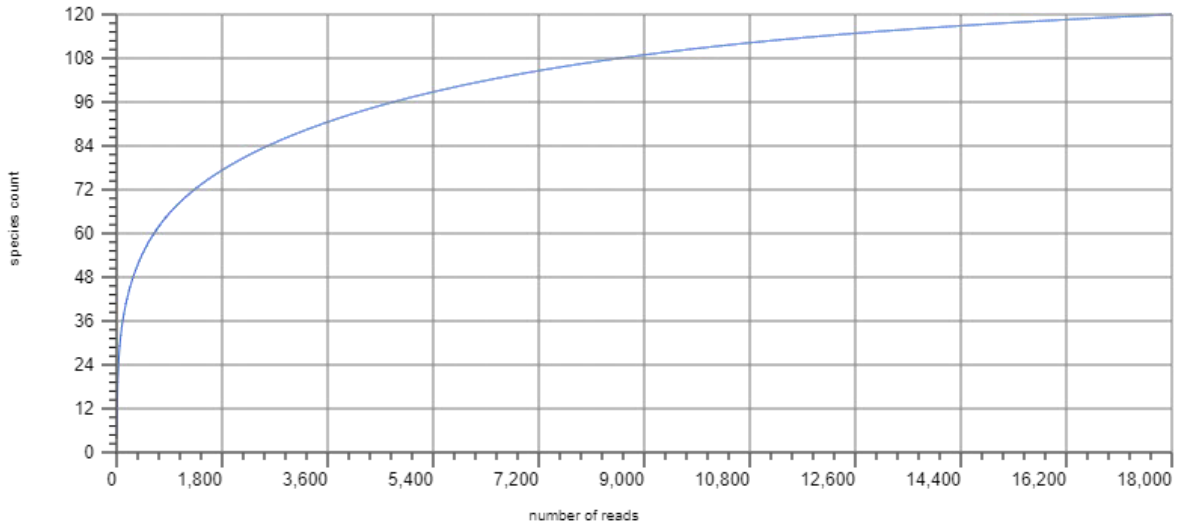

The Rarefaction Curve of the 18S Analysis for the ST Pond.

Sequence Breakdown

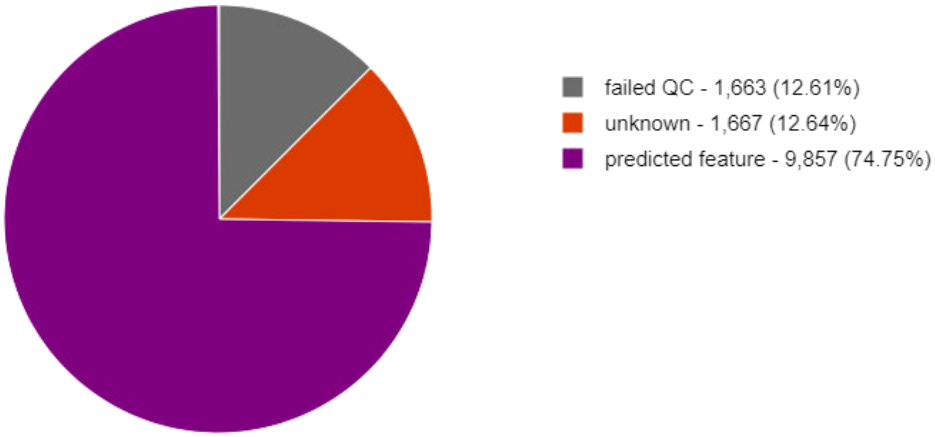

The Sequence Breakdown of the 16S Analysis for the NS Pond.

Of the sequences tested, 1,663 sequences (12.61%) failed to pass the QC pipeline. Of those, dereplication identified 10,138 sequences as artificial duplicate reads.

Analysis Statistics

Table 7.1: The Analysis Statistics of the 16S Analysis for the NS Pond.

UPLOAD bp COUNT	**3 428 192 bp**
UPLOAD SEQUENCES COUNT	**13 187**
UPLOAD MEAN SEQUENCE LENGTH	**260 ± 92 bp**
UPLOAD MEAN GC PERCENT	**56 ± 13 %**
ARTIFICIAL DUPLICATE READS SEQUENCE COUNT	**10 138**
POST QC bp COUNT	**292 945 bp**
POST QC SEQUENCES COUNT	**1 385**
POST QC MEAN SEQUENCE LENGTH	**212 ± 69 bp**
POST QC MEAN GC PERCENT	**59 ± 6 %**
PROCESSED PREDICTED PROTEIN FEATURES	**54**
PROCESSED PREDICTED rRNA FEATURES	**3 897**
ALIGNMENT IDENTIFIED PROTEIN FEATURES	**11**
ALIGNMENT IDENTIFIED rRNA FEATURES	**3 706**
ANNOTATION IDENTIFIED FUNCTIONAL CATEGORIES	**UNDEFINED**

Domain

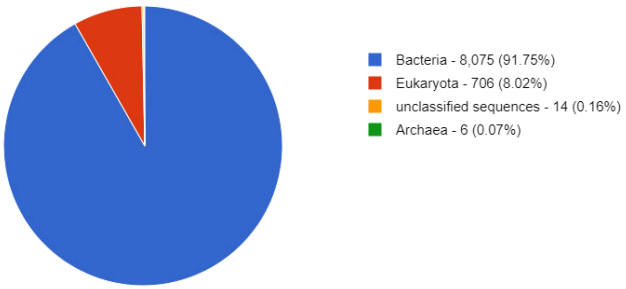

The Domain Distribution of the 16S Analysis for the NS Pond.

Phylum

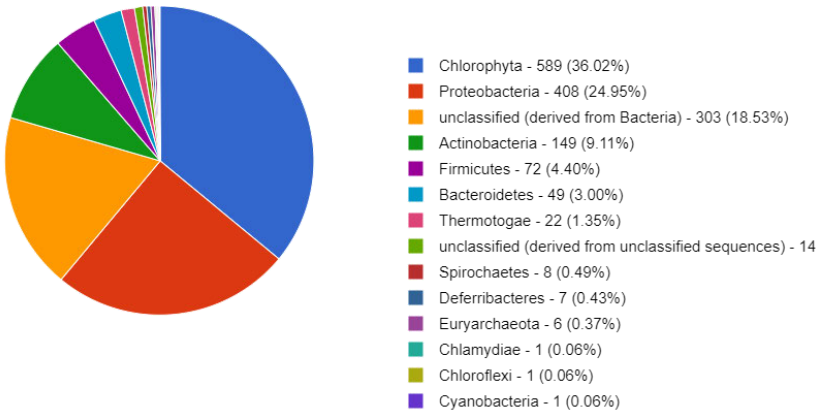

The Phylum Distribution of the 16S Analysis for the NS Pond.

Class

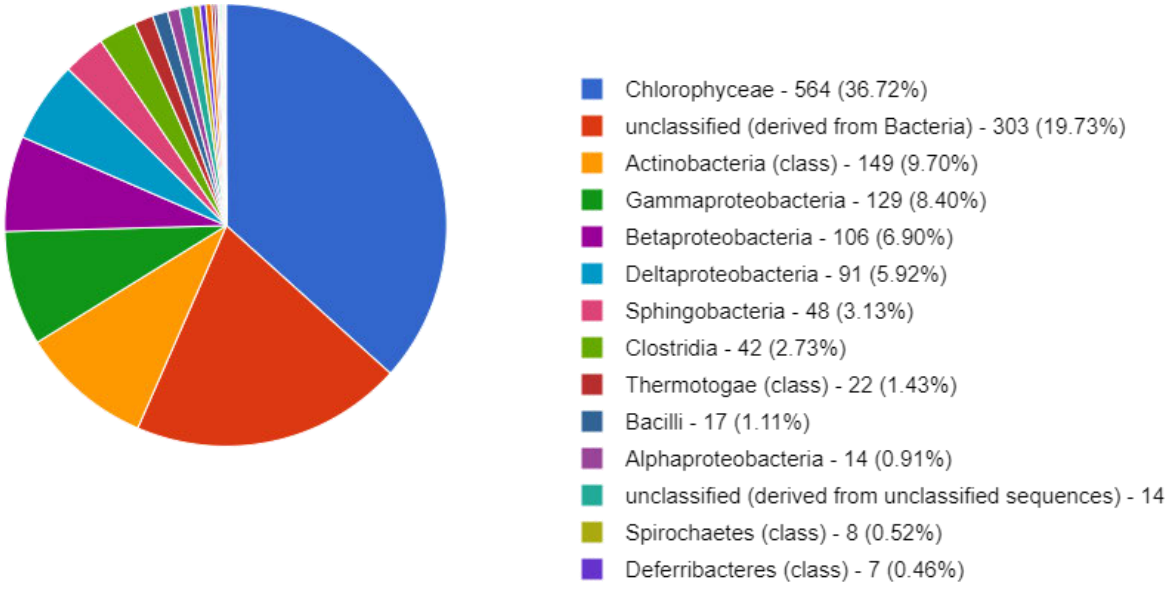

The Class Distribution of the 16S Analysis for the NS Pond.

Order

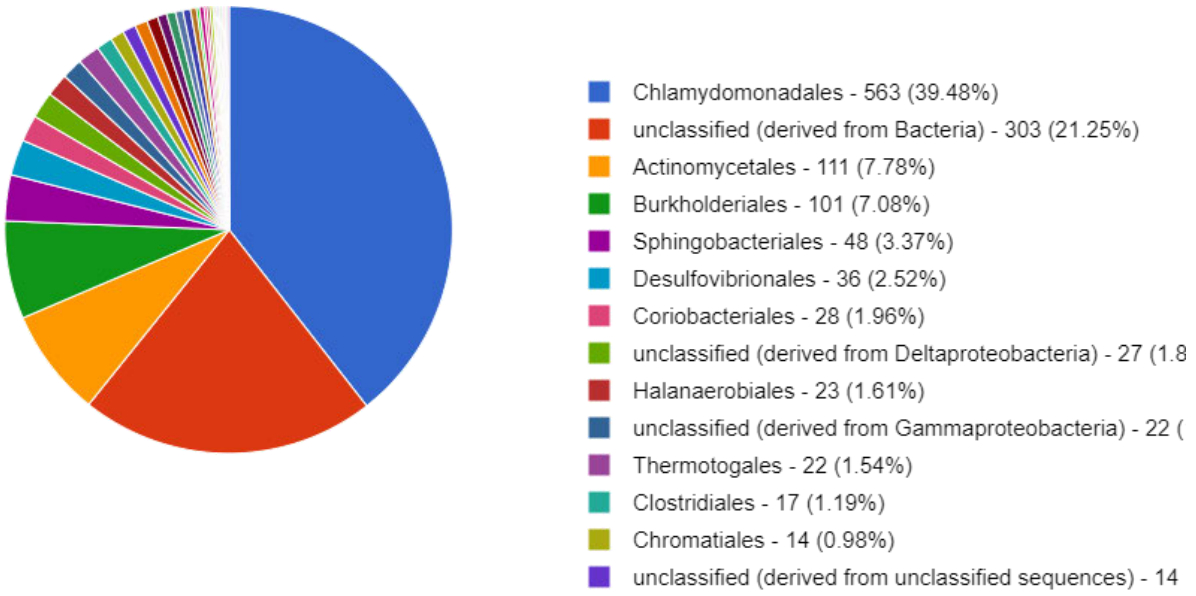

The Order Distribution of the 16S Analysis for the NS Pond.

Family

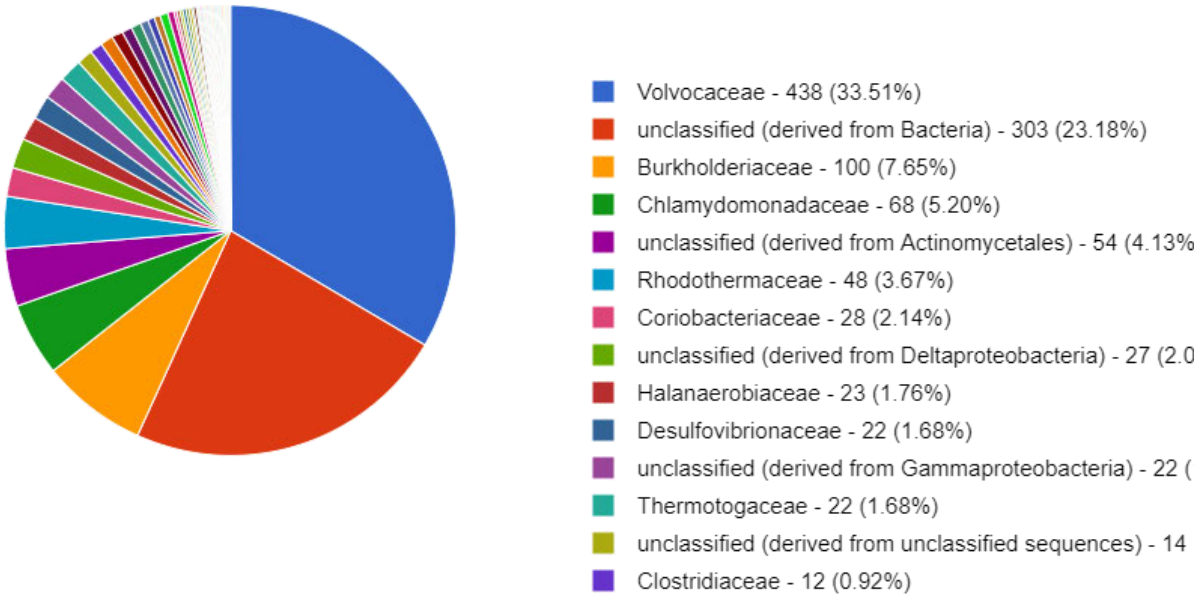

The Family Distribution of the 16S Analysis for the NS Pond.

Rarefaction Curve

The plot below shows the rarefaction curve of annotated species richness. This curve is a plot of the total number of distinct species annotations as a function of the number of sequences sampled. On the left, a steep slope indicates that a large fraction of the species diversity remains to be discovered. If the curve becomes flatter to the right, a reasonable number of individuals is sampled. More intensive sampling is likely to yield only a few additional species.

Sampling curves generally rise very quickly at first and then level off toward an asymptote as fewer new species are found per unit of individuals collected. These rarefaction curves are calculated from the table of species abundance. The curves represent the average number of different species annotations for subsamples of the complete data set.

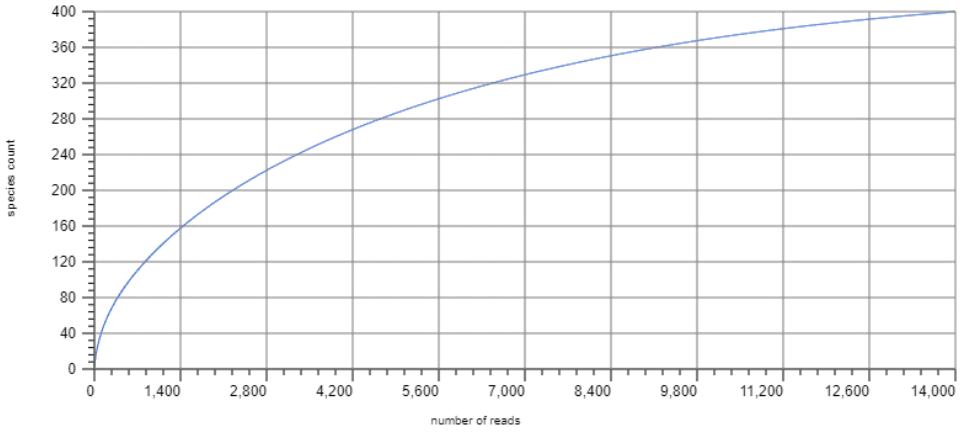

The Rarefaction Curve of the 16S Analysis for the NS Pond.

Sequence Breakdown

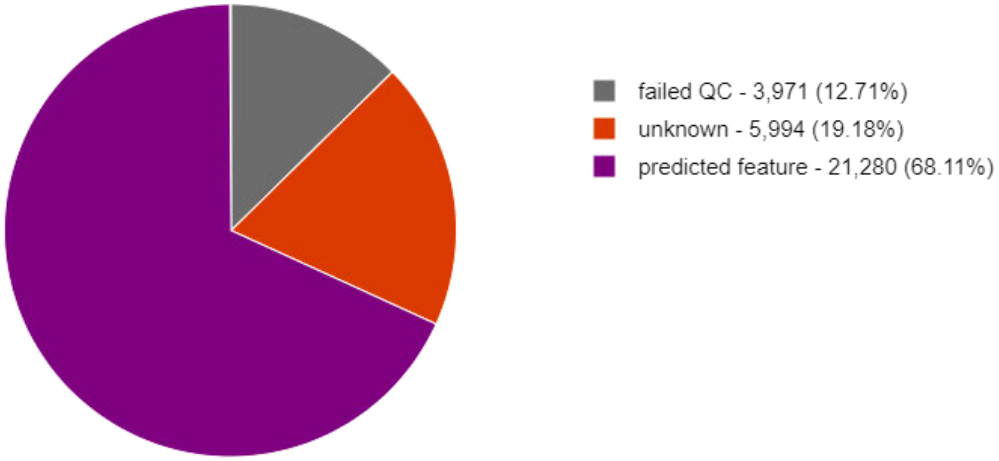

The Sequence Breakdown of the 16S Analysis for the WI Pond.

Of the sequences tested, 3,971 sequences (12.71%) failed to pass the QC pipeline. Of those, dereplication identified 24,577 sequences as artificial duplicate reads.

Analysis Statistics

Table 7.2: The Analysis Statistics of the 16S Analysis for the WI Pond.

UPLOAD bp COUNT	**7 962 514 bp**
UPLOAD SEQUENCES COUNT	**31 245**
UPLOAD MEAN SEQUENCE LENGTH	**255 ± 92 bp**
UPLOAD MEAN GC PERCENT	**54 ± 13 %**
ARTIFICIAL DUPLICATE READS SEQUENCE COUNT	**24 577**
POST QC bp COUNT	**684 086 bp**
POST QC SEQUENCES COUNT	**2 695**
POST QC MEAN SEQUENCE LENGTH	**254 ± 66 bp**
POST QC MEAN GC PERCENT	**60 ± 7 %**
PROCESSED PREDICTED PROTEIN FEATURES	**171**

PROCESSED PREDICTED rRNA FEATURES	**5 654**
ALIGNMENT IDENTIFIED PROTEIN FEATURES	**94**
ALIGNMENT IDENTIFIED rRNA FEATURES	**5 641**
ANNOTATION IDENTIFIED FUNCTIONAL CATEGORIES	**UNDEFINED**

Domain

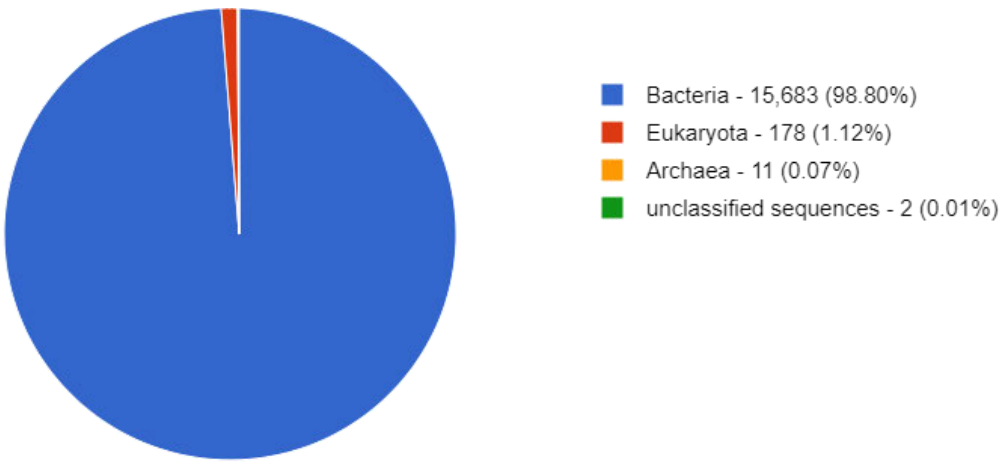

The Domain Distribution of the 16S Analysis for the WI Pond.

Phylum

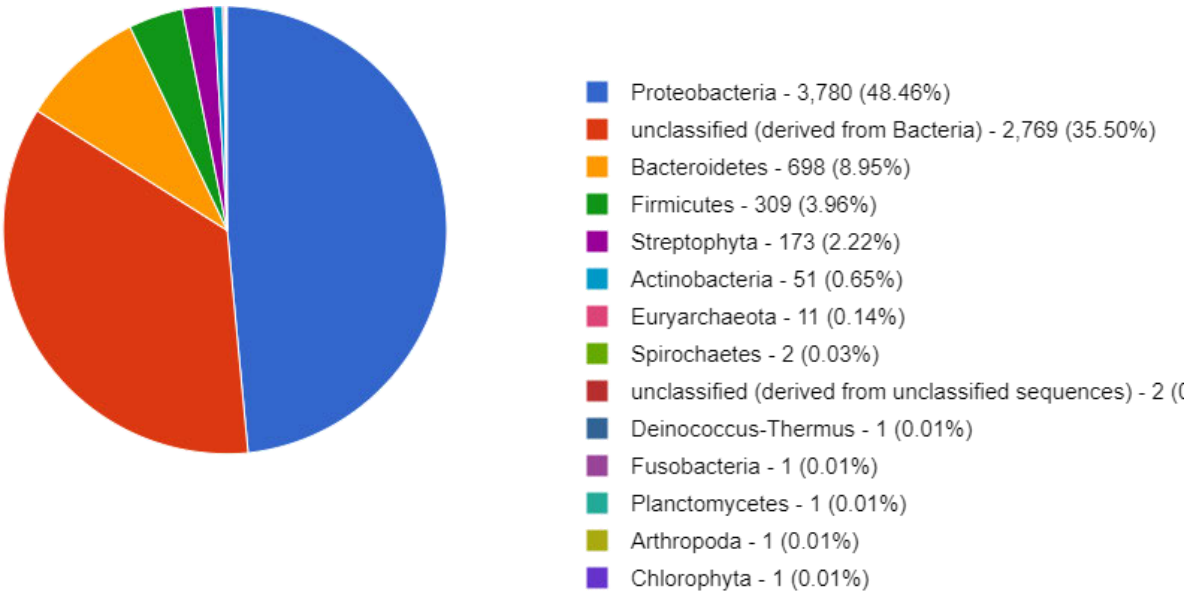

The Phyla Distribution of the 16S Analysis for the WI Pond.

Class

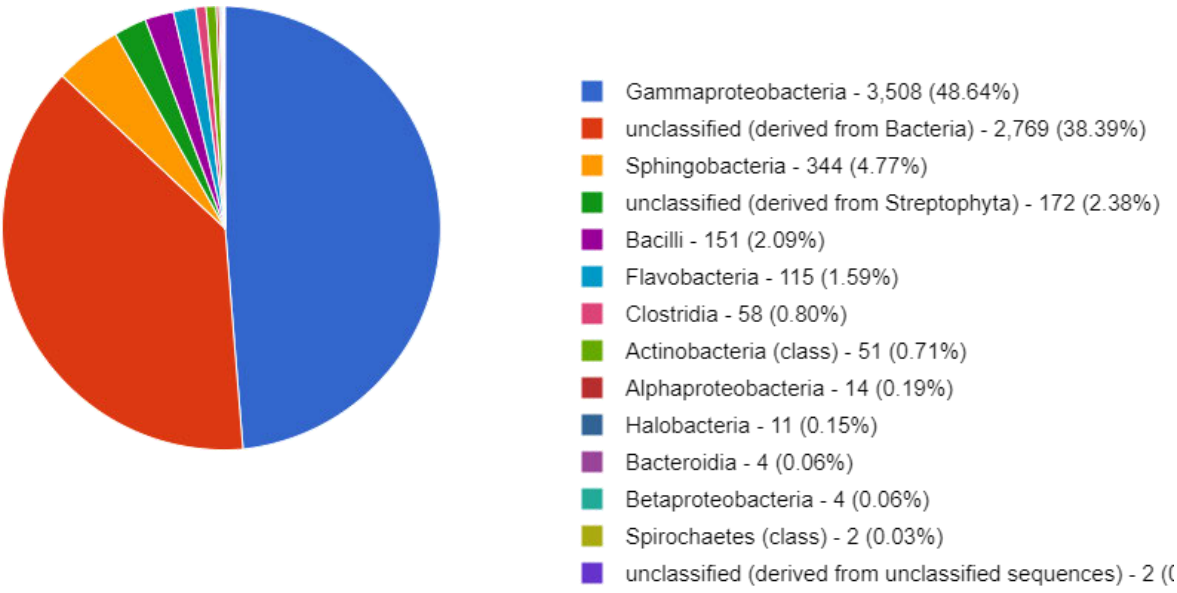

The Class Distribution of the 16S Analysis for the WI Pond.

Order

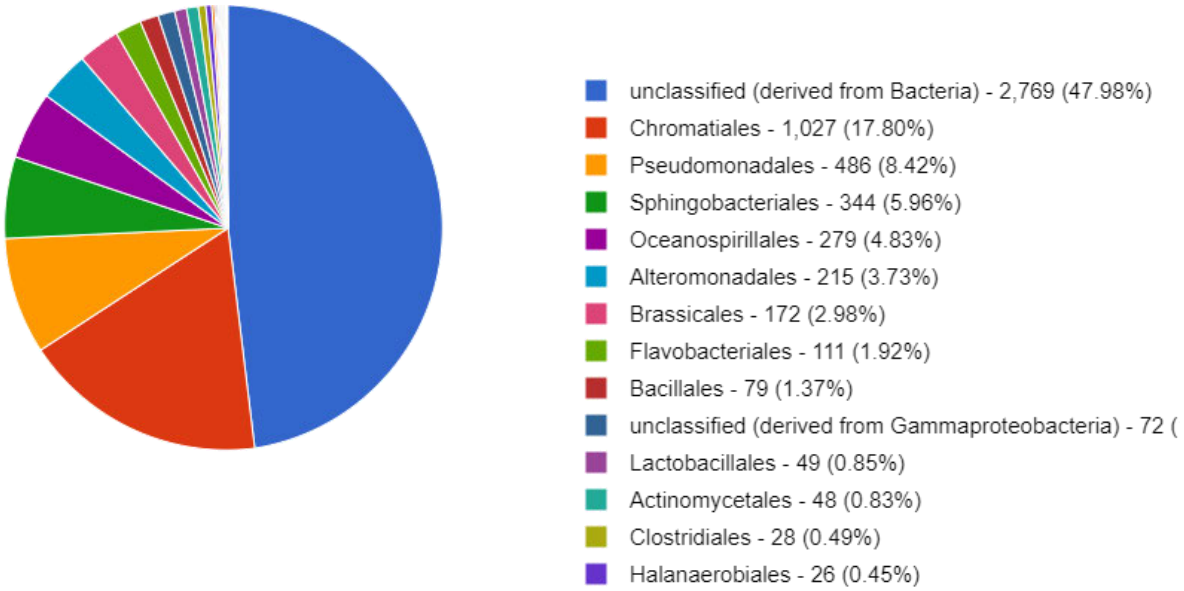

The Order Distribution of the 16S Analysis for the WI Pond.

Family

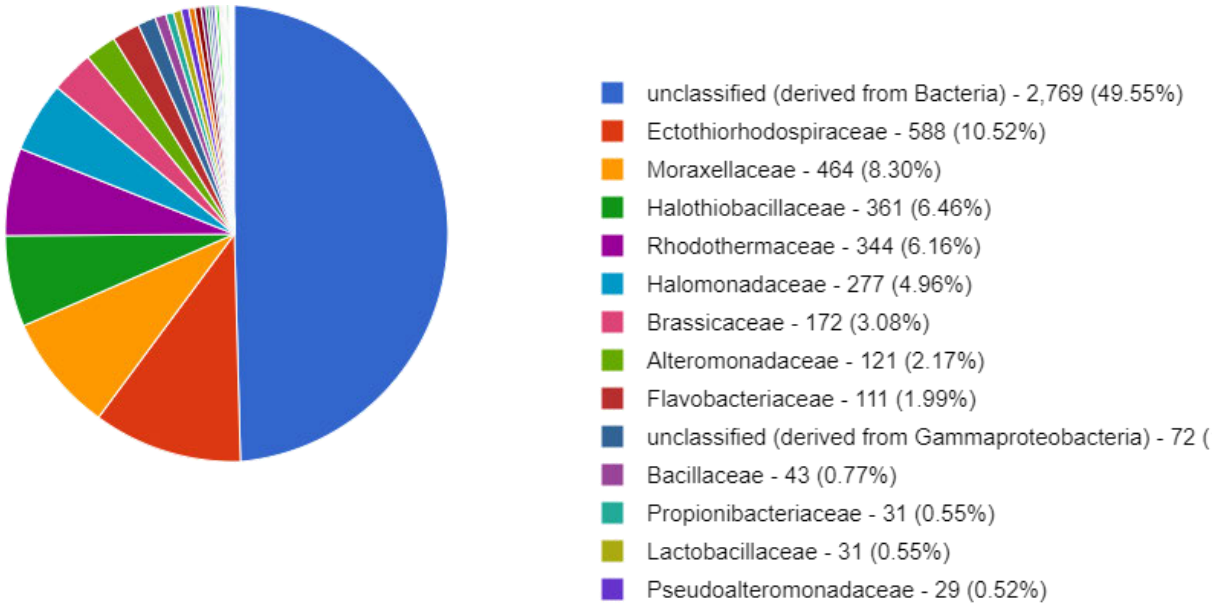

The Family Distribution of the 16S Analysis for the WI Pond.

Rarefaction Curve

The plot below shows the rarefaction curve of annotated species richness. This curve is a plot of the total number of distinct species annotations as a function of the number of sequences sampled. On the left, a steep slope indicates that a large fraction of the species diversity remains to be discovered. If the curve becomes flatter to the right, a reasonable number of individuals is sampled. More intensive sampling is likely to yield only few additional species.

Sampling curves generally rise very quickly at first and then level off toward an asymptote as fewer new species are found per unit of individuals collected. These rarefaction curves are calculated from the table of species abundance. The curves represent the average number of different species annotations for subsamples of the complete data set.

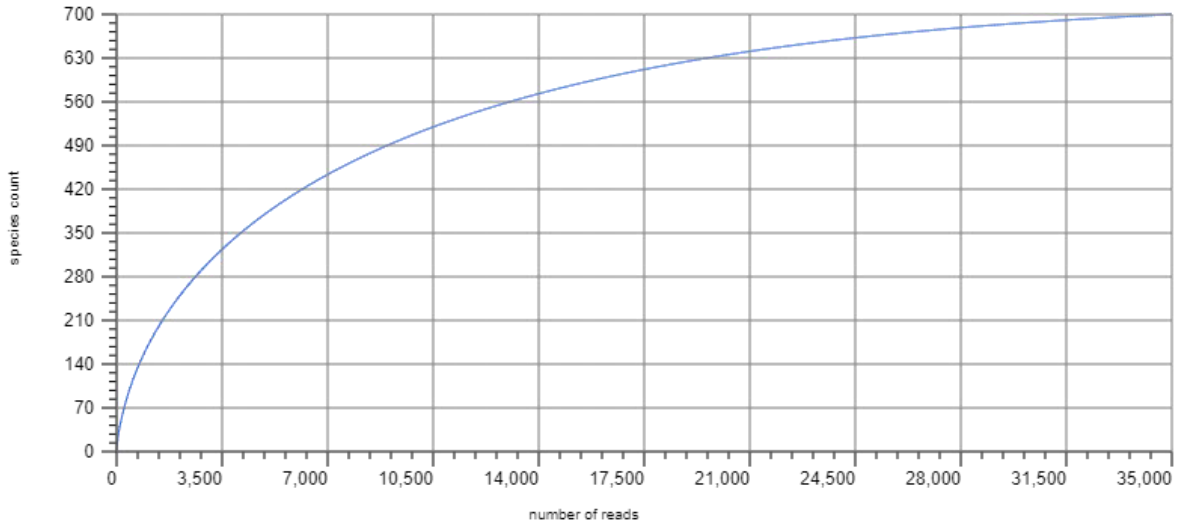

The Rarefaction Curve of the 16S Analysis of the WI Pond.

Sequence Breakdown

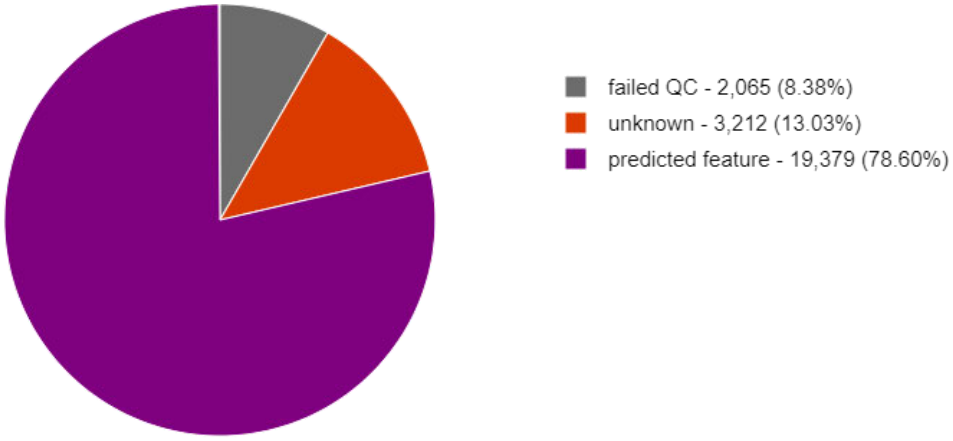

The Sequence Breakdown of the 16S Analysis for the ST Pond.

Of the sequences tested, 2,065 sequences (8.38%) failed to pass the QC pipeline. Of those, dereplication identified 20,981 sequences as artificial duplicate reads.

Analysis Statistics

The Analysis Statistics of the 16S Analysis for the ST Pond.

UPLOAD bp COUNT	**6 625 519 bp**
UPLOAD SEQUENCES COUNT	**24 656**
UPLOAD MEAN SEQUENCE LENGTH	**269 ± 79 bp**
UPLOAD MEAN GC PERCENT	**55 ± 11 %**
ARTIFICIAL DUPLICATE READS SEQUENCE COUNT	**20 981**
POST QC bp COUNT	**403 776 bp**
POST QC SEQUENCES COUNT	**1 608**
POST QC MEAN SEQUENCE LENGTH	**251 ± 68 bp**
POST QC MEAN GC PERCENT	**59 ± 5 %**
PROCESSED PREDICTED PROTEIN FEATURES	**68**

PROCESSED PREDICTED rRNA FEATURES	**3 175**
ALIGNMENT IDENTIFIED PROTEIN FEATURES	**25**
ALIGNMENT IDENTIFIED rRNA FEATURES	**3 159**
ANNOTATION IDENTIFIED FUNCTIONAL CATEGORIES	**UNDEFINED**

Domain

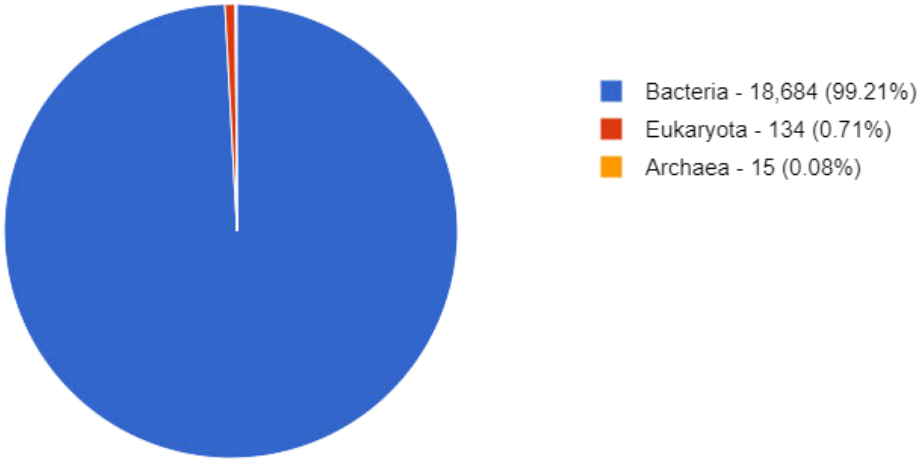

The Domain Distribution of the 16S Analysis for the ST Pond.

Phylum

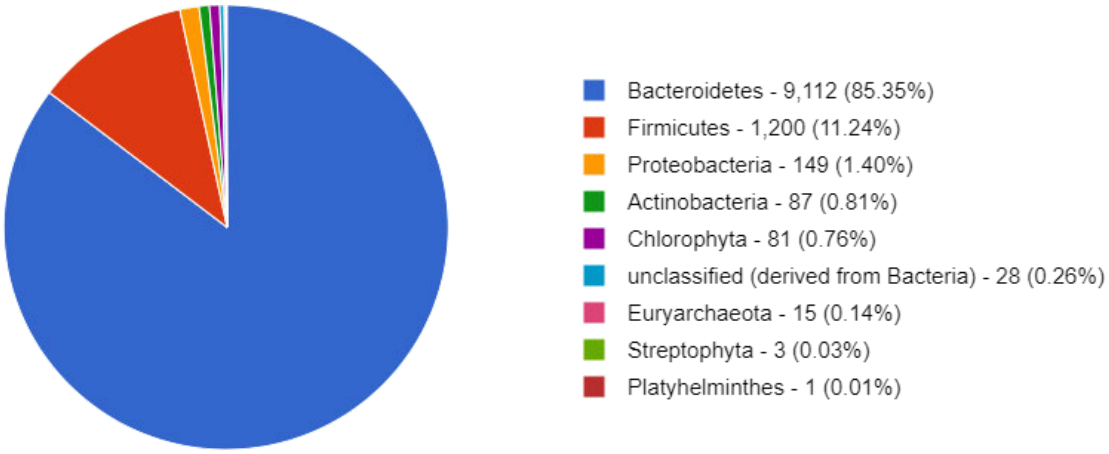

The Phylum Distribution of the 16S Analysis for the ST Pond.

Class

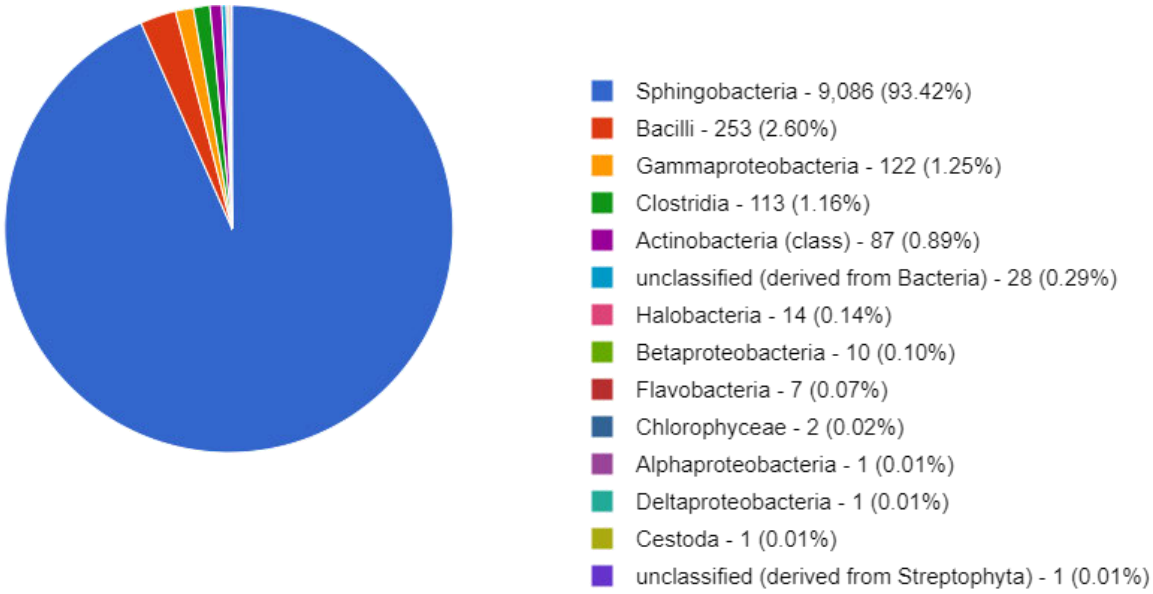

The Class Distribution of the 16S Analysis for the ST Pond.

Order

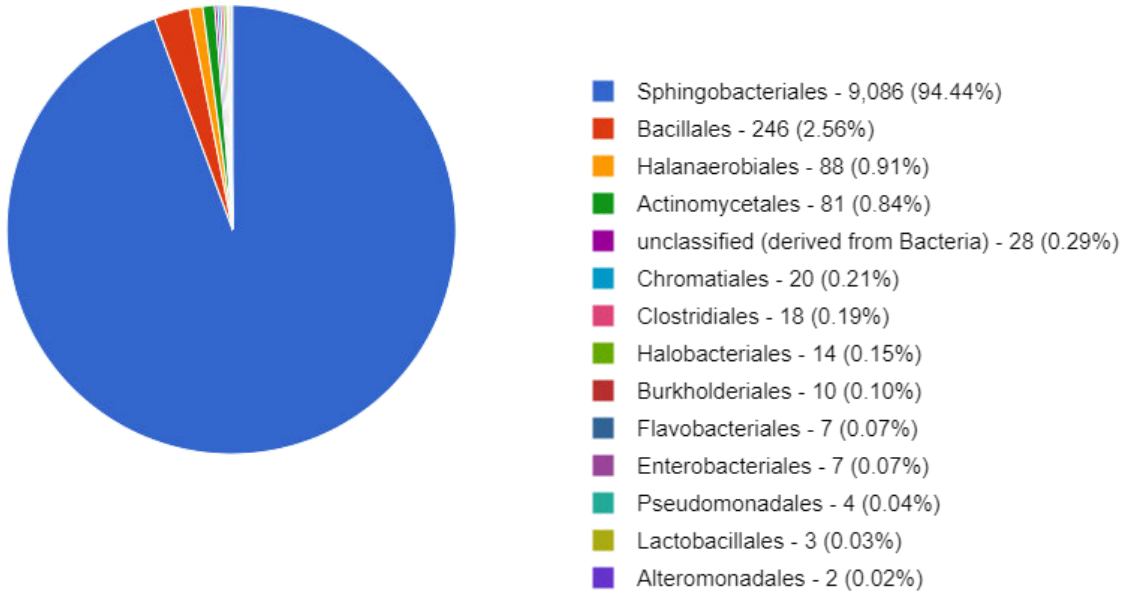

The Order Distribution of the 16S Analysis for the ST Pond.

Family

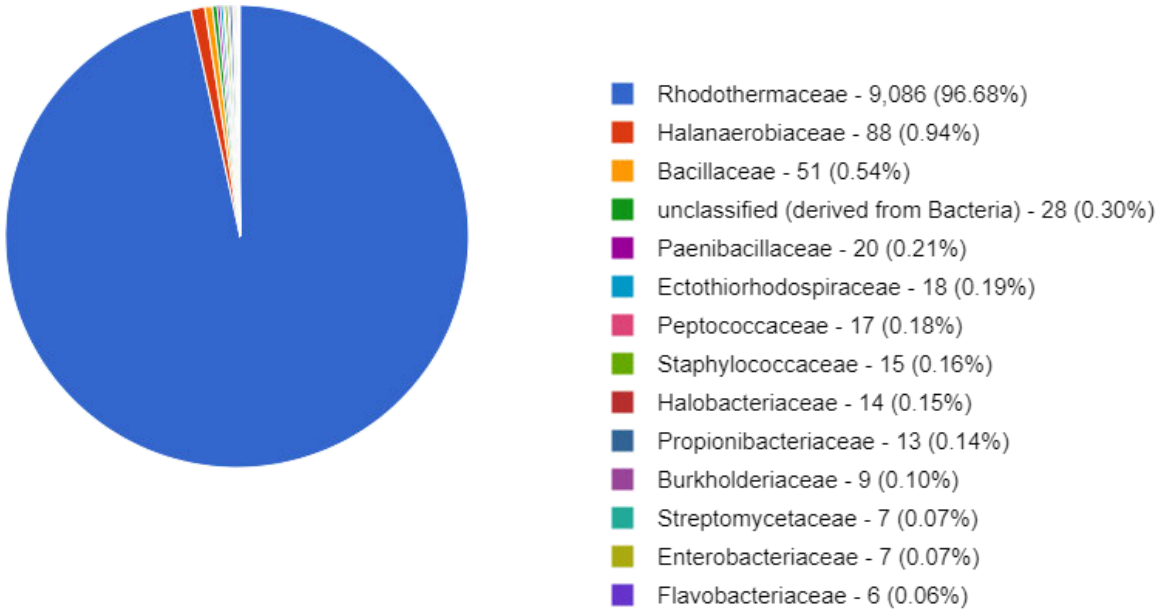

The Family Distribution of the 16S Analysis for the ST Pond.

Rarefaction Curve

The plot below shows the rarefaction curve of annotated species richness. This curve is a plot of the total number of distinct species annotations as a function of the number of sequences sampled. On the left, a steep slope indicates that a large fraction of the species diversity remains to be discovered. If the curve becomes flatter to the right, a reasonable number of individuals is sampled. More intensive sampling is likely to yield only few additional species.

Sampling curves generally rise very quickly at first and then level off toward an asymptote as fewer new species are found per unit of individuals collected. These rarefaction curves are calculated from the table of species abundance. The curves represent the average number of different species annotations for subsamples of the complete data set.

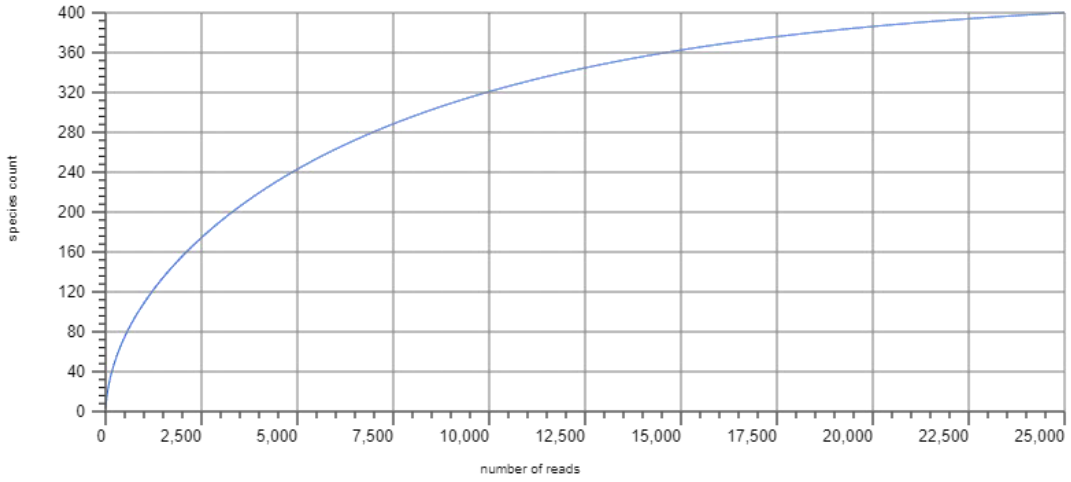

The Rarefaction Curve of the 16S Analysis for the ST Pond.

Chapter 3

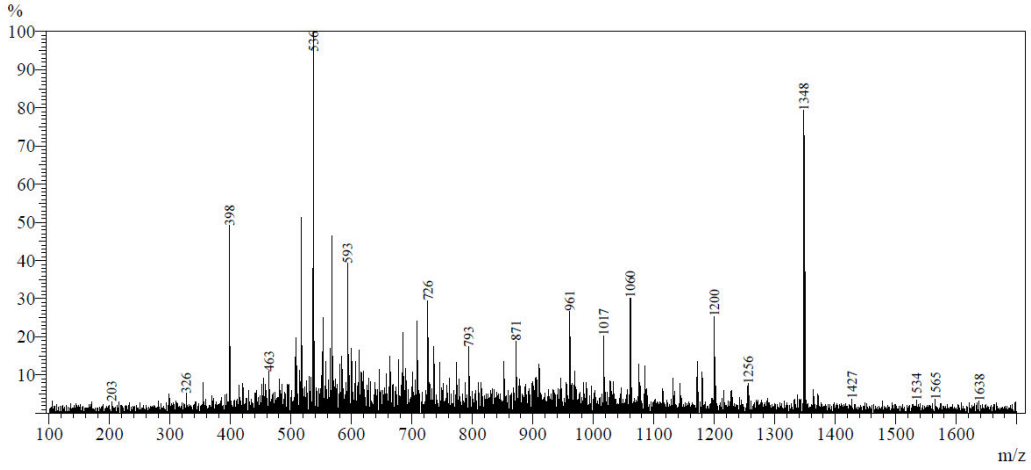

The LCMS Results for the 2M NaCl Treatment.

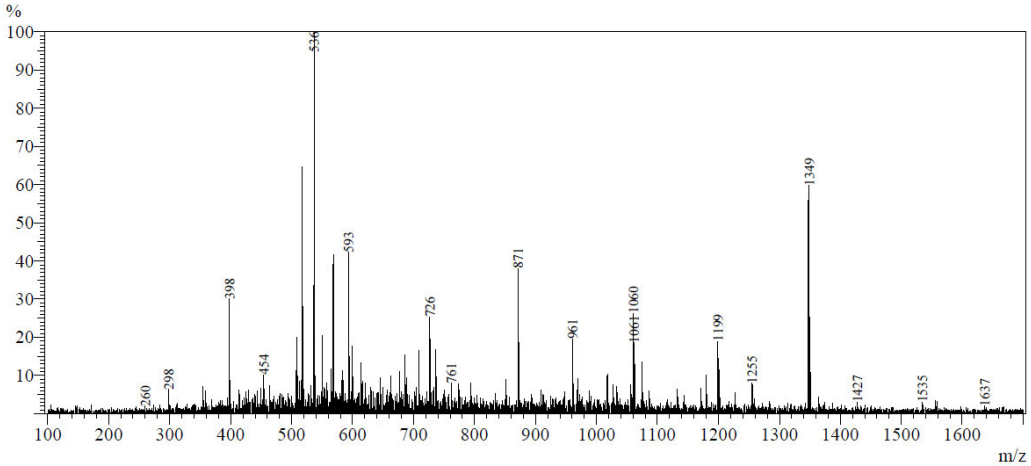

The LCMS Results for the 2,5M NaCl Treatment.

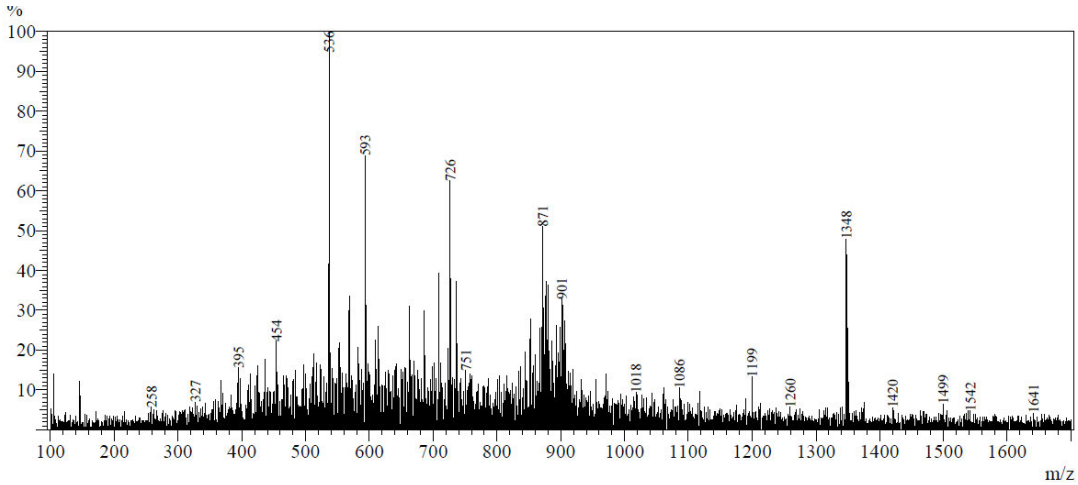

The LCMS Results of the 3M NaCl Treatment.

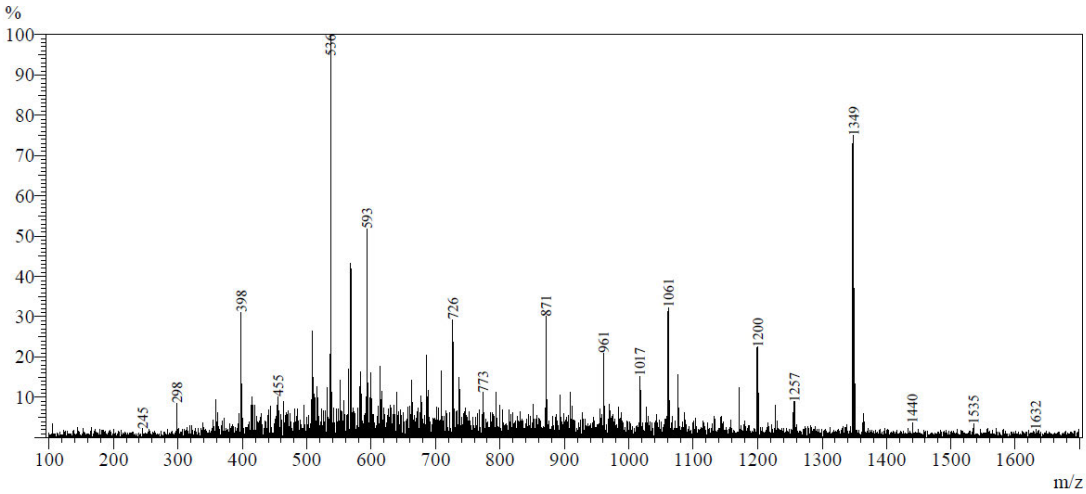

The LCMS Results of the 3,5M NaCl Treatment.

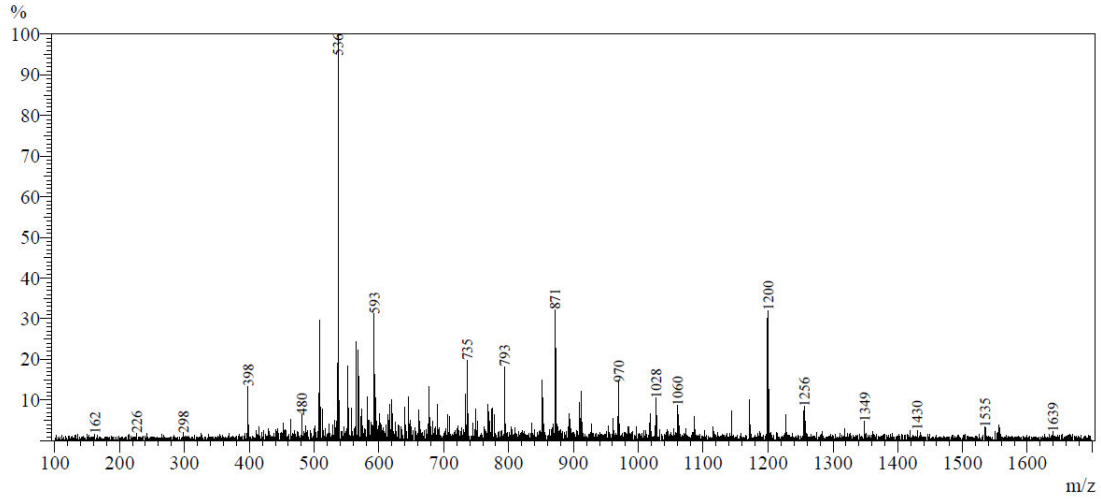

The LCMS Results for the NO_3 Treatment.

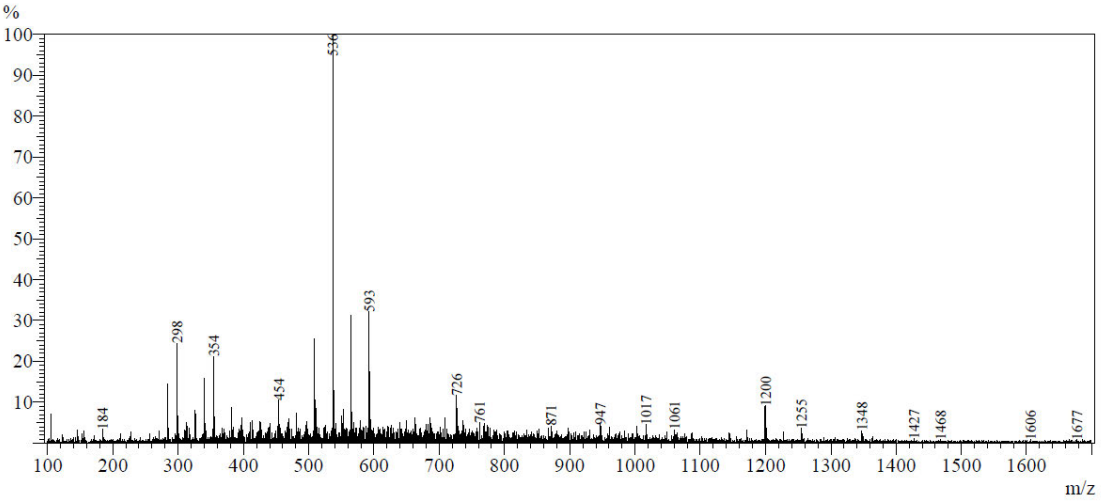

The LCMS Results for the Ammonia Treatment.

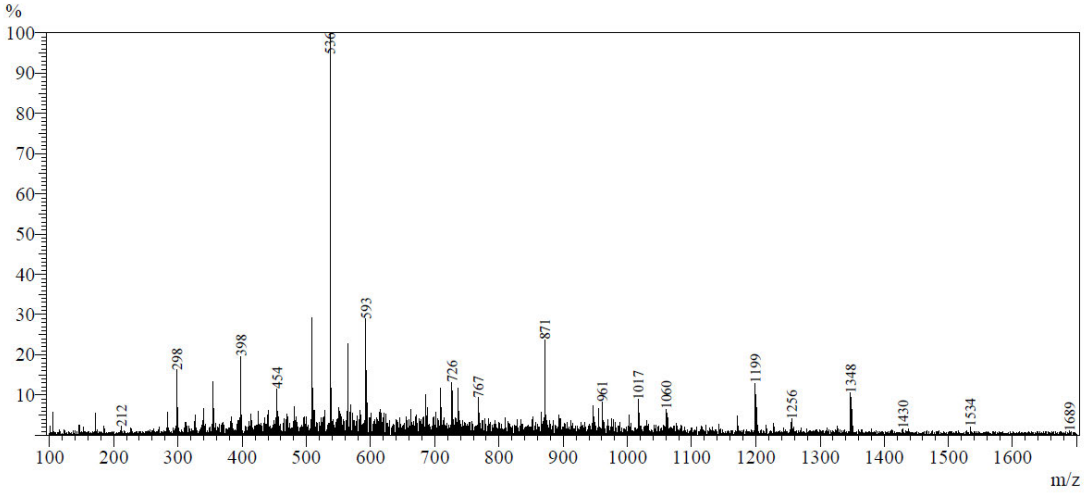

The LCMS Results for the Urea Treatment.

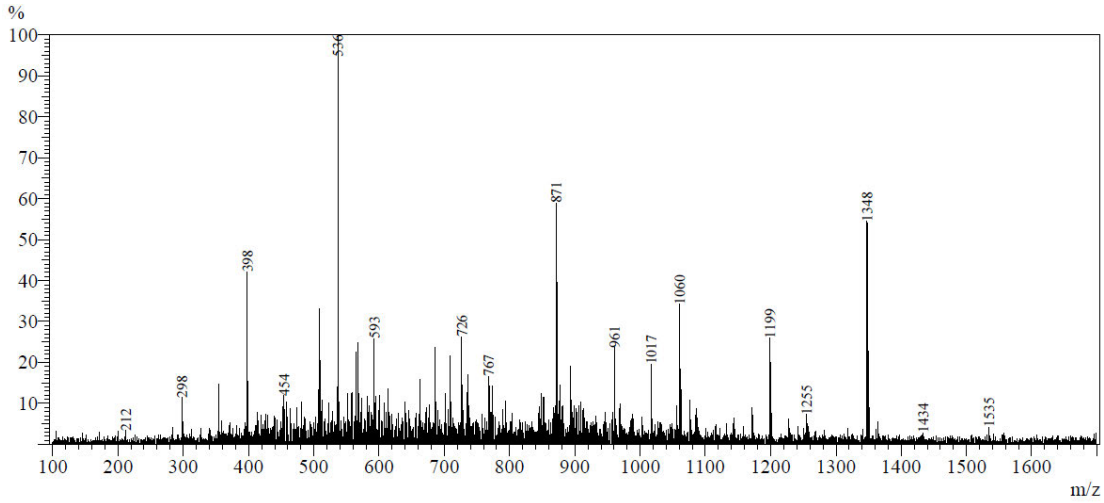

The LCMS Results for the Control Treatment.

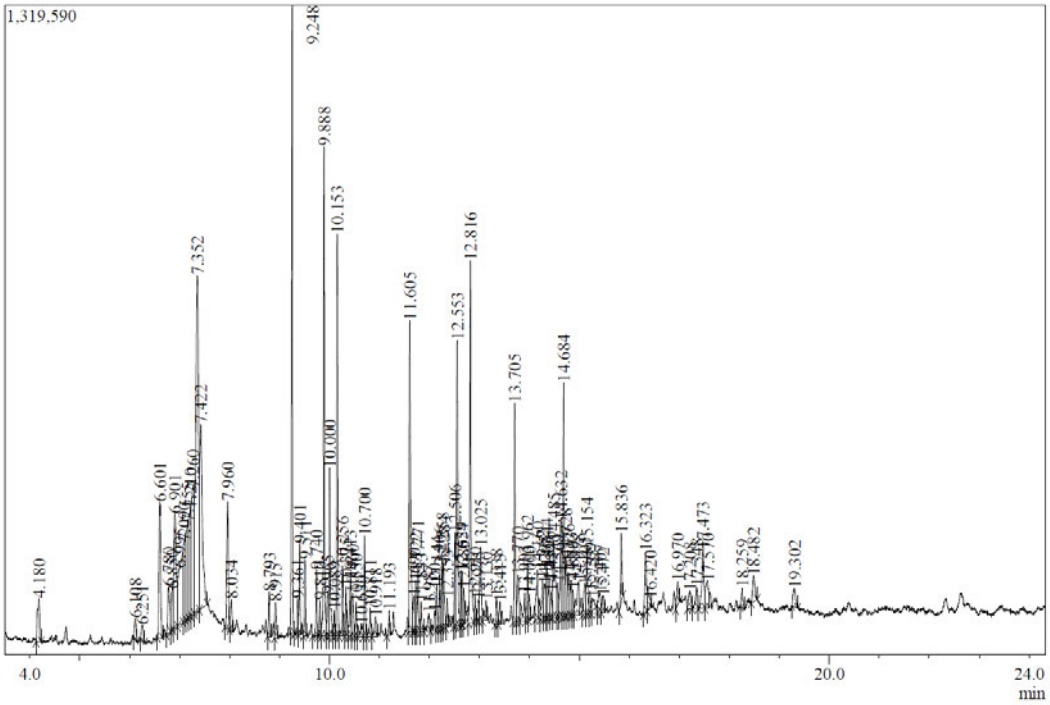

The GC-MS Chromatogram for the 2M NaCl treatment.

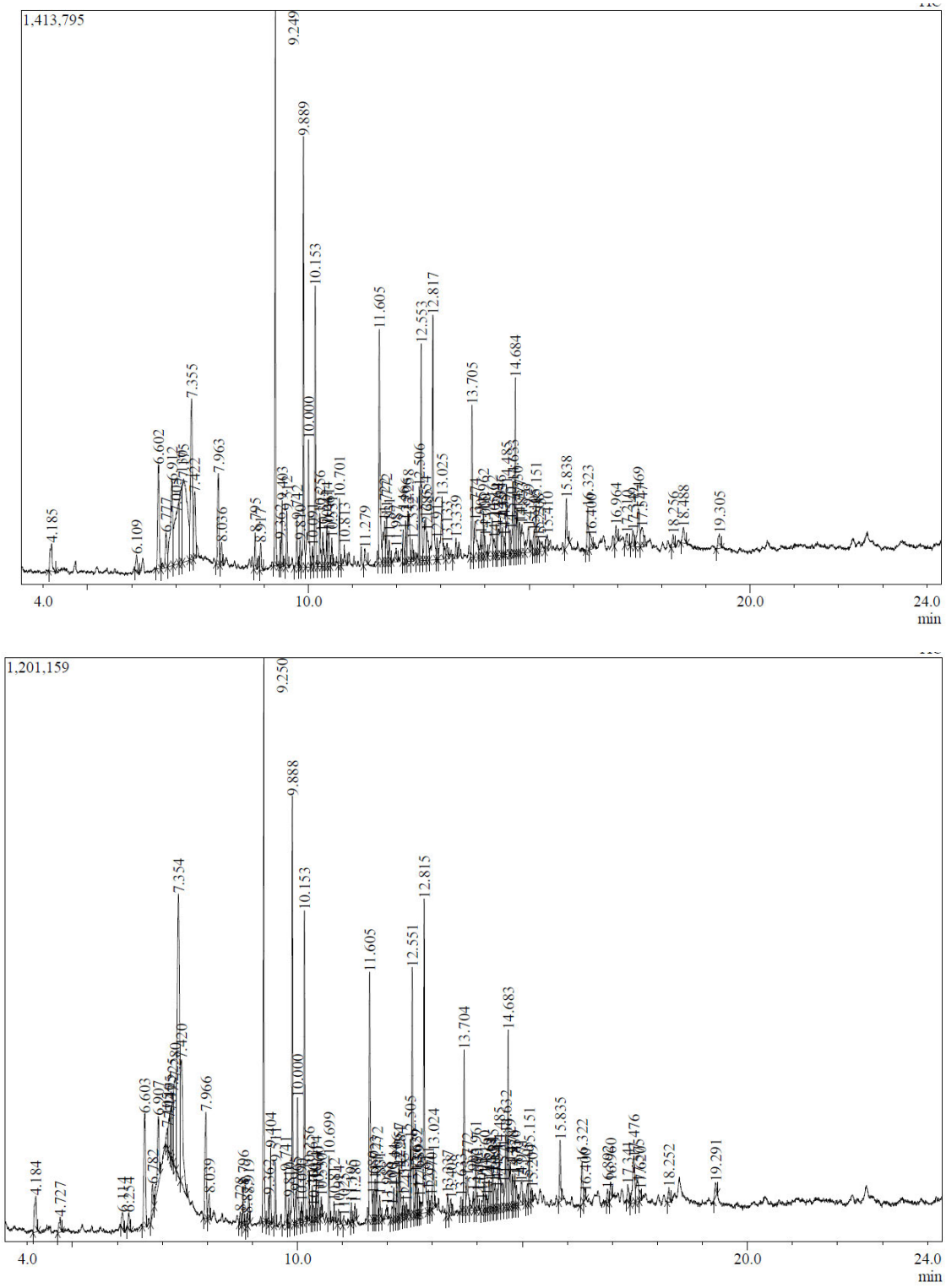

The GC-MS Chromatogram for the 2,5M NaCl treatment.

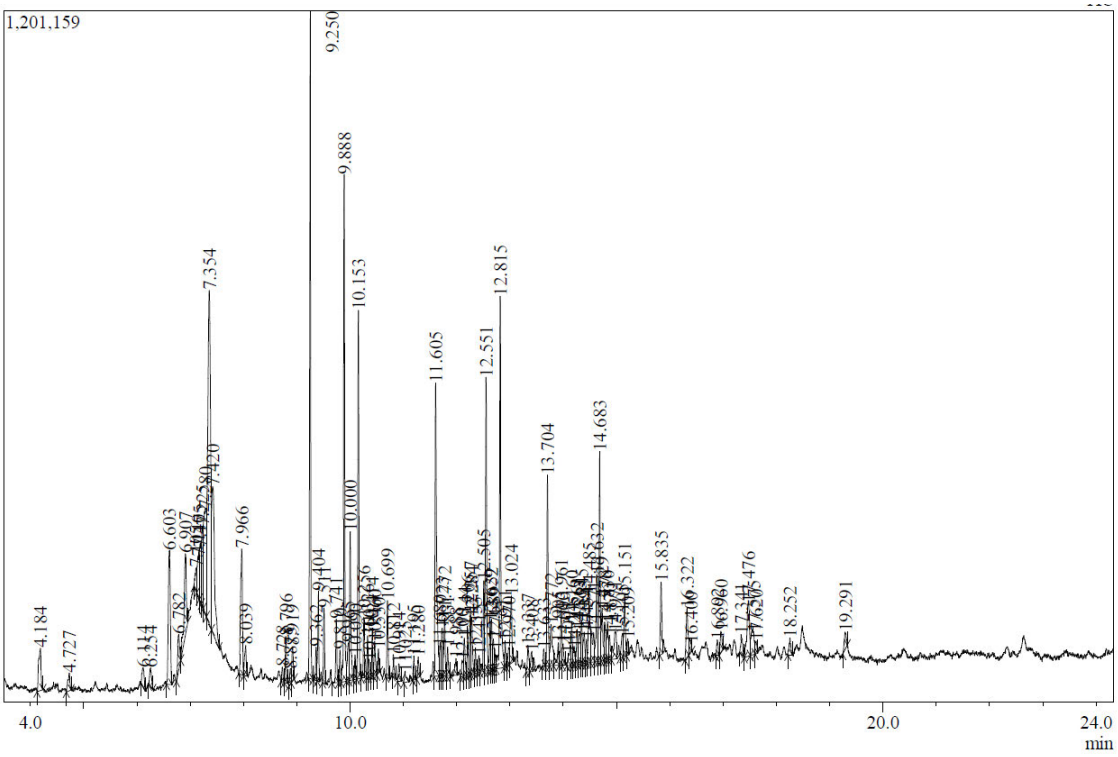

The GC-MS Chromatogram for the 3M NaCl treatment.

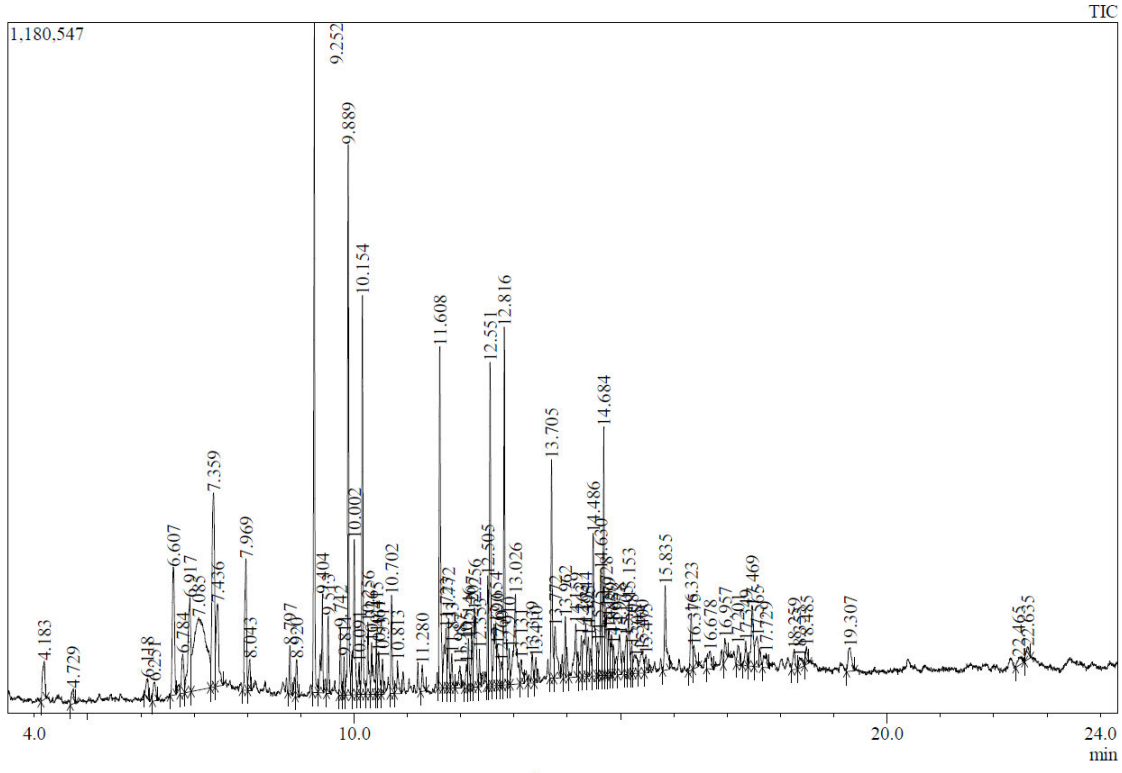

The GC-MS Chromatogram for the 3,5M NaCl treatment.

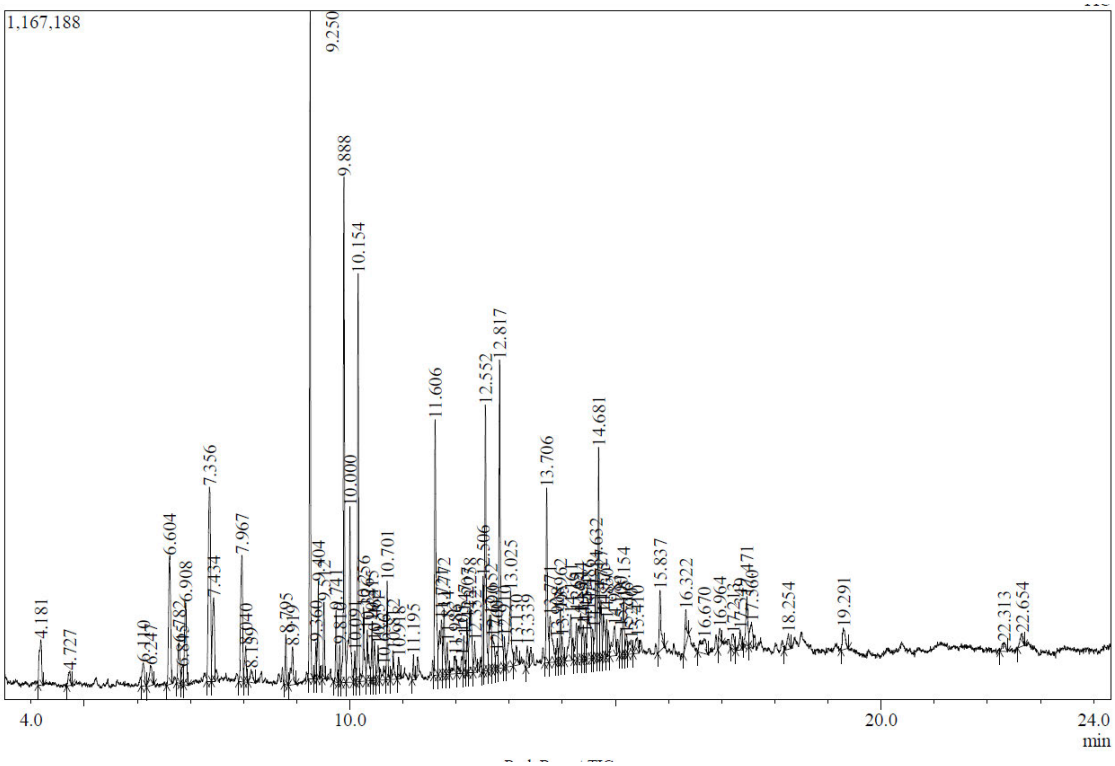

The GC-MS Chromatogram of the NO_3 treatment.

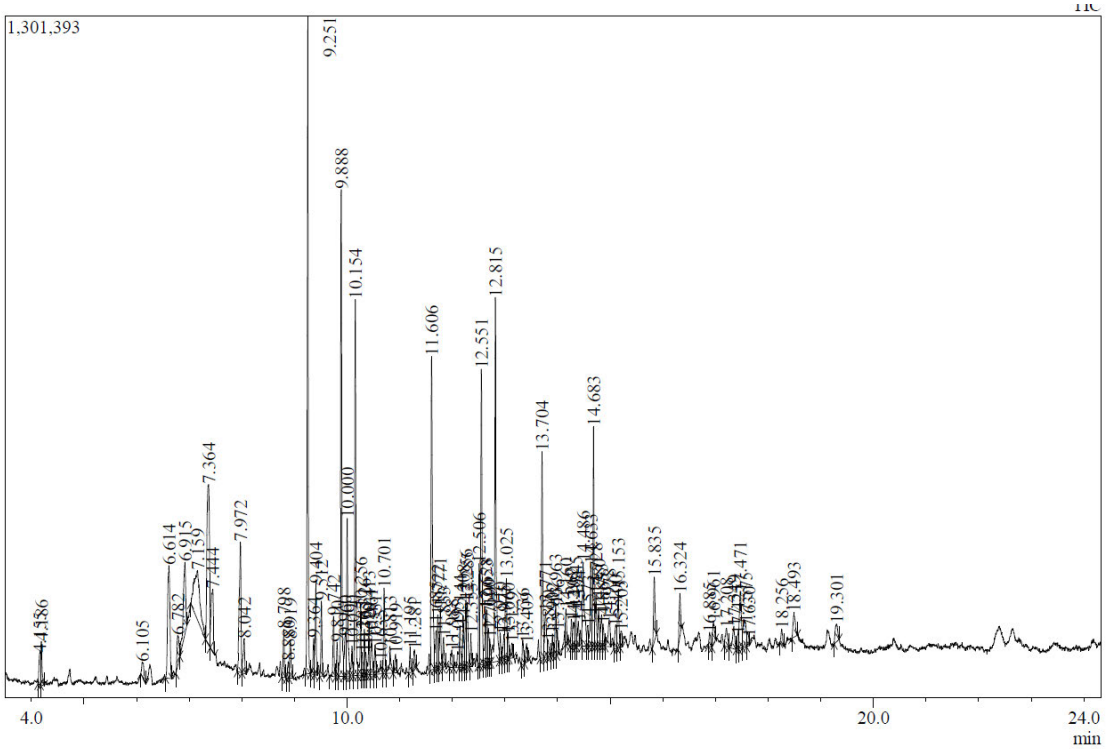

The GC-MS Chromatogram of the Ammonia treatment.

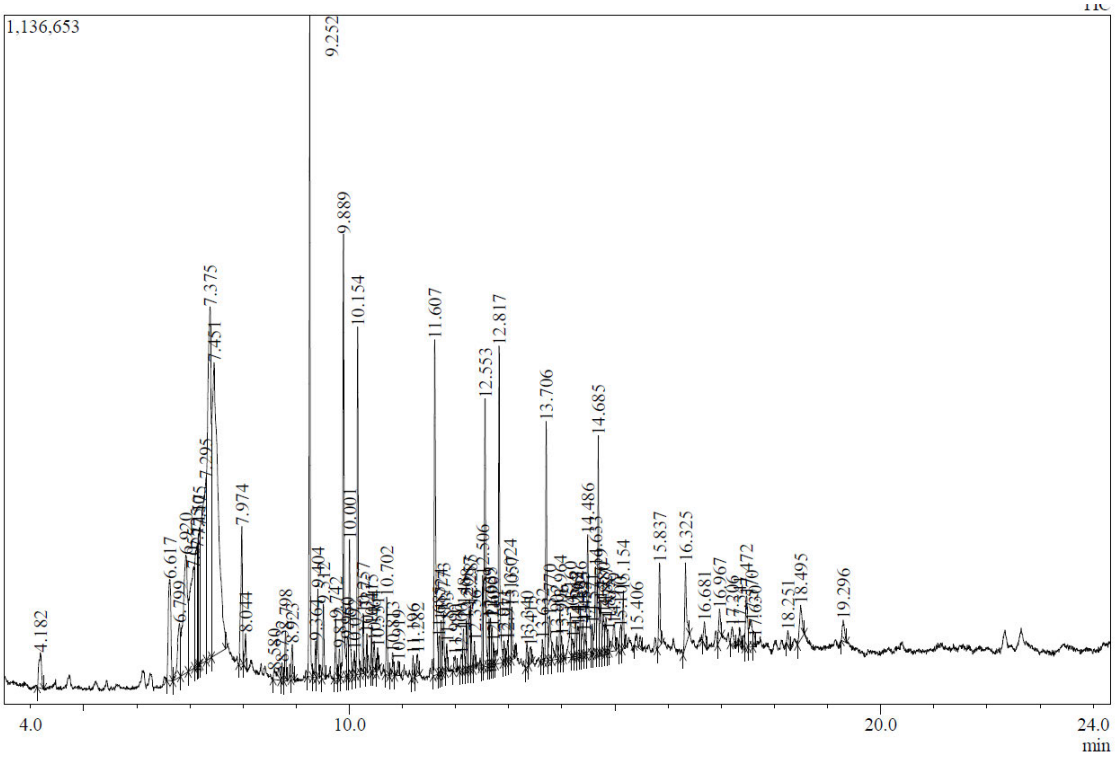

The GC-MS Chromatogram of the Urea treatment.

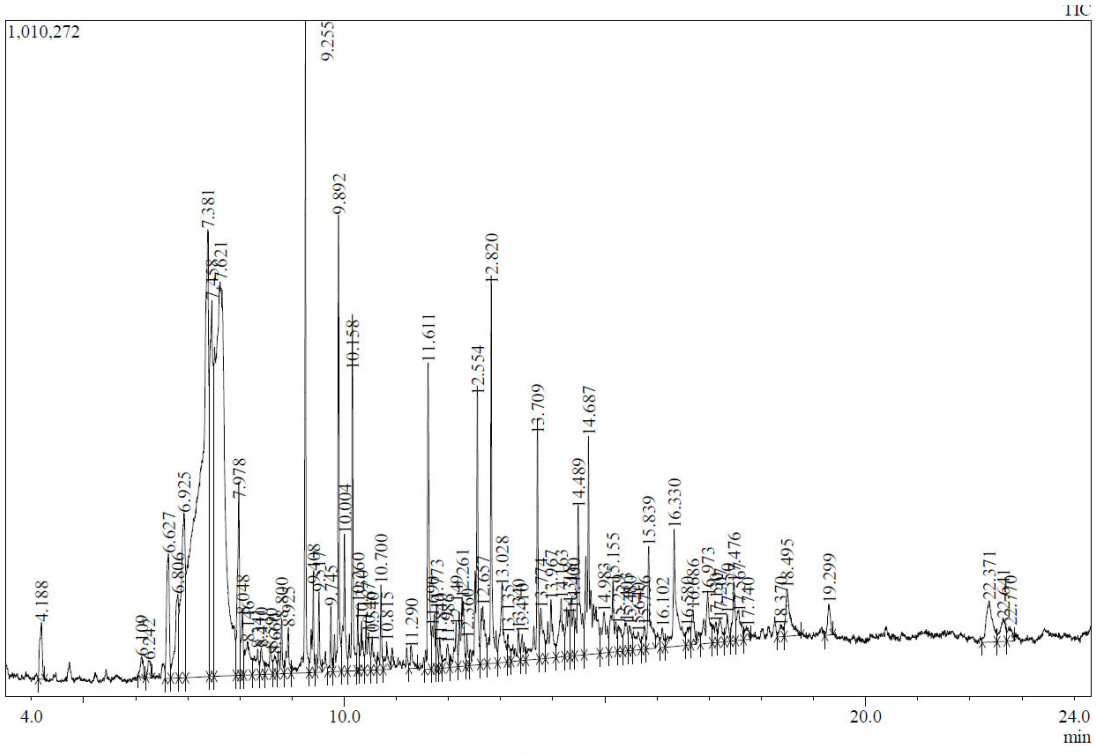

The GC-MS Chromatogram of the Control treatment.

Table A 1: 100 Chemical Compounds identified in the 2M Treatment of *D. salina*.

Peak#	R.Time	Area	Area%	Height	Height%	A/H	Name
1	4.180	259334	0.78	87781	0.55	2.95	Heptane, 2,4-dimethyl-
2	6.108	92624	0.28	42518	0.27	2.18	Nonane, 2-methyl-
3	6.251	78945	0.24	32776	0.21	2.41	Nonane, 2,5-dimethyl-
4	6.601	672511	2.03	276289	1.75	2.43	Octane, 3,5-dimethyl-
5	6.780	284618	0.86	94465	0.60	3.01	Nonane, 2,5-dimethyl-
6	6.850	213794	0.64	83682	0.53	2.55	Nonane, 2,5-dimethyl-
7	6.901	820166	2.47	232571	1.47	3.53	Octane, 3,3-dimethyl-
8	6.995	802595	2.42	115779	0.73	6.93	Propylamine, N,N,2,2-tetramethyl-, N-oxide
9	7.090	582921	1.76	161392	1.02	3.61	Oxirane, [[(2-ethylhexyl)oxy]methyl]-
10	7.155	569073	1.71	196202	1.24	2.90	Methane, nitro-
11	7.210	638822	1.92	221038	1.40	2.89	Propane, 2-fluoro-2-methyl-
12	7.260	1044108	3.14	256464	1.62	4.07	Octane, 6-ethyl-2-methyl-
13	7.352	2661420	8.02	682460	4.31	3.90	Nonane, 5-(2-methylpropyl)-
14	7.422	1334001	4.02	375057	2.37	3.56	Octane, 2,3,6,7-tetramethyl-
15	7.960	548404	1.65	258031	1.63	2.13	Dodecane, 4,6-dimethyl-
16	8.034	133451	0.40	64980	0.41	2.05	Octane, 6-ethyl-2-methyl-
17	8.793	153150	0.46	91947	0.58	1.67	Nonane, 5-(2-methylpropyl)-
18	8.915	144157	0.43	72853	0.46	1.98	Undecane, 4,6-dimethyl-
19	9.248	1902640	5.73	1275797	8.06	1.49	Dodecane
20	9.361	93974	0.28	71063	0.45	1.32	Undecane, 2,4-dimethyl-
21	9.401	265373	0.80	184287	1.16	1.44	Undecane, 4,6-dimethyl-
22	9.511	207056	0.62	154534	0.98	1.34	Dodecane, 4-methyl-
23	9.740	176972	0.53	134692	0.85	1.31	Tetradecane
24	9.810	105874	0.32	71717	0.45	1.48	Tetradecane
25	9.888	1483595	4.47	995015	6.29	1.49	Benzene, 1,3-bis(1,1-dimethylethyl)-
26	9.965	186874	0.56	85019	0.54	2.20	Decane, 2,3,4-trimethyl-

Peak#	R.Time	Area	Area%	Height	Height%	A/H	Name
27	10.000	507258	1.53	341691	2.16	1.48	Tetradecane, 5-methyl-
28	10.089	82391	0.25	53093	0.34	1.55	Tetradecane, 4-methyl-
29	10.153	1041142	3.14	817336	5.17	1.27	Dodecane, 2,6,11-trimethyl-
30	10.256	220138	0.66	144015	0.91	1.53	Octane, 2,3,6,7-tetramethyl-
31	10.325	137064	0.41	101082	0.64	1.36	Nonane, 5-(2-methylpropyl)-
32	10.413	183891	0.55	117485	0.74	1.57	Dodecane, 2,6,11-trimethyl-
33	10.460	172378	0.52	88490	0.56	1.95	Heptadecane, 2,6,10,15-tetramethyl-
34	10.530	110411	0.33	70069	0.44	1.58	Decane, 2,3,7-trimethyl-
35	10.630	107735	0.32	25515	0.16	4.22	Nonane, 1-iodo-
36	10.700	267097	0.80	203737	1.29	1.31	Dodecane, 2,6,11-trimethyl-
37	10.811	132391	0.40	58865	0.37	2.25	Octane, 6-ethyl-2-methyl-
38	10.918	100472	0.30	40521	0.26	2.48	Nonane, 3-methyl-5-propyl-
39	11.193	77034	0.23	51071	0.32	1.51	Heptadecane, 2,6,10,15-tetramethyl-
40	11.605	1158679	3.49	632493	4.00	1.83	Tetradecane
41	11.690	122488	0.37	72417	0.46	1.69	Dodecane, 2,6,11-trimethyl-
42	11.722	192613	0.58	103103	0.65	1.87	Pentadecane, 2,6,10-trimethyl-
43	11.771	202174	0.61	128313	0.81	1.58	Eicosane
44	11.833	103784	0.31	60557	0.38	1.71	Tetradecane, 4-methyl-
45	11.987	104841	0.32	36892	0.23	2.84	Hexadecane
46	12.100	112899	0.34	38847	0.25	2.91	Octane, 2,3,6,7-tetramethyl-
47	12.144	161198	0.49	92366	0.58	1.75	Heptadecane
48	12.206	201376	0.61	111018	0.70	1.81	Heptadecane
49	12.258	221338	0.67	137684	0.87	1.61	Dodecane, 4-methyl-
50	12.284	221319	0.67	130221	0.82	1.70	Eicosane, 2,4-dimethyl-
51	12.353	102394	0.31	59674	0.38	1.72	2,3-Dimethyldodecane
52	12.506	274055	0.83	190479	1.20	1.44	Eicosane
53	12.553	1001826	3.02	580300	3.67	1.73	Eicosane
54	12.629	167138	0.50	109800	0.69	1.52	Heptadecane
55	12.654	148024	0.45	107503	0.68	1.38	Eicosane
56	12.685	125152	0.38	73288	0.46	1.71	Pentadecane
57	12.816	1264286	3.81	735714	4.65	1.72	Phenol, 2,4-bis(1,1-dimethylethyl)-
58	12.910	85881	0.26	54440	0.34	1.58	Eicosane
59	12.975	88676	0.27	44007	0.28	2.02	Tridecane, 7-propyl-
60	13.025	329988	0.99	150128	0.95	2.20	Dodecane, 2,6,11-trimethyl-
61	13.130	92358	0.28	39875	0.25	2.32	Sulfurous acid, dodecyl pentyl ester
62	13.338	96463	0.29	55561	0.35	1.74	Heptadecane, 2,6,10,15-tetramethyl-
63	13.413	90903	0.27	45562	0.29	2.00	Hexadecane, 2-methyl-
64	13.705	637129	1.92	445043	2.81	1.43	Hexadecane
65	13.770	242346	0.73	93610	0.59	2.59	Eicosane
66	13.903	193162	0.58	55052	0.35	3.51	Hexadecane, 4-methyl-
67	13.962	188736	0.57	116477	0.74	1.62	Eicosane
68	14.000	82254	0.25	52362	0.33	1.57	Eicosane
69	14.160	239139	0.72	100337	0.63	2.38	Heptadecane
70	14.262	166601	0.50	80171	0.51	2.08	Dodecane, 4-methyl-
71	14.295	188568	0.57	69236	0.44	2.72	Sulfurous acid, dodecyl pentyl ester
72	14.344	155575	0.47	104835	0.66	1.48	Hexadecane, 1-iodo-
73	14.396	165030	0.50	76053	0.48	2.17	Eicosane
74	14.434	91417	0.28	53427	0.34	1.71	Eicosane
75	14.485	479903	1.45	155514	0.98	3.09	1-Decanol, 2-hexyl-
76	14.569	119215	0.36	69691	0.44	1.71	Eicosane
77	14.632	393111	1.18	197126	1.25	1.99	Eicosane
78	14.684	783485	2.36	474986	3.00	1.65	Eicosane
79	14.728	204592	0.62	121983	0.77	1.68	Eicosane
80	14.776	224268	0.68	87974	0.56	2.55	Eicosane
81	14.833	160186	0.48	71835	0.45	2.23	Dodecane, 2,6,11-trimethyl-
82	14.870	90510	0.27	52128	0.33	1.74	Eicosane
83	14.978	254544	0.77	67711	0.43	3.76	Eicosane
84	15.105	166961	0.50	59483	0.38	2.81	Octadecane, 5-methyl-
85	15.154	258375	0.78	138968	0.88	1.86	Eicosane
86	15.209	90715	0.27	45401	0.29	2.00	Tetracosane
87	15.255	149148	0.45	31117	0.20	4.79	Tetradecane, 4-methyl-
88	15.407	140742	0.42	40067	0.25	3.51	Eicosane
89	15.472	88233	0.27	32881	0.21	2.68	Heptadecane, 3-methyl-
90	15.836	235328	0.71	141069	0.89	1.67	Heptadecane
91	16.323	292935	0.88	122920	0.78	2.38	Isophytol, acetate
92	16.420	134471	0.41	18956	0.12	7.09	Nonadecane, 9-methyl-
93	16.970	112029	0.34	46093	0.29	2.43	2-methyltetracosane
94	17.208	112733	0.34	36082	0.23	3.12	Eicosane
95	17.348	125340	0.38	42799	0.27	2.93	Eicosane
96	17.473	363803	1.10	118732	0.75	3.06	Eicosane
97	17.570	213431	0.64	52820	0.33	4.04	Hexadecane, 1-iodo-
98	18.259	85014	0.26	40164	0.25	2.12	Eicosane
99	18.482	174593	0.53	52000	0.33	3.36	l-(+)-Ascorbic acid 2,6-dihexadecanoate
100	19.302	131046	0.39	36464	0.23	3.59	Heneicosane
		33200375	100.00	15823188	100.00		

Table A 2: 85 Chemical Compounds identified in the 2,5M Treatment of *D. salina*.

Peak#	R.Time	Area	Area%	Height	Height%	A/H	Name
1	4.185	223950	0.79	68068	0.52	3.29	Heptane, 2,4-dimethyl-
2	6.109	94720	0.33	40020	0.31	2.37	Nonane, 2-methyl-
3	6.602	651376	2.29	257305	1.96	2.53	Octane, 3,5-dimethyl-
4	6.777	271542	0.95	85437	0.65	3.18	Nonane, 2,5-dimethyl-
5	6.912	857187	3.01	207528	1.58	4.13	Decane, 4-methyl-
6	7.005	906663	3.18	125969	0.96	7.20	Carbamic acid, acetylthio-, O-methyl ester
7	7.130	834862	2.93	190218	1.45	4.39	Ethanethiol, 2-(diethylboryloxy)-
8	7.175	1552885	5.45	205005	1.56	7.57	Glycerin
9	7.355	1135235	3.99	396592	3.03	2.86	Nonane, 5-(2-methylpropyl)-
10	7.422	436541	1.53	161321	1.23	2.71	Octane, 2,3,6,7-tetramethyl-
11	7.963	507935	1.78	224166	1.71	2.27	Dodecane, 4,6-dimethyl-
12	8.036	121054	0.43	55977	0.43	2.16	Octane, 6-ethyl-2-methyl-
13	8.795	136629	0.48	88956	0.68	1.54	Nonane, 5-(2-methylpropyl)-
14	8.917	129917	0.46	66240	0.51	1.96	Tridecane
15	9.249	1965764	6.90	1368254	10.44	1.44	Dodecane
16	9.362	88613	0.31	65055	0.50	1.36	Undecane, 2,4-dimethyl-
17	9.403	242284	0.85	161667	1.23	1.50	Undecane, 2,5-dimethyl-
18	9.512	198495	0.70	139087	1.06	1.43	Dodecane, 4-methyl-
19	9.742	182041	0.64	117091	0.89	1.55	Tetradecane
20	9.810	101116	0.36	67589	0.52	1.50	Pentadecane
21	9.889	1487223	5.22	1061656	8.10	1.40	Benzene, 1,3-bis(1,1-dimethylethyl)-
22	10.000	645865	2.27	314001	2.40	2.06	Tetradecane, 5-methyl-
23	10.091	89218	0.31	51386	0.39	1.74	Dodecane, 2,6,11-trimethyl-
24	10.153	928272	3.26	692060	5.28	1.34	Dodecane, 2,6,11-trimethyl-
25	10.256	230817	0.81	130725	1.00	1.77	Dodecane, 2,6,11-trimethyl-
26	10.325	166925	0.59	84084	0.64	1.99	Dodecane, 2,6,11-trimethyl-

Peak#	R.Time	Area	Area%	Height	Height%	A/H	Name
27	10.414	158295	0.56	101486	0.77	1.56	Dodecane, 2,6,11-trimethyl-
28	10.461	160130	0.56	86891	0.66	1.84	Decane, 2,3,5,8-tetramethyl-
29	10.531	93364	0.33	69150	0.53	1.35	Decane, 2,3,7-trimethyl-
30	10.701	224220	0.79	165169	1.26	1.36	Dodecane, 2,6,11-trimethyl-
31	10.813	112699	0.40	50849	0.39	2.22	Dodecane, 2,6,11-trimethyl-
32	11.279	100474	0.35	40999	0.31	2.45	Tetradecane
33	11.605	1088988	3.82	573810	4.38	1.90	Tetradecane
34	11.722	291512	1.02	100628	0.77	2.90	Hexadecane
35	11.772	182621	0.64	112897	0.86	1.62	Eicosane
36	11.831	88298	0.31	53785	0.41	1.64	Tetradecane, 4-methyl-
37	11.987	80016	0.28	33799	0.26	2.37	Heptadecane, 2,6,10,15-tetramethyl-
38	12.146	141332	0.50	78658	0.60	1.80	Heptadecane
39	12.206	174309	0.61	100929	0.77	1.73	Heptadecane
40	12.258	383673	1.35	121387	0.93	3.16	Decane, 3,7-dimethyl-
41	12.352	92806	0.33	53594	0.41	1.73	2,3-Dimethyldodecane
42	12.506	277695	0.98	182770	1.39	1.52	Eicosane
43	12.553	901602	3.17	534952	4.08	1.69	Eicosane
44	12.654	310698	1.09	102777	0.78	3.02	Dodecane, 2,6,11-trimethyl-
45	12.685	176782	0.62	70977	0.54	2.49	Pentadecane
46	12.817	1229550	4.32	603672	4.61	2.04	Phenol, 2,4-bis(1,1-dimethylethyl)-
47	12.915	85969	0.30	51769	0.40	1.66	Nonane, 5-methyl-5-propyl-
48	13.025	464881	1.63	154543	1.18	3.01	Eicosane
49	13.133	92154	0.32	39536	0.30	2.33	Eicosane
50	13.339	108261	0.38	51018	0.39	2.12	Heptadecane, 2,6,10,15-tetramethyl-
51	13.705	560799	1.97	375742	2.87	1.49	Hexadecane
52	13.774	320476	1.13	88870	0.68	3.61	Heptadecane
53	13.905	114327	0.40	55309	0.42	2.07	Hexadecane, 4-methyl-
54	13.962	183803	0.65	111258	0.85	1.65	Eicosane
55	14.000	92041	0.32	49577	0.38	1.86	Eicosane
56	14.162	286254	1.01	92375	0.71	3.10	Pentadecane, 2,6,10-trimethyl-
57	14.205	95406	0.34	40939	0.31	2.33	Tetradecane, 5-methyl-
58	14.264	116918	0.41	71998	0.55	1.62	Dodecane, 4-methyl-
59	14.346	306754	1.08	92171	0.70	3.33	Eicosane
60	14.395	140294	0.49	66960	0.51	2.10	Eicosane
61	14.435	76110	0.27	44380	0.34	1.71	Eicosane
62	14.485	493186	1.73	172828	1.32	2.85	3-Eicosene, (E)-
63	14.570	94248	0.33	60352	0.46	1.56	Dodecane, 4-methyl-
64	14.633	348159	1.22	177421	1.35	1.96	Eicosane
65	14.684	678656	2.38	433579	3.31	1.57	Eicosane
66	14.730	189687	0.67	110377	0.84	1.72	Eicosane
67	14.777	195170	0.69	76503	0.58	2.55	Eicosane
68	14.833	247081	0.87	70345	0.54	3.51	Decane, 5-ethyl-5-methyl-
69	14.979	240922	0.85	63791	0.49	3.78	Eicosane
70	15.105	143120	0.50	51504	0.39	2.78	Tetradecane, 5-methyl-
71	15.151	222699	0.78	117380	0.90	1.90	Eicosane
72	15.208	74522	0.26	37108	0.28	2.01	Eicosane
73	15.255	105898	0.37	24747	0.19	4.28	Tetradecane, 4-methyl-
74	15.410	129499	0.45	39766	0.30	3.26	Eicosane
75	15.838	257165	0.90	120250	0.92	2.14	Heneicosane
76	16.323	253539	0.89	104790	0.80	2.42	Tetrapentacontane, 1,54-dibromo-
77	16.400	141875	0.50	31205	0.24	4.55	Tridecane, 4,8-dimethyl-
78	16.964	97138	0.34	44291	0.34	2.19	2-methyltetracosane
79	17.210	85077	0.30	29491	0.23	2.88	Eicosane
80	17.349	104815	0.37	39137	0.30	2.68	Eicosane
81	17.469	338023	1.19	92173	0.70	3.67	Eicosane
82	17.547	196615	0.69	47439	0.36	4.14	Hexadecane, 2,6,11,15-tetramethyl-
83	18.256	86922	0.31	31929	0.24	2.72	Eicosane
84	18.488	126437	0.44	37971	0.29	3.33	l-(+)-Ascorbic acid 2,6-dihexadecanoate
85	19.305	122076	0.43	36422	0.28	3.35	Eicosane
		28473169	100.00	13101880	100.00		

Table A 3: 105 Chemical Compounds identified in the 3M Treatment of *D. salina*.

Peak#	R.Time	Area	Area%	Height	Height%	A/H	Name
1	4.184	227836	0.94	73337	0.59	3.11	Heptane, 2,4-dimethyl-
2	4.727	83646	0.35	30873	0.25	2.71	Octane, 4-methyl-
3	6.114	85103	0.35	33376	0.27	2.55	Nonane, 2-methyl-
4	6.254	74587	0.31	33385	0.27	2.23	Nonane, 2,5-dimethyl-
5	6.603	640987	2.66	232646	1.86	2.76	Octane, 3,5-dimethyl-
6	6.782	164661	0.68	61642	0.49	2.67	Nonane, 2,5-dimethyl-
7	6.907	431100	1.79	141654	1.13	3.04	Decane, 4-methyl-
8	7.105	78197	0.32	39052	0.31	2.00	Glycerin
9	7.140	196887	0.82	66442	0.53	2.96	o-Ethylhydroxylamine
10	7.175	206613	0.86	91025	0.73	2.27	Methane, (methylsulfinyl)(methylthio)-
11	7.225	272585	1.13	138662	1.11	1.97	Glycerin
12	7.280	620582	2.57	182975	1.46	3.39	2-Butanone, 4-hydroxy-3-methyl-
13	7.354	2188760	9.07	579705	4.63	3.78	Dodecane, 2,6,11-trimethyl-
14	7.420	866724	3.59	253789	2.03	3.42	Octane, 2,3,6,7-tetramethyl-
15	7.966	497810	2.06	218450	1.74	2.28	Dodecane, 4,6-dimethyl-
16	8.039	104497	0.43	52715	0.42	1.98	Octane, 6-ethyl-2-methyl-
17	8.728	39087	0.16	25446	0.20	1.54	Undecane, 4-methyl-
18	8.796	122855	0.51	81172	0.65	1.51	Nonane, 5-(2-methylpropyl)-
19	8.875	50656	0.21	25061	0.20	2.02	Undecane, 3-methyl-
20	8.919	105495	0.44	60397	0.48	1.75	Undecane, 4,6-dimethyl-
21	9.250	1642711	6.81	1160813	9.26	1.42	Dodecane
22	9.362	96389	0.40	58055	0.46	1.66	Undecane, 2,4-dimethyl-
23	9.404	218864	0.91	157246	1.25	1.39	Undecane, 4,6-dimethyl-
24	9.511	174529	0.72	131286	1.05	1.33	Dodecane, 4-methyl-
25	9.741	149415	0.62	110401	0.88	1.35	Tetradecane
26	9.810	80080	0.33	56503	0.45	1.42	Pentadecane

Peak#	R.Time	Area	Area%	Height	Height%	A/H	Name
27	9.888	1246151	5.17	881516	7.03	1.41	Benzene, 1,3-bis(1,1-dimethylethyl)-
28	9.965	150459	0.62	65539	0.52	2.30	Decane, 2,3,4-trimethyl-
29	10.000	403787	1.67	258836	2.07	1.56	Tetradecane, 5-methyl-
30	10.090	65001	0.27	42787	0.34	1.52	Tetradecane, 4-methyl-
31	10.153	830400	3.44	640335	5.11	1.30	Dodecane, 2,6,11-trimethyl-
32	10.256	156465	0.65	104633	0.83	1.50	Octane, 2,3,6,7-tetramethyl-
33	10.326	96654	0.40	71185	0.57	1.36	Dodecane, 2,6,11-trimethyl-
34	10.360	42323	0.18	28162	0.22	1.50	Heptane, 3,3,5-trimethyl-
35	10.414	103307	0.43	82567	0.66	1.25	Dodecane, 2,6,11-trimethyl-
36	10.460	98263	0.41	59454	0.47	1.65	Heptadecane, 2,6,10,15-tetramethyl-
37	10.530	50661	0.21	42402	0.34	1.19	Decane, 2,3,7-trimethyl-
38	10.699	186765	0.77	133735	1.07	1.40	Dodecane, 2,6,11-trimethyl-
39	10.812	61817	0.26	37943	0.30	1.63	Nonane, 5-(2-methylpropyl)-
40	10.914	57036	0.24	30442	0.24	1.87	Dodecane, 4-methyl-
41	11.025	60469	0.25	17818	0.14	3.39	Dodecane, 4,6-dimethyl-
42	11.195	53298	0.22	41111	0.33	1.30	2,3-Dimethyldodecane
43	11.280	59183	0.25	35716	0.29	1.66	Eicosane
44	11.605	978809	4.06	509597	4.07	1.92	Tetradecane
45	11.680	117354	0.49	51628	0.41	2.27	1-Undecene, 4-methyl-
46	11.723	126036	0.52	82919	0.66	1.52	Tridecane, 2,5-dimethyl-
47	11.772	162627	0.67	100739	0.80	1.61	Eicosane
48	11.831	75022	0.31	49520	0.40	1.51	Tetradecane, 4-methyl-
49	11.988	57368	0.24	28889	0.23	1.99	Nonane, 3-methyl-5-propyl-
50	12.100	61835	0.26	28904	0.23	2.14	Sulfurous acid, pentyl undecyl ester
51	12.144	119698	0.50	65776	0.52	1.82	Heptadecane
52	12.206	143158	0.59	84944	0.68	1.69	Heptadecane
53	12.257	169880	0.70	106982	0.85	1.59	Dodecane, 4,6-dimethyl-
54	12.284	161360	0.67	98153	0.78	1.64	Eicosane
55	12.353	68018	0.28	43912	0.35	1.55	Decane, 5-ethyl-5-methyl-
56	12.415	39963	0.17	29268	0.23	1.37	Tetradecane, 1-chloro-
57	12.505	234707	0.97	157548	1.26	1.49	Eicosane
58	12.551	785430	3.26	510352	4.07	1.54	Eicosane
59	12.629	130397	0.54	85071	0.68	1.53	Hexadecane, 1-iodo-
60	12.652	112821	0.47	88312	0.70	1.28	Dodecane, 2,6,11-trimethyl-
61	12.689	79431	0.33	53081	0.42	1.50	Pentadecane
62	12.715	52167	0.22	34340	0.27	1.52	Undecane, 3,3-dimethyl-
63	12.815	1120838	4.65	646780	5.16	1.73	Phenol, 2,4-bis(1,1-dimethylethyl)-
64	12.911	60550	0.25	45837	0.37	1.32	Eicosane
65	12.970	64629	0.27	30561	0.24	2.11	Tetradecane, 4-ethyl-
66	13.024	240184	1.00	116965	0.93	2.05	Eicosane
67	13.337	90216	0.37	46544	0.37	1.94	Heptadecane, 2,6,10,15-tetramethyl-
68	13.408	69144	0.29	35442	0.28	1.95	Tetradecane, 2-methyl-
69	13.633	36913	0.15	29350	0.23	1.26	3-Eicosene, (E)-
70	13.704	488582	2.03	331599	2.65	1.47	Hexadecane
71	13.772	195979	0.81	71759	0.57	2.73	Eicosane
72	13.905	109243	0.45	39435	0.31	2.77	Hexadecane, 4-methyl-
73	13.961	156481	0.65	95845	0.76	1.63	Eicosane
74	14.000	67016	0.28	36885	0.29	1.82	Eicosane
75	14.095	78666	0.33	20546	0.16	3.83	Sulfurous acid, 2-ethylhexyl tridecyl este
76	14.160	143984	0.60	75893	0.61	1.90	Pentadecane, 2,6,10-trimethyl-
77	14.205	48351	0.20	28397	0.23	1.70	Tetradecane, 5-methyl-
78	14.261	104919	0.43	61013	0.49	1.72	Eicosane
79	14.313	152454	0.63	56389	0.45	2.70	Eicosane, 2,4-dimethyl-
80	14.345	113369	0.47	75652	0.60	1.50	Eicosane
81	14.395	113558	0.47	54439	0.43	2.09	Eicosane
82	14.434	58917	0.24	41348	0.33	1.42	Tetradecane, 2,6,10-trimethyl-
83	14.485	250229	1.04	119811	0.96	2.09	3-Eicosene, (E)-
84	14.571	202038	0.84	50936	0.41	3.97	Dodecane, 4-methyl-
85	14.632	278103	1.15	151338	1.21	1.84	Eicosane
86	14.683	605068	2.51	363964	2.90	1.66	Eicosane
87	14.729	160935	0.67	91040	0.73	1.77	Eicosane
88	14.778	138085	0.57	66137	0.53	2.09	Eicosane
89	14.830	131355	0.54	65478	0.52	2.01	Tetratetracontane
90	14.870	85668	0.36	42341	0.34	2.02	Eicosane
91	14.971	178311	0.74	47123	0.38	3.78	Eicosane
92	15.105	83304	0.35	38307	0.31	2.17	5,5-Dibutylnonane
93	15.151	218749	0.91	108293	0.86	2.02	Eicosane
94	15.209	41453	0.17	28505	0.23	1.45	Dodecane, 4-methyl-
95	15.835	232776	0.96	125843	1.00	1.85	Heptadecane
96	16.322	208511	0.86	85297	0.68	2.44	Tetrapentacontane, 1,54-dibromo-
97	16.400	69054	0.29	15340	0.12	4.50	Heptadecane, 2,3-dimethyl-
98	16.892	50761	0.21	27183	0.22	1.87	Eicosane
99	16.960	85088	0.35	37036	0.30	2.30	2-methylhexacosane
100	17.341	80626	0.33	34308	0.27	2.35	Eicosane
101	17.476	317337	1.32	91944	0.73	3.45	Eicosane
102	17.575	185914	0.77	39133	0.31	4.75	Dodecane, 2,6,11-trimethyl-
103	17.620	40831	0.17	21690	0.17	1.88	Nonadecane, 4-methyl-
104	18.252	70745	0.29	30010	0.24	2.36	Eicosane
105	19.291	75006	0.31	29473	0.24	2.54	Eicosane
		24122716	100.00	12531433	100.00		

Table A 4: 90 Chemical Compounds identified in the 3,5M Treatment of *D. salina*.

Peak#	R.Time	Area	Area%	Height	Height%	A/H	Name
1	4.183	212897	0.77	65202	0.52	3.27	Heptane, 2,4-dimethyl-
2	4.729	81412	0.29	25915	0.21	3.14	Octane, 4-methyl-
3	6.118	93675	0.34	33282	0.27	2.81	Nonane, 2-methyl-
4	6.251	99304	0.36	32234	0.26	3.08	Nonane, 2,5-dimethyl-
5	6.607	644671	2.34	218740	1.76	2.95	Decane
6	6.784	201623	0.73	66735	0.54	3.02	Nonane, 2,5-dimethyl-
7	6.917	586314	2.12	160558	1.29	3.65	Decane, 4-methyl-
8	7.085	1943055	7.04	123786	1.00	15.70	Glycerin
9	7.359	1067233	3.87	331815	2.67	3.22	Nonane, 5-(2-methylpropyl)-
10	7.436	485261	1.76	141032	1.14	3.44	Octane, 2,3,6,7-tetramethyl-
11	7.969	517256	1.87	224223	1.80	2.31	Dodecane, 4,6-dimethyl-
12	8.043	110616	0.40	52937	0.43	2.09	Octane, 6-ethyl-2-methyl-
13	8.797	132120	0.48	82515	0.66	1.60	Undecane, 2-methyl-
14	8.920	129548	0.47	63664	0.51	2.03	Octane, 3,5-dimethyl-
15	9.252	1715946	6.22	1145531	9.22	1.50	Dodecane
16	9.404	349994	1.27	167769	1.35	2.09	Undecane, 4,6-dimethyl-
17	9.513	181071	0.66	131683	1.06	1.38	Dodecane, 4-methyl-
18	9.742	162874	0.59	115420	0.93	1.41	Tetradecane
19	9.811	103132	0.37	65561	0.53	1.57	Tetradecane
20	9.889	1359634	4.93	940806	7.57	1.45	Benzene, 1,3-bis(1,1-dimethylethyl)-
21	10.002	515580	1.87	265381	2.14	1.94	Tetradecane, 5-methyl-
22	10.091	111215	0.40	54835	0.44	2.03	Tetradecane, 4-methyl-
23	10.154	930547	3.37	682196	5.49	1.36	Dodecane, 2,6,11-trimethyl-
24	10.256	245510	0.89	123213	0.99	1.99	Dodecane, 2,6,11-trimethyl-
25	10.326	216400	0.78	88309	0.71	2.45	Dodecane, 2,6,11-trimethyl-
26	10.415	149579	0.54	104513	0.84	1.43	Dodecane, 2,6,11-trimethyl-

Peak#	R.Time	Area	Area%	Height	Height%	A/H	Name
27	10.461	153110	0.55	72712	0.59	2.11	Decane, 2,3,5,8-tetramethyl-
28	10.531	98541	0.36	59569	0.48	1.65	Decane, 2,3,7-trimethyl-
29	10.702	260429	0.94	168408	1.36	1.55	Dodecane, 2,6,11-trimethyl-
30	10.813	153532	0.56	55894	0.45	2.75	Dodecane, 2,6,11-trimethyl-
31	11.280	90184	0.33	45190	0.36	2.00	Tetradecane
32	11.608	1057283	3.83	583202	4.69	1.81	Tetradecane
33	11.723	308976	1.12	100883	0.81	3.06	Hexadecane
34	11.772	185226	0.67	118336	0.95	1.57	Eicosane
35	11.833	97828	0.35	58702	0.47	1.67	Tetradecane, 4-methyl-
36	11.987	107576	0.39	37914	0.31	2.84	Pentadecane, 7-methyl-
37	12.105	82177	0.30	40651	0.33	2.02	Dodecane, 2,6,11-trimethyl-
38	12.146	143329	0.52	83975	0.68	1.71	Heptadecane
39	12.207	189312	0.69	102567	0.83	1.85	Heptadecane
40	12.256	411922	1.49	131256	1.06	3.14	Dodecane, 4-methyl-
41	12.353	106502	0.39	64250	0.52	1.66	2,3-Dimethyldodecane
42	12.505	264673	0.96	188459	1.52	1.40	Eicosane
43	12.551	894935	3.24	553757	4.46	1.62	Eicosane
44	12.654	358769	1.30	106145	0.85	3.38	Eicosane
45	12.690	178048	0.65	69144	0.56	2.58	3,5-Dimethyldodecane
46	12.760	96933	0.35	40197	0.32	2.41	Nonane, 4,5-dimethyl-
47	12.816	1104000	4.00	612302	4.93	1.80	Phenol, 2,4-bis(1,1-dimethylethyl)-
48	12.910	113599	0.41	61962	0.50	1.83	Dodecane, 2,6,11-trimethyl-
49	13.026	604911	2.19	153369	1.23	3.94	Eicosane
50	13.131	112365	0.41	41128	0.33	2.73	Dodecane, 2,6,11-trimethyl-
51	13.339	125425	0.45	51292	0.41	2.45	Heptadecane, 2,6,10,15-tetramethyl-
52	13.410	80212	0.29	43264	0.35	1.85	Pentadecane, 3-methyl-
53	13.705	577546	2.09	374220	3.01	1.54	Hexadecane
54	13.772	291242	1.06	88071	0.71	3.31	Eicosane
55	13.962	171277	0.62	104155	0.84	1.64	Eicosane
56	14.159	275308	1.00	90368	0.73	3.05	Heptadecane
57	14.263	148956	0.54	70003	0.56	2.13	Dodecane, 4-methyl-
58	14.344	305513	1.11	90216	0.73	3.39	Eicosane
59	14.395	140605	0.51	66734	0.54	2.11	Eicosane
60	14.486	619915	2.25	243758	1.96	2.54	3-Heptadecene, (Z)-
61	14.575	96259	0.35	56563	0.46	1.70	Dodecane, 4-methyl-
62	14.630	362428	1.31	179615	1.45	2.02	Eicosane
63	14.684	690284	2.50	424866	3.42	1.62	Eicosane
64	14.728	190458	0.69	114062	0.92	1.67	Eicosane
65	14.779	210888	0.76	79695	0.64	2.65	Eicosane
66	14.829	132486	0.48	68845	0.55	1.92	Dodecane, 2,6,11-trimethyl-
67	14.865	101358	0.37	51351	0.41	1.97	3-Ethyl-3-methylheptane
68	14.978	197655	0.72	68386	0.55	2.89	Eicosane
69	15.105	173697	0.63	64149	0.52	2.71	Tetradecane, 4-ethyl-
70	15.153	270437	0.98	127838	1.03	2.12	Eicosane
71	15.208	100627	0.36	47344	0.38	2.13	Nonane, 5-methyl-5-propyl-
72	15.305	143905	0.52	26636	0.21	5.40	Sulfurous acid, pentadecyl pentyl ester
73	15.400	170836	0.62	37437	0.30	4.56	Eicosane
74	15.475	83451	0.30	31259	0.25	2.67	Hexadecane, 1-iodo-
75	15.835	345452	1.25	144796	1.17	2.39	Heptadecane
76	16.323	240958	0.87	97330	0.78	2.48	Tetrapentacontane, 1,54-dibromo-
77	16.375	116554	0.42	39958	0.32	2.92	Tetradecane, 5-methyl-
78	16.678	143066	0.52	30587	0.25	4.68	Isophytol, acetate
79	16.957	91678	0.33	39755	0.32	2.31	2-methylhexacosane
80	17.201	97584	0.35	33855	0.27	2.88	Eicosane
81	17.349	100851	0.37	42290	0.34	2.38	Eicosane
82	17.469	317076	1.15	101791	0.82	3.11	Eicosane
83	17.565	232357	0.84	50850	0.41	4.57	Hexatriacontane
84	17.729	102761	0.37	24225	0.19	4.24	Eicosane
85	18.259	101144	0.37	33747	0.27	3.00	Eicosane
86	18.355	83785	0.30	18742	0.15	4.47	Squalane
87	18.485	85717	0.31	30622	0.25	2.80	l-(+)-Ascorbic acid 2,6-dihexadecanoate
88	19.307	184688	0.67	40164	0.32	4.60	Eicosane
89	22.465	86876	0.31	14497	0.12	5.99	Phytol
90	22.635	91145	0.33	22001	0.18	4.14	Octadecane, 2,6,10,14-tetramethyl-
		27603087	100.00	12423164	100.00		

Table A 5: 90 Chemical Compounds identified in the NO_3 Treatment of *D. salina*.

Peak#	R.Time	Area	Area%	Height	Height%	A/H	Name
1	4.181	237145	1.05	76981	0.70	3.08	Heptane, 2,4-dimethyl-
2	4.727	69172	0.31	24608	0.22	2.81	Octane, 4-methyl-
3	6.110	118028	0.52	39307	0.36	3.00	Nonane, 2-methyl-
4	6.247	124842	0.55	34187	0.31	3.65	Nonane, 2,5-dimethyl-
5	6.604	589994	2.60	218554	1.98	2.70	Decane
6	6.782	191110	0.84	68629	0.62	2.78	Nonane, 2,5-dimethyl-
7	6.845	76116	0.34	28180	0.26	2.70	Nonane, 2,5-dimethyl-
8	6.908	376530	1.66	139020	1.26	2.71	Octane, 3,3-dimethyl-
9	7.356	936866	4.13	329014	2.99	2.85	Octane, 6-ethyl-2-methyl-
10	7.434	375043	1.65	141194	1.28	2.66	Octane, 2,3,6,7-tetramethyl-
11	7.967	519994	2.29	214392	1.95	2.43	Dodecane, 4,6-dimethyl-
12	8.040	126786	0.56	61701	0.56	2.05	Octane, 6-ethyl-2-methyl-
13	8.139	78357	0.35	22055	0.20	3.55	Undecane, 4-methyl-
14	8.795	128907	0.57	84579	0.77	1.52	Nonane, 5-(2-methylpropyl)-
15	8.919	184918	0.82	63907	0.58	2.89	Tridecane
16	9.250	1632602	7.20	1132567	10.28	1.44	Dodecane
17	9.360	98276	0.43	62141	0.56	1.58	Undecane, 2,4-dimethyl-
18	9.404	226925	1.00	164420	1.49	1.38	Undecane, 4,6-dimethyl-
19	9.512	179792	0.79	130837	1.19	1.37	Dodecane, 4-methyl-
20	9.741	166844	0.74	121262	1.10	1.38	Tetradecane
21	9.810	99508	0.44	64351	0.58	1.55	Tetradecane
22	9.888	1279596	5.65	856745	7.78	1.49	Benzene, 1,3-bis(1,1-dimethylethyl)-
23	10.000	619301	2.73	297813	2.70	2.08	Tetradecane, 5-methyl-
24	10.091	81080	0.36	52297	0.47	1.55	Tetradecane, 4-methyl-
25	10.154	894297	3.95	691963	6.28	1.29	Dodecane, 2,6,11-trimethyl-
26	10.256	259137	1.14	124940	1.13	2.07	Dodecane, 2,6,11-trimethyl-

Peak#	R.Time	Area	Area%	Height	Height%	A/H	Name
27	10.326	205078	0.90	86854	0.79	2.36	Dodecane, 2,6,11-trimethyl-
28	10.415	143849	0.63	100501	0.91	1.43	Dodecane, 2,6,11-trimethyl-
29	10.462	135438	0.60	66086	0.60	2.05	Heptadecane, 2,6,10,15-tetramethyl-
30	10.531	94738	0.42	59524	0.54	1.59	Dodecane, 4-methyl-
31	10.636	96882	0.43	23747	0.22	4.08	Tetradecane, 4-methyl-
32	10.701	227340	1.00	167244	1.52	1.36	Dodecane, 2,6,11-trimethyl-
33	10.812	120256	0.53	48602	0.44	2.47	Dodecane, 2,6,11-trimethyl-
34	10.918	68528	0.30	36944	0.34	1.85	Nonane, 3-methyl-5-propyl-
35	11.195	65594	0.29	42028	0.38	1.56	Eicosane, 10-methyl-
36	11.606	842511	3.72	433498	3.93	1.94	Tetradecane
37	11.721	306671	1.35	92770	0.84	3.31	Hexadecane
38	11.772	197432	0.87	111717	1.01	1.77	Eicosane
39	11.834	95882	0.42	54061	0.49	1.77	Tetradecane, 4-methyl-
40	11.986	109756	0.48	30537	0.28	3.59	Heptadecane, 2,6,10,15-tetramethyl-
41	12.105	82248	0.36	28812	0.26	2.85	Decane, 3-ethyl-3-methyl-
42	12.147	124259	0.55	63217	0.57	1.97	Hexadecane
43	12.207	136319	0.60	91196	0.83	1.49	Heptadecane
44	12.258	390578	1.72	108528	0.98	3.60	Dodecane, 4-methyl-
45	12.352	112673	0.50	51949	0.47	2.17	Heptadecane
46	12.506	232342	1.03	161038	1.46	1.44	Eicosane
47	12.552	823254	3.63	450580	4.09	1.83	Eicosane
48	12.652	291610	1.29	92948	0.84	3.14	Eicosane
49	12.690	148742	0.66	54635	0.50	2.72	Pentadecane
50	12.760	75400	0.33	28720	0.26	2.63	Tetradecane, 5-methyl-
51	12.817	1095680	4.83	522927	4.75	2.10	Phenol, 2,4-bis(1,1-dimethylethyl)-
52	12.910	81843	0.36	51865	0.47	1.58	Eicosane
53	13.025	404757	1.79	127023	1.15	3.19	Eicosane
54	13.130	106058	0.47	33486	0.30	3.17	Dodecane, 2,6,11-trimethyl-
55	13.339	79220	0.35	37441	0.34	2.12	Eicosane
56	13.706	502797	2.22	296214	2.69	1.70	Hexadecane
57	13.771	289898	1.28	78405	0.71	3.70	Eicosane
58	13.908	80271	0.35	39241	0.36	2.05	Hexadecane, 4-methyl-
59	13.962	157853	0.70	87750	0.80	1.80	Eicosane
60	13.995	76961	0.34	42276	0.38	1.82	Eicosane
61	14.161	243597	1.07	77450	0.70	3.15	Heptadecane
62	14.265	132711	0.59	62052	0.56	2.14	Dodecane, 4-methyl-
63	14.344	270589	1.19	77884	0.71	3.47	Eicosane
64	14.395	123996	0.55	57396	0.52	2.16	Heptadecane, 2,6,10,15-tetramethyl-
65	14.435	66322	0.29	43146	0.39	1.54	Dodecane, 4-methyl-
66	14.486	332778	1.47	80699	0.73	4.12	1-Decanol, 2-hexyl-
67	14.571	90660	0.40	49162	0.45	1.84	Eicosane
68	14.632	289468	1.28	149308	1.36	1.94	Eicosane
69	14.681	618052	2.73	356359	3.23	1.73	Eicosane
70	14.727	170987	0.75	95749	0.87	1.79	Eicosane
71	14.775	197664	0.87	73337	0.67	2.70	Eicosane
72	14.830	116524	0.51	63189	0.57	1.84	2-methylhexacosane
73	14.983	195626	0.86	50648	0.46	3.86	Eicosane
74	15.100	98936	0.44	45649	0.41	2.17	5,5-Diethyltridecane
75	15.154	209428	0.92	95820	0.87	2.19	Eicosane
76	15.206	65742	0.29	34321	0.31	1.92	Nonane, 5-methyl-5-propyl-
77	15.290	92750	0.41	24273	0.22	3.82	Eicosane
78	15.410	105671	0.47	27453	0.25	3.85	Tridecanol, 2-ethyl-2-methyl-
79	15.837	248820	1.10	102435	0.93	2.43	Heptadecane
80	16.322	147269	0.65	60094	0.55	2.45	Tetrapentacontane, 1,54-dibromo-
81	16.670	168009	0.74	25727	0.23	6.53	2-methyltetracosane
82	16.964	80799	0.36	31760	0.29	2.54	2-methyltetracosane
83	17.213	77810	0.34	25272	0.23	3.08	Eicosane
84	17.349	93106	0.41	34229	0.31	2.72	Eicosane
85	17.471	222827	0.98	82968	0.75	2.69	Eicosane
86	17.560	154422	0.68	44117	0.40	3.50	5-Butyl-5-ethylpentadecane
87	18.254	85836	0.38	26746	0.24	3.21	Eicosane
88	19.291	133931	0.59	36623	0.33	3.66	Eicosane
89	22.313	70691	0.31	15060	0.14	4.69	2-methyloctacosane
90	22.654	87257	0.38	22013	0.20	3.96	Squalane
		22666162	100.00	11018947	100.00		

Table A 6: 100 Chemical Compounds identified in the Ammonia Treatment of *D. salina*.

Peak#	R.Time	Area	Area%	Height	Height%	A/H	Name
1	4.155	111622	0.46	59257	0.46	1.88	Heptane, 2,4-dimethyl-
2	4.186	159700	0.66	83166	0.64	1.92	Heptane, 2,4-dimethyl-
3	6.105	77734	0.32	27804	0.21	2.80	Nonane, 2-methyl-
4	6.614	670673	2.79	215294	1.65	3.12	Decane
5	6.782	154207	0.64	56050	0.43	2.75	Nonane, 2,5-dimethyl-
6	6.915	446242	1.86	137748	1.06	3.24	Nonane, 2,6-dimethyl-
7	7.159	717010	2.99	94808	0.73	7.56	Glycerin
8	7.364	963146	4.01	305377	2.35	3.15	Nonane, 5-(2-methylpropyl)-
9	7.444	331361	1.38	118708	0.91	2.79	Octane, 2,3,6,7-tetramethyl-
10	7.972	557363	2.32	249023	1.91	2.24	Octane, 5-ethyl-2-methyl-
11	8.042	135412	0.56	66364	0.51	2.04	Octane, 6-ethyl-2-methyl-
12	8.798	135948	0.57	91797	0.71	1.48	Undecane, 2-methyl-
13	8.880	53104	0.22	31726	0.24	1.67	Undecane, 3-methyl-
14	8.919	146265	0.61	72709	0.56	2.01	Tridecane
15	9.251	1815715	7.56	1255576	9.65	1.45	Dodecane
16	9.364	110063	0.46	68456	0.53	1.61	Undecane, 2,4-dimethyl-
17	9.404	255684	1.06	174148	1.34	1.47	Undecane, 4,6-dimethyl-
18	9.512	184506	0.77	142771	1.10	1.29	Dodecane, 4-methyl-
19	9.742	167413	0.70	114923	0.88	1.46	Tetradecane
20	9.810	93768	0.39	65926	0.51	1.42	Tetradecane
21	9.888	1379278	5.74	929487	7.14	1.48	Benzene, 1,3-bis(1,1-dimethylethyl)-
22	9.960	174333	0.73	75298	0.58	2.32	Dodecane, 4-methyl-
23	10.000	468690	1.95	301037	2.31	1.56	2,4-Dimethyldodecane
24	10.090	96319	0.40	56604	0.43	1.70	Tetradecane, 4-methyl-
25	10.154	965185	4.02	718351	5.52	1.34	Dodecane, 2,6,11-trimethyl-
26	10.256	222875	0.93	128348	0.99	1.74	Dodecane, 2,6,11-trimethyl-

Peak#	R.Time	Area	Area%	Height	Height%	A/H	Name
27	10.285	50918	0.21	43453	0.33	1.17	Undecane, 2,10-dimethyl-
28	10.326	129934	0.54	86883	0.67	1.50	Dodecane, 2,6,11-trimethyl-
29	10.355	58337	0.24	42881	0.33	1.36	Nonane, 2,6-dimethyl-
30	10.413	163971	0.68	101018	0.78	1.62	Dodecane, 2,6,11-trimethyl-
31	10.461	147679	0.61	67444	0.52	2.19	Decane, 2,3,5,8-tetramethyl-
32	10.531	81472	0.34	55744	0.43	1.46	Decane, 2,3,7-trimethyl-
33	10.635	89512	0.37	24688	0.19	3.63	Tetradecane, 4-methyl-
34	10.701	236366	0.98	163461	1.26	1.45	Dodecane, 2,6,11-trimethyl-
35	10.813	127169	0.53	50956	0.39	2.50	Dodecane, 4-methyl-
36	10.919	62271	0.26	35391	0.27	1.76	Dodecane, 4-methyl-
37	11.195	72062	0.30	48555	0.37	1.48	Eicosane, 10-methyl-
38	11.281	68534	0.29	37866	0.29	1.81	Eicosane, 10-methyl-
39	11.606	1092556	4.55	598448	4.60	1.83	Tetradecane
40	11.685	150116	0.63	69601	0.53	2.16	Tetradecane, 5-methyl-
41	11.722	171156	0.71	102031	0.78	1.68	Hexadecane
42	11.771	181803	0.76	115111	0.88	1.58	Eicosane
43	11.833	83432	0.35	56804	0.44	1.47	Tetradecane, 4-methyl-
44	11.988	73744	0.31	33920	0.26	2.17	Pentadecane
45	12.095	86108	0.36	28398	0.22	3.03	Octadecane, 5,14-dibutyl-
46	12.144	141457	0.59	79790	0.61	1.77	Hexadecane
47	12.208	170653	0.71	98730	0.76	1.73	Heptadecane
48	12.256	225389	0.94	127863	0.98	1.76	Decane, 4-methyl-
49	12.285	205821	0.86	122915	0.94	1.67	Eicosane, 2,4-dimethyl-
50	12.353	97738	0.41	63084	0.48	1.55	Dodecane, 4,6-dimethyl-
51	12.506	264922	1.10	194629	1.50	1.36	Eicosane
52	12.551	936556	3.90	564593	4.34	1.66	Eicosane
53	12.628	183437	0.76	105512	0.81	1.74	Heptadecane
54	12.653	159727	0.67	102704	0.79	1.56	Dodecane, 2,6,11-trimethyl-
55	12.690	98590	0.41	63266	0.49	1.56	3,5-Dimethyldodecane
56	12.710	49373	0.21	46845	0.36	1.05	Hexadecane, 1-iodo-
57	12.815	1286772	5.36	695664	5.35	1.85	Phenol, 2,4-bis(1,1-dimethylethyl)-
58	12.910	76946	0.32	52810	0.41	1.46	Dodecane, 2,6,11-trimethyl-
59	12.975	95466	0.40	46418	0.36	2.06	Tridecane, 3-ethyl-
60	13.025	304849	1.27	154002	1.18	1.98	Dodecane, 4-methyl-
61	13.060	74993	0.31	47970	0.37	1.56	Thiophene-2-carboxamide, 3-ethoxy-N-(4-chlo
62	13.129	69535	0.29	28534	0.22	2.44	Sulfurous acid, dodecyl pentyl ester
63	13.336	85842	0.36	47986	0.37	1.79	Heptadecane, 2,6,10,15-tetramethyl-
64	13.409	61069	0.25	35512	0.27	1.72	Tetradecane, 2-methyl-
65	13.704	579704	2.41	394590	3.03	1.47	Hexadecane
66	13.771	225967	0.94	86826	0.67	2.60	Eicosane
67	13.820	50149	0.21	30592	0.24	1.64	3-Ethyl-3-methylheptadecane
68	13.902	65153	0.27	41270	0.32	1.58	Hexadecane, 4-methyl-
69	13.963	153092	0.64	96476	0.74	1.59	Hexadecane, 1-iodo-
70	13.996	63304	0.26	46179	0.35	1.37	Heptadecane
71	14.160	90789	0.38	67484	0.52	1.35	Pentadecane, 2,6,10-trimethyl-
72	14.262	71394	0.30	51856	0.40	1.38	Hexadecane, 4-methyl-
73	14.295	115911	0.48	45874	0.35	2.53	Dodecane, 2,6,11-trimethyl-
74	14.345	91080	0.38	74777	0.57	1.22	Heptadecane
75	14.394	93377	0.39	47951	0.37	1.95	Eicosane
76	14.486	398871	1.66	160550	1.23	2.48	3-Eicosene, (E)-
77	14.573	69165	0.29	39289	0.30	1.76	Eicosane
78	14.633	291216	1.21	157358	1.21	1.85	Eicosane
79	14.683	656409	2.73	420610	3.23	1.56	Eicosane
80	14.728	151004	0.63	99854	0.77	1.51	Eicosane
81	14.780	146948	0.61	70331	0.54	2.09	Eicosane
82	14.833	124214	0.52	60684	0.47	2.05	Tetratetracontane
83	14.865	61185	0.25	43052	0.33	1.42	Hexadecane, 2,6,11,15-tetramethyl-
84	14.978	149511	0.62	50913	0.39	2.94	Eicosane
85	15.100	119266	0.50	42395	0.33	2.81	Octadecane, 5-methyl-
86	15.153	203452	0.85	112392	0.86	1.81	Eicosane
87	15.205	55311	0.23	30591	0.24	1.81	Eicosane
88	15.835	231399	0.96	124816	0.96	1.85	Heptadecane
89	16.324	168968	0.70	82194	0.63	2.06	Tetrapentacontane, 1,54-dibromo-
90	16.885	49370	0.21	25415	0.20	1.94	Eicosane
91	16.961	98510	0.41	43479	0.33	2.27	2-methylhexacosane
92	17.208	90480	0.38	35300	0.27	2.56	Eicosane
93	17.349	117979	0.49	43161	0.33	2.73	Eicosane
94	17.425	58675	0.24	26692	0.21	2.20	2-Bromopropionic acid, 2-ethylhexyl ester
95	17.471	305545	1.27	107506	0.83	2.84	Eicosane
96	17.575	192889	0.80	45689	0.35	4.22	Undecane, 4,8-dimethyl-
97	17.630	61143	0.25	15389	0.12	3.97	Hexatriacontane
98	18.256	60708	0.25	28582	0.22	2.12	Eicosane
99	18.493	137641	0.57	46871	0.36	2.94	l-(+)-Ascorbic acid 2,6-dihexadecanoate
100	19.301	108450	0.45	33519	0.26	3.24	Eicosane
		24018120	100.00	13012743	100.00		

Table A 7: 100 Chemical Compounds identified in the Urea Treatment of *D. salina*.

Peak#	R.Time	Area	Area%	Height	Height%	A/H	Name
1	4.182	201092	0.66	57920	0.45	3.47	Heptane, 2,4-dimethyl-
2	6.617	575964	1.88	166865	1.30	3.45	Decane
3	6.799	338010	1.10	88301	0.69	3.83	Nonane, 2,5-dimethyl-
4	6.920	1126592	3.67	194566	1.52	5.79	Octane, 3,3-dimethyl-
5	7.055	1038615	3.38	162962	1.27	6.37	Glycerin
6	7.125	623579	2.03	192331	1.50	3.24	Glycerin
7	7.150	315620	1.03	211566	1.65	1.49	Methane, nitro-
8	7.175	334281	1.09	226341	1.76	1.48	Methanamine, N-methoxy-
9	7.295	1813676	5.91	298909	2.33	6.07	Propylamine, N,N,2,2-tetramethyl-, N-oxide
10	7.375	2736874	8.92	580369	4.52	4.72	Nonane, 5-(2-methylpropyl)-
11	7.451	3752106	12.23	483587	3.77	7.76	Dimethylamine, N-(neopentyloxy)-
12	7.974	466918	1.52	227461	1.77	2.05	Octane, 5-ethyl-2-methyl-
13	8.044	90844	0.30	56963	0.44	1.59	Octane, 6-ethyl-2-methyl-
14	8.580	101059	0.33	13871	0.11	7.29	Disiloxane, 1,1,3,3-tetramethyl-1,3-bis[3-(oxir
15	8.732	45862	0.15	29455	0.23	1.56	Undecane, 4-methyl-
16	8.798	125610	0.41	82512	0.64	1.52	Undecane, 2-methyl-
17	8.923	98899	0.32	57623	0.45	1.72	Dodecane, 2,7,10-trimethyl-
18	9.252	1558271	5.08	1091465	8.51	1.43	Dodecane
19	9.364	107014	0.35	60059	0.47	1.78	Undecane, 2,4-dimethyl-
20	9.404	218180	0.71	146638	1.14	1.49	Undecane, 2,5-dimethyl-
21	9.512	171717	0.56	123129	0.96	1.39	Dodecane, 4-methyl-
22	9.742	137122	0.45	98020	0.76	1.40	Tetradecane
23	9.812	69499	0.23	47360	0.37	1.47	Tetradecane
24	9.889	1071683	3.49	730839	5.70	1.47	Benzene, 1,3-bis(1,1-dimethylethyl)-
25	9.960	128210	0.42	61252	0.48	2.09	Dodecane, 4-methyl-
26	10.001	369486	1.20	225464	1.76	1.64	Decane, 4-ethyl-

Peak#	R.Time	Area	Area%	Height	Height%	A/H	Name
27	10.092	73536	0.24	40096	0.31	1.83	Tetradecane, 4-methyl-
28	10.154	763354	2.49	573887	4.47	1.33	Dodecane, 2,6,11-trimethyl-
29	10.257	144451	0.47	98986	0.77	1.46	Dodecane, 2,6,11-trimethyl-
30	10.327	92399	0.30	65049	0.51	1.42	Dodecane, 2,6,11-trimethyl-
31	10.415	93764	0.31	77618	0.60	1.21	Dodecane, 2,6,11-trimethyl-
32	10.464	90930	0.30	50472	0.39	1.80	Decane, 2,3,5,8-tetramethyl-
33	10.531	47797	0.16	38448	0.30	1.24	Decane, 4-ethyl-
34	10.702	183016	0.60	128146	1.00	1.43	Dodecane, 2,6,11-trimethyl-
35	10.813	90593	0.30	38026	0.30	2.38	Dodecane, 2,6,11-trimethyl-
36	10.919	47315	0.15	23967	0.19	1.97	Nonane, 5-methyl-5-propyl-
37	11.196	60295	0.20	37355	0.29	1.61	2,3-Dimethyldodecane
38	11.282	71160	0.23	35650	0.28	2.00	Dodecane, 2,6,11-trimethyl-
39	11.607	1062572	3.46	553897	4.32	1.92	Tetradecane
40	11.685	111334	0.36	59786	0.47	1.86	Tetradecane, 5-methyl-
41	11.724	155175	0.51	87177	0.68	1.78	Pentadecane, 2,6,10-trimethyl-
42	11.773	151217	0.49	97067	0.76	1.56	Eicosane
43	11.833	70734	0.23	46070	0.36	1.54	Tetradecane, 4-methyl-
44	11.990	58730	0.19	26101	0.20	2.25	Heptadecane, 2,6,10,15-tetramethyl-
45	12.100	55706	0.18	25829	0.20	2.16	Hexadecane, 1-iodo-
46	12.148	123948	0.40	68402	0.53	1.81	Heptadecane
47	12.208	136743	0.45	82006	0.64	1.67	Heptadecane
48	12.257	203398	0.66	101066	0.79	2.01	Nonane, 2,6-dimethyl-
49	12.285	148840	0.49	104792	0.82	1.42	Tetradecane, 5-methyl-
50	12.356	66534	0.22	44611	0.35	1.49	Decane, 5-ethyl-5-methyl-
51	12.506	230165	0.75	151159	1.18	1.52	Eicosane
52	12.553	743290	2.42	441462	3.44	1.68	Eicosane
53	12.629	112061	0.37	77724	0.61	1.44	Heptadecane
54	12.655	126462	0.41	77780	0.61	1.63	Hexadecane, 1-iodo-
55	12.690	87097	0.28	61280	0.48	1.42	Undecane, 4,7-dimethyl-
56	12.710	47756	0.16	36732	0.29	1.30	2-Butene, 1-butoxy-3-methyl-
57	12.817	955654	3.11	523919	4.08	1.82	Phenol, 2,4-bis(1,1-dimethylethyl)-
58	12.911	55022	0.18	35920	0.28	1.53	Eicosane
59	12.975	65817	0.21	34073	0.27	1.93	Tetradecane, 4-ethyl-
60	13.024	243033	0.79	115252	0.90	2.11	Dodecane, 2,6,11-trimethyl-
61	13.057	124156	0.40	85847	0.67	1.45	Phosphoric acid, diethyl nonyl ester
62	13.340	73547	0.24	41353	0.32	1.78	Pentadecane, 2,6,10,14-tetramethyl-
63	13.413	55878	0.18	27962	0.22	2.00	Pentadecane, 3-methyl-
64	13.632	48250	0.16	36322	0.28	1.33	Trichloroacetic acid, dodecyl ester
65	13.706	563599	1.84	395106	3.08	1.43	Hexadecane
66	13.770	185024	0.60	73470	0.57	2.52	Eicosane
67	13.902	131066	0.43	37321	0.29	3.51	Hexadecane, 4-methyl-
68	13.964	133383	0.43	86144	0.67	1.55	Eicosane
69	13.996	56252	0.18	37024	0.29	1.52	Hexadecane, 2,6,10,14-tetramethyl-
70	14.160	198487	0.65	73274	0.57	2.71	Heneicosane
71	14.205	48709	0.16	29512	0.23	1.65	Tetradecane, 5-methyl-
72	14.263	112695	0.37	55345	0.43	2.04	Dodecane, 4-methyl-
73	14.295	128316	0.42	49838	0.39	2.57	Hexadecane, 2,6,11,15-tetramethyl-
74	14.346	101637	0.33	70542	0.55	1.44	Eicosane
75	14.395	104132	0.34	53785	0.42	1.94	Eicosane
76	14.433	62288	0.20	36648	0.29	1.70	Eicosane
77	14.486	482870	1.57	198139	1.54	2.44	3-Heptadecene, (Z)-
78	14.571	78051	0.25	49460	0.39	1.58	Dodecane, 4-methyl-
79	14.633	275742	0.90	143041	1.11	1.93	Eicosane
80	14.685	568381	1.85	358470	2.79	1.59	Eicosane
81	14.729	142204	0.46	87277	0.68	1.63	Eicosane
82	14.780	158761	0.52	63609	0.50	2.50	Eicosane
83	14.827	108035	0.35	56380	0.44	1.92	1-(5-Ethyl-tetrahydrofuran-2-yl)-3,3-dimethyl-
84	14.875	69852	0.23	34278	0.27	2.04	Eicosane
85	14.979	157458	0.51	44214	0.34	3.56	Eicosane
86	15.100	97657	0.32	35969	0.28	2.72	Octadecane, 5-methyl-
87	15.154	165721	0.54	95528	0.74	1.73	Eicosane
88	15.406	101940	0.33	21533	0.17	4.73	10-Methylnonadecane
89	15.837	264110	0.86	137639	1.07	1.92	Heptadecane
90	16.325	352472	1.15	138966	1.08	2.54	Phytol, acetate
91	16.681	84530	0.28	36701	0.29	2.30	3,7,11,15-Tetramethyl-2-hexadecen-1-ol
92	16.967	118897	0.39	51799	0.40	2.30	Tetrapentacontane, 1,54-dibromo-
93	17.206	88583	0.29	30648	0.24	2.89	Eicosane
94	17.341	53048	0.17	23313	0.18	2.28	Hexatriacontane
95	17.472	214991	0.70	84544	0.66	2.54	Eicosane
96	17.570	192614	0.63	41765	0.33	4.61	Dodecane, 4-methyl-
97	17.630	48972	0.16	15672	0.12	3.12	Hexatriacontane
98	18.251	59033	0.19	24292	0.19	2.43	Eicosane
99	18.495	194395	0.63	56900	0.44	3.42	l-(+)-Ascorbic acid 2,6-dihexadecanoate
100	19.296	96138	0.31	34905	0.27	2.75	Eicosane
		30688555	100.00	12830168	100.00		

Table A 8: 80 Chemical Compounds identified in the Control Treatment of *D. salina*.

Peak#	R.Time	Area	Area%	Height	Height%	A/H	Name
1	4.188	282866	0.58	84565	0.78	3.34	Heptane, 2,4-dimethyl-
2	6.109	118391	0.24	31136	0.29	3.80	Nonane, 2-methyl-
3	6.242	101889	0.21	25796	0.24	3.95	Nonane, 2,5-dimethyl-
4	6.627	680602	1.40	185927	1.71	3.66	Octane, 3,5-dimethyl-
5	6.806	610331	1.26	125030	1.15	4.88	Decane, 2,4-dimethyl-
6	6.925	1402949	2.89	246434	2.27	5.69	Octane, 3,3-dimethyl-
7	7.381	8358798	17.24	666148	6.13	12.55	Nonane, 5-(2-methylpropyl)-
8	7.458	2683063	5.53	557838	5.13	4.81	Octane, 2,3,6,7-tetramethyl-
9	7.621	7681138	15.84	588396	5.41	13.05	Glycerin
10	7.978	741520	1.53	275784	2.54	2.69	Dodecane, 4,6-dimethyl-
11	8.048	226185	0.47	94290	0.87	2.40	Octane, 6-ethyl-2-methyl-
12	8.146	334074	0.69	48763	0.45	6.85	Octane, 2,3,6,7-tetramethyl-
13	8.341	212273	0.44	37104	0.34	5.72	Nonane, 5-(2-methylpropyl)-
14	8.410	139641	0.29	38896	0.36	3.59	1,3-bis(2,2-Dimethylpropoxy)-1,1,3,3-tetrame
15	8.590	179635	0.37	39703	0.37	4.52	Disiloxane, 1,1,3,3-tetramethyl-1,3-bis[3-(oxir
16	8.660	100846	0.21	25569	0.24	3.94	Undecane, 6-methyl-
17	8.800	217250	0.45	78115	0.72	2.78	Nonane, 5-(2-methylpropyl)-
18	8.925	217172	0.45	62272	0.57	3.49	Tridecane
19	9.255	1640420	3.38	841232	7.74	1.95	Dodecane
20	9.408	346558	0.71	139446	1.28	2.49	Undecane, 4,6-dimethyl-
21	9.517	247444	0.51	109026	1.00	2.27	Dodecane, 4-methyl-
22	9.745	160501	0.33	83568	0.77	1.92	Tetradecane
23	9.892	1151161	2.37	636138	5.85	1.81	Benzene, 1,3-bis(1,1-dimethylethyl)-
24	10.004	525074	1.08	180324	1.66	2.91	Decane, 4-ethyl-
25	10.158	930222	1.92	490742	4.52	1.90	Dodecane, 2,6,11-trimethyl-
26	10.260	154745	0.32	98707	0.91	1.57	Dodecane, 2,6,11-trimethyl-

Peak#	R.Time	Area	Area%	Height	Height%	A/H	Name
27	10.330	227254	0.47	70429	0.65	3.23	Octane, 2,3,6,7-tetramethyl-
28	10.467	294983	0.61	52626	0.48	5.61	Decane, 2,3,5,8-tetramethyl-
29	10.540	152673	0.31	45534	0.42	3.35	Decane, 2,3,7-trimethyl-
30	10.700	269200	0.56	108596	1.00	2.48	Dodecane, 2,6,11-trimethyl-
31	10.815	150766	0.31	38557	0.35	3.91	Dodecane, 2,6,11-trimethyl-
32	11.290	111373	0.23	31978	0.29	3.48	Hexadecane
33	11.611	1020801	2.11	457451	4.21	2.23	Tetradecane
34	11.690	301688	0.62	63773	0.59	4.73	2,6-Dimethyldecane
35	11.773	140604	0.29	87492	0.81	1.61	Eicosane
36	11.840	98943	0.20	41107	0.38	2.41	Tetradecane, 4-methyl-
37	11.986	144418	0.30	33748	0.31	4.28	Tetradecane
38	12.149	232988	0.48	63784	0.59	3.65	Hexadecane
39	12.261	503998	1.04	98467	0.91	5.12	Dodecane, 4-methyl-
40	12.360	103296	0.21	43721	0.40	2.36	Tridecane, 4-methyl-
41	12.554	1054192	2.17	368970	3.40	2.86	Eicosane
42	12.657	429085	0.89	82005	0.75	5.23	Dodecane, 2,6,11-trimethyl-
43	12.820	1235327	2.55	573247	5.27	2.15	Phenol, 2,4-bis(1,1-dimethylethyl)-
44	13.028	507758	1.05	116279	1.07	4.37	Eicosane
45	13.135	118706	0.24	37873	0.35	3.13	Dodecane, 2,6,11-trimethyl-
46	13.340	205669	0.42	45710	0.42	4.50	Heptadecane, 2,6,10,15-tetramethyl-
47	13.410	133144	0.27	36065	0.33	3.69	Pentadecane, 3-methyl-
48	13.709	773998	1.60	347372	3.20	2.23	Hexadecane
49	13.774	326906	0.67	74535	0.69	4.39	Eicosane
50	13.967	443529	0.91	84115	0.77	5.27	Eicosane
51	14.163	443006	0.91	84104	0.77	5.27	Heptadecane
52	14.318	335764	0.69	63747	0.59	5.27	Eicosane
53	14.400	320553	0.66	69939	0.64	4.58	Heptadecane, 2,6,10,15-tetramethyl-
54	14.489	832229	1.72	222211	2.04	3.75	3-Heptadecene, (Z)-
55	14.687	1544388	3.19	305119	2.81	5.06	Eicosane
56	14.983	391191	0.81	60234	0.55	6.49	Eicosane
57	15.155	479134	0.99	98630	0.91	4.86	Eicosane
58	15.259	182104	0.38	36875	0.34	4.94	Dodecane, 2,6,11-trimethyl-
59	15.403	205058	0.42	41535	0.38	4.94	Dodecane, 2,6,11-trimethyl-
60	15.480	151406	0.31	36251	0.33	4.18	Hexadecane, 1-iodo-
61	15.640	189051	0.39	25883	0.24	7.30	Eicosane
62	15.756	130194	0.27	33951	0.31	3.83	Docosyl pentafluoropropionate
63	15.839	493392	1.02	152687	1.40	3.23	Heptadecane
64	16.102	98273	0.20	28924	0.27	3.40	Octadecane, 4-methyl-
65	16.330	874849	1.80	171698	1.58	5.10	Phytol, acetate
66	16.580	139556	0.29	25224	0.23	5.53	Tetracosane, 11-decyl-
67	16.686	179038	0.37	51490	0.47	3.48	3,7,11,15-Tetramethyl-2-hexadecen-1-ol
68	16.973	437889	0.90	71924	0.66	6.09	Phytol, acetate
69	17.130	133700	0.28	29805	0.27	4.49	Eicosane
70	17.207	157825	0.33	34343	0.32	4.60	Eicosane
71	17.350	137479	0.28	39556	0.36	3.48	Eicosane
72	17.476	285290	0.59	82759	0.76	3.45	Eicosane
73	17.567	251582	0.52	43374	0.40	5.80	Eicosane
74	17.740	98386	0.20	17272	0.16	5.70	5-Ethyl-5-methylnonadecane
75	18.370	93078	0.19	16413	0.15	5.67	Dodecane, 4-methyl-
76	18.495	431090	0.89	69661	0.64	6.19	l-(+)-Ascorbic acid 2,6-dihexadecanoate
77	19.299	172620	0.36	44864	0.41	3.85	Eicosane
78	22.371	504061	1.04	61419	0.57	8.21	Phytol
79	22.641	237483	0.49	34562	0.32	6.87	Eicosane
80	22.770	127781	0.26	18718	0.17	6.83	Sulfurous acid, hexyl octyl ester
		48483497	100.00	10867555	100.00		

Chapter 4

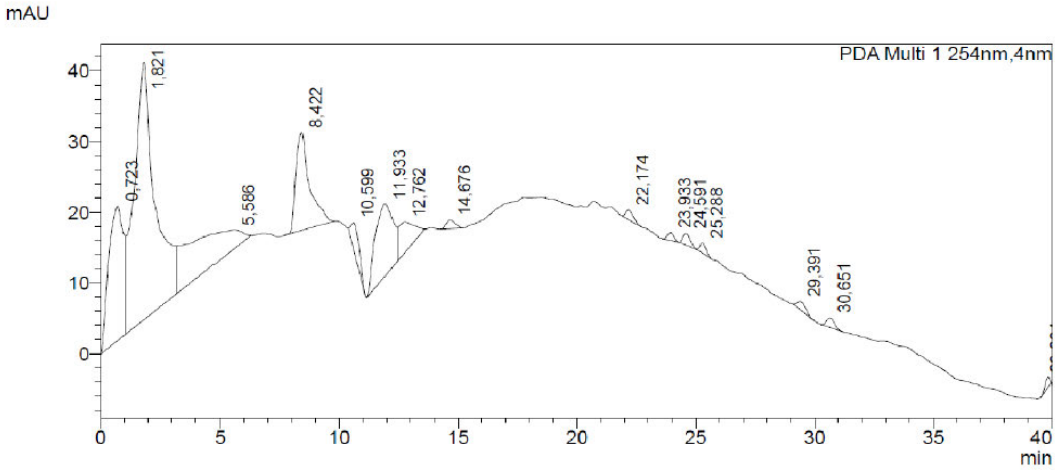

The Chromatogram indicating the retention times of the compounds detected in the 2M NaCl sample.

As shown the above figure depicts the results observed for the 2M NaCl sample, the chromatogram indicates the presence of various different polysaccharides excluding arabinose.

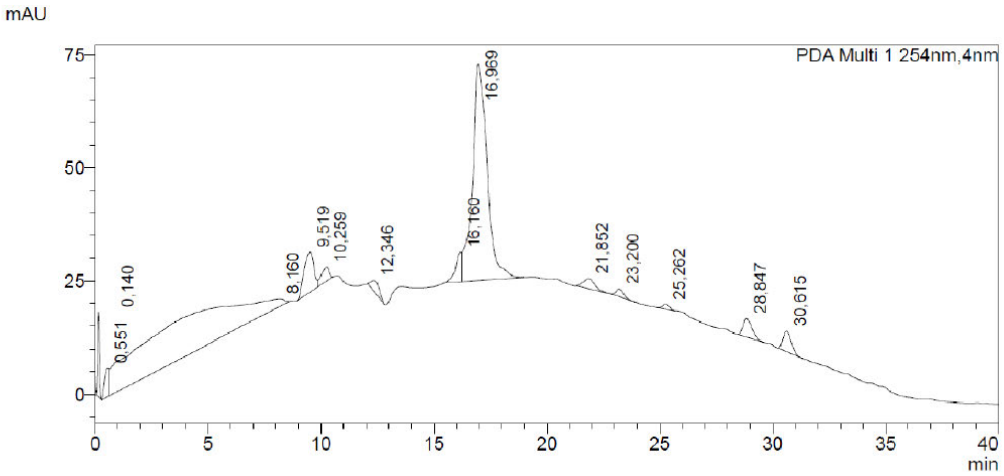

The Chromatogram indicating the retention times for the compounds detected in the 2,5M NaCl sample.

As shown in the chromatogram of the 2,5M NaCl treatment shows the presence of various polysaccharides such as arabinose.

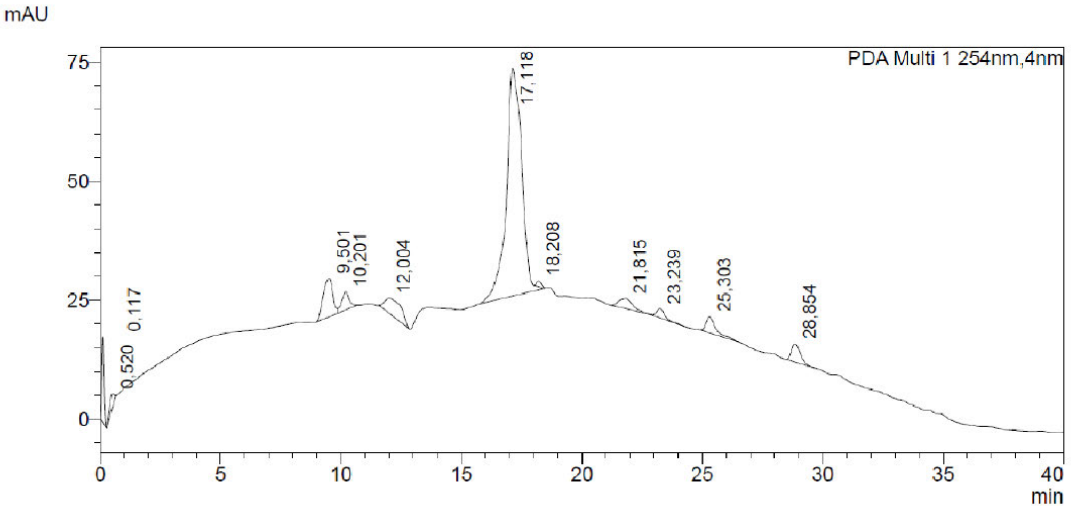

The Chromatogram indicating the retention times of the compounds detected in the 3M NaCl sample.

The Figure above, depicts the results of the EPS analysis for the 3M NaCl treatment, the results depict the presence of various polysaccharides.

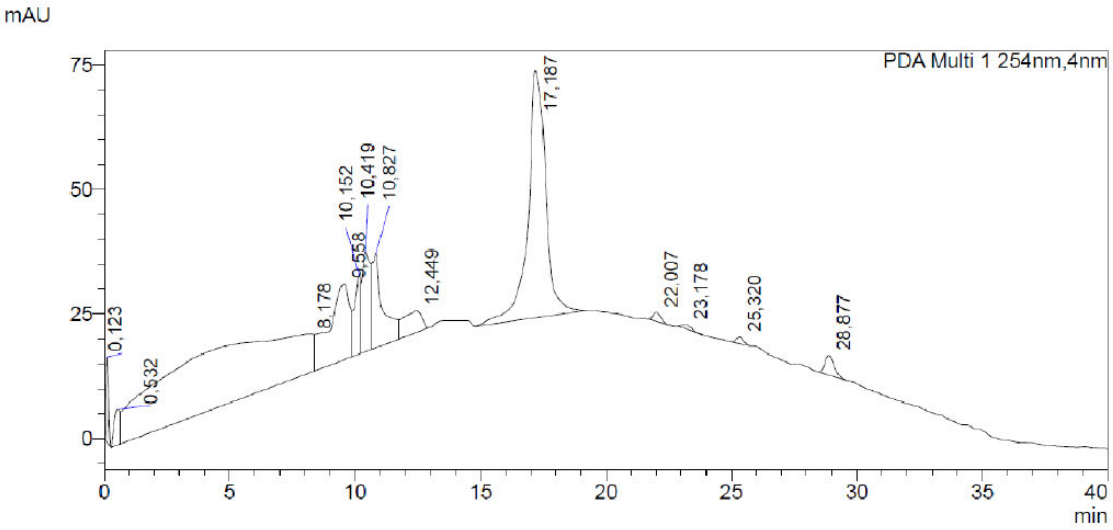

The Chromatogram indicating the retention times of the compounds detected in the 3,5M NaCl sample.

As shown in the Figure above, the results for the EPS analysis of the 3,5M NaCl treatment depicts the presence of polysaccharides such as ribose.

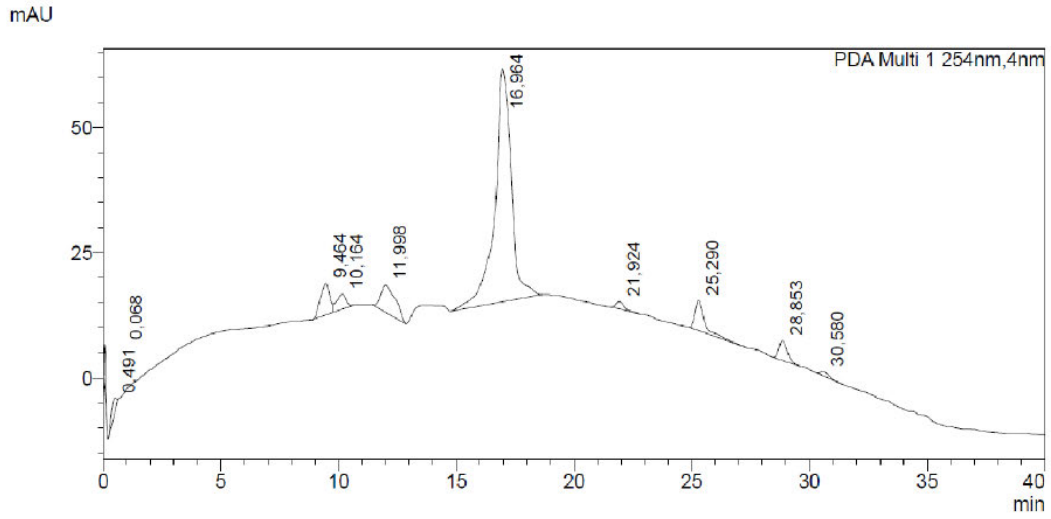

The Chromatogram indicating the retention times of the compounds detected in the NO_3 Treatment sample.

As shown in the Figure above, the EPS analysis for the Nitrate treatment of *D. salina* displays the presence of polysaccharides similar to the polysaccherides found in the NaCl experiment.

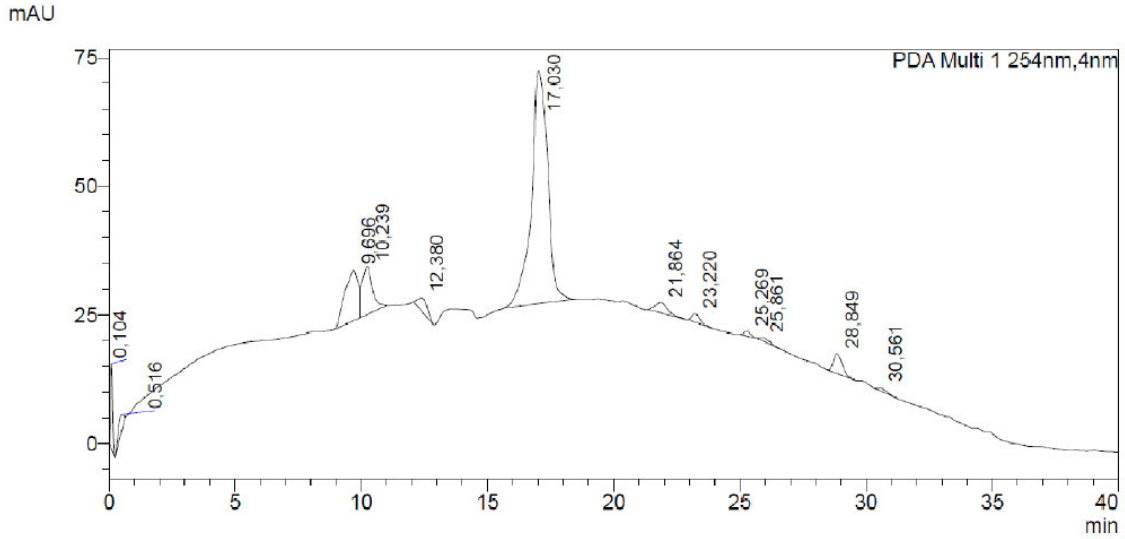

The Chromatogram indicating the retention times of the compounds detected in the Ammonia Treatment.

As shown in the Figure above, the ammonia treatment produces a chromatogram that is like the results obtained for the nitrate treatment.

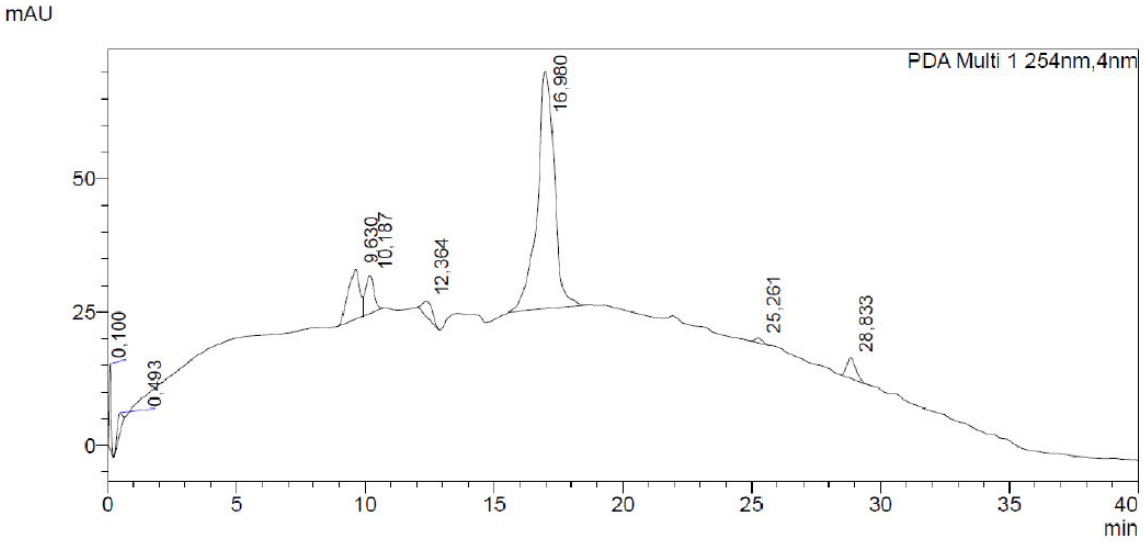

The Chromatogram indicating the retention times of the compounds detected in the Urea Treatment sample.

As shown in the Figure above, the urea treatment depicts the presence of fewer polysaccharides as opposed to other treatments.

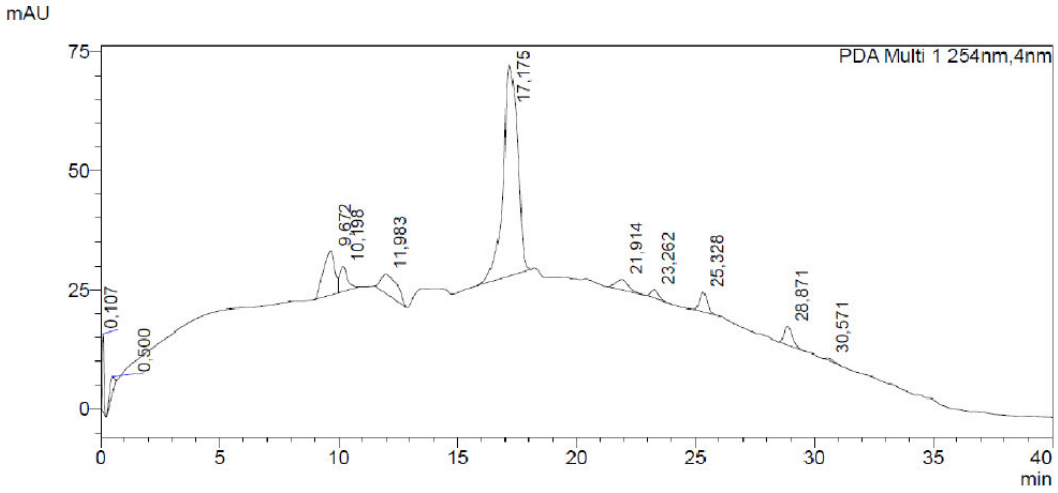

The Chromatogram indicating the retention times of the compounds detected in the Control Treatment sample.

As shown in the Figure above the control treatment for the nitrogen source experiment has extremely low concentrations of polysaccharides.

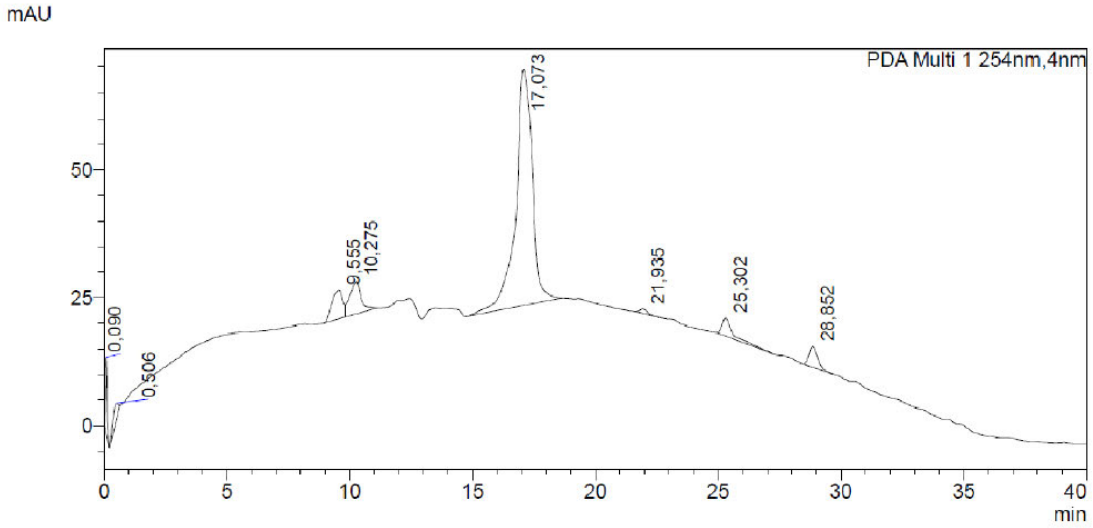

The Chromatogram indicating the retention times of the compounds detected in the NO_3, 2M NaCl and 25ºC Treatment sample for the RSM study.

The Figure shown above shows the chromatogram for the RSM treatment containing 2M NaCl and nitrate at 25ºC. The results depict the presence of few polysaccharides as seen by the peaks.

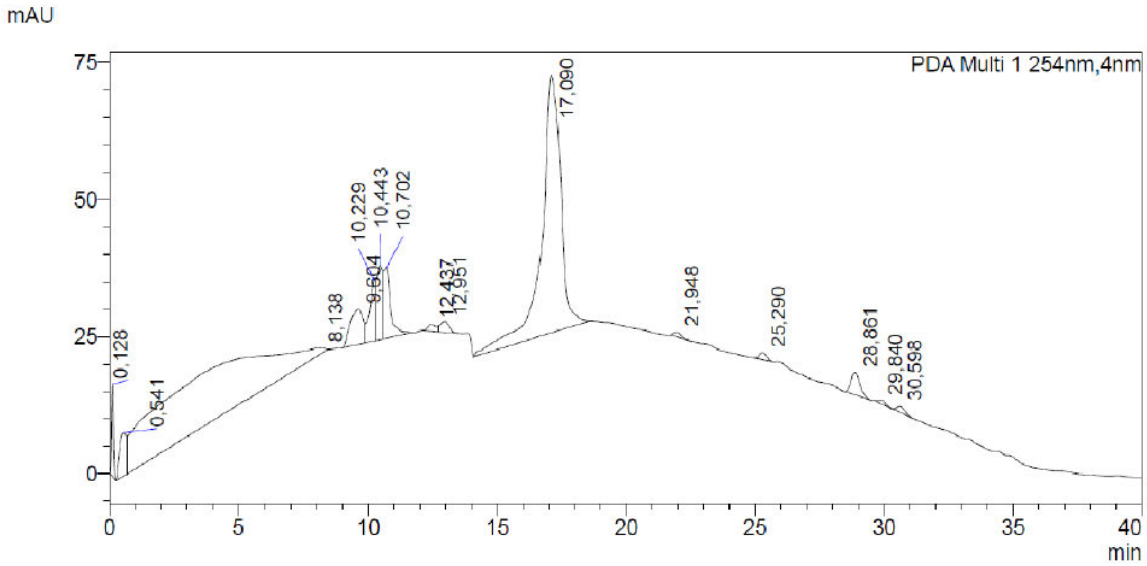

The Chromatogram indicating the retention times of the compounds detected in the Ammonia, 3M NaCl and 25ºC Treatment sample for the RSM study.

As shown in the Figure above, the RSM treatment containing ammonia, 3M NaCl at 25ºC has produced many EPS molecules within the *D. salina* cells.

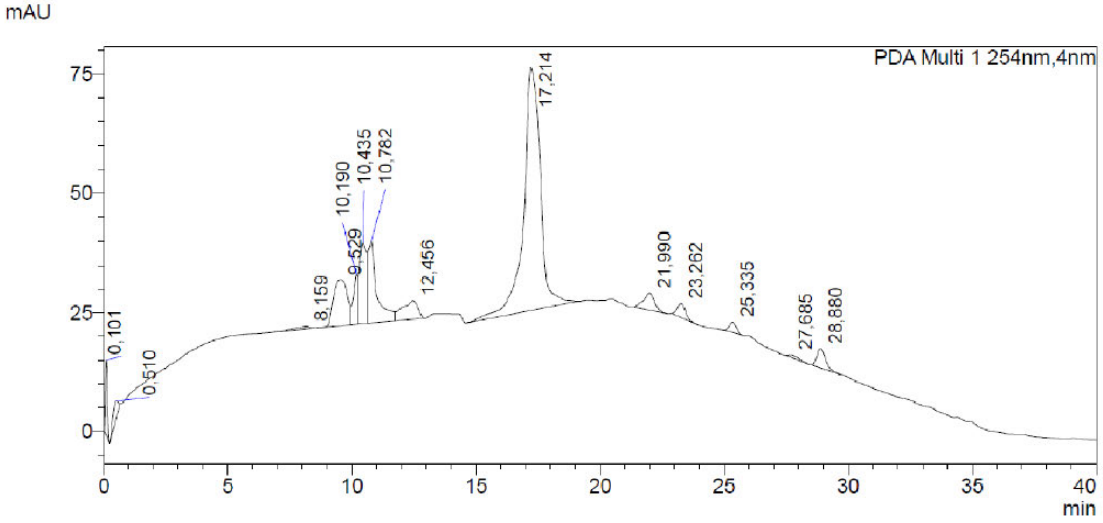

The Chromatogram indicating the retention times of the compounds detected in the Urea, 3M NaCl and 25ºC Treatment sample for the RSM study.

As shown in the Figure above, the presence of polysaccharides such as arabinose and ribose are clearly depicted within the chromatogram.

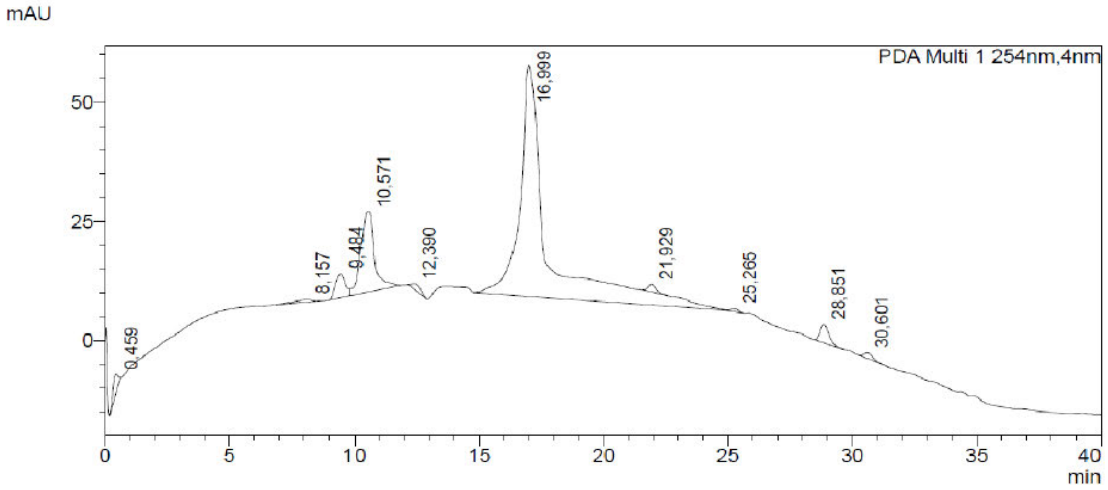

The Chromatogram indicating the retention times of the compounds detected in the NO_3, 4M NaCl and 25ºC Treatment sample for the RSM study.

As shown in the Figure above, the nitrate, 4M NaCl and 25ºC RSM treatment produces many polysaccharides due to the high NaCl salinity.

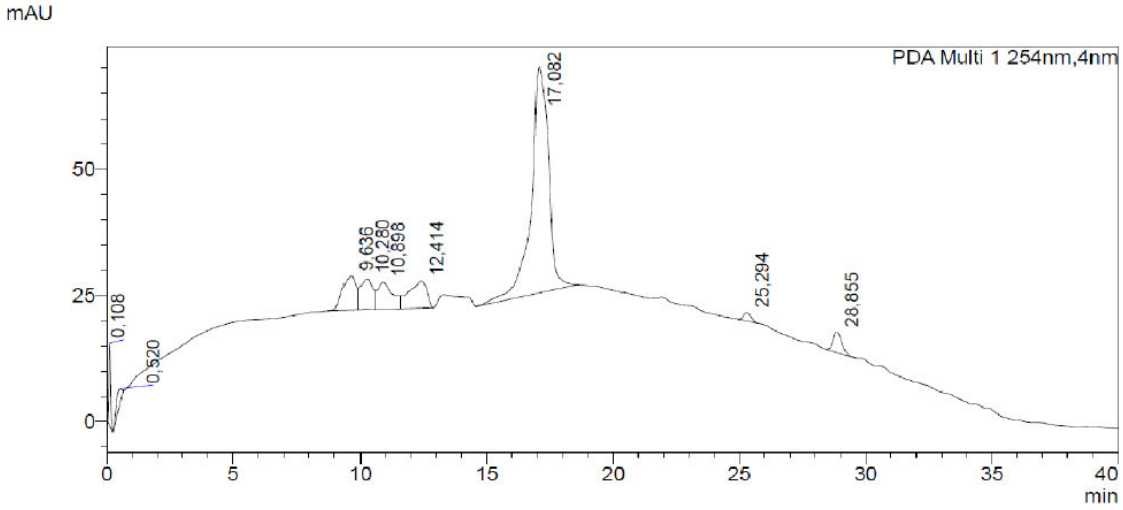

The Chromatogram indicating the retention times of the compounds detected in the Ammonia, 2M NaCl and 28ºC Treatment sample for the RSM study.

As shown in the Figure above, very few polysaccharides are produced when ammonia is used as the nitrogen source at 28ºC, this is due to the cells lack of affinity to using ammonia as a nitrogen source.

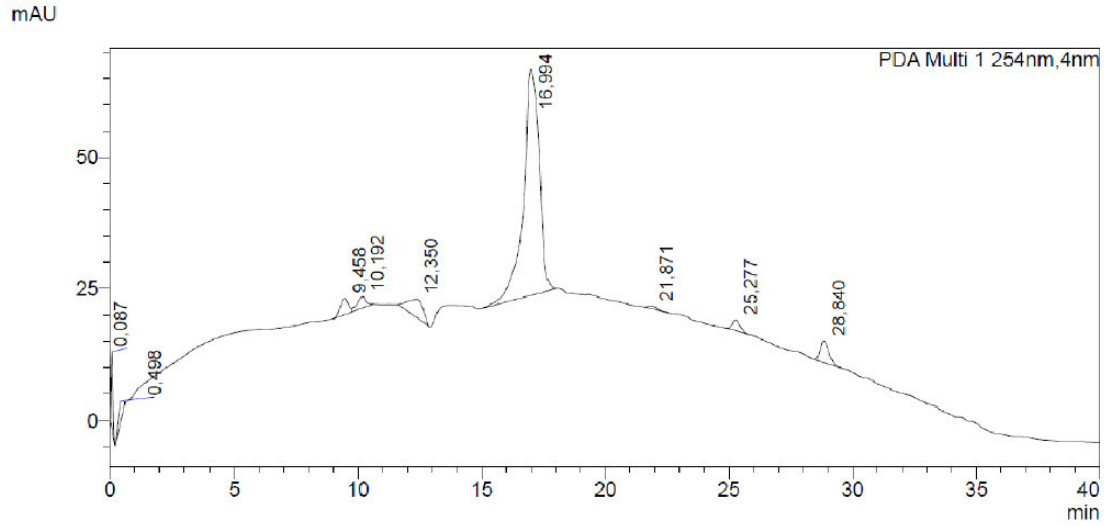

The Chromatogram indicating the retention times of the compounds detected in the Urea, 2M NaCl and 28ºC Treatment sample for the RSM study.

As shown in the Figure above, the use of urea as the nitrogen source produces less polysaccharides in the EPS. Another reason could be due to the low NaCl salinity.

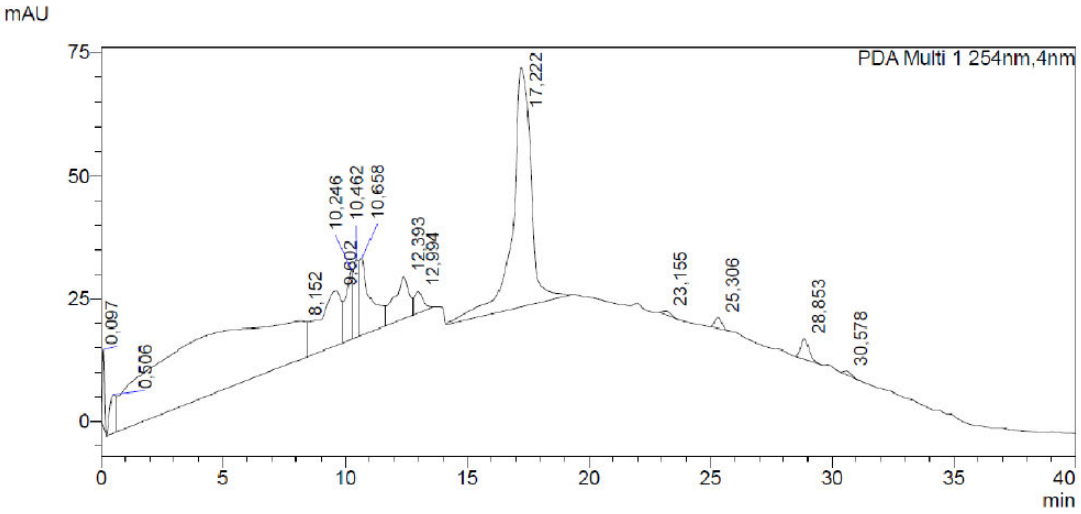

The Chromatogram indicating the retention times of the compounds detected in the NO_3, 3M NaCl and 28ºC Treatment sample for the RSM study.

As shown in the Figure above, the in NaCl salinity causes an increase in EPS production regardless of the nirogen source.

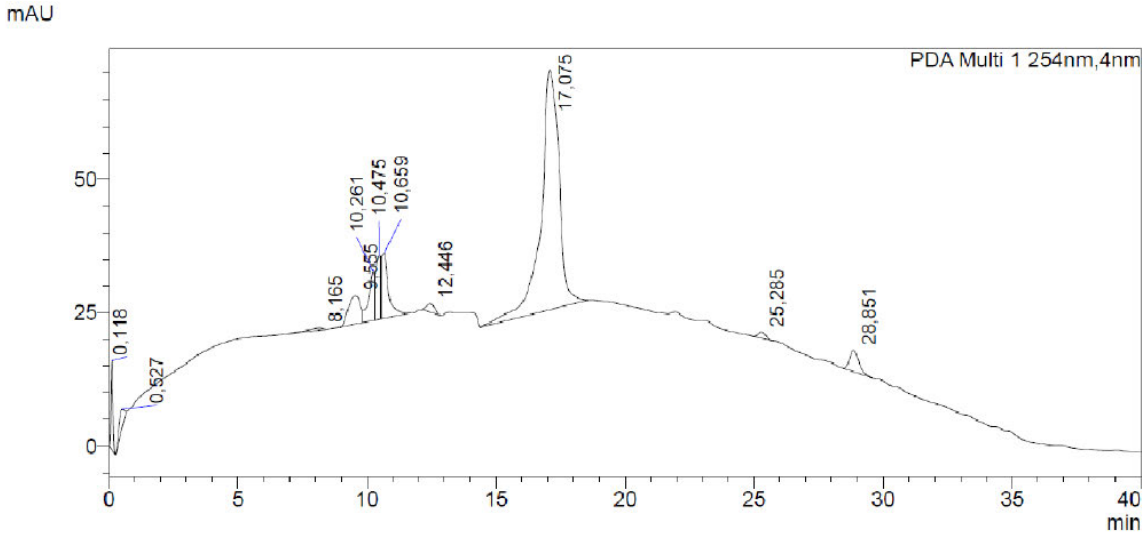

The Chromatogram indicating the retention times of the compounds detected in the Ammonia, 4M NaCl and 28ºC Treatment sample for the RSM study.

As shown in the Figure above, the presence of ammonia affects the EPS production regardless of the NaCl salinity.

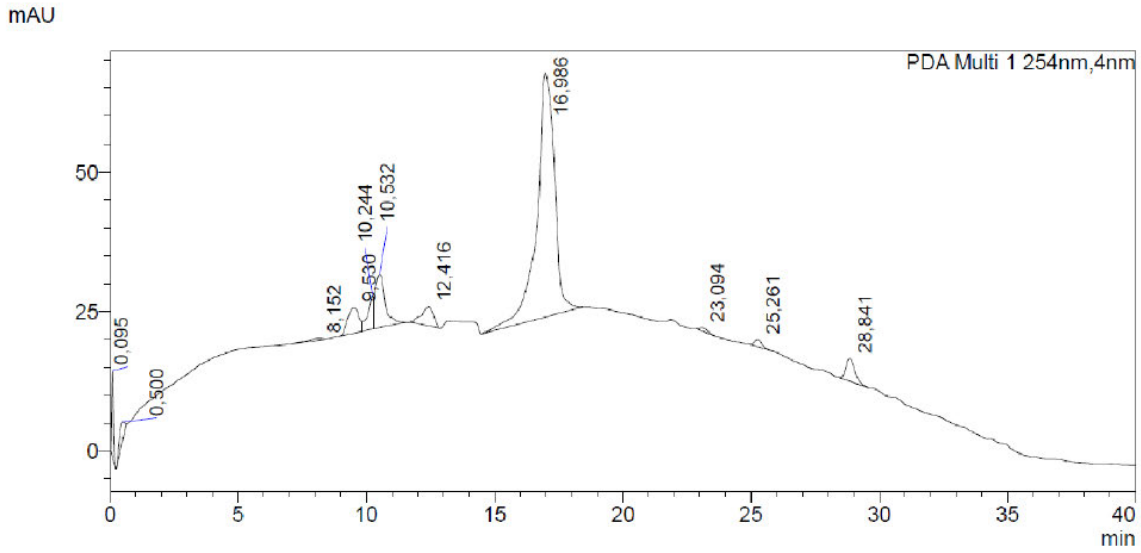

The Chromatogram indicating the retention times of the compounds detected in the Urea, 4M NaCl and 28ºC Treatment sample for the RSM study.

As shown in the Figure above the treatment containing urea as the nitrogen source and 4M NaCl at 28ºC, has lower amounts of polysaccharides, this could be due to the temperature as the temperature could impact the EPS production.

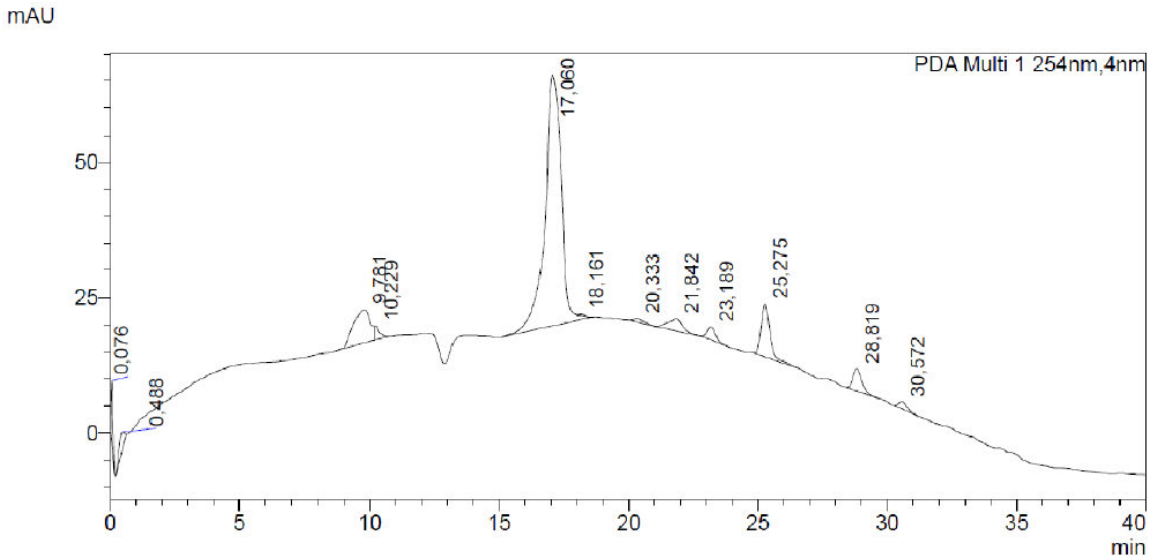

The Chromatogram indicating the retention times of the compounds detected in the NO_3, 2M NaCl and 32ºC Treatment sample for the RSM study.

As shown in the figure above, the presence of nitrate and 2M NaCl at 32ºC stimulates high EPS production.

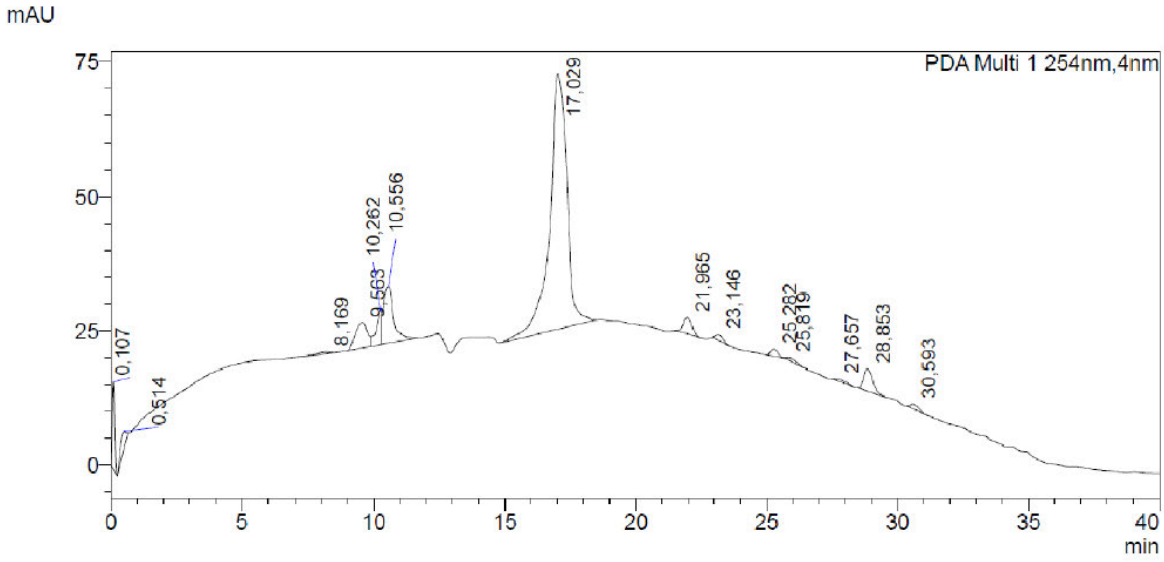

The Chromatogram indicating the retention times of the compounds detected in the Ammonia, 3M NaCl and 32ºC Treatment sample for the RSM study.

As shown in the Figure above, the presence of 3M NaCl has the highest impact on EPS production.

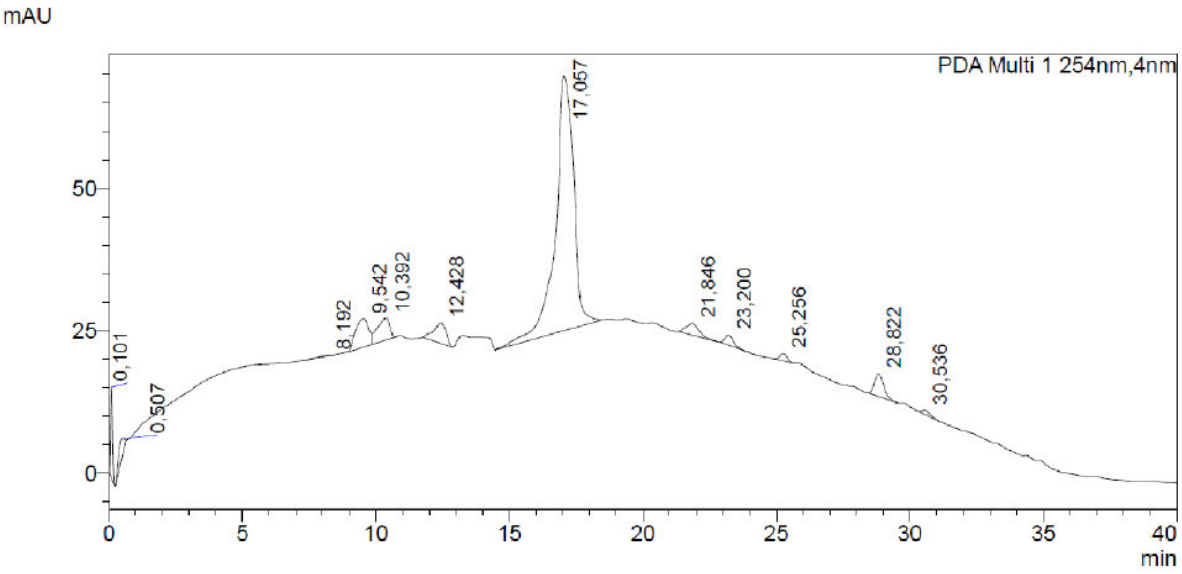

The Chromatogram indicating the retention times of the compounds detected in the Urea, 3M NaCl and 32ºC Treatment sample for the RSM study.

As shown in the Figure above, the temperature has an impact on the EPS production, the higher the temperatures the less EPS is produced.

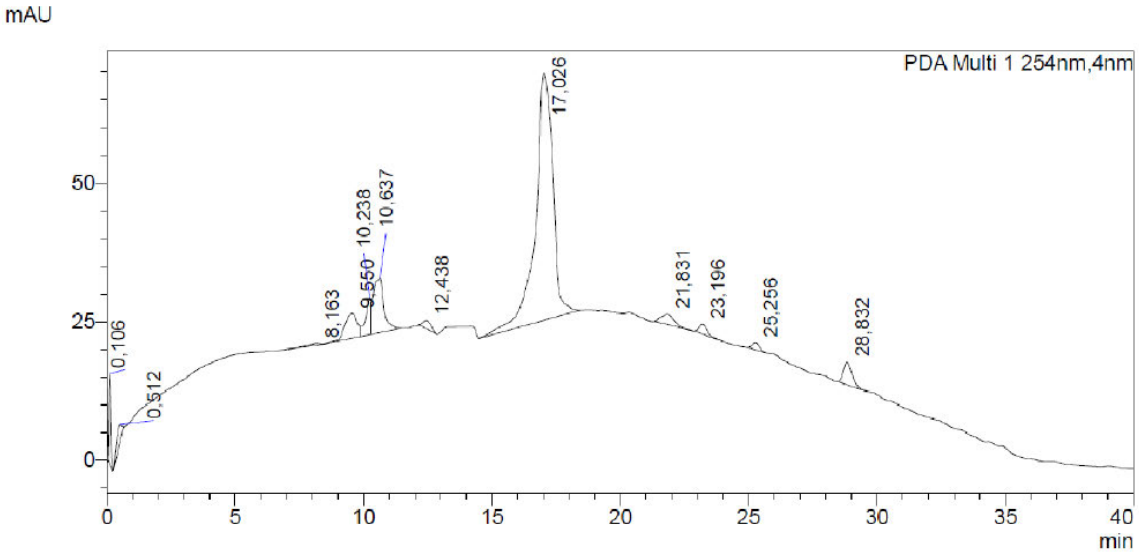

The Chromatogram indicating the retention times of the compunds detected in the NO_3, 4M NaCl and 32ºC Treatment sample for the RSM study.

As shown in the Figure above, the presence of 4M Nacl produces high levels of the polysaccharide arabinose which is indicated by the peak at the 17 min retention time.